SOUTHWEST RESEARCH INSTITUTE®

SOUTHWEST RESEARCH INSTITUTE®

Internal Research and Development 2017

The SwRI IR&D Program exists to broaden the Institute's technology base and to encourage staff professional growth. Internal funding of research enables the Institute to advance knowledge, increase its technical capabilities, and expand its reputation as a leader in science and technology. The program also allows Institute engineers and scientists to continually grow in their technical fields by providing freedom to explore innovative and unproven concepts without contractual restrictions and expectations.

- Space Science
- Materials Research & Structural Mechanics
- Intelligent Systems, Advanced Computer & Electronic Technology, & Automation
- Measurement & Nondestructive Evaluation of Materials & Structures
- Engines, Fuels, Lubricants, & Vehicle Systems
- Geology & Nuclear Waste Management
- Fluid & Machinery Dynamics
- Electronic Systems & Instrumentation
- Chemistry & Chemical Engineering

SOUTHWEST RESEARCH INSTITUTE®

SwRI IR&D 2017 – Space Science

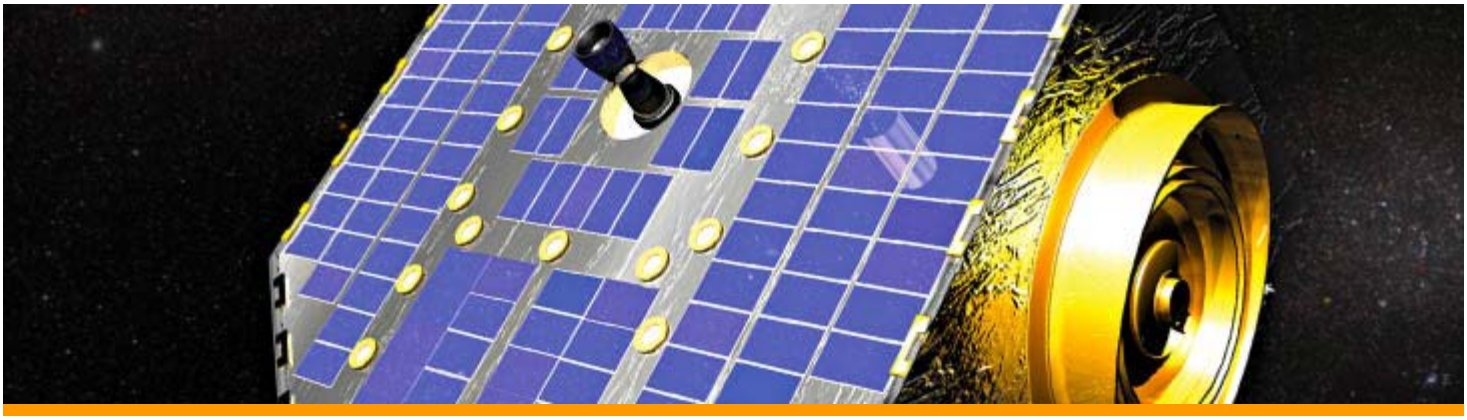

- Augmenting a Novel Magnetohydrodynamics Code for Studying Astrophysical Plasmas and Space Weather, 15-R8568
- Constant Pressure Stratospheric Balloon (CPSB), 15-R8663
- Testing Graphene Foils in a Space Plasma Instrument, 15-R8674
- Experimental Investigation of the Organic Solar System, 15-R8756
- The Investigation into High Altitude Lighter-Than-Air Mission Concept of Operations Scenarios as Defined by Persistence, Risk and Cost, 15-R8764

SOUTHWEST RESEARCH INSTITUTE®

SwRI IR&D 2017 – Materials Research & Structural Mechanics

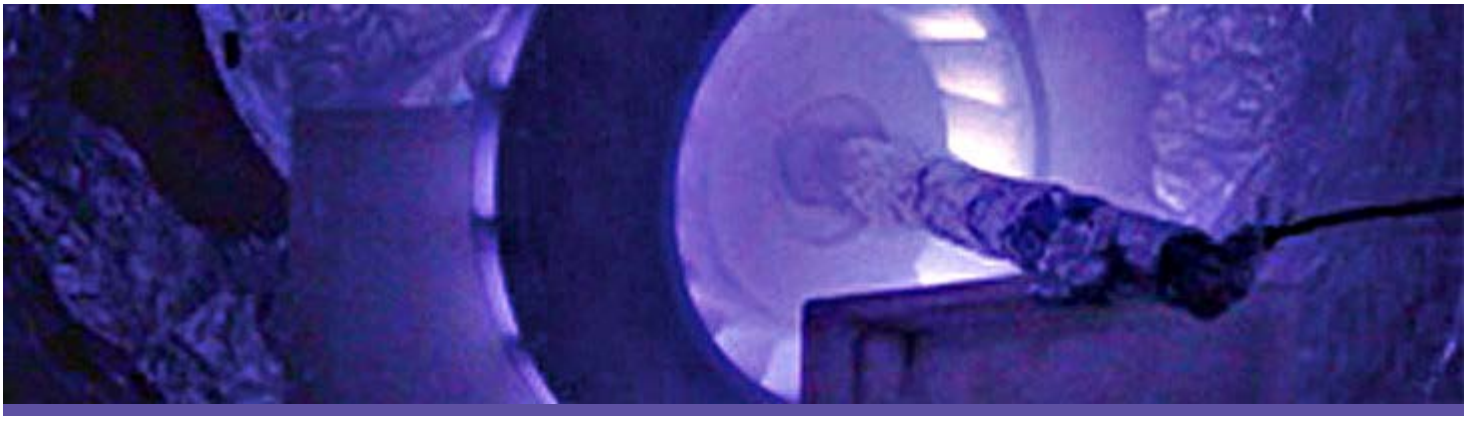

- Large-Scale Additive Manufacturing Using Concrete Composite Materials, 14-R8610
- Effect of Cyclic Relative Humidity on Environmentally Assisted Cracking, 18-R8554
- Development of a New Numerical Model to Simulate Chemotaxis-driven Bacterial Transport for Treatment of Tumor Cells and Mitigation of Bacterially-mediated Pipeline Corrosion Problems, 18-R8602
- Hydrogen and Methane Gas-Phase Detonations, 18-R8614
- Development of Artificial Muscle Actuator for Physical Joint Simulator, 18-R8616
- A Fundamental Assessment of K_{ISSC} and J_R Tearing Resistance Curves in Sour Brine Environments, 18-R8618
- Impact of Carbon Fiber-Reinforced Composites, 18-R8619
- Statistical Shape Modeling of the Temporomandibular Joint, 18-R8684
- 3-D Printed Human Surrogates for Injury RDT&E, 18-R8692
- Analysis of Corrosion Damage on Samples Exposed to Accelerated and Outdoor Corrosion Environments, 18-R8745
- Additive Manufacturing and the 3rd Sandia Fracture Challenge, 18-R8747
- Scaling Issues in Hypervelocity Impact, 18-R8779
- Develop, Test, and Validate a Corrosion Monitoring Cell to Quickly Evaluate Effectiveness of the Corrosion Control Measures, 20-R8784

SOUTHWEST RESEARCH INSTITUTE®

SwRI IR&D 2017 – Intelligent Systems, Advanced Computer & Electronic Technology, & Automation

- Development of a Reactive Automated Mixed Palletizing (RAMP Algorithm), 10-R8752
- Feasibility Investigation of Determining the Condition of Distribution Equipment in Live Power Systems Using Radar Technology, 10-R8761
- Investigation of the Use of Machine Learning to Traffic Profile Prediction Capabilities, 10-R8762
- Investigation of the Application of Machine Learning to Distributed Temperature Sensing Data, 10-R8773
- Generation and Auto-Annotation of High-Precision Road Geometry Maps from Multi-Modal Sensor Data, 10-R8781
- Multivariate Statistical Process Control for Cooling Towers, 14-R8656
- Fusion of Intelligence Data from Observables, 16-R8670

SOUTHWEST RESEARCH INSTITUTE®

SwRI IR&D 2017 – Measurement & Nondestructive Evaluation of Materials & Structures

- Development of an Omnidirectional MsT Probe for Guided Wave Testing of Plates, 18-R8707

SOUTHWEST RESEARCH INSTITUTE®

SwRI IR&D 2017 – Engines, Fuels, Lubricants, & Vehicle Systems

- Experimental Investigation of Co-direct Injection of Natural Gas and Diesel in a Heavy-duty Engine, 03-R8522
- Investigation of the Durability of High-Efficiency Gasoline Engines, 03-R8596
- Advanced Model-Based SCR Controller for Advanced Multiple Component Catalyst Systems, 03-R8599
- Fast Catalyst Light-Off on a Heavy-Duty Natural Gas Engine, 03-R8620
- Dynamic Fast Charging of a Battery Pack without Significant Degradation in Capacity and Power Capability, 03-R8647
- Fuel Economy Effect of Advanced Vehicle Hardware, 03-R8649
- Evaluation of Ionization Current as a Combustion Monitoring Tool in a Dual Fuel Engine, 03-R8668
- SULEV Potential for D-EGR Light Duty Passenger Vehicles, 03-R8689
- Investigation of Dual-Fuel Engine to Achieve Tier 4 Final Emission Levels with no NOx Exhaust Aftertreatment, 03-R8694
- Methanol Fuel Testing on Port Fuel Injected Internal EGR, HPL-EGR and D-EGR® Engine Configurations, 03-R8713
- Development of Low Flow Capability and Lean / Rich Switching for SwRI's ECTO-Lab (formerly HGTR®) Technology, 03-R8714
- Investigation of Regeneration Frequency, Ash Rate, and Soot/Ash Ratio Impact on Ash Loaded Diesel Particulate Filters, 03-R8716

- Combustion Performance of CO_2 Only EGR and its Separation from an Exhaust Gas Stream Through Membrane Technology, 03-R8727
- Comparison of Accelerated Ash Loading Methods for Gasoline Particulate Filters, 03-R8729
- Heat Transfer Prediction in Internal Combustion Engines using Simulation, 03-R8755
- Characterization of High Pulse Energy Turbochargers, 03-R8757
- Evaluating System-Level Transient Performance of a Plug-In Hybrid-Electric Vehicle, 03-R8778
- Development of a New Automotive Fuel Filter Test Method Incorporating Vibration and Cyclic Flow Test Parameters, 08-R8723

SOUTHWEST RESEARCH INSTITUTE®

SwRI IR&D 2017 – Geology & Nuclear Waste Management

- Investigation of Drought Intensity and Periodicity in South Texas Using Chemical Records in Bat Guano Cores, 15-R8519
- Understanding the Fluid Behavior of Planetary Regolith Materials, 15-R8651
- Development of an Integrated Surface Water-Groundwater Model for Semi-Arid Environments, 15-R8759
- Predicting Induced Permeability from Geomechanical Modeling of Hydraulic Fracturing, 15-R8760
- Injection Wells and Induced Seismicity, South Central Texas, 15-R8772
- Development of Computational Fluid Dynamics Framework for Characterization of High Energy Arcing Faults (HEAF) in Nuclear Power Plants, 20-R8680
- Assessment of Limitations in Current Approaches to Analyses of Seismic Liquefaction Potential, 20-R8698
- Proof-of-Concept Biosphere Model to Calculate Human Radon Doses Applicable to Buried Radioactive Waste Exposure Scenarios, 20-R8775

SOUTHWEST RESEARCH INSTITUTE®

SwRI IR&D 2017 – Fluid & Machinery Dynamics

- Model Based Gas Turbine Health Monitoring, Diagnostics, and Optimization Using Typically Sparse Performance Data, 18-R8601
- Field Testing of Rotating Equipment Vibration Modes Using Operational Modal Analysis, 18-R8608
- Development and Validation of Liquid-Liquid Separation Modeling Techniques, 18-R8622
- Acoustic-Induced Vibration Testing, Modeling, and Mitigation, 18-R8730
- Tie Bolt Rotor Modeling and Design: Joint Bending Stiffness and Tie Bolt Preload Requirements, 18-R8766
- Optical Level Sensor for Cryogenic Applications, 18-R8771
- Investigation of the Effects of Inlet Flow Distortion on the Performance of Centrifugal Compressors, 18-R8780

SOUTHWEST RESEARCH INSTITUTE®

SwRI IR&D 2017 – Electronic Systems & Instrumentation

- Inexpensive and Rapid Production of Microfluidic Parts, 11-R8719
- Method Development for Production of Energetic Bimetallic Materials, 11-R8770
- A Bundt Pan Electrostatic Analyzer for an Open Ion Source for MASPEX, 15-R8709
- Fabrication and Testing of High Voltage Optocouplers for Space Applications, 15-R8712
- Development of a Lunar Advanced Vacuum Apparatus (LAVA), 15-R8734

SOUTHWEST RESEARCH INSTITUTE®

SwRI IR&D 2017 – Chemistry & Chemical Engineering

- Enhancing the Efficacy of a Chlamydia Subunit Vaccine Through Encapsulation, 01-R8584

SOUTHWEST RESEARCH INSTITUTE®

2017 IR&D Annual Report

Augmenting a Novel Magnetohydrodynamics Code for Studying Astrophysical Plasmas and Space Weather, 15-R8568

Principal Investigators
Derek A. Lamb
Craig E. DeForest

Inclusive Dates: 07/01/15 – 09/01/17

Background — Magnetohydrodynamics (MHD) is the study of electrically conductive, magnetized fluids. The solar atmosphere exists in a state in which the equations of MHD apply, and researchers use simulations to understand this complex system. Conventional simulations are hundreds to thousands of times more dissipative (electrically resistive) than real solar plasma, so conventional simulations use far finer grids than are necessary to represent the system under study. This makes simulations computationally expensive, and severely limits the fidelity with which conventional simulations can represent electric-current-bearing systems on the Sun, such as solar flares and the magnetically stressed regions that release coronal mass ejections (CMEs). With prior internal and external funding, we have developed a code, the Field Line Universal relaXer (FLUX), that reformulates the equations of MHD to take advantage of the analogy between magnetic field lines and the magnetic fields they represent.

Our approach discretizes the magnetic field, automatically preserves the magnetic field topology, and results in a thousand-fold increase in efficiency compared to conventional codes. While the modeling approach has advantages over traditional codes, the development had stalled. The objective of this project was to revive, augment, and demonstrate new capabilities of the FLUX code.

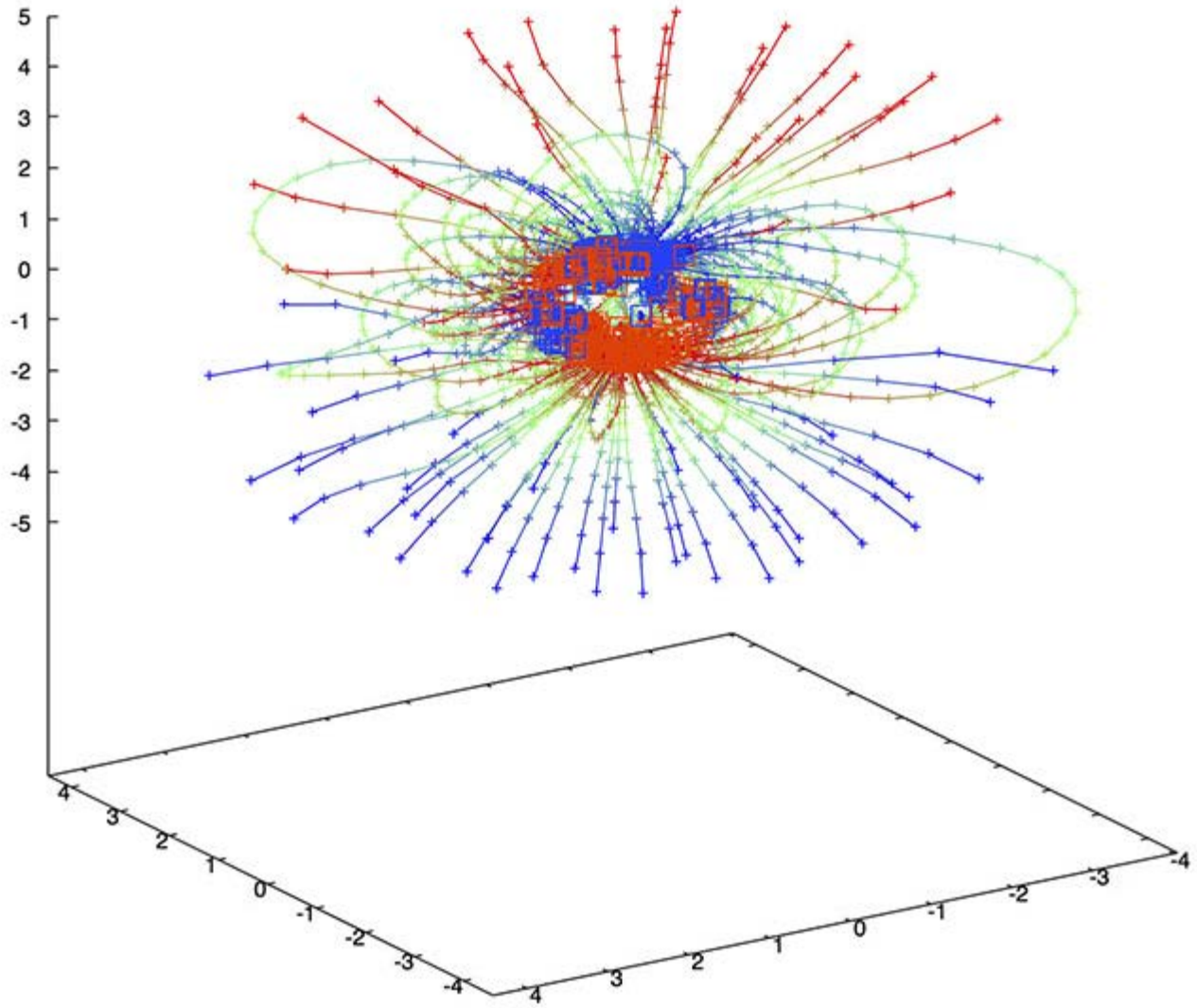

Figure 1: FLUX rendering of the 3-D magnetic field structure of the solar corona near the time of August's total solar eclipse, showing open magnetic structures from the north and south poles, and closed magnetic structures that form the bases of streamers near the equator.

Approach — We devoted substantial effort to revive this code and bring it up to modern coding and development standards. We extended the code to enable it to model and map the steady solar wind. We used synoptic measurements of the solar surface magnetic field as a boundary condition, and created models of the steady-state corona to compare with the 2017 total solar eclipse.

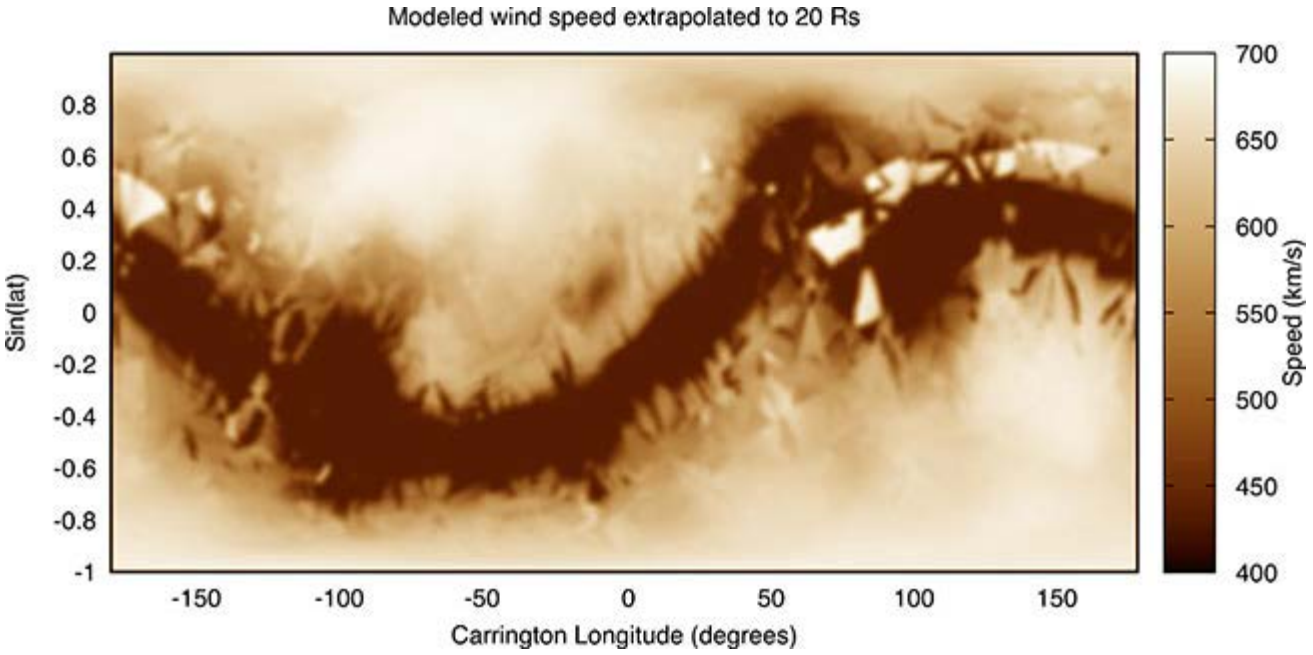

Figure 2: The solar wind flow through a FLUX model, extrapolated to 20 R☉, shows slower wind speeds in the "S"-shaped streamer belt, and the higher speeds near the polar coronal holes.

Accomplishments — Having been revived from a several-year dormancy, the FLUX code now uses a modern version control system, public source code repository, and issue tracker. The user manual and documentation have been substantially updated and simplified. The complex code compiles cleanly, and we have created a test suite that automatically runs whenever the code is changed to help detect incompatible changes. We rewrote the 3-D visualization software used by FLUX to render the simulations (Figure 1). The new visualization interface is well-supported and maintained, stable, and produces publication-quality 3-D renders and plots. We added a one-fluid flow model to FLUX, enabling us to use FLUX to model and map the steady solar wind flow that forms a backdrop to space weather events (Figure 2). Finally, we performed relaxations of a global coronal magnetic field simulation, using synoptic solar surface magnetic field measurements as input, to compare with the observations made during the recent total solar eclipse (Figure 1).

The magnetic structure of the relaxation is highly evocative of the eclipse, with large loops (associated with a streamer) on the left side of the Sun, and two smaller bundles of loops (associated with two smaller streamers) on the right side of the Sun, and open field lines from the north and south polar regions filling up most of the space.

2017 IR&D | IR&D Home

SOUTHWEST RESEARCH INSTITUTE®

2017 IR&D Annual Report

Constant Pressure Stratospheric Balloon (CPSB), 15-R8663

Principal Investigators
William D. Perry
Ethan Chaffee

Inclusive Dates: 05/23/16 – 01/24/17

Background — Stratospheric balloons are used for a wide range of science, military, and commercial applications. In many of these applications, flight durations of days or weeks are needed. These balloons provide a platform to support instruments, surveillance, and communication systems above most of the Earth's atmosphere, providing clear view of the sky and a wide view of the Earth. Constellations of balloons can provide communications and internet service to large areas of the world that presently do not have the needed telecommunications infrastructure.

This project investigated a concept for a novel constant pressure stratospheric balloon system. Presently, there are two basic types of stratospheric balloons: zero pressure and super pressure. Zero pressure balloons are cost effective and reliable, but the flight duration is limited. Super pressure balloons provide long duration flight, but are much less reliable and must be fabricated from expensive, very high strength material.

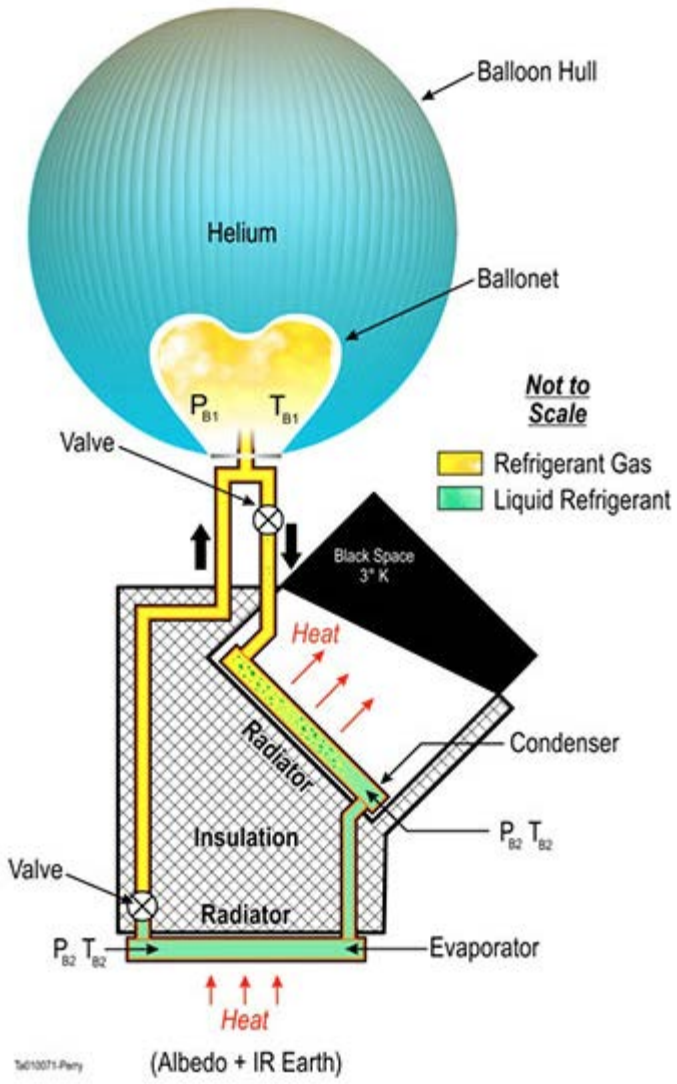

Figure 1: Schematic of CPSB concept

The SwRI-develped CPSB (Constant Pressure Stratospheric Balloon) concept uses a dual gas methodology to produce a balloon design that has the advantages of both zero pressure and super pressure balloons. This dual gas balloon system allows for extended constant altitude flights, since the need for expendable ballast is eliminated, while maintaining a very low differential hull pressure and keeping the hull volume constant. The sealed, low-pressure hull design is made of low-cost, ductile polyethylene film filled with helium or hydrogen. It has an internal ballonet that can be filled with a refrigerant like ammonia, butane, or propane. The refrigerant in the ballonet would be in a gas form, while reserve refrigerant would be stored in a liquid state. The balloon would be filled with just enough lifting gas to completely fill the hull at the maximum expected gas temperature at the target altitude. At night when the

lifting gas cools and contracts, refrigerant gas would be released into the ballonet to maintain the volume of the balloon. Since the mass and the volume are unchanged, the balloon system will not lose altitude during the night. In the morning when the lifting gas temperature starts to rise, the refrigerant gas is removed by condensing it to a liquid state. By using a combination of a condenser that radiates heat to "black space" and an evaporator that radiates to the "surface of the Earth," little or no electrical energy will be needed. The schematic in Figure1 illustrates the concept configured to use butane as the refrigerant gas, which can be condensed without additional compression.

SwRI has been awarded a patent on this novel technology, U.S. Patent No. 9,568,918, February 14, 2017, William D. Perry, inventor.

Patent Abstract: The present disclosure relates to a balloon system that includes a flexible volume balloon hull configured to contain a lifting gas, a flexible volume ballonet contained within said balloon hull configured to contain a refrigerant gas and a refrigerant gas transfer device in fluid communication with the ballonet to control the balloon's vertical ascent and descent.

Approach — Our approach involved the following tasks:

- Define the performance requirements for a CPSB.
- Develop a detailed thermal model of the proposed concept.
- Evaluate different refrigerant gases (ammonia, Freon, propane and etc.) and system configurations to determine which combination produces the optimum performance.

Based on the thermal analysis results, the team determined the size of the condenser and evaporator radiators needed for a configuration and refrigerant gas type for a prototype system, suitable for demonstrating the concept.

Accomplishments — During Phase 1 of this project, the team defined the CPSB performance requirements and specifications, created a thermal model of the proposed system, and evaluated a number of candidate refrigerant gases. Based on the results of this model, the size and mass of the required closed loop refrigerant assembly was determined. The team evaluated and selected refrigerants that could best achieve the required performance, while maximizing the mass available for the payload. Many refrigerants were eliminated during this evaluation, but ethane, propane, and butane all look feasible. In this investigation it was determined that a closed-loop refrigerant assembly using ethane will have the lowest mass, resulting in a greater percentage of the CPSB total mass being available for the user payload. The team looked at several different possible designs for implementing the concepts. While all of these implementations appear to be achievable, one was selected to be the basis for the preliminary CPSB design planned for the second phase of this project. Based on Phase 1 results, all of the GO/NO-GO criteria were met, and the team proceeded with Phase 2, Design of a CPSB Prototype.

The goal of Phase 2 was to develop a design for a CPSB prototype that can be used as a testbed to evaluate the performance of the concept. The challenge was to convert the results of the model into a design for a functional prototype that can be fabricated and tested using available technologies and at a reasonable cost. During Phase 2, a full-scale 3-D CAD model of the CPSB prototype was developed, as shown in Figure 2. While the actual fabrication and testing of the CPSB prototype is beyond the scope of this project, the team has completed a preliminary design that will be the basis for a future prototype. The results of this project have elevated the technology readiness level to TRL-4 and have given the team the information needed to propose a CPSB test flight project for funding from DOD, NASA, or an SwRI internal research project.

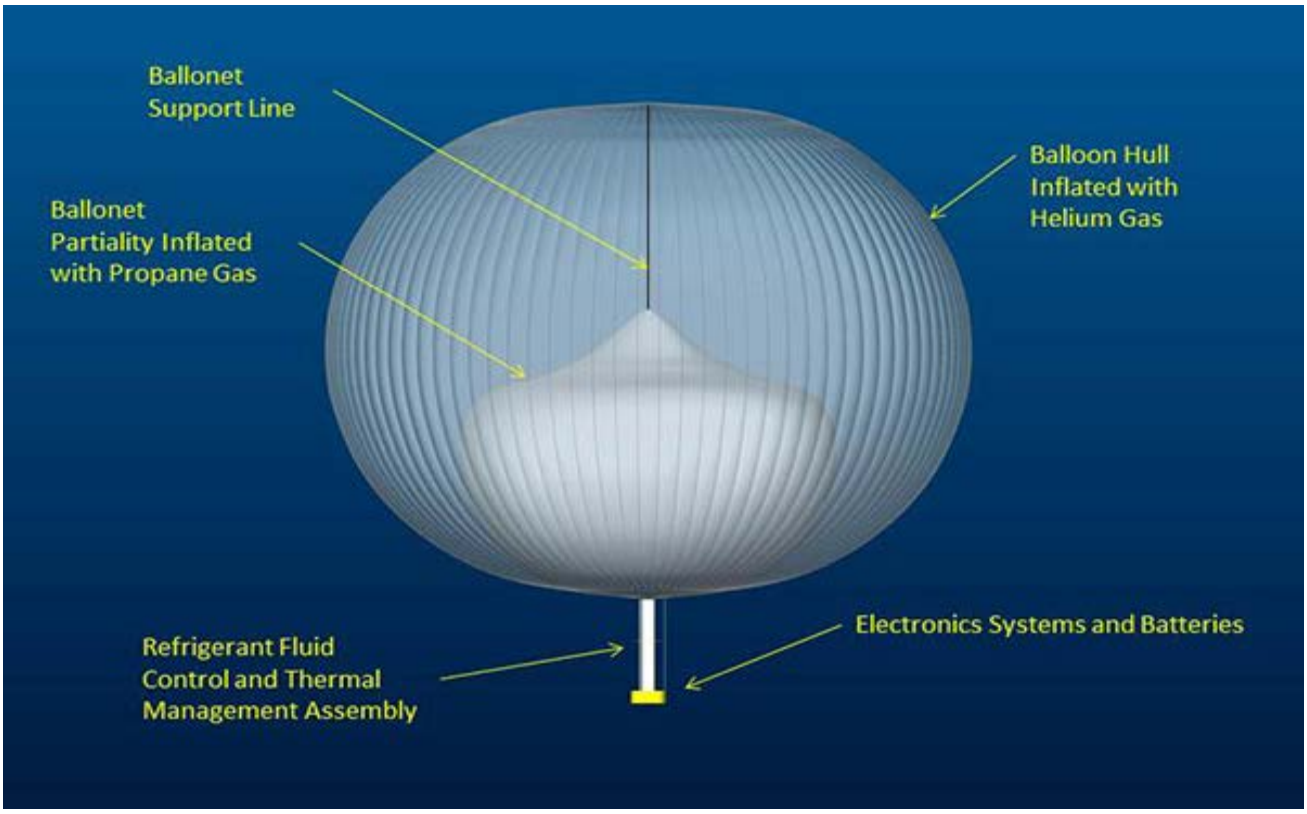

Figure 2: CPSB demonstrator design.

2017 IR&D | IR&D Home

SOUTHWEST RESEARCH INSTITUTE®

2017 IR&D Annual Report

Testing Graphene Foils in a Space Plasma Instrument, 15-R8674

Principal Investigators
Frédéric Allegrini
Robert Ebert
Greg Dirks
Stephen Fuselier
Roman Gomez
Tim Orr
Paul Wilson

Inclusive Dates: 07/01/16 – 12/31/17

Background — In this project, we will test graphene foils in a space plasma instrument to increase their technology readiness level (TRL). Foils, until now made of amorphous carbon, are used for coincidence and time-of-flight (TOF) measurements. The interaction of particles with the foil results in multiple processes, which either enable or negatively affect the measurement. For example, 1) the particle-induced secondary electron emission enables coincidence and time-of-flight measurements, and 2) the particle charge state modification enables detection and measurement of energetic neutral atoms (ENAs). However, 3) the angular scattering perturbs the particle trajectory and may result in particle loss in the detector, and 4) the energy straggling reduces the particle energy. Processes 3) and 4) scale with foil thickness, while 1) and 2) are at most marginally affected by it. Thus, using the thinnest practical foil is always a goal. Current state-of-the-art carbon foils are about 9-nm thick.

Recently, the emergence of graphene (single atomic layer of carbon, 0.345-nm thick) has opened the possibility to reduce the foil thickness and, thus, tremendously advance foil performance by reducing angular scattering and energy straggling. In fact, we showed in recent studies (partially funded by SwRI's IR&D Program and a NASA grant) that graphene foils outperform carbon foils in angular scattering by a factor of 2 to 3. Graphene foils could therefore replace carbon foils in future space plasma instruments.

Approach — We divided the project into three objectives:

- Perform environmental tests on graphene and carbon foils by themselves
- Compare the performance of graphene foils with carbon foils in an instrument with time-of-flight
- Perform environmental tests on graphene and carbon foils in an instrument.

Accomplishments — We are in the final steps of improving the transfer method of graphene to support grids. During transfer, the graphene is supported with a polymer that is subsequently removed. All steps involved in the transfer are challenging and can cause defects in the graphene foil. With the graphene we have successfully transferred, we have shown that coverage can be better than 96 percent while the angular scattering is a factor of 1.2 to 1.8 lower than for our thinnest carbon foils. We have established a baseline of the performance of a space plasma instrument that contains carbon foils, which will later be replaced with graphene foils. We also designed and manufactured the fixtures for testing the foils.

Experimental Investigation of the Organic Solar System, 15-R8756

Principal Investigators
Kelly Miller
Mark Libardoni
Ryan Blase
Madeline Colley
Chris Glein
Ed Patrick
Ben Teolis

Inclusive Dates: 04/01/17 – Current

Background — The goals of this project are twofold. First, we aim to develop a laboratory setup for hydrothermal experiments on geologic samples. Second, we will use that setup to characterize volatile production during thermal decomposition of complex, kerogen-like organics that may be abundant in the interiors of icy satellites and other solid bodies in the outer solar system. Many of these bodies including Europa, Titan, and Enceladus are hypothesized to have liquid oceans underneath their icy shells. Titan also has a thick atmosphere composed primarily of nitrogen and methane, and liquid seas of hydrocarbons. The volatile cycles of these bodies may include input via outgassing from their rocky cores; this idea is supported by evidence for hydrothermal vents on Enceladus' ocean floor, the presence of outgassed ^{40}Ar in Titan's atmosphere, and the importance of outgassing to terrestrial volatile cycles. Constraining what volatiles may be produced in the rocky cores of these bodies is therefore key to understanding their volatile cycles and their potential habitability. Our experiments will provide new insight into volatile chemistry in the interiors of these bodies, where radioactive decay and accretional and tidal heating may lead to decomposition of complex organics.

Approach — Our experimental setup includes a Ni alloy vessel with an inert coating that is rated to 1,000 psi at 850 C with a built-in thermocouple to monitor the vessel temperature. Gases evolved during heating experiments will be captured and measured via a combination of gas chromatography-thermal conductivity detector (TCD) and state-of-the-art gas chromatography-mass spectrometry (GC-MS). Our target sample is an organic-rich meteorite that has been characterized extensively in the literature. This meteorite preserves the chemistry of planetary building blocks, including the icy satellites. The complex material that comprises the majority of the meteorite organics is similar to organics observed in primitive outer solar system building blocks like comets, and the meteorite is therefore a good analog for the satellite interior material. We will heat aliquots of the sample to a range of temperature conditions relevant to satellite interiors, and then collect and characterize the product gases.

Accomplishments — Our laboratory setup is nearly completed, and we will begin conducting experiments in early 2018. The setup features a custom-made reaction vessel with dual outlets and a sample holder insert that reduces the volume to concentrate the product gases. Our new GC-MS has been set up and calibrated, and is ready for application.

SOUTHWEST RESEARCH INSTITUTE®

2017 IR&D Annual Report

The Investigation into High Altitude Lighter-Than-Air Mission Concept of Operations Scenarios as Defined by Persistence, Risk and Cost, 15-R8764

Principal Investigators
Ethan Chaffee
I. Steve Smith Jr.
James Noll

Inclusive Dates: 04/21/17 – 08/21/17

Background — The SwRI Lighter-Than-Air (LTA) team was presented with an opportunity to respond to a request for information regarding the design of a concept of operations (CONOPS) to locate a payload package over areas of interest and maintain a persistent presence for an extended period of time. A preferred method to achieve this stated goal is to use high altitude LTA vehicle platforms such as stratospheric balloons and airships. The capability of stratospheric balloons and airships to maintain a persistent presence over a specified target has long been a goal pursued by the LTA community. The SwRI LTA team is currently leading a number of programs related to this challenge, including the "ALTA" (Adaptable Lighter-Than-Air) program which is incorporating trajectory control of free balloons achieved through altitude excursions for a diverse range of military and civilian applications. Alternatively, SwRI has led the way in developing stratospheric airships for station keeping applications. With the Sounder project and its successor HiSentinel, SwRI has successfully flown six airships to altitude. These projects have led to increased interest in the use of airships at stratospheric altitudes for persistence missions.

The objective of this effort was to conduct an investigation into high altitude LTA mission CONOPS scenarios and to develop CONOPS and cost estimation capabilities to quickly assess the needs of the client. No CONOPS evaluation tool previously existed within SwRI to provide a cost/benefit analysis for mission operations. The model built upon past work involving airship and free balloon characterization along with atmospheric predictions to evaluate cost, risk, and persistence capabilities over a specified area to satisfy mission objectives. The work performed under this project allows SwRI to provide quantitative answers to client inquisitions as evidence for selecting LTA platforms to meet their stated mission requirements as compared to competing concepts.

Approach — Two separate phases of development constituted the efforts of this project. The first phase regarded the design of vehicles that meet client needs. The design of the vehicles is based upon the specified altitude range for operation, the total payload mass which will be carried onboard, and the vehicle performance specifications. The resulting analysis of each vehicle design included both the risk and cost for each type of system to be incorporated into the mission trade space. The second phase of model development looked to quantify the ability to achieve persistence. This model required incorporating global wind data at many varying altitudes and time periods to include the potential for many different operating arenas. The model also took into account the vehicle performance specifications for altitude variation capabilities and vectored thrust. The resulting data provides information as to how long a vehicle can stay within a given target region to obtain a more accurate calculation of the cost to meet the mission requirements. The diagram in Figure 1 represents the structure of the CONOPS evaluation tool. The resulting data is used to form a trade space matrix with regard to persistence, risk, and cost to demonstrate the reasoning for selecting a specified CONOPS scenario and to provide quantitative evidence to the client justifying that decision.

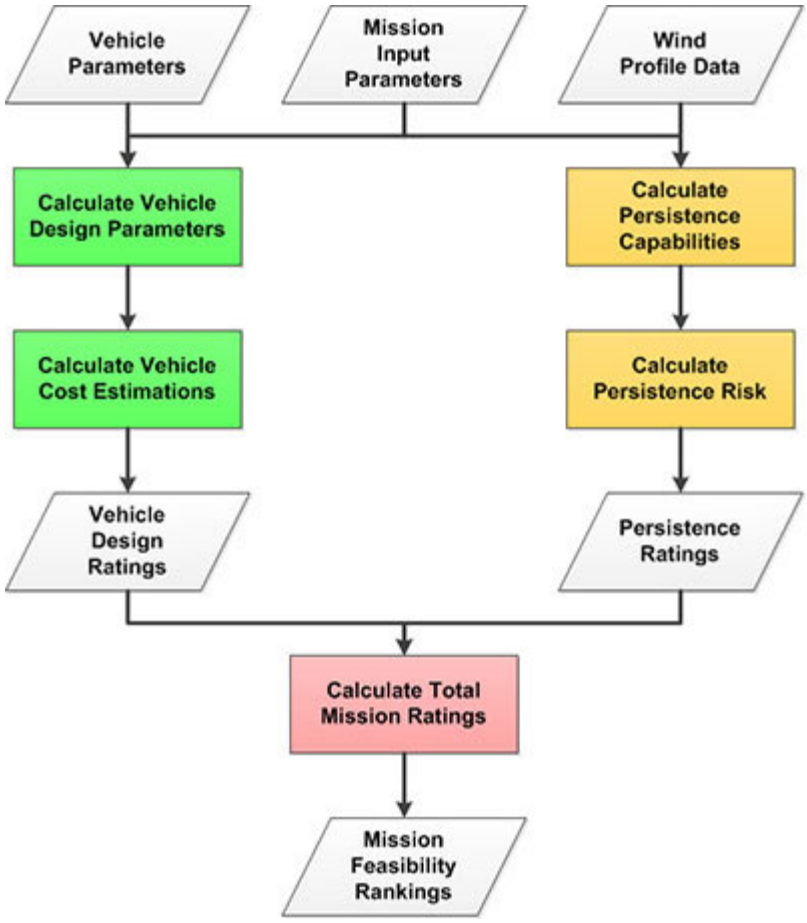

Figure 1: Model flow diagram for mission CONOPS evaluation tool.

Accomplishments — The purpose of this project was to identify and research the interdependencies of the many factors affecting an LTA-based mission CONOPS and attempt to quantify each factor's impact upon a mission. A quantification method to prioritize various LTA systems and mission elements was developed. Using this information, the team developed an integrated model composed of LTA system design capabilities, atmospheric circulation, trajectory modeling, costing, and reliability data. The integrated model generates a list of CONOPS scenarios addressing LTA systems, cost, and risk levels. This model has successfully allowed the SwRI LTA team to provide quicker responses to customer requests with quantitative results and higher consistency in evaluating CONOPS scenarios. As a result, better comparative analyses require significantly fewer man hours to develop a full CONOPS plan with increased confidence.

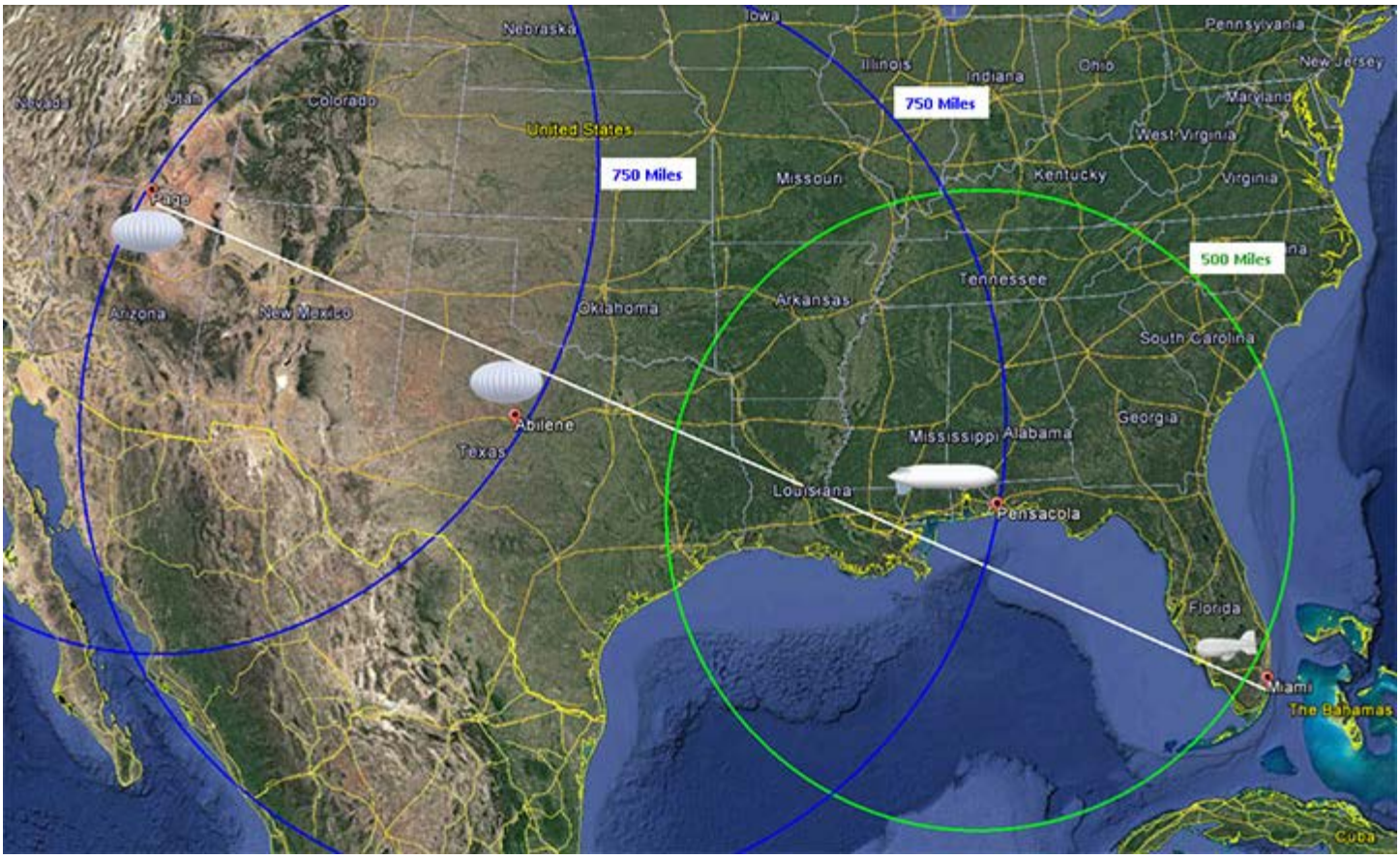

Figure 2: Example CONOPS map showing vehicle placement to create over-the-horizon comms link.

The resulting analysis showed that for missions that allow for a large target area of operations, a super pressure balloon with a ballonet capable of altitude control resulted in the most optimal CONOPS plan given all other requirements. This system is cheap enough to accommodate using multiple vehicles to maintain a persistent presence while being able to take advantage of the full wind profile of the altitude range desired. Missions that require a smaller target area of operations demand the use of an airship system for finer trajectory control. It is not necessary to include a ballonet in the design of these stratospheric airships if the wind profiles are variable enough to provide trajectory control with moderate propulsive capabilities. The exact point where the mission requirements switch to needing the use of an airship is situationally dependent and will require further analysis of more defined mission requirements.

SOUTHWEST RESEARCH INSTITUTE®

2017 IR&D Annual Report

Large-Scale Additive Manufacturing Using Concrete Composite Materials, 14-R8610

Principal Investigators
Cliff Scribner
Paul Hvass

Inclusive Dates: 12/01/15 – 06/01/17

Background — Large-scale additive manufacturing using concrete design mixes have gained popularity recently within small startup domains and with collaborations between the U.S., European and local as well as regional University ecosystems. Layer-by-layer construction methods are being explored using fixed-gantry as well as mobile-robot delivery methods. However, minimal information is available regarding the process limitations of the material, including generalized physical attributes of formed layer-by-layer structures.

Approach — For this project, we focused on three research elements:

- Mortar-based wet concrete composite rheological shear strength (real-time in kilopascals using a four-sided shear vane paddle) and process limitations of the material using a continuous additive layer-by-layer process (1.22 x 1.83 meter aerial gantry) for extrudability, workability, pot life, layer-by-layer buildability limitations, nozzle velocity and volume deposition flow rate. Design mixes were developed using water, sand, a polycarboxylate plasticizer, rheology mineral modifier, silica fume, and class-C fly ash.
- Evaluation of numerous chemical additive candidates to potentially accelerate set-time control to improve buildability of the concrete composite, including alkali chlorides, nitrates and nitrite salts, thiocynates, alkali carbonates, carboxylic acids and salts, alkanolamines, alkali metal aluminates, and shotcrete admixtures.
- Post-process physical strength measurement limitations of the formed structures via layer-by-layer interlocking with formed steel staple inserts.

Accomplishments — Using the same research elements above, we accomplished the following:

- Characterized the wet design mix with a preferable real-time shear strength of 0.75 ± 0.25 kilopascals for layer-by-layer deposition with an effective pot life of about 120 minutes. Some commercially available concrete mixes have distinctly different requirements to achieve similar rheological profile results based on water-to-cement ratios from 40 to 43 percent, respectively. We also achieved a 25-mm diameter nozzle linear slew rate of 50mm/sec., using a flow rate range of 1 to 2 liters per minute.
- Tested approximately two dozen set time accelerant chemical candidates. Calcium formate - $3Ca(HCO_2)_2$ demonstrated the best reduction from 300 down to approximately 50 minutes over a range of 2 to 5 weight percent per total dry mix content. However, this limits pot life of a standard concrete mixing/pumping process.
- The interlocking layer study results indicate that a 28-day cure of as-deposited layer-by-layer composite structures in simple shear perform about the same as continuously molded samples having similar dimensions. Steel staples seem to only have the effect of mitigating catastrophic structural failure. Compression results for design mixes tested achieved a favorable 28-day cure strength of about 27.6MPa (4,000 psi), depending on water content.

Figure 1: Example of 25mm wide x 17mm thick layer-by-layer serpentine pattern testing.

2017 IR&D | IR&D Home

SOUTHWEST RESEARCH INSTITUTE®

2017 IR&D Annual Report

Effect of Cyclic Relative Humidity on Environmentally Assisted Cracking, 18-R8554

Principal Investigators
James Dante
Todd Mintz
Erica Macha
James Feiger

Inclusive Dates: 04/01/15 – 04/03/17

Background — The annual cost of corrosion for U.S. Department of Defense aircraft systems is estimated to be over $10 billion. It is estimated that over 80 percent of structural cracks that have been detected initiate at corrosion sites, raising concerns that corrosion has a potentially high impact on structural integrity. In an attempt to compensate for these environmental effects, a margin of safety during design considerations is employed. These margins of safety are based on crack growth rate (CGR) data that has been collected under immersion conditions. Recent work, however, has shown that CGR can be as much as 10 times higher than values acquired in lab air under certain environmental conditions. Measurements of CGR under aggressive atmospheric conditions are required not only to understand the specific effects of environmental spectra on CGR but also to define how environmentally assisted cracking should be addressed in engineering design approaches for components and structures.

Approach — The goal of this work was to develop an initial framework to address atmospheric environmentally assisted cracking. The approach included developing an atmospheric test cell with controlled relative humidity (RH) and temperature constructed around a standard fatigue test system. Testing under controlled environmental conditions and dynamic loading conditions was used to demonstrate how atmospheric parameters directly affected CGR. Using well-established multi-electrode array techniques developed at SwRI, correlations between corrosion modes and changes in crack growth rate were established. Finally, existing environmental sensor data was analyzed in a manner analogous with structural usage spectra.

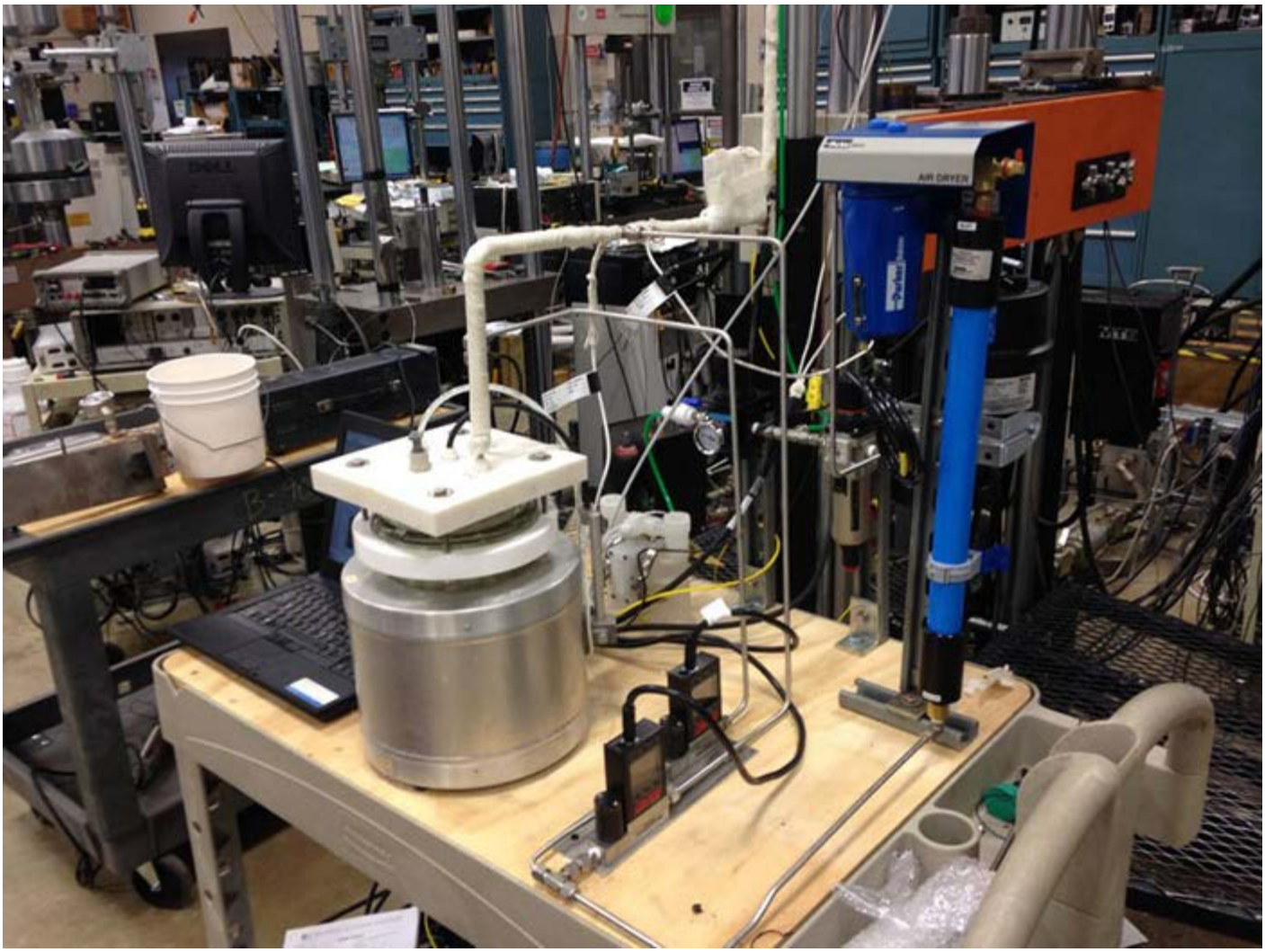

Figure 1: Test equipment to control temperature and relative humidity in test chamber.

Accomplishments — An environmental control system (Figure 1) was integrated around a CT fatigue sample. Testing using this apparatus reveals that RH does play a significant effect on cracking behavior of both 304L stainless steel and 7075-T6 aluminum. Fatigue crack growth rates were increased in high humidity environments. Specifically, the fatigue crack growth rate in 7075 aluminum increases about 30 percent when the RH increases from 20 percent to 90 percent (Figure 2). However, when the RH is decreased from 90 percent to roughly 70 percent, the crack growth rate increases almost 300 percent compared to the crack growth rate in dry air. Corrosion currents inside a simulated crevice are up to six times greater than the currents on the boldly exposed surface, and current inside the crevice increases with increasing RH. Corrosion continues inside the crevice even when the surrounding RH is dry due to capillary forces acting to keep the crevice wet.

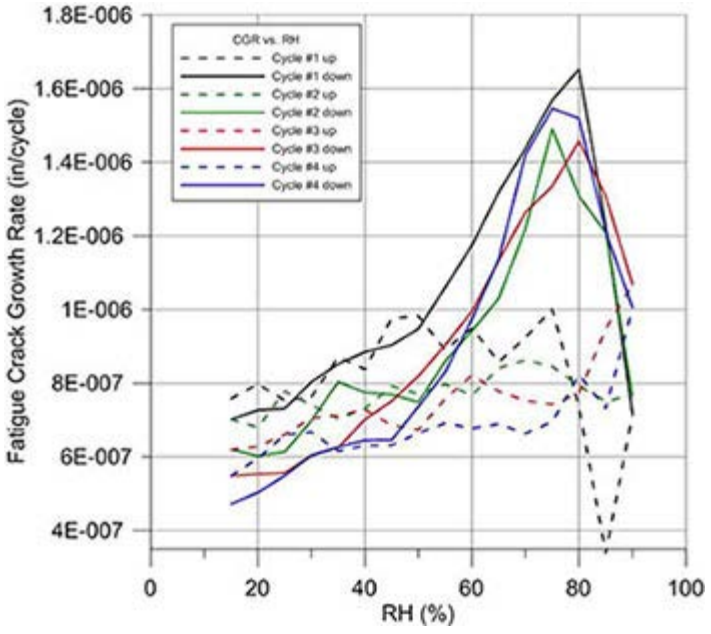

Figure 2: 7075-T651 fatigue crack growth rate as a function of relative humidity between 15 to 90 percent.

A program to quickly import and categorize
corrosion and humidity sensor readings was developed and is helpful to quickly determine the severity of an exposure location. In particular, because corrosion and cracking is strongly adversely affected by decreasing RH when RH is between 76 percent and 50 percent, rankings of time spent in this intermediate condition are important to determine the overall severity of a location.

SOUTHWEST RESEARCH INSTITUTE®

2017 IR&D Annual Report

Development of a New Numerical Model to Simulate Chemotaxis-driven Bacterial Transport for Treatment of Tumor Cells and Mitigation of Bacterially-mediated Pipeline Corrosion Problems, 18-R8602

Principal Investigators
Hakan Başağaoğlu
Alexander Carpenter
Spring Cabiness
Miriam Juckett

Inclusive Dates: 10/01/15 – 04/01/17

Background — The objective of this project was to develop a new, computationally efficient, multiscale numerical model to simulate the directional and tumble motions of self-propelled chemotactic particles (live bacteria, or bacterial or chemical robots) in spatially and temporarily varying chemoattractant (e.g., nutrients) gradients in geometrically complex domains by accommodating cells scale adaptation dynamics and signal processing, and particle-scale fluid-particle hydrodynamics. The project objectives also involved developing new modules to simulate non-Newtonian fluid flows, arbitrary-shape particles flows, and advective-diffusive-reactive transport of substrates to extend the model use for targeted applications in biomedical and oil and gas fields. Prior to this project, such a comprehensive numerical model with these capabilities did not exist. The project involved experimental tasks to study chemotactic motility of an E. coli bacterial strain, with the intention that the experimental data would produce good quality data for the validation of the proposed numerical model.

Approach — Major components of the new numerical model were developed based on the Lattice-Boltzmann (LB). An existing RapidCell (RC) model was coupled with our-in-house colloidal LB model to simulate chemotactic motility of chemotactic particles. The coupling involved a new set of equations we derived to calculate the position of receptor clusters on the chemotactic particle surfaces through which chemotactic particles would detect and orient toward the transient chemoattractant gradients. The coupling also involved calculations of forces and torques on chemotactic particles due to their run and tumble motions as part of their adaption dynamics The non-Newtonian flow module was developed by relating the local fluid viscosity to the second invariant of the rate-of-strain tensor. The arbitrary-shape particles flow module was developed through new geometrical relations to locate surface boundary nodes via the winding number algorithm of any arbitrary-shaped particles' surfaces along which the particle and the fluid exchange momentum. The advective-diffusive substrate transport module was formulated by relating the relaxation parameter to the molecular diffusion of the substrate through the Chapman Enskog expansion. We impended a series of optimization techniques, including optimizing array memory layouts, data structure simplification, random number generation outside the simulation thread(s), code parallelization via OpenMP, and intra- and inter-timestep task pipelining to enhance the computational performance of the new model. Microfluidic experiments were set up to generate data for model validation.

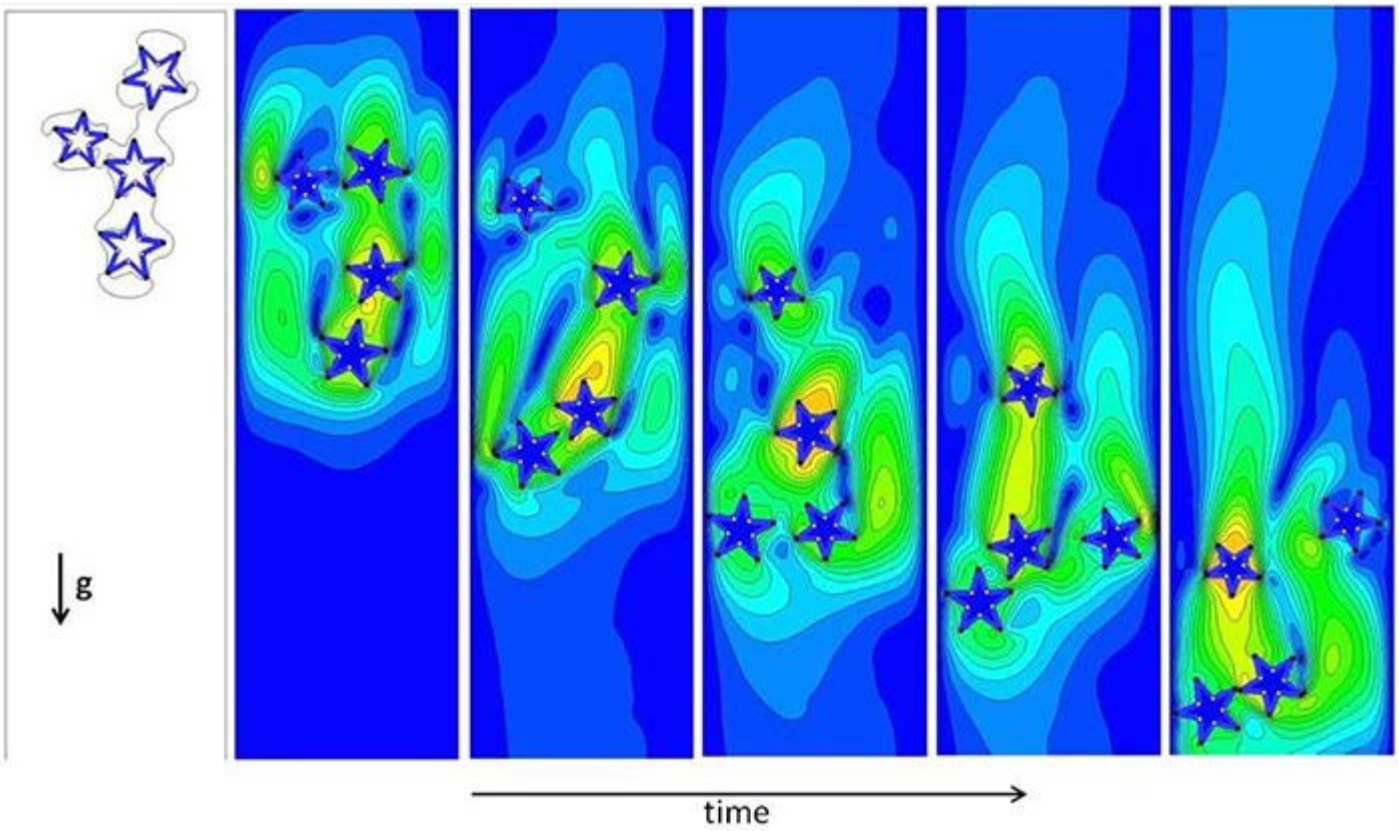

Figure 1: Gravity-driven settling of star-shaped particles of different sizes in an initially quiescent fluid in a bounded domain.

Accomplishments — We successfully developed a new multi-scale model to simulate motility of chemotactic particles in complex fluidic environments. We also successfully formulated new modules for non-Newtonian fluid flows (for pseduoplastic and dilatant fluid flows), advective-diffusive substrate transport, and arbitrary-shaped particles flows (e.g., snapshots from gravity-driven settling of four star-shaped particles in an initially quiescent fluid in a bounded domain) and validated these new modules with benchmark problems. Moreover, we successfully implemented optimization techniques to enhance the computational performance of the new model, which resulted in 15 to 40 times computational speed-ups. As for the experimental tasks, although we gained substantial experience in the design and performance of microfluidic experiments to study chemotactic particle motion, the experiments did not produce good quality data to validate the RC-CLB model.

2017 IR&D | IR&D Home

SOUTHWEST RESEARCH INSTITUTE®

2017 IR&D Annual Report

Hydrogen and Methane Gas-Phase Detonations, 18-R8614

Principal Investigators
Nicholas Mueschke
Alexandra Joyce

Inclusive Dates: 01/01/16 – 06/30/17

Background — The explosive combustion of hydrogen (H_2), methane (CH_4), and other gases results in a rapidly expanding volume of hot gaseous reaction products. Depending upon the conditions, the combusting gases may result in a detonation. The high-pressure shock waves created by detonations are hazardous and can cause serious injury or significant damage to surrounding structures. Better understanding such hazardous events and their mitigations are of significant concern to the chemical processing, aerospace, defense, nuclear, automotive, and marine industries. Current tools used to predict detonation overpressures may not provide accurate blast loads in situations involving enclosed gaseous releases, complex geometries, inhomogeneous mixtures, and large gas volumes. The goal of this work is to develop a state-of-the-art predictive capability for simulating the dynamics of gas phase detonations. One challenge in this work includes addressing the multiscale nature of the problem. The combustion zone and detonation wave are sub-millimeter in scale and move at supersonic speeds while the structural domain of interest can be on the scale of an entire building. Furthermore, within the small region where combustion occurs, complex chemical kinetics dictates the rate at which energy is released. Accurately capturing this energy release is critical to accurately modeling the propagation and strength of detonation waves.

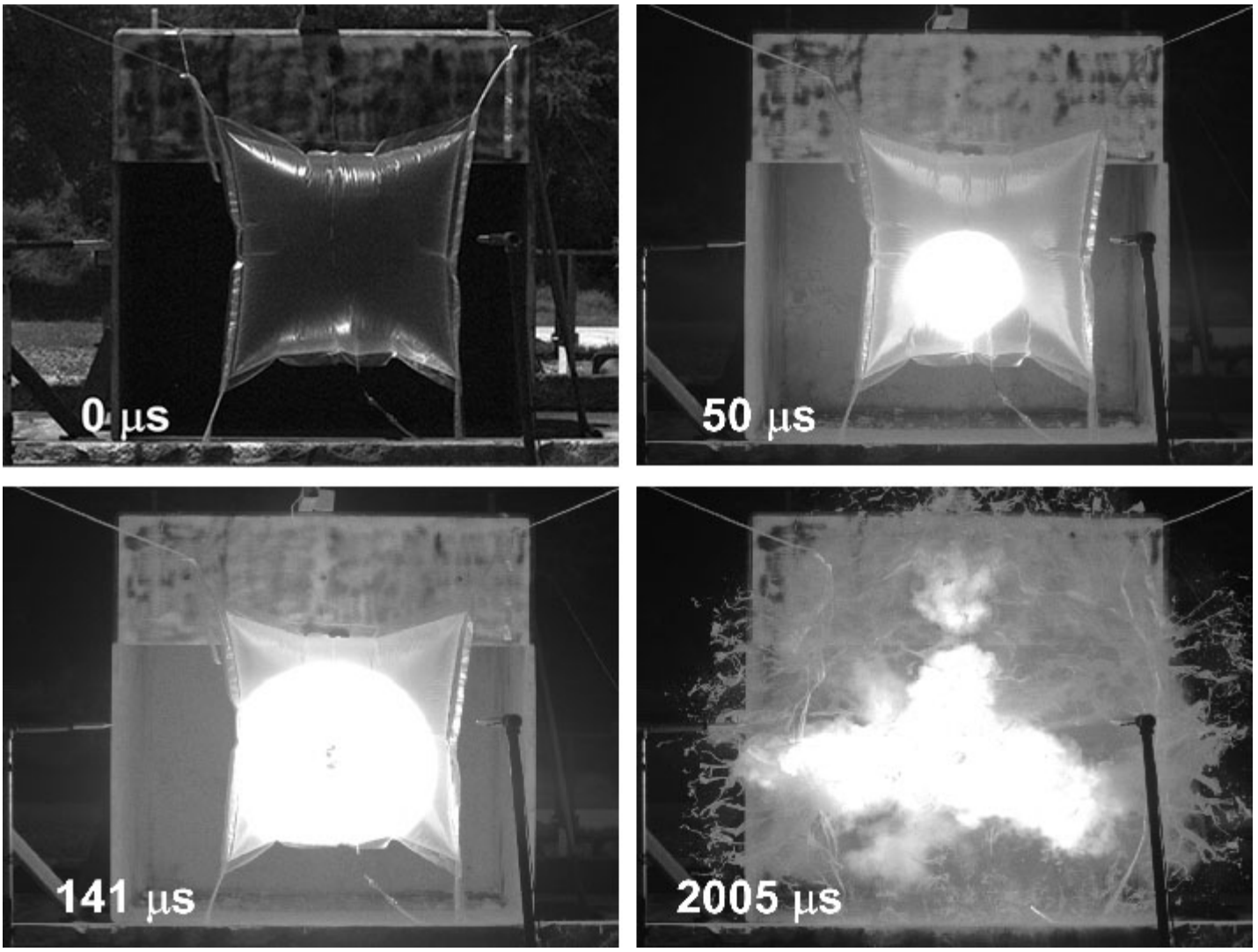

Figure 1: Detonation of methane-oxygen gas mixture. View video of detonation.

Approach — The primary objective of this work was to develop a new computational capability to simulate gas-phase detonations for real-world scenarios that involve large domains and complex gas mixtures. This was accomplished through a combined numerical and experimental approach. Different chemical reaction kinetics models and numerical integration strategies were evaluated to determine their predictive accuracy, computational efficiency, and numerical resolution requirements. In particular, both simplified global reaction kinetics and complex complete reaction kinetics schemes were evaluated. In addition, this work investigated methods that allow for detonation simulations to be performed more efficiently by using coarse computational meshes. These simulation approaches were tested by comparing numerical results with a new set of gas detonation experiments. Experiments were performed to measure the blast overpressures that happen when a detonation occurs in a partially confined structure. The overpressures exerted on the test fixture structure by the blast waves were measured using an array of high-resolution pressure transducers and directly compared with simulations.

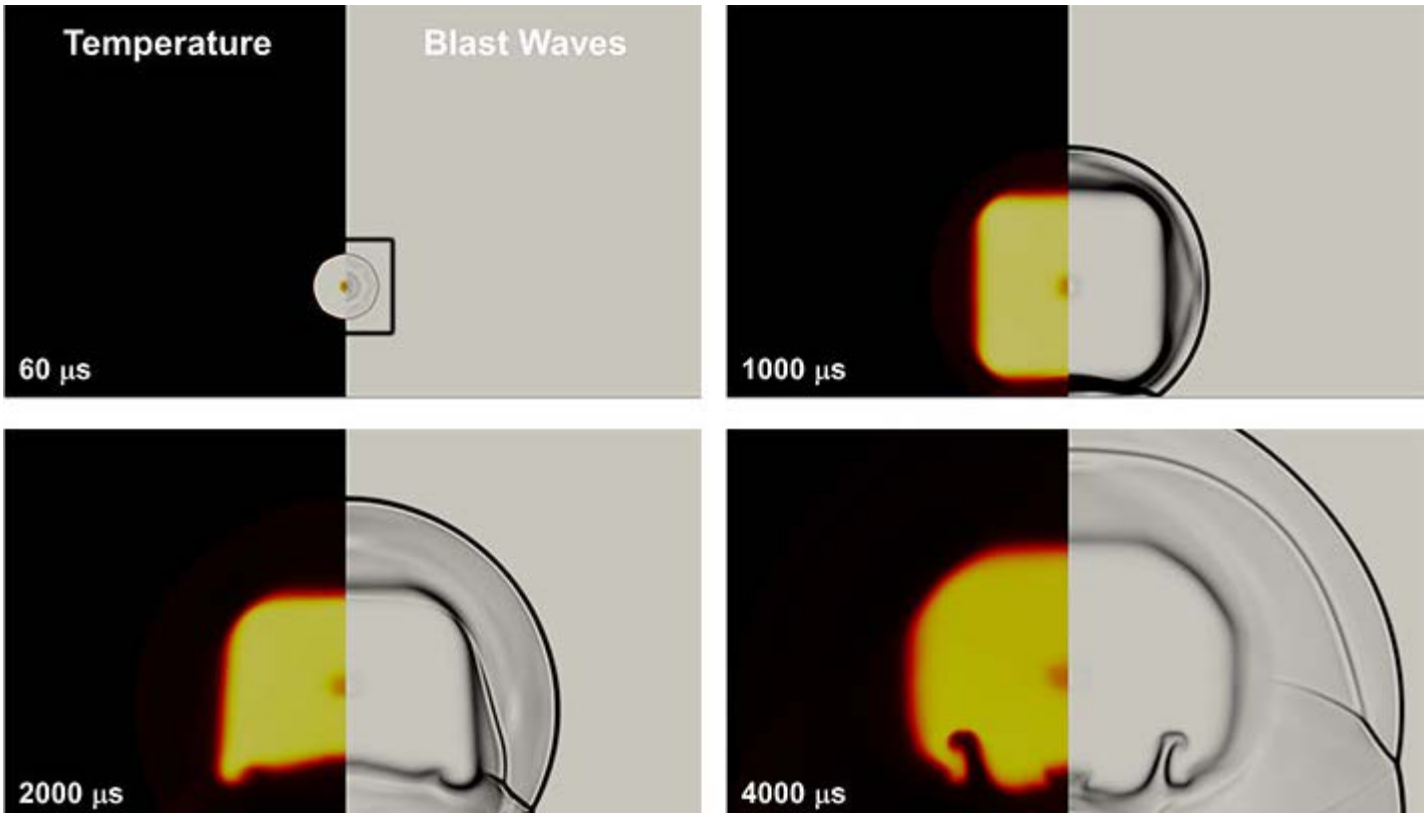

Figure 2: Simulation of hydrogen-oxygen detonation. View video of simulation.

Accomplishments — A novel set of gas detonation experiments has been completed. These tests measured the loads imparted on a structure containing hydrogen-air and methane-oxygen detonations. Figure 1 shows the results from one of these tests where a bag filled with a stoichiometric methane-oxygen mixture was detonated. The spherical expanding detonation wave was recorded using high speed videography at 22,000 frames per second. Additional tests measured blast loads for a range of gas mixture volumes, effects of interior wall placements, and fuel-air stratifications.

These experiments were used to validate a new simulation code developed to model gas detonation and blast events. Figure 2 shows a series of images from a simulated hydrogen-oxygen detonation. In this simulation, the detonation wave expands until all of the fuel-air mixture is consumed. The detonation wave then continues to migrate away from the ignition point as a supersonic blast wave. The simulation models developed as part of this work are capable of simulating both simplified chemical kinetics as well as complex, multi-step chemical reactions. A significant accomplishment of this work is developing and validating efficient modeling techniques that allow for detonations and blast loads on structures to be simulated while using a minimum amount of computing resources. This allows SwRI to examine a range of hazardous, large-scale gas explosion scenarios accurately and efficiently.

SOUTHWEST RESEARCH INSTITUTE®

2017 IR&D Annual Report

Development of Artificial Muscle Actuator for Physical Joint Simulator, 18-R8616

Principal Investigators
Travis Eliason
Andrew Moore

Inclusive Dates: 01/01/16 – 07/01/17

Background — While great advances have been made into understanding the biomechanical environment within human joints, large gaps in our knowledge of the basic mechanics still exist. These gaps are a direct result of limitations in our ability to experimentally characterize detailed internal joint mechanics during *in vivo* human motion. This lack of fundamental knowledge underlies a multitude of basic and applied research areas in musculoskeletal biomechanics. For example, a comprehensive understanding of internal human joint mechanics is critical to deciphering the underlying mechanisms leading to the onset and progression of osteoarthritis, determining the optimal course of treatment for repairing torn ligaments, developing artificial ligaments that restore normal joint function, designing joint braces, developing optimal rehabilitation strategies, developing better prosthetics, improving treatment strategies for muscle injury, etc. Studying the mechanics of joints presents a series of technical challenges that severely limits the type of experiments that can be performed and the data that can be collected. First and foremost is the challenge of experimentally collecting data from inside the joint while replicating natural boundary conditions and realistic muscle forces. Muscle forces are a significant driver of the mechanics within a joint, and current joint simulators are unable to replicate the complex multicomponent force generation of natural muscle.

Approach — The objective of this project was to develop and characterize a biomimetic artificial muscle utilizing thermally actuated polymer artificial muscle (TPAM) fibers. In pursuit of this objective a methodology for consistently and accurately producing the individual TPAM fibers was developed. These TPAM fibers were then tested in different mechanical conditions (various loads, strains, activation currents, etc.) to determine their performance, repeatability, and limitations. Next, control strategies were developed to allow for the scalable, coordinated control of multiple TPAM fibers working together. These strategies were inspired by the methodologies that natural muscles use to coordinate the activation of their individual muscle fibers, allowing groups of actuators to accomplish tasks that they could not do alone. Lastly, this control strategy was incrementally scaled up to a system of 100 individual TPAM fibers working together to lift 32.5 lbs. This corresponds to the amount of force the bicep has to exert to perform a curl exercise with a 5-lb weight.

Accomplishments — A semi-automated methodology for TPAM fiber production was developed and used to produce all the TPAMs used over the course of the project. During the characterization of the individual actuators several significant limitations of TPAMs were discovered. Most significant of these limitations is the variability in the supply of conductive nylon sewing thread used as raw material in the production of TPAMs. Using material from different supply lots produced performance variations that far exceeded the inherent variation that was characterized between fibers with material from the same lot. Despite the limitations that were discovered, we were able to successfully create and control systems of individual TPAM actuators whose capabilities far exceeded that of the individual components. We were able to successfully control 100 individual TPAM actuators working together to lift 32.5 lbs, compared to an individual TPAM actuator, which can lift approximately 1/3 lb. Even with the limitations that were

discovered over the course of this project, TPAMs have the potential to have a major impact on biomechanics research. With the knowledge gained we believe that we can take this technology combined with our other work in 3-D printing of biomimetic human surrogates and make functional artificial muscles relevant for biomechanics research.

SOUTHWEST RESEARCH INSTITUTE®

2017 IR&D Annual Report

A Fundamental Assessment of K_{ISSC} and J_R Tearing Resistance Curves in Sour Brine Environments, 18-R8618

Principal Investigators
Baotong Lu
Carl F. Popelar
W. Fassett Hickey
Guadalupe B. Robledo

Inclusive Dates: 01/01/16 – 06/30/17

Background — Sulfide stress cracking (SSC) and reduced fracture toughness in sour brine (SB) environments are potential threats to safety of offshore structures in oil/gas production. These threats are not yet properly considered in offshore structure design. The SSC threshold, K_{ISSC}, is the parameter currently used to assess potential occurrence of SSC in pipes under operational loading. However, K_{ISSC} measured as per the NACE standard is not a material property in the test environment, increasing with $K_{Applied}$ (K initially applied on the wedge-loaded specimen). The fracture toughness in SB ($J_{c,SB}$) is the key parameter to ensure the failure will not occur in sour service pipe under the extreme loading conditions. The method to measure Jc,SB is not yet standardized. This project is a response to the requests from the oil industry on the concerns outlined above.

Approach — Based on experimental investigations and fundamental understandings of the cracking mechanism achieved in our preceding research, the objectives of this project were to develop (1) a method to determine K_{ISSC} as a material property in a test environment based on the fundamental understanding of the SSC mechanism, (2) a theoretical framework to quantify the environmental dependence of SSC, and (3) a theoretical framework to quantify the environmental dependence of fracture toughness based on a theoretical model of crack-tip strain rate (CTSR).

Accomplishments — The main

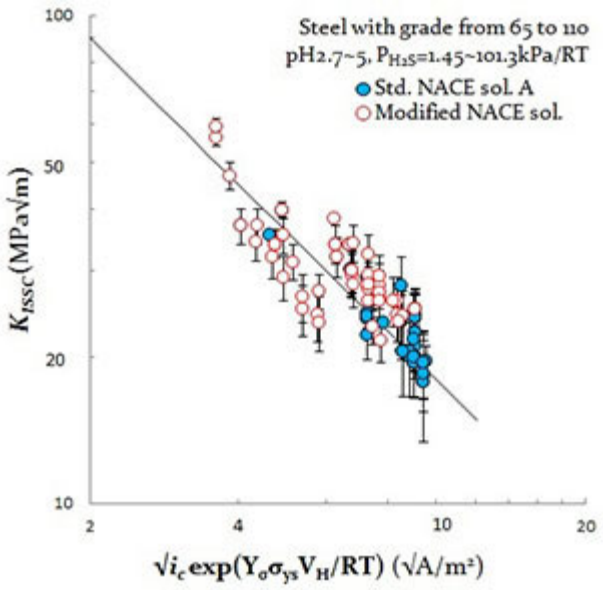

Figure 1. Correlation between K_{ISSC} and $C_{FPZ}\left\{\propto \sqrt{i_c}\exp\left(\frac{Y_\sigma\sigma_{ys}V_H}{RT}\right)\right\}$: i_c –corrosion current density; Y_σ –crack-tip constraint factor; σ_{ys} –yield strength; V_H –partial molar volume of hydrogen in steel; R – gas constant; T – temperature

accomplishments of this project are as follows.

- The experimental results revealed that the changing of solution chemistry during testing would be the mechanism for the $K_{Applied}$-dependence of apparent K_{ISSC} as measured per NACE standard. Based on this understanding, a simple method was proposed to determine K_{ISSC} in the test environment.
- A theoretical framework was established to assess potential risk due to SSC during pipe operation based on the quantitative SSC models developed in this effort, which formulated K_{ISSC} as a function of C_{FPZ}, the hydrogen concentration in the fracture process zone (FPZ) ahead of the crack tip (Figure 1); and the plateau crack propagation rate as a function of product of C_{FPZ} and the hydrogen flux into the FPZ (Figure 2).
- A theoretical model for the CTSR of growing crack was developed.
- Based on the CTSR model, a theoretical framework was developed for the model characterizing the loading-rate dependence of fracture toughness in SB (Figure 3).
- According to the fundamental understandings of the SSC mechanism of line pipe steel, a theoretical model was developed to formulate the knockdown factor (KDF) of fracture toughness as a function of C_{FPZ} that was proportional to hydrogen permeability for a given material in the testing environment (Figure 4). The KDF was defined as the ratio of the lower bound fracture toughness in SB and fracture toughness in air (Figure 3).

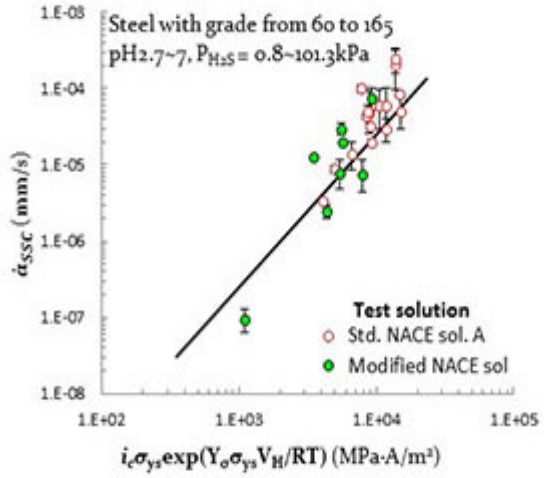

Figure 2. Correlation between $\dot{a}_{SSC}$ and $\dot{Q}_H C_{FPZ}$ $\left\{\propto i_c\sigma_{ys}\exp\left(\frac{Y_o\sigma_{ys}V_H}{RT}\right)\right\}$

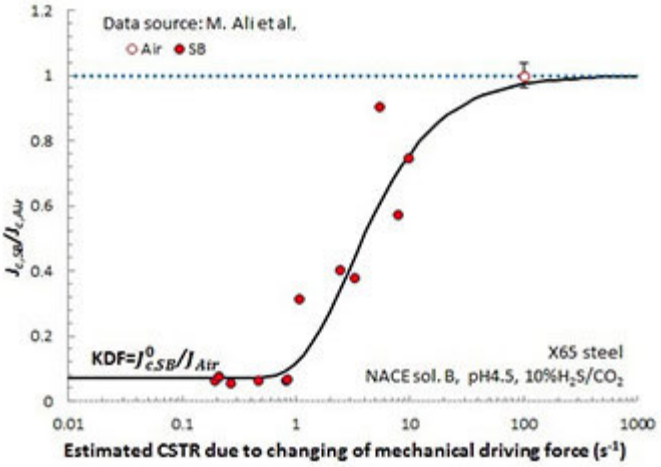

Figure 3. Comparison of model prediction with measured fracture toughness of X65 steel exposed to SB under different loading rates

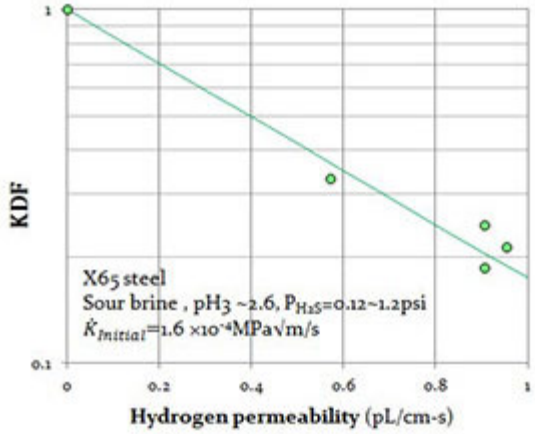

Figure 4. Comparison of model prediction with the KDF determined from the lower bound fracture toughness of X65 steel exposed to SB

Based on fundamental understandings realized in this project, technical proposals for two joint industry programs have been written as responses to the

requests from the oil companies. These will be submitted to the oil industry before the end of 2017.

2017 IR&D | IR&D Home

SOUTHWEST RESEARCH INSTITUTE®

2017 IR&D Annual Report

Impact of Carbon Fiber-Reinforced Composites, 18-R8619

Principal Investigators
Sidney Chocron
Alexander J. Carpenter
Rory Bigger
Nikki L. Scott
Adam Cobb

Inclusive Dates: 01/01/17 – Current

Background — Carbon fiber-reinforced plastics (CFRP) have become very popular as an aerospace material due to their high strength and stiffness combined with a very low weight. The behavior of CFRPs under ballistic impacts and blasts is still not well understood. No computer code can provide reliable predictions on deflection, delamination, or failure of these materials. The goal of this research project is to obtain experimental data to better understand the dynamic response and damage mechanics of carbon fiber-reinforced composites due to high velocity impact, and to use the experimental data to develop a meso-scale model for high-fidelity predictions of the dynamic response of the carbon-fiber reinforced composite materials under impact and blast.

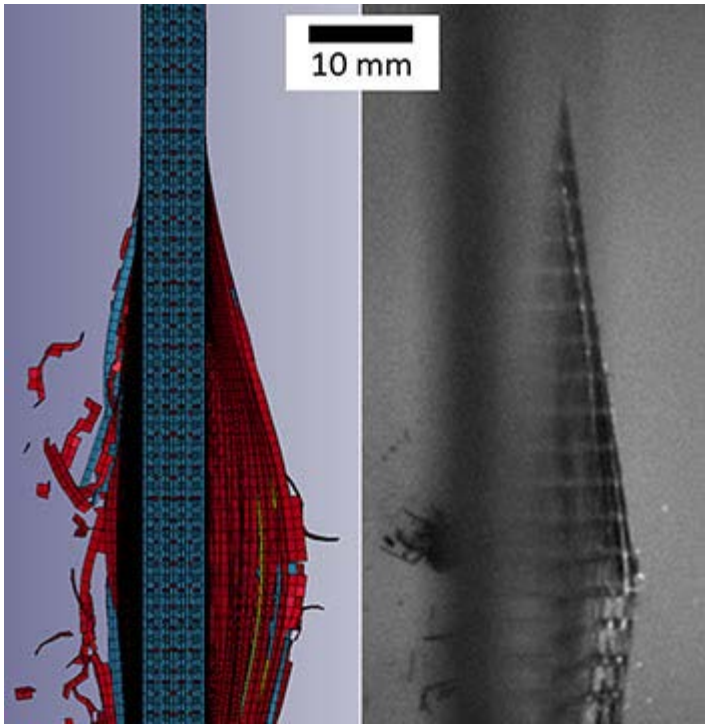

Figure 1: The (a) simulated and (b) actual ballistic pyramids formed 70 μs after impact of the 0.25-inch-thick CRFP with a 0.30-cal FSP at 350 m/s are compared.

Approach — An extensive experimental program was conducted. Material and ballistic tests were performed. The materials of interest in this research were unidirectional and 3D-weave CFRP panels provided by Albany Engineered Composites, a partner for the project. The material tests included tension, compression, torsion, and delamination tests at low and high strain rates of coupons machined from panels and standalone resin specimens. Ballistic tests were performed with the 0.30 cal fragment simulating projectile. Some of the ballistic panels were inspected using X-ray computer tomography. The material data was used to build a mesoscale computer model of the unidirectional and 3-D CFRP.

Accomplishments — Figure 1 compares a computer simulation with the image taken from ultra-high-speed cameras. The computer simulations for the unidirectional composite are accurately predicting the ballistic limit (minimum velocity for perforation of the panel). The computations also provide good deflection histories when compared to the ones measured experimentally.

SOUTHWEST RESEARCH INSTITUTE®

2017 IR&D Annual Report

Statistical Shape Modeling of the Temporomandibular Joint, 18-R8684

Principal Investigators
Dan Nicolella
Jessica Coogan

Inclusive Dates: 07/13/16 – 11/13/16

Background — Disorders of the temporomandibular joint (TMJ) are widespread, afflicting between 5 and 40 percent of the adult population. TMJ disorder (TMJD) encompasses several conditions including orofacial pain, restricted mandibular movement, clicking and popping sounds from the jaw joint, and locked jaws. About 10 to 15 percent of TMJD patients have osteoarthritis, characterized by a degenerative joint which results from erosion of articular cartilage and degeneration of subchondral cortical and trabecular bone. Symptoms can become chronic and difficult to manage, severely reducing quality of life. However, the exact etiology for TMJD has not been fully understood. While TMJD is reported in virtually all populations and age groups, many studies have consistently indicated that TMJD is more prevalent for women than men. While the etiology of TMJD is clearly multifactorial, it is widely believed that local joint tissue level biomechanics resulting from daily functional mastication or other jaw motion plays a major role in the development and progression of TMJD. Several studies have investigated the correlation of TMJ anatomy with TMJD, revealing associations between TMJD and occlusal curvature, dental occlusion, and articular eminence inclination. However, significant controversy exists over these relationships, since other studies did not find correlations between anatomy and TMJD. We hypothesize that differences in TMJ anatomy between males and females could result in different biomechanics that leads to a higher prevalence of the disease in females. Furthermore, while individual anatomical measures may not show correlations with TMJD or sex, combinations of anatomical traits represented using a statistical shape and trait model (SSTM) may show correlations. Thus, the objective of this study was to elucidate sex differences in the anatomy of human temporomandibular joint mandibular condyles using an SSTM.

Approach — Mandibles were obtained from 16 human cadavers (9 males, 7 females, 79±13 years). The condyles were dissected at the point of the sigmoid notch concavity and scanned using micro-computed tomography with 27 micron resolution. An image processing algorithm was used to segment the bone and determine the border of the entire mandibular condyle and trabecular bone compartments. Triangulated meshes of the compartments were created. One subject was chosen as the template and was registered to the other individuals using a coherence point drift algorithm. This process positioned all vertices at corresponding anatomic locations. For the trabecular bone region, around each vertex position, the average bone image intensity, which is proportional to bone density, and microstructural traits, including trabecular bone volume fraction, thickness, separation, connectivity, and connectivity density were calculated. For the entire mandibular condyle mesh, the surface vertices were extracted to represent the overall anatomy of the condyle. Using an SSTM, the shape and trait information was reduced to a small set of independent and uncorrelated variables for each individual. Wilcoxon rank sum tests were used to test for differences in the variables between sexes. A lasso approach was used to determine a set of variables that differentiate between sexes.

Accomplishments — Male condyles were on average larger than female condyles, with complex differences in the microstructural traits. Two out of 15 principal components were statistically different between males and females ($p<0.1$). The lasso approach determined a set of seven principal components that fully described the complex shape and trait differences between males and females. An SSTM was able to determine sex-dependent differences in the shape of the mandibular condyle. These differences

may alter the biomechanics of the joint and contribute to developing temporomandibular joint disease.

SOUTHWEST RESEARCH INSTITUTE®

2017 IR&D Annual Report

3-D Printed Human Surrogates for Injury RDT&E, 18-R8692

Principal Investigators
Dan Nicolella
Travis Eliason
Art Nicholls

Inclusive Dates: 08/30/16 – 02/17/17

Background — Musculoskeletal injury is a significant problem in the U.S. Military and civilian populations. As such, there is a critical need to develop methods and systems to accurately assess the risk of injury during military operational activities, vehicular accidents, and other potentially injurious environments in order to develop countermeasures and systems to mitigate this risk. However, advances in developing injury countermeasures have been severely restricted by the limitations of available tools to determine the biomedical basis of human injury. Current methods of investigating musculoskeletal injuries include *in vivo* (both human and animal), cadaver, and surrogate testing (anthropomorphic test device (ATD)), as well as computational modeling. Each of these approaches has limitations that limit its applicability to developing injury criteria and injury countermeasures, personal protection equipment (PPE), and safety systems.

Human *in vivo* investigations are limited by the inability to investigate injurious loading conditions and to directly measure tissue responses to loading. Cadaver testing is limited by the availability of cadavers representing target populations, the large number of specimens and significant costs required to obtain statistically significant results, and the extensive safety protocols and methods required when handling and testing human tissue. Human surrogates (ATDs) do not faithfully represent human anatomy or injury, only represent a limited slice of the population (e.g., 50th percentile male, 5th percentile female), cannot be used to investigate population variability, are only valid when subjected to specific loading conditions (e.g., frontal accelerations), and only measure gross responses that then must be correlated to expected human tissue injuries. Finally, computational modeling requires extensive model verification and validation along with significant training and expertise for users to obtain reliable and credible results.

Approach — The objective of this project was to investigate the use of 3-D printing to develop a highly biofidelic, low-cost, biomechanically verified and validated, physical surrogate of the human cervical spine for human injury and injury countermeasure research, development, testing, and evaluation (RDT&E). To achieve this overall goal, an existing benchtop 3-D-fused deposition modeling printer was used to construct soft tissue surrogates that represent the major soft tissue components of the human cervical spine: anterior longitudinal ligament, posterior longitudinal ligament, ligamentum flavum, interspinous ligament, joint capsule, and the intervertebral disc. The project team developed custom printable architectures and material composites that resulted in "3-D printable" surrogate materials that closely mimic the biomechanical behavior of the target human soft biological tissues. Using techniques derived from our experience in hierarchical, probabilistic computational model development, verification, and validation, procedures were applied to evaluate the biomechanical behavior of the surrogate system in comparison to human biomechanical data.

Accomplishments — In Phase I, the resulting 3-D printable surrogate materials closely matched the target cervical spine soft biological tissue material elastic modulus. All developed surrogate materials matched their target human soft tissue elastic modulus to within 10 percent with a minimum 90 percent probability. Phase II focused on developing 3-D printed cervical spine motion segments (two vertebra and all associated soft tissues) that are both anatomically and biomechanically biofidelic. While the tension-

compression behavior of the vertebral body-intervertebral disc-vertebral body construct closely matched the behavior of cadaver specimens reported in the literature, when tested in flexion-extension bending, the 3-D printed surrogate motion segments were significantly stiffer than equivalent cadaver specimens. This behavior was a result of the printed surrogate ligaments exhibiting compressive behavior significantly stiffer than natural ligaments. In conclusion, we have shown that it is feasible to custom design printable architectures and material composites using a "metamaterial" approach that resulted in "3-D printable" surrogate materials that closely mimic the biomechanical behavior of the target human soft biological tissues.

SOUTHWEST RESEARCH INSTITUTE®

2017 IR&D Annual Report

Analysis of Corrosion Damage on Samples Exposed to Accelerated and Outdoor Corrosion Environments, 18-R8745

Principal Investigators
James Dante
Marta Zuflacht

Inclusive Dates: 02/21/17 – 06/21/17

Background — Accelerated corrosion tests are widely used by industry and the U.S. Department of Defense to determine the environmental performance of materials and coatings. Currently used continuous and cyclic accelerated corrosion tests have very poor correlation to outdoor exposures, or the correlations are only valid for very specific sets of performance metrics and generalizations often cannot be made. The existing accelerated tests show especially poor correlation with the performance ranking of different chromate-free coating systems. Recently, SwRI completed a seven-year effort with the goal of developing a new accelerated corrosion test that predicts the corrosion behavior of a variety of materials in operational environments (Strategic Environmental Research and Development Program WP-1673). This effort investigated the relationship between environmental variables and corrosion failure modes of various material systems in detail. The SERDP program provided us with an understanding of how relative humidity (RH) and, more importantly, RH cycling changes the mode and severity of corrosion under atmospheric conditions. It is therefore hypothesized that the corrosion mode and severity observed in the field can be replicated under accelerated laboratory conditions by fine-tuning the RH cycle of the exposure test.

Approach — The objective of this effort was to quantitatively analyze the corrosion morphology of a suite of AA7075-T6 test specimens after accelerated testing and three years of outdoor exposures to gain a better understanding of the effect of relative humidity cycling on the mode and degree of corrosion. Additionally, the corrosion morphology of specimens exposed to the newer iteration of the new accelerated corrosion test was quantitatively compared to that of the outdoor specimens to help us prove the utility of the new accelerated test. Sample analysis was performed using techniques developed by SwRI to quantify area of attack, depth of attack, and volume of attack.

Accomplishments — Analysis of the mass loss specimens revealed that intergranular corrosion (IGC) occurred along the fastener hole of the AA7075-T6 alloy (Figure 1). The severity of the IGC was greatly dependent upon the type of primer used to coat the substrate surfaces. Water-borne primer was found to be more susceptible to IGC compared to solvent-borne primer due its greater sensitivity to moisture.

The test specimens exposed outdoors at coastal sites for three years showed very extensive damage, especially in the case of the chromate-free primers. IGC was found along the fastener holes. The quantitative analysis method developed in this work indicated that the IGC fissures in the case of the hexavalent chrome primers were fewer in number compared with the chromate-free primers (Figure 2). The fissures found in the case of the chromate-free coatings were predominantly longer than those for the chromate-coated samples (Figure 2). These results suggest that the hexavalent chrome provided the most protection against corrosion of the primers investigated.

Overall, this project resulted in a better understanding of the relationship between environmental parameters and galvanic corrosion of aluminum alloys. More importantly, in this effort, a new quantitative analysis method was developed to evaluate the degree of intergranular corrosion using cross-sectional micrograph images.

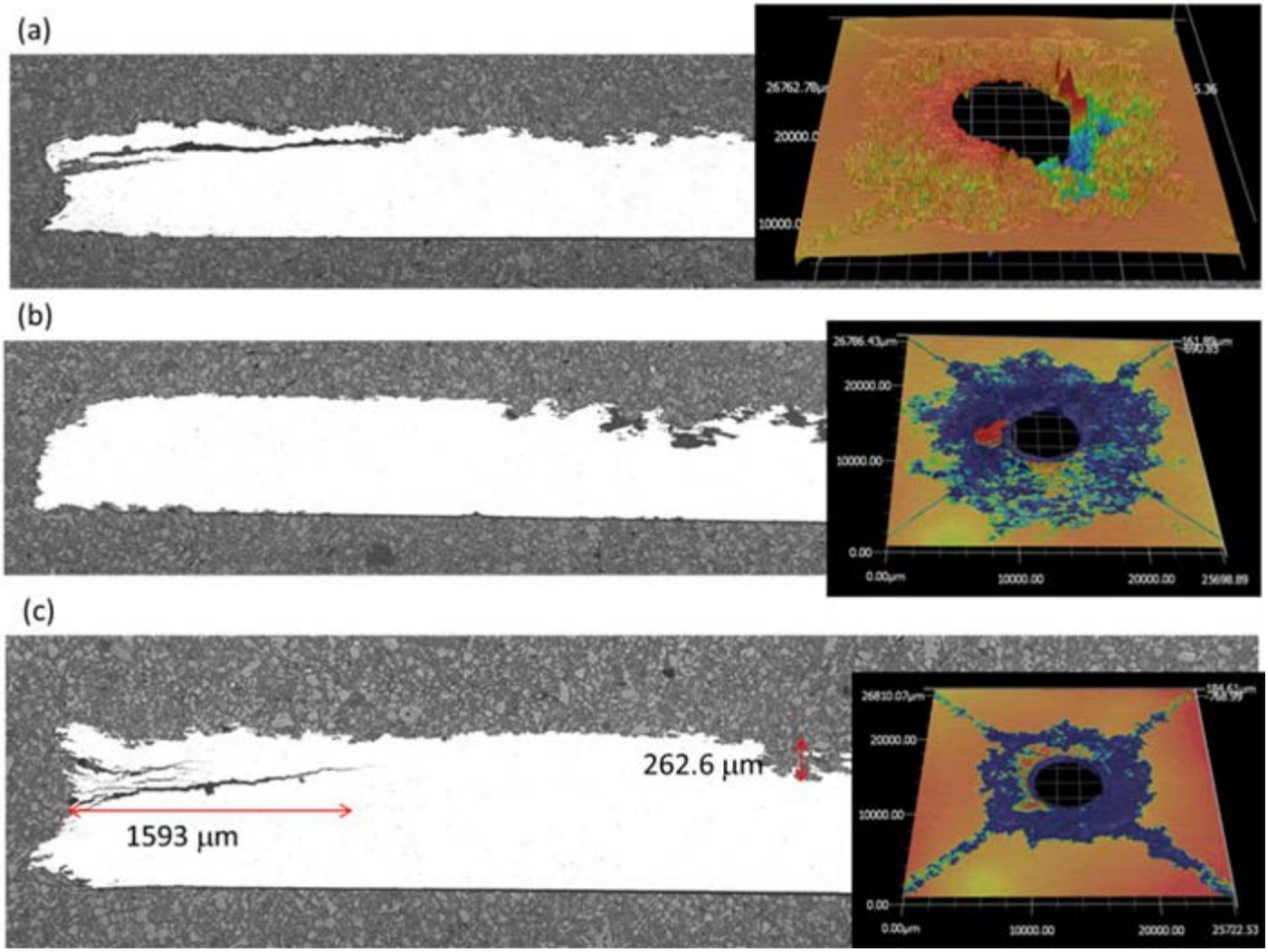

Figure 1: Cross-sectional and 3D surface images of samples coated with solvent-borne chromate-free primer after 1,320 hours exposure in an environmental chamber using different RH cycles.

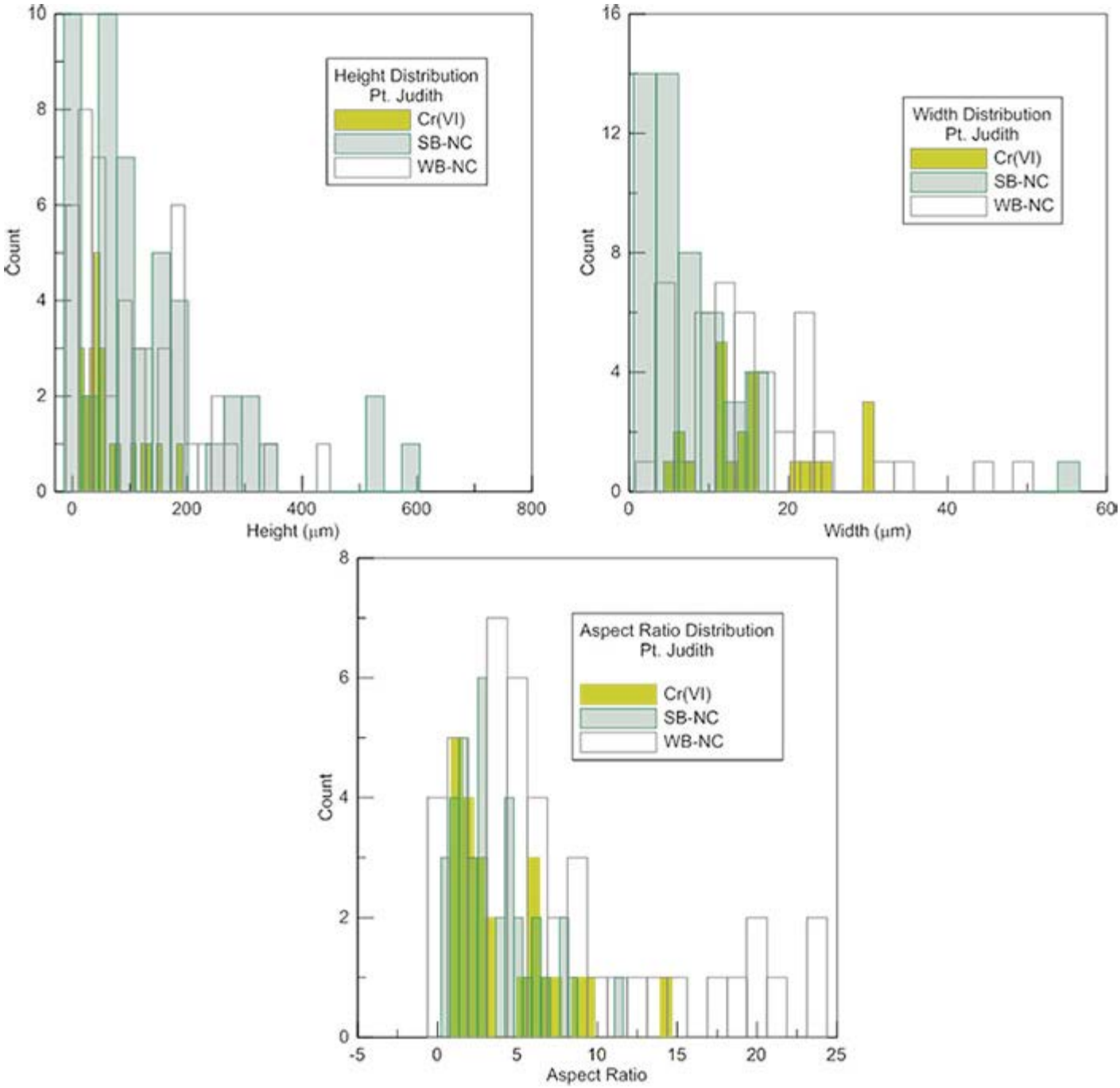

Figure 2: Quantitative analysis results of the IGC fissure analysis of AA7075-T6 panels exposed at Point Judith, R.I., for three years. The panels were coated with hexavalent chrome (yellow bars); solvent-borne, chromate-free (green bars) primer; and water-borne, chromate-free (white bars) primer.

2017 IR&D | IR&D Home

SOUTHWEST RESEARCH INSTITUTE®

2017 IR&D Annual Report

Additive Manufacturing and the 3rd Sandia Fracture Challenge, 18-R8747

Principal Investigators
James C. Sobotka
John M. McFarland
Robert Duran
Jeremy Stein

Inclusive Dates: 02/22/17 – 10/13/17

Background — Additive manufacturing enables the rapid production of new and replacement components by joining successive layers of material to build 3D geometries. However, many questions regarding performance remain unanswered from this class of materials with markedly different microstructures and generally more variability than traditionally formed materials. SwRI participated in the third Sandia Fracture Challenge (SFC) to demonstrate our modeling and simulation capabilities with respect to additive manufacturing. In the SFC, Sandia National Laboratories (SNL) provided participants with select experimental results to calibrate yield and damage models for a material formed by an additive process. SNL then asked participants to predict various quantities of interest (e.g., a load-displacement curve) for a non-standard geometry made from this material. Participants then had a limited amount of time (on the order of six months) to predict and report quantities of interest to SNL.

Approach — We developed a comprehensive analysis framework to predict the elastic, plastic, and damage response of components built using an additive manufacturing process. This framework was applied to the challenge problem presented by SNL: a unique geometry with voids, holes, and intersections that demonstrates the capabilities of additive manufacturing and that introduces potential issues in existing modeling and simulation approaches. Our process recognizes ensemble studies as the fundamental unit of simulation (i.e., a set of analyses with variable inputs), and, as a result, it directly incorporates variability in the quantities of interest due to variability in the geometry and the material properties. This process may be particularly suitable for additive manufacturing processes that have increase variability and material properties that vary from build-to-build.

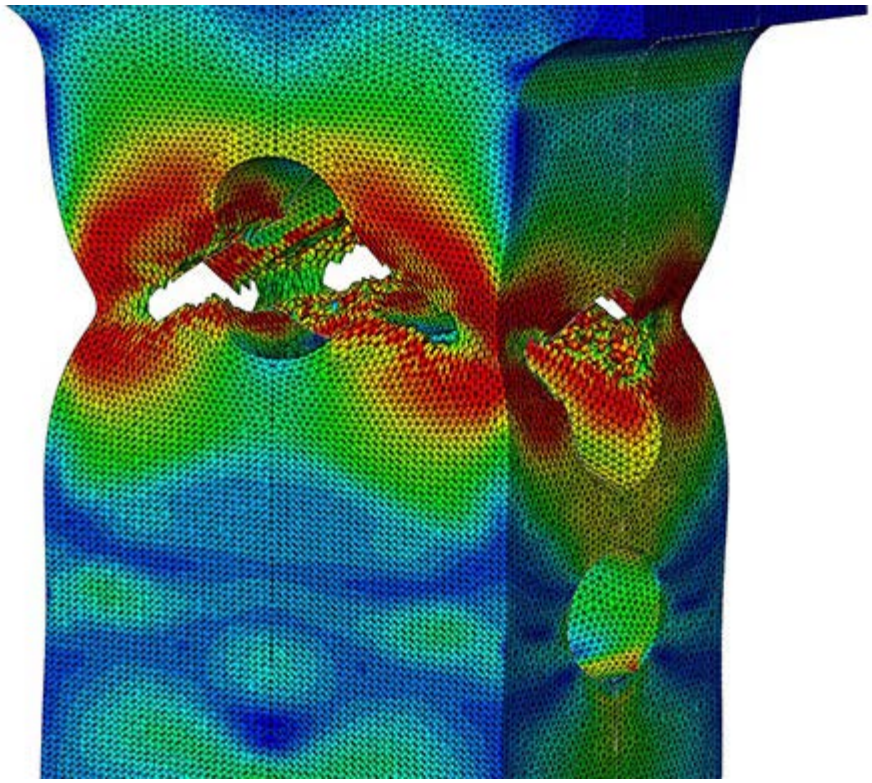

Figure 1: Simulation of the challenge geometry.

Accomplishments — Using this analysis framework, we predicted the quantities of interest requested by SNL for the SFC. First, we selected appropriate material models for the elastic, plastic, and damage regimes, including a novel ductile damage model based on micromechanics considerations and recent experimental work of void growth rates measured *in situ* during loading. Then, we calibrated distributions of the material properties using results from witness coupons and a Bayesian updating scheme. Finally, we propagated relevant uncertainties in the material response and in the geometric dimensions through detailed 3D finite element analyses to predict the nominal response and its variability at requested confidence intervals. Figure 1 shows the damage process predicted by one analysis. These results were provided to SNL by the relevant deadline. More information on our results for the SFC will be provided in the forthcoming review article.

SOUTHWEST RESEARCH INSTITUTE®

2017 IR&D Annual Report

Scaling Issues in Hypervelocity Impact, 18-R8779

Principal Investigators
James D. Walker
Donald J. Grosch
Sidney Chocron

Inclusive Dates: 07/01/17 – Current

Background — Historically, it has been observed that impact events do not undergo linear geometric size scaling, i.e., if you double the size of the projectile, for example, you don't exactly double the crater size, it turns out to be a little larger than double the size. There are other aspects to size scaling that are even more dramatic. This work will explore the size scaling of momentum enhancement and the role of damage evolution in its size scaling. We are also going to explore a novel impactor and how its impact results scale.

Approach — In the summer of 2017, SwRI completed the facility to house a large two-stage light gas gun (Figure 1). The experimental capabilities of the two-stage light gas gun facility are unique, but in particular it can launch large projectiles at high speeds (up to 7 km/s). This launcher allows us to explore advanced and novel penetrators, hypervelocity impact phenomena, and armor response. We will use this facility to explore the scaling question, in one case focusing on the target response and in the other focusing on the impactor type.

Accomplishments — So far, computational simulations of impacts of interest have been performed to aid in the design of experiments. Though the new gun facility has been used for external client work, the impact experiments are still being designed and will be performed in the future.

Figure 1: The centerpiece of a new 7,050 square foot facility at SwRI is a two-stage light-gas launcher featuring a 38-mm-diameter launch tube (1.50 caliber) with the ability to achieve velocities up to 7 kilometers per second (15,660 miles per hour).

2017 IR&D | IR&D Home

SOUTHWEST RESEARCH INSTITUTE®

2017 IR&D Annual Report

Develop, Test, and Validate a Corrosion Monitoring Cell to Quickly Evaluate Effectiveness of the Corrosion Control Measures, 20-R8784

Principal Investigators
Xihua S. He
Jay L. Fisher
Adam Cobb

Inclusive Dates: 07/10/17 – Current

Background — Aboveground storage tanks (ASTs) are widely used in the oil and gas and nuclear industries. In both industries, the ASTs often are constructed using a concrete ring wall, a high-density polyethylene liner as a secondary containment, and tank foundation material, which is usually sand. The tank bottom plates, which are usually 0.25 inch thick bare A36 steel, sit on the sand pad foundation, which is approximately 12 to 18 inches thick. Electrolyte with aggressive chemical species promoting corrosion may accumulate in the pad foundation over time, leading to a corrosive environment and severe corrosion of the tank bottom plates, even under cathodic protection (CP). AST operators need to develop corrosion control measures based on the sand electrolyte corrosivity near the bottom plate. Design of an appropriate corrosion control measure depends on the tank-specific sand conditions; therefore, it must be customized for each tank location. The focus of this project is to develop a laboratory corrosion monitoring cell to quickly evaluate the effectiveness of various corrosion control measures involving combined application of CP and vapor corrosion inhibitors (VCIs) to meet the industry need.

Approach — A glass cell filled with field-grade sand was used in the laboratory tests. A coupon assembly was developed with an ultrasonic testing (UT) probe on it (hereafter referred to as the UT coupon assembly). The UT coupon assembly was used to monitor the thickness of the metal as a function of time, as an indicator of metal loss through corrosion. The glass cell plus UT coupon assembly was used to evaluate the effectiveness of corrosion control measures under various test conditions by making thickness measurements as a function of time. Because the coupon thickness is continuously measured, the approach provides a quick way to evaluate the effectiveness of various corrosion control measures.

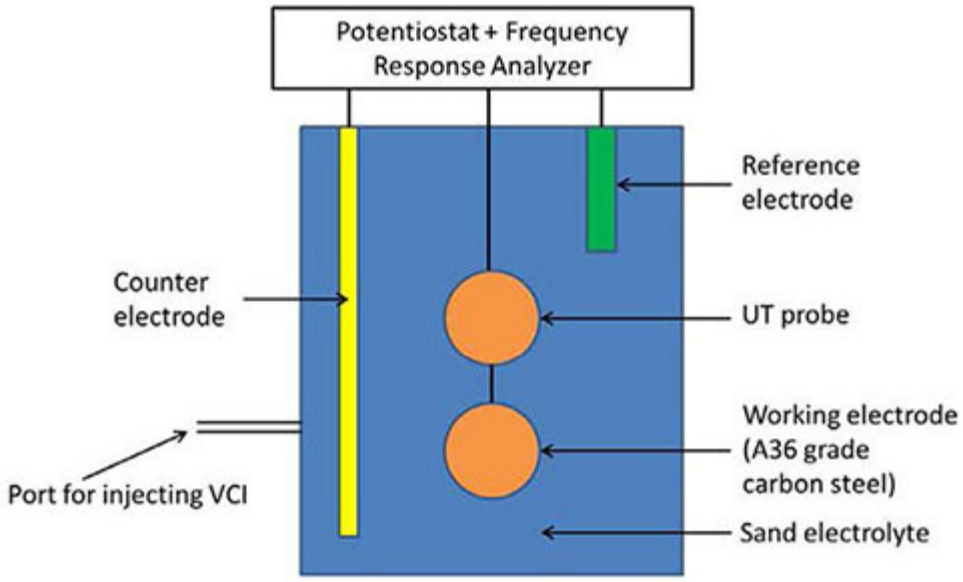

Figure 1: Schematic of the corrosion cell to evaluate effectiveness of the corrosion control measures involving a combination of cathodic protection plus the vapor corrosion inhibitor.

Accomplishments — The corrosion cell, schematically shown in Figure 1, was set up. Standard three-electrode glass cells were constructed with a counter electrode, saturated calomel reference electrode, and a piece of A36 grade carbon steel as the working electrode. The cell has penetrations for the working electrode, UT probe, reference electrode, and counter electrode. Three experiments were conducted in parallel: experiment without any corrosion control measure, application of -850 $_{m}V_{CSE}$ CP, and application of -850 $_{m}V_{CSE}$ CP plus VCI. The last two tests helped to determine the relative effectiveness of the two corrosion control measures for the sand-electrolyte mix, and whether their effectiveness can be measured using the UT probe. Results show that the system and the UT probe were functioning. The CP to the carbon steel coupon was turned on and off, and the corrosivity of the electrolyte in contact with the sand was adjusted to confirm the functionality of the UT probe in detecting metal loss. After the tests were completed, the coupons were examined under the microscope and with laser profilometry to determine metal loss, and the results were compared to the *in situ* data from the UT probe.

The general progress of the corrosion process and the absence of corrosion were successfully detected. The fundamental accuracy of the sensors was shown to be on the order of 1-3 µm when the surface being measured was very uniform. However, when the sensor was located over a non-uniform surface, it underestimated the amount of thickness loss; the adhered corrosion product on the coupons may have affected the thickness readings.

SOUTHWEST RESEARCH INSTITUTE®

2017 IR&D Annual Report

Deep Learning System for Robotic Pick Selection, 10-R8600

Principal Investigators
Michael Rigney
Alex Goins
Johnathan Meyers
David Chambers

Inclusive Dates: 10/01/15 – 03/01/17

Background — Robotic sorting operations are challenged by the task of interpreting 2-D/3-D image data to identify a pick point within a pile of mixed product types (boxes, widgets, parts, bags). Varying object colors, labels, sealing tapes, decoration, and occlusions contribute to scene complexity.

Perception systems are typically developed by exploring and selecting engineered feature detectors and machine vision algorithms to interpret sensor data. High-level results from feature extraction operations may be input to a machine learning algorithm for classification or ranking.

Deep convolutional neural networks (DCNN) have recently attained top performance scores among machine learning paradigms in image-based object recognition competitions and similar challenges. DCNNs are composed of several CNN layers followed by a traditional fully convolutional neural network (FCN). Through a progression of layers, CNNs implement low-level feature detectors and produce higher-level abstract representations of the input data. Importantly, CNNs are trained from example data, alleviating the feature engineering burden of traditional perception solution development.

Figure 1: Parcel sorting work cell with ABB robot, vacuum gripper, and 2-D/3-D sensors.

Approach — A DCNN development environment was integrated with a robotic parcel sorting testbed that included 2-D and 3-D vision sensors (Figure 1). A database of 30,000 observations with single and multiple pick locations was used for offline training and alternate 2-D and 3-D data encodings were tested. Pick performance of a range of DCNN architectures was evaluated. Baseline architectures mirrored those used for image-based object recognition and output for a single parcel location and orientation. Final architectures output maps (images) indicating location, orientation, and confidence score of multiple parcel pick selections. Pick performance was scored by the

accuracy of robotic parcel placement at the work cell output conveyor.

Accomplishments — Best DCNN performance was comparable to that of a conventional machine vision approach, but achieved using a machine learning paradigm. Training data augmentation to simulate parcel piles with multiple known parcel locations and orientations was key to obtaining our best observed performance.

SOUTHWEST RESEARCH INSTITUTE®

2017 IR&D Annual Report

Improved Spatial Resolution for an Earth-Observing Infrared Spectrometer, 10-R8621

Principal Investigators
Robert A. Klar
Yvette D. Tyler

Inclusive Dates: 01/01/16 – 6/30/17

Background — Within the last decade, there has been rising awareness of climate change and its potentially detrimental consequences. Recognition that methane is a potent greenhouse gas has urged stricter governmental regulations and renewed focus on monitoring atmospheric methane. At SwRI, a concept for an atmospheric methane monitoring instrument was conceived a few months ago. After researching several instruments, we found that those currently fielded do not have sufficient spatial resolution to meet the increasing demand for improved environmental monitoring.

Approach — The objective of this research is to devise, test, and validate a data processing approach for reducing data volume while accurately measuring methane concentrations. To meet demands for improved environmental monitoring and improve upon the capabilities of predecessor instruments, we established the performance goals shown in Table 1.

Table 1: Performance Goals and Results

PERFORMANCE GOALS	GOAL	RESULT
Minimum Signal-to-Noise Ratio	100[1]	113 at poles, 337 at equator (land) 120 at poles, 360 at equator (ocean)
Spatial Resolution	2 km x 2 km (land) 25 km x 25 km (ocean)	2 km x 2 km (land) 25 km x 25 km (ocean)
Spectral Resolution (Resolvance R=λ/Δλ, λ=1640 nm and 760 nm)	0.1 (16,400 and 7,600)	0.1 (16,400 and 7,600)

[1] measured at the poles (80° latitude)

This research seeks to take advantage of recent advancements in detector and readout technologies. In particular, we seek to exploit the processing capabilities included within the Teledyne SIDECAR® Application Specific Integrated Circuit (ASIC), which miniaturizes the drive electronics for infrared detectors. We also introduce a simplification to our original instrument concept by using a single larger detector (H2RG) instead of the two smaller ones.

Accomplishments — Windowing and Accumulation data processing were implemented using the embedded processor on the SIDECAR. Images were acquired with the H2RG, demonstrating the feasibility of doing data reduction at the front end. A lossless data compression algorithm was implemented using the Cobham-Gaisler GR712RC on the back end. The compression uses a one-dimensional predictor with lossless compression (an implementation of CCSDS 121.0-B-2). Based on analysis of data processing tests, we can satisfy our desired performance goals.

We completed the design, fabrication, and assembly of a SIDECAR Interface Board (SCIB). A prototype instrument data processing chain was assembled consisting of the SCIB and a GR712RC development

board. We created a breakout board for the H2RG Hirose connector and are using it to integrate and test the SCIB with the H2RG detector in our lab.

SOUTHWEST RESEARCH INSTITUTE®

2017 IR&D Annual Report

Large-Scale Robotic Aircraft Painting Technology Research and Development, 10-R8640

Principal Investigators
Carl Bargainer
Crystal Parrott
Chris Lewis
Branson Brockschmidt

Inclusive Dates: 11/01/16 – 11/01/17

Background — In late 2014, SwRI was awarded an externally funded large-scale laser depaint program for passenger-sized aircraft. The system under development is being designed with the concept of extensibility for a variety of other large-scale aerospace processes. Aircraft painting represents the most significant process opportunity, with market potential estimated to exceed depaint. Multiple coatings will be applied during an aircraft's lifespan. In addition, coatings are re-applied due to branding and marketing positions by aircraft owners. Aircraft manufacturers and maintainers are actively seeking paint system solutions that reduce cost, improve quality, speed the process, and allow easy application of complex paint schemes such as logos and images for advertising and branding.

Figure 1: Inkjet EoAT on laboratory robot

Approach — Our goal is to adapt the approach for use with the large-scale robotic platform developed for laser depaint, and develop end effectors for painting and direct-print inkjet applications. We designed and fabricated an inkjet end-of-arm tool (EoAT) with a printhead stabilization system to absorb vibrations induced by the large-scale robotic platform. To identify the effects of variable printhead orientation and the limits of key process parameters such as standoff distance, we integrated a commercial printhead with support systems and tested it in a lab setting. The goal was to define parameters for printing in arbitrary orientations and on curved surfaces.

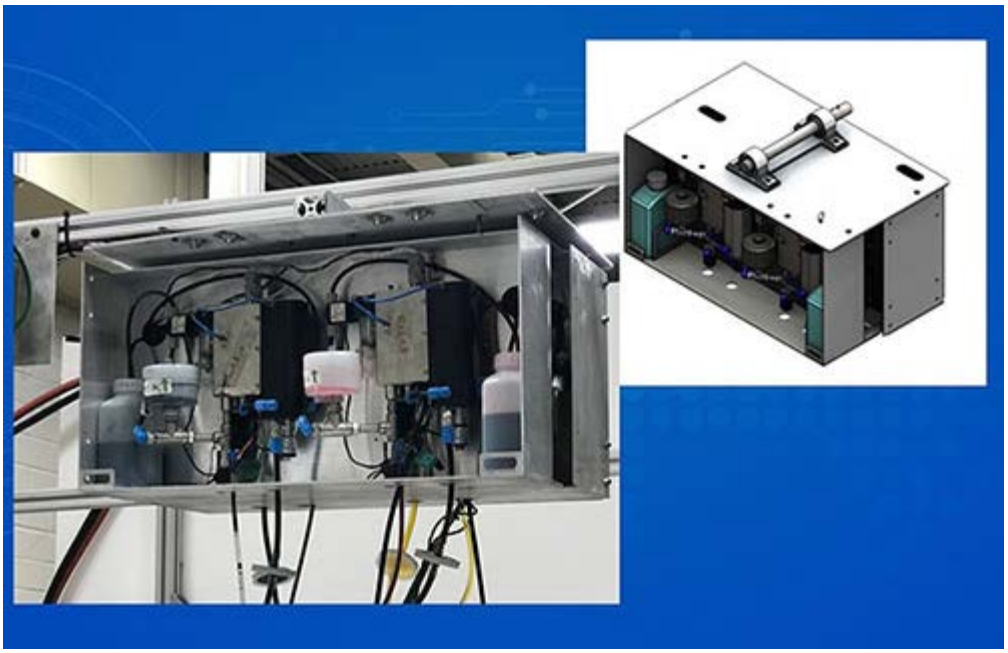

Figure 2: Inkjet fluid handling system

The final challenge was to address print path alignment over large surfaces so the image is seamless. We solved this problem by developing a vision-based solution that uses specialized print patterns to detect, at high precision, the alignment of the previous print pass and position the print head accordingly to achieve the necessary alignment. We integrated the EoAT onto a robotic platform to demonstrate direct inkjet printing within our robotics laboratory.

Accomplishments — The inkjet EoAT and ink delivery enclosure were designed. A 3-axis printhead stabilization platform was assembled, and stabilization software developed for 2-axis vibration compensation. The inkjet printhead was selected and integrated with drive electronics, fluid handling system, and printing control software. The inkjet EoAT was fabricated and mounted to a 6-DOF laboratory robot for testing. Color images were printed with test fluid at varying angles and on curved surfaces. The effects of printing distance, ink inlet and outlet pressure, printhead orientation, and drive voltage waveform were investigated. Demonstration of the inkjet EoAT was performed on a laboratory robot.

We attained the following results:

- Speed range from 10 to 400 mm/s demonstrated
- Print angles from 0° to 145° demonstrated using aqueous test fluid (limited by robot reach)
- Vibration Compensation Validation for control to ±0.004 in.
- Curved Surface Radius of 675 mm demonstrated with distortion less than 0.007 in.

SOUTHWEST RESEARCH INSTITUTE®

2017 IR&D Annual Report

High Performance Streaming Data Processing, 10-R8677

Principal Investigators
Stephen A. Kilpatrick
Wayne Timme
Todd Newton
Phil Westhart
Glen Mabey
Ben Abbott

Inclusive Dates: 07/01/16 – 07/01/17

Background — In 2004 as part of the Boeing 787 team, SwRI developed the first large-scale, network-based data acquisition and telemetry flight test system. While our success in this arena continues today, the increasing momentum of standardized network technologies has led to unrealizable expectations. When technologies become commoditized, the industry expects the increased capabilities to be incorporated smoothly and quickly into their systems. While the core unifying technology, Internet Protocol (IP), eases this process, unique challenges unanticipated by our clients in the flight-test telemetry domain are impeding the introduction of the next generation of high speed IP technologies. These challenges have led some down the expensive path of attempting to develop special purpose hardware. While likely to create an expensive working solution for the short term, we believe a more open, commodity-driven approach that will have demand for the long term is possible. This project evaluated the efficacy of using commodity central processing unit (CPU) and general-purpose graphics processing unit (GPGPU) technologies to offload the processing challenges associated with the ever-increasing demands on network-based telemetry.

Approach — We based our approach around the belief that the high packet rate nature of flight test data systems offers a good opportunity for packet-level parallelism to be explored. Four computational approaches were investigated to determine the optimal way to partition the packet processing between the CPU and GPGPU. The four approaches used the same method for receiving packets, but varied in how they performed the packet processing and monitoring for completion. The four unique approaches were performed on three different sets of hardware (i.e. a high-end desktop computer; a mid-range, ruggedized embedded system; a low-power, compact embedded system) to prove out the scalability of the solutions.

Accomplishments — All approaches were shown to scale well with the numbers of packets processed, with packet processing rate not strongly affected by the number of packets processed. Some minor packet rate slowdowns are observed in the GPU approach due to the overhead of initializing the GPUs. The same trends were observed across the three different computers, with a "Full CPU" approach performing best under low packet load, and the GPU approaches scaling better across higher packet loads. These results are consistent with the architecture of the GPU. The GPU cannot perform conditional branching as efficiently as the CPU, but given enough parallelization, the GPU will begin to outperform the CPU in overall performance. Encouraged by these results, an end-to-end experiment of GPU-enhanced packet processing was conducted using a hard-coded configuration with 10,500 filter rules and data word extractions. The setup included IP packets generated from multiple simulation sources, a multicast video stream, and a real flight test data acquisition unit (DAU), generating a total of 6.6 Gb/s of input load. With this experiment, we had no packets lost and achieved processing latencies averaging ~350 microseconds, with a maximum latency of 1 ms.

SOUTHWEST RESEARCH INSTITUTE®

2017 IR&D Annual Report

Autonomous Trailer Docking, 10-R8683

Principal Investigators
Elliot R. Johnson
Kristopher C. Kozak

Inclusive Dates: 07/11/16 – 11/11/16

Background — SwRI has identified a strong interest for autonomous systems that can reduce the operating costs of trailer yards where many trailers are shuttled between loading docks and parking yards. The Automated Trailer Docking project sought to develop and evaluate a prototype autonomous system to drive a trailer in reverse to a shipping dock. The purpose of this research was to demonstrate that SwRI's technology is uniquely suited for these applications and to make an accurate determination of the level of effort required to develop new systems for client facilities.

Approach — An actuated commercial semi-trailer truck was outfitted with SwRI's Ranger localization system and existing autonomy software. A single-plane light detection and ranging was installed on the truck to measure the truck-trailer angle without modifications to the trailer. A steering controller was developed to provide accurate path following in reverse. The steering controller is based on a pure-pursuit steering law and kinematic model of the truck-trailer system. The steering controller provides accurate path tracking that is robust against error in the localization and angle measurements, and errors in the kinematic model parameters.

Accomplishments — This project developed a prototype that can successfully back a trailer to a shipping dock, placing the rear bumper within 0.5 meters of lateral alignment and within a 0.25-meter gap to the dock (See Figure 1). This project demonstrated the feasibility of achieving this task, characterized the achievable tolerances with SwRI's existing autonomous technologies, and identified cost-effective approaches to improve performance.

Figure 1: SwRI Class VIII truck autonomously backed up to a loading dock.

SOUTHWEST RESEARCH INSTITUTE®

2017 IR&D Annual Report

Advanced Technology for Quantifying and Optimizing Human Physical Performance, 10-R8690

Principal Investigators
Kase Saylor
Dan Nicolella

Inclusive Dates: 09/06/16 – 09/06/17

Background — Human performance is defined as physical performance, cognitive performance, and social/organizational performance. This project specifically focused on physical performance. The research team spent a great deal of time with practitioners within the tactical athlete (i.e., U.S. Special Operations) and professional sports physical performance communities, and discovered that there is a strong desire to use 3-D motion capture analysis for biomechanical assessment; however, current practices and technologies are not able to meet this need (either too labor intensive [marker-based] or measurement accuracies are too low [markerless-based]). Thus, the objective of this research effort was to design, integrate, and evaluate the performance of a novel model-based markerless motion measurement system.

Approach — We developed a new markerless 3-D motion capture system that provides measurement accuracies comparable to traditional marker-based 3-D motion capture systems, but requires a minimal setup time that aligns with the operational needs of the human performance community. The new SwRI markerless biomechanics system was developed by combining biomechanical modeling, deep neural networks, and sensor fusion techniques. Some advantages of this new system are:

- Commercial-off-the-shelf video components are used compared to specialized infrared cameras used with traditional marker-based systems
- A minimal number of cameras are required to capture 3-D motion compared to traditional systems (two cameras vs. eight or more)
- No external markers are required to be placed on the subject compared to up to 60 markers when using a traditional system
- The system can be extended to capture multiple subjects
- The methodology will allow for a complete biomechanical analysis using a single system compared to multiple systems (e.g. marker-based motion capture, force plates, separate data analysis and modeling codes) using traditional methods.

Accomplishments — This research project was successful in accomplishing the goal of researching and developing an SwRI-developed markerless 3-D motion capture system that provides measurement accuracies comparable to marker-based 3-D motion capture systems, while requiring a minimal setup time to align with the operational needs of the human performance community. The results of this project have defined a framework for a paradigm-shifting foundational technology for biomechanical human performance measurement. We anticipate that with further development, this technology will be widely adopted across multiple disciplines that can benefit from the accurate quantification of human motion.

SOUTHWEST RESEARCH INSTITUTE®

2017 IR&D Annual Report

Convolutional Neural Network Gesture Recognition in Low Light Conditions, 10-R8697

Principal Investigators
Douglas A. Brooks
Edmond M. DuPont

Inclusive Dates: 09/30/16 – 01/30/17

Background — The purpose of this project was to measure the performance (accuracy and speed of detection and interpretation) of a tactically relevant gesture recognition system using an adaptation of SwRI's Convolutional Neural Network (CNN) object detection algorithms. Having a quantitative performance measure of the system would give us the ability to more accurately bid our support tasks for specific clients.

Approach — For this project, the team used a military grade vehicle equipped with its own set of infrared (IR) emitters. The vehicle was evaluated at SwRI's test track. An IR camera system was installed on the vehicle and the detection metrics of interest were collected. Due to the lack of available low-light pedestrian data for training, the team also had to create labeled data of pedestrians in low-light scenarios (specifically using an IR camera) to train the CNN to detect people and gestures in those conditions.

To test the system, the team collected data of four different gestures, at two different times of day (dusk and night), at four different angles, and at seven different distances. The team collected data to analyze the following metrics:

- The angle and range of gesture recognition
- The impact of lighting to the range of gesture recognition
- The detection rate and false positive rate
- The acquisition rate (speed) in which the system positively recognized each gesture

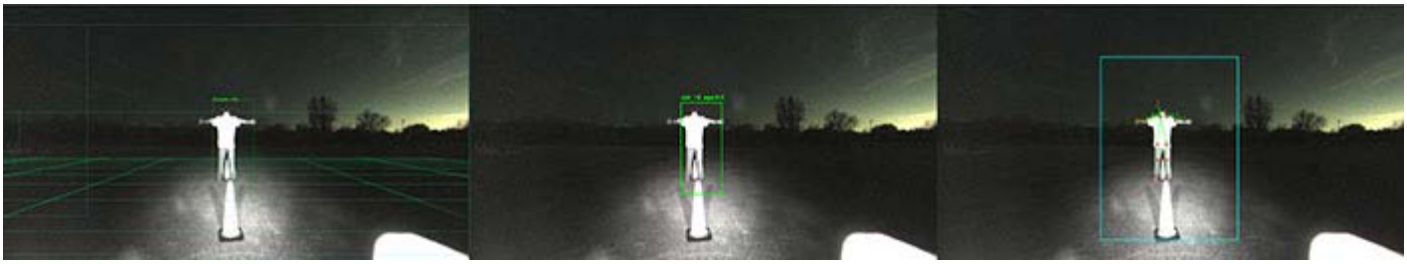

Figure 1: Accurate pedestrian and gesture recognition in low-light conditions.

Accomplishments — During dusk, the overall pedestrian detection rate of the system is 99.5 percent, and the false positive rate is 10^{-5}. The gesture recognition algorithm is intermittent at times because it is highly dependent on the accuracy of the pedestrian detection and tracking boxes. The operation range was 5 m to 20 m and ±30 degrees. During night, the detection rate and false positive rate remained consistent, but the operation range decreased to 10 m and ±15 degrees, due to limited illumination ranges of the IR emitters. It is worth noting that the detection at night works at distances up to 20 m, but only with a 0 degree offset because the IR emitter's illumination radius is reasonably strong at 0 degrees and less so as

the angle increases. The detector processes detections at 6.65 Hz (~150 ms), and the tracker and gesture recognizer process at 19.5 Hz (~50 ms) and 3.32 Hz (~300 ms), respectively. Figure 1 illustrates the system detecting the pedestrian and accurately determining a gesture during night conditions at a 0 degree offset.

SOUTHWEST RESEARCH INSTITUTE®

2017 IR&D Annual Report

Radio Frequency (RF) Detection of Gunfire, 10-R8703

Principal Investigators
Jay D. Thomas
Thomas C. Untermeyer
Brad D. Moore
Carl E. Weiss

Inclusive Dates: 10/01/16 – 10/01/17

Background — For defense purposes, the military has an interest in detecting weapons as soon as possible after their firing or launching from as far away as possible. Optical, Infrared (IR), and acoustic systems exist today that can detect a variety of weapon fire. However, these detection methods do not work as well during obscured environmental conditions caused by phenomena such as clouds, fog, and rain. Acoustic systems also provide much slower response time and limited range. Radio frequency (RF) sensors could provide an additional method of detection and location not only to reduce the number of overall false positives but also to provide some additional capability such as providing better detection through obscured environments. This project builds on previous work in this technical area.

Approach — This project focused on AK-47 gunfire to determine if the firing of this weapon also produced a repeatable RF recognizable signature of sufficient strength for reliable detection at extended ranges. The general technical approach included testing first within an indoor RF-shielded enclosure to initially minimize outdoor interference from other externally generated RF signals followed by outdoor testing using software/hardware filtration techniques based on the RF signal characteristics discovered during the indoor testing to adequately isolate the RF emissions in an outdoor environment.

The project team began by modeling the anticipated electromagnetic environment of a transmitter inside a shielded enclosure to determine the best test setup. The modeling revealed the expected best location for placing anechoic material to reduce reflections that can cause standing waves. A log periodic antenna, horn antennas, and omnidirectional antennas were used to cover the frequency bands of interest. Analysis of the captured data confirmed the precise timing of any RF emissions. The project team then assembled and set up test equipment at SwRI's outdoor ballistics range to validate the detection algorithms based on the data results from the RF-shielded enclosure.

Accomplishments — The project team collected RF data in the RF-shielded enclosure during the AK-47 test and detected multiple signals during the firing of the weapon. During the outdoor tests, the project team successfully detected an RF emission from the AK-47 weapon at a distance of 15 feet from the weapon.

In summary, our test results indicate that an AK-47 small arms weapon does emit unique RF signatures that are detectable at significant ranges from the weapon with enough fidelity to identify not only the type of weapon fired but probably also the type of ammunition used. This should allow the development of passive gunfire detection systems using RF sensors in collaboration with other types of sensors.

SOUTHWEST RESEARCH INSTITUTE®

2017 IR&D Annual Report

Robotic Path Planning for Geometry-Constrained Processes, 10-R8706

Principal Investigator
Chris Lewis

Inclusive Dates: 10/01/16 – 09/30/17

Background — We developed, demonstrated, and tested a robotic path planning framework for industrial processes. The work focused on developing software modules that analyze 3-D geometric data to automatically generate robot plans for processing complex parts efficiently. The first major set of modules analyzed scanned 3-D data to perform tasks such as segmentation, boundary detection, and mesh generation. These features are salient to many industrial processing tasks. The second module set generated tool paths to perform the process on the particular features selected. Another module simulated the process to provide an estimate of the performance of the generated tool path. The final module determined the ordering of path segments to process the entire part. The framework is integrated directly into ROS-Industrial, which provides collision-free robotic path planning and generic interfaces to a variety of industrial robots. The work flows seamlessly from scanning to path execution on industrial robots and can significantly reduce the cost of production processes with a high mix of parts.

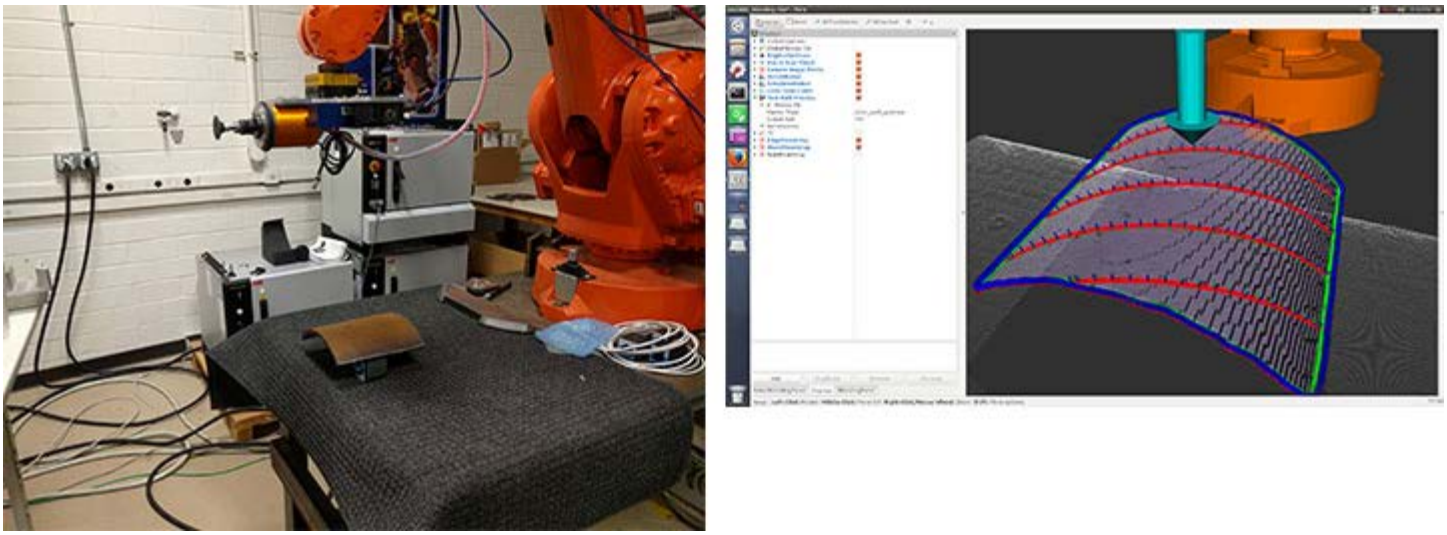

Figure 1: In a fully automated work-flow, a curved part is scanned by a robot using a 3-D camera. Paths are automatically generated to surface grind the part to remove rust, and to edge grind to remove flashing residue from the plasma cutting.

Approach — Our approach focused on developing the necessary software modules to generate the task points for edge and area coverage tasks, with a strong linkage with ROS-Industrial capabilities to generate collision-free robot joint trajectories and to execute these trajectories on robots. With this in mind, SwRI researchers developed software to automatically analyze 3-D data to find the salient edges and surfaces and then generate the tool paths to process or cover these features. A subsequent tool interleaves sub-segments from different features to improve the overall part processing efficiency.

Area-covering tool paths are characterized by their pitch, or distance between adjacent paths. Process results depend on both the pitch and on application-specific process execution parameters (e.g. the paint

flow rate). To allow users to tune the pitch to meet desired process specifications, SwRI researchers developed methods and interfaces for general tool process simulation and a specific paint thickness process simulator.

All of the software modules were combined into an end-to-end system complete with a user interface that generates tool paths, displays the expected process result, allows the user to refine re-plan paths, and then generate and execute joint trajectories on industrial robots.

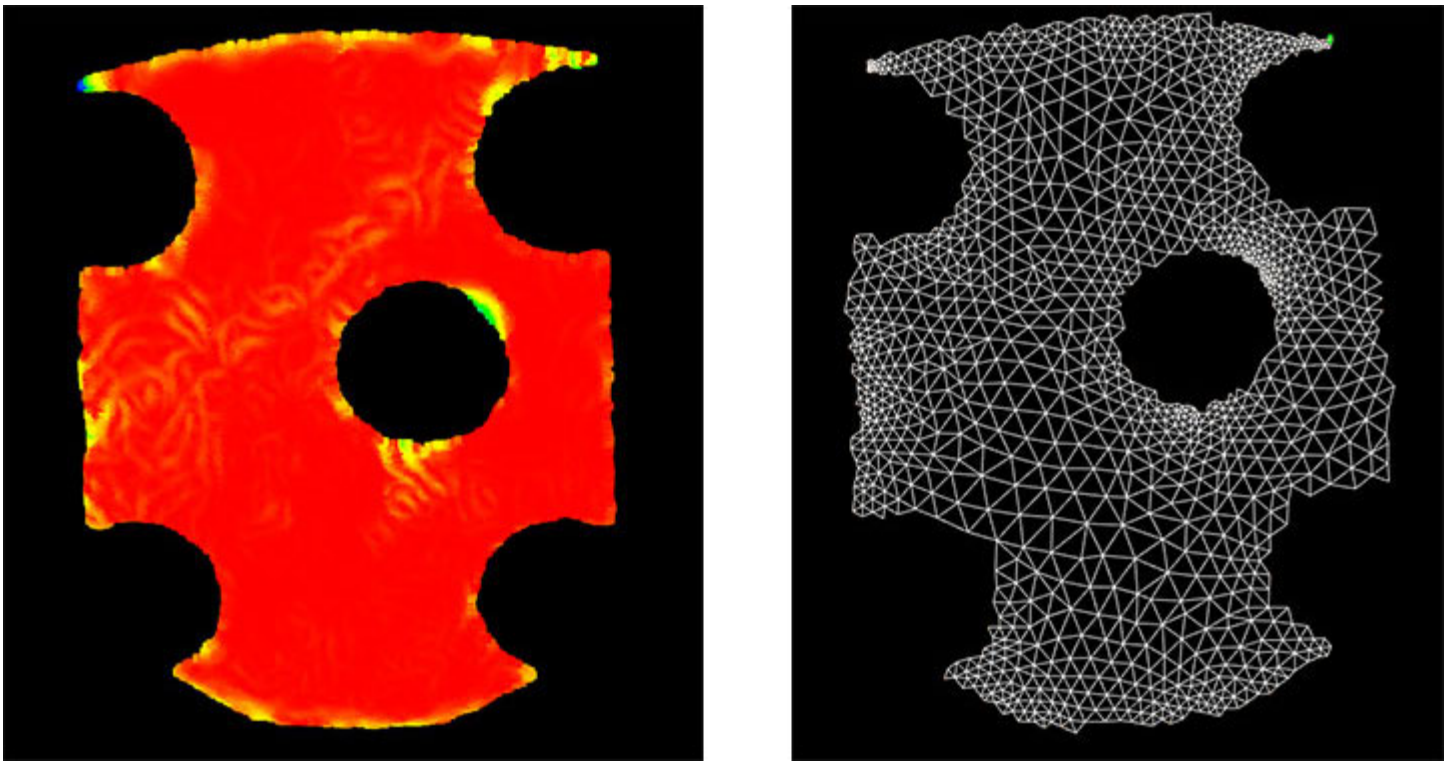

Figure 2: Meshes automatically generated from the scanned 3-D data has increased density in high curvature regions.

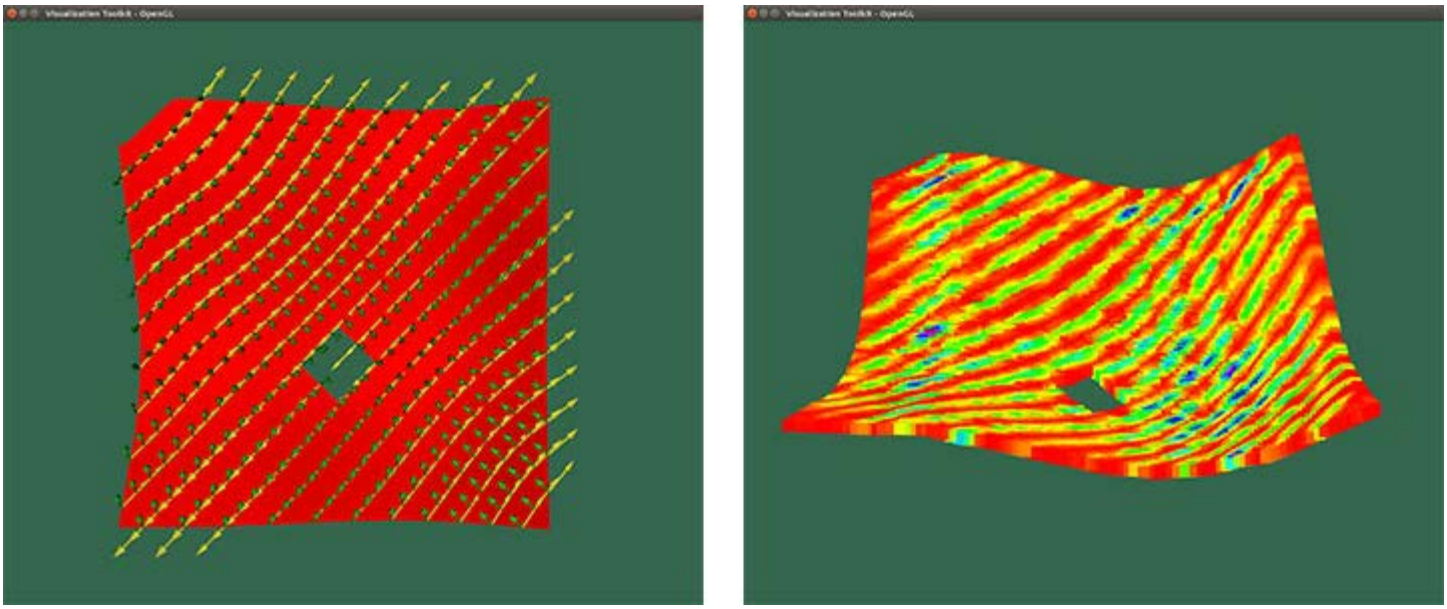

Figure 3: Simulation to evaluate whether expected paint thickness variations are acceptably small.

Accomplishments — The project developed the following software modules and demonstrated the system:

- Region growing segmentation of raw point clouds
- Boundary detection and refinement
- Boundary path plan generation
- Mesh generation using the Advancing Front Algorithm
- Uniform surface coverage of arbitrary mesh surfaces
- Simulation and evaluation tools for paint processing
- Automatic sequence planning.

SOUTHWEST RESEARCH INSTITUTE®

2017 IR&D Annual Report

Automated Detection of Oil Spills Using SAR and Visible Satellite Imagery, 10-R8721

Principal Investigators
Samantha Blaisdell
Adam Van Horn
Daniel Davila

Inclusive Dates: 12/19/16 – 04/19/17

Background — The Deepwater Horizon blowout and subsequent oil spill in the Gulf of Mexico resulted in one of the largest accidental oil disasters in U.S. history and caused significant damage to the marine life and regional economies that rely on sea-related activities. Due to this accident and others, there has been an increase in environmental and regulatory policies. As a result, oil slick detection in bodies of water has become an area of exponential growth and interest by many safety and environmental agencies and organizations.

This project builds on a previous project, 10-R8552, Automated Detection of Small Hazardous Liquid Pipeline Leaks, which concluded in September 2016 and resulted in a technology known as the Smart Leak Detection (SLED) technology, which can detect and classify various hazardous liquids using ground-based sensor fusion and machine learning. Based on our experience developing SLED, we developed a similar technology using satellite-based imagery. While others have focused on either visible or Synthetic Aperture Radar (SAR) imagery, we have shown that visible and SAR imagery of spatiotemporal disparity can be registered in space and time and used as input to a machine-learning algorithm for the reliable detection of marine oil spills.

Approach — We focused on the following tasks using publicly available and widely studied imagery of the Deepwater Horizon oil spill from different instruments on different satellites (not aligned spatially nor temporally):

- Investigation of tools and techniques for working with diverse satellite imagery sources
- Labeling visible and SAR satellite imagery with ground truth
- Developing a registration algorithm for fusing different types of satellite sensor data
- Adapting existing deep learning segmentation algorithms to satellite sensor data
- Testing and evaluating the machine learning-based oil slick detection technology

Accomplishments — We met the aforementioned objectives successfully. Additionally, the successful completion of this project has favorably positioned SwRI to develop capabilities in the market of satellite remote sensing for the oil and gas industry, as well as satellite-based analytics for other applications and industries. This project focused on developing a deep learning-based technology for detecting marine oil spills using sensor fusion of visible and SAR satellite imagery.

SOUTHWEST RESEARCH INSTITUTE®

2017 IR&D Annual Report

End-to-End Learning of Robotic Navigation Using Deep Convolutional Neural Networks with Structural Projection Layers, 10-R8728

Principal Investigators
Samuel Slocum
David Chambers
David Anthony

Inclusive Dates: 01/01/17 – Current

Background — "End-to-end" deep learning, as applied to ground vehicle autonomy, is an active field of research studied by a number of major companies. Current implementations focus on an attempt to leverage using human control of the vehicle as the primary mode of training supervision. While these attempts have been somewhat successful in very limited situations such as highway driving on previously learned roads, this method results in a whole-scale abandonment of previously developed and understood techniques for controlling ground vehicles. In particular, this method of training limits the ability of the system to handle complicated maneuvering, and is only able to handle unusual cases if the driver has already handled a similar situation. This project is investigating the methods by which established autonomy system components can be used as part of a complete end-to-end convolutional neural network (CNN) based system.

Approach — SwRI's approach has been to focus on using previously designed CNNs as components of a larger network. This network then provides the best quality data to the parts of the system for which CNNs are not well suited, such as control systems and longer-term planning. By starting with network components already well-trained on the individual problems, the overall optimization for the network starts from a state that is already well suited to the problem of controlling the vehicle. In addition, the network is responsible for learning the correct parameters to turn the observed classification data into an overall cost map, something that has, to date, depended on hand-tuned values based on human intuition and experience rather than an optimization process. Existing maps collected by human drivers are used as ground truth for traversability and perception.

Accomplishments — We accomplished the following:

- Each individual component was developed and trained. Figure 1 gives an example of the kind of component data being included in the overall network. FLOWNET is a CNN system for determining motion estimates based on changes in a scene from frame to frame. The images represent the motion in each of the X and Y directions of the view. By decomposing the motion into motion caused by the vehicle and motion of other objects, the system can better understand dangers in its environment.
- The "end-to-end" network was designed.
- The necessary training data was collected and processed and is ready for training.

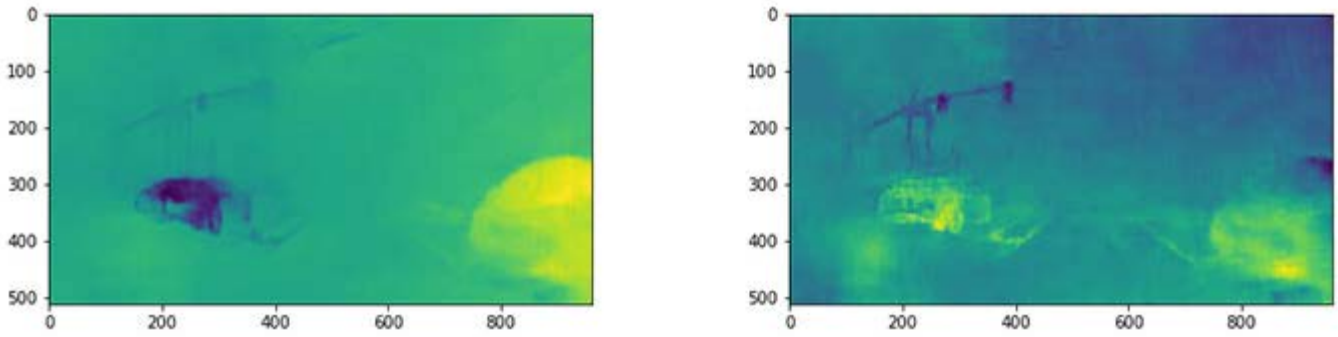

Figure 1: FLOWNET X (left) and Y (right) optical flows

SOUTHWEST RESEARCH INSTITUTE®

2017 IR&D Annual Report

Network Scheduling Policy Selection Based on Fluctuating Network Parameters, 10-R8732

Principal Investigators
Daniel Rossiter
Greg Fletcher
Todd Newton

Inclusive Dates: 01/01/17 – Current

Background — The purpose of this project is to address some of the universal challenges encountered by networked nomadic software applications that travel across many access points (AP) potentially over many communication link types and varying signal strengths. This investigation focused on two known problem areas – space and terrestrial mobile networks. While the terrestrial mobile network is an established, well-known concept, the Space Mobile Network (SMN) is a proposed next-generation solution to an ever-expanding fleet of space assets that increasingly rely on communication both between themselves and with ground stations. To address these challenges in a generalized way, a network scheduler could be developed to dynamically track and react to changes in network capabilities, queuing packets in a way most effective in the current environment and re-queuing these packets as the environment changes to make use of improved capabilities or gracefully degrade in the case of poor network performance. In the most extreme cases, delay/disruption tolerant network (DTN) techniques may be applied, storing packets for extended periods when no route is available and transmitting when possible, as is often the case in space networks.

Approach — To address these challenges in a generalized way across disciplines (e.g.: terrestrial and space mobile networks) our approach is to place an intelligent network scheduler between the software application and the network interface. This scheduler, informed by domain specific knowledge passed in by the application, would then track network capabilities in near real time and (re)schedule these packets as network capabilities change. To evaluate the efficacy of this scheduler, ns-3 (an industry-standard discrete-event network simulator) will be used to run simulations in representative network environments both with and without this scheduler.

Accomplishments — To date, the project team has devised methods to collect near real-time network health metrics using a combination of open-source libraries and in-house algorithms. Additionally, a baseline ns-3 network simulation has been devised that simulates the fluctuating network capabilities of satellites as they orbit the Earth with each other and with ground stations. This simulation will later be tied into simulated satellite data already collected from Systems Tool Kit (STK).

SOUTHWEST RESEARCH INSTITUTE®

2017 IR&D Annual Report

Machine Learning for Space Data Compression, 10-R8733

Principal Investigators
Daniel Davila
Keith Pickens
Scott Miller
Mike Koets
Samantha Blaisdell
Heath Spidle
Joshua Anderson

Inclusive Dates: 01/01/17 – Current

Background — The objective of this research was to investigate the adaptation of machine learning algorithms to the task of space science data compression. This capability is pivotal for reducing the strain on the telemetry links of many science missions that is imposed by a combination of the high (and ever increasing) data volume and low telemetry bandwidths of modern spacecraft instrumentation systems.

Approach — Compression was achieved using a machine learning algorithm to intelligently select the portions of the signal that represented relevant data. This approach was motivated by observation that within most scientific instrumentation data, only a small fraction of the data is non-noise. In this case, the regions of interest corresponded to specie peaks from mass spectrometer data acquisitions. Data from the instrument was used to train a neural network that has the ability to accurately segment the data for relevant peaks. The rest of the signal was rejected as noise. The resultant compressed signal was the combination of the extracted peaks and some necessary metadata for establishing where in the original time of flight spectrum these peaks occurred.

Accomplishments — This effort resulted in an algorithm that performed well on simulated data, correctly extracting 95 percent of the relevant peaks and reducing the signal by a factor of 10:1. Initial work was also performed for determining the feasibility of embedding a neural network onto a space flight field programmable gate array. The successful completion of this project positions SwRI favorably for pursuing immediate leads:

- The application of machine learning for intelligent data handling for ground and space Internet of things (IoT)
- The application of machine learning tools to space instrumentation data
- The deployment of machine learning to hardware-constrained space mission hardware

Artifacts and results from this project also have direct applicability in other industries that utilize embedded intelligence at the edge, including automotive, energy, and aerospace applications.

SOUTHWEST RESEARCH INSTITUTE®

2017 IR&D Annual Report

Data Collection Analysis for Fuel Economy Improvement through Connected and Autonomous Vehicle Technology, 10-R8749

Principal Investigator
Edmond M. DuPont

Inclusive Dates: 04/03/17 – 08/03/17

Background — To date, the automotive industry has pursued Connected and Automated Vehicle (CAV) technology to improve safety, driver comfort, and fuel economy. The recent Department of Energy's Advanced Research Projects Agency-Energy Next-Generation Energy Technologies for Connected and Automated On-Road Vehicles program targets fuel economy improvements of at least 20 percent by using CAV technology to optimize both vehicle dynamics and powertrain control. One way in which CAV technology can have a large impact on fuel economy is through collaborative adaptive cruise control, which begins with robust detection of road markings and lane lines. SwRI performed repetitive on-road experiments collecting data using SwRI's Engineering Technology Demonstrator 2 (ETD2) (Figure 1).

Figure 1: SwRI ETD2 enclosure

Approach — The objective of this project was to use SwRI's ETD2 to collect data and analyze if and how CAV technology can best be used to improve fuel economy. The ETD2 includes stereo cameras, an inertial measurement unit (IMU), and a global positioning systems (GPS) receiver inside an enclosure that was mounted on a test vehicle's roof. SwRI implemented a lane detection algorithm that was optimized to run on the integrated embedded processor. The lane detection algorithm provides a parametric model of the lane curvature for the detected left and right lanes. In addition, the confidence of the detected lane was provided as an output for later comparison to commercial off-the-shelf (COTS) lane departure warning systems.

Figure 2: ETD2 mounted on SwRI vehicle

Accomplishments — SwRI installed the ETD2 on a vehicle for data collection and system evaluation (Figure 2). The data collection resulted in 15 Gb of data files that captures approximately 1.3 km of on-road driving. The data includes daytime and nighttime views, more than 8,000 frames per camera, of the road with the vehicle traveling up to 25 miles per hour. SwRI maintains this data on network storage and incrementally parses and annotates the data to determine relevant events, estimate the vehicle's state, and perform statistical analysis to quantify the environmental effects on the driver's responses. The data collected will allow the team to build a consistent database for developing more advanced CAV algorithms to handle various conditions. There exist various academic datasets for automated driving but these datasets are restricted or require licenses for commercial use. The datasets and mechanism for capturing them that were created on this project will allow SwRI the flexibility to capture independent data for training new artificial intelligence algorithms and develop automated driving behaviors to handle complex environments not currently being addressed by the industry.

SOUTHWEST RESEARCH INSTITUTE®

2017 IR&D Annual Report

Development of a Reactive Automated Mixed Palletizing (RAMP Algorithm), 10-R8752

Principal Investigators
Jeremy Zoss
Clay Flannigan

Inclusive Dates: 03/01/17 – 05/01/17

Background — Most manufactured goods are transported on standard shipping pallets. The process of stacking individual packages onto a pallet is labor intensive, so the palletizing process is a frequent target of automation. Traditionally, automated palletizing has only been applied when the incoming product stream is consistent and known in advance. Automation systems use fixed algorithms to place packages of known size in specific patterns. While this approach works well for some applications, large distribution and fulfillment centers still use manual palletizing due to their highly variable product mix. Existing software designed for mixed-size palletizing typically requires up-front knowledge of all incoming packages and full control of the placement ordering. This project developed an algorithm for planning pallets of mixed case sizes in a "reactive" scenario, where the algorithm has only limited visibility or control of the incoming package stream.

Approach — The primary challenge with mixed palletizing operations is not the package handling or sensing, as these are similar to existing automated palletizing solutions. This research focused on developing an algorithm for determining place positions of incoming packages given limited knowledge of the remaining packages. Sample pallet plans are shown in Figure 1.

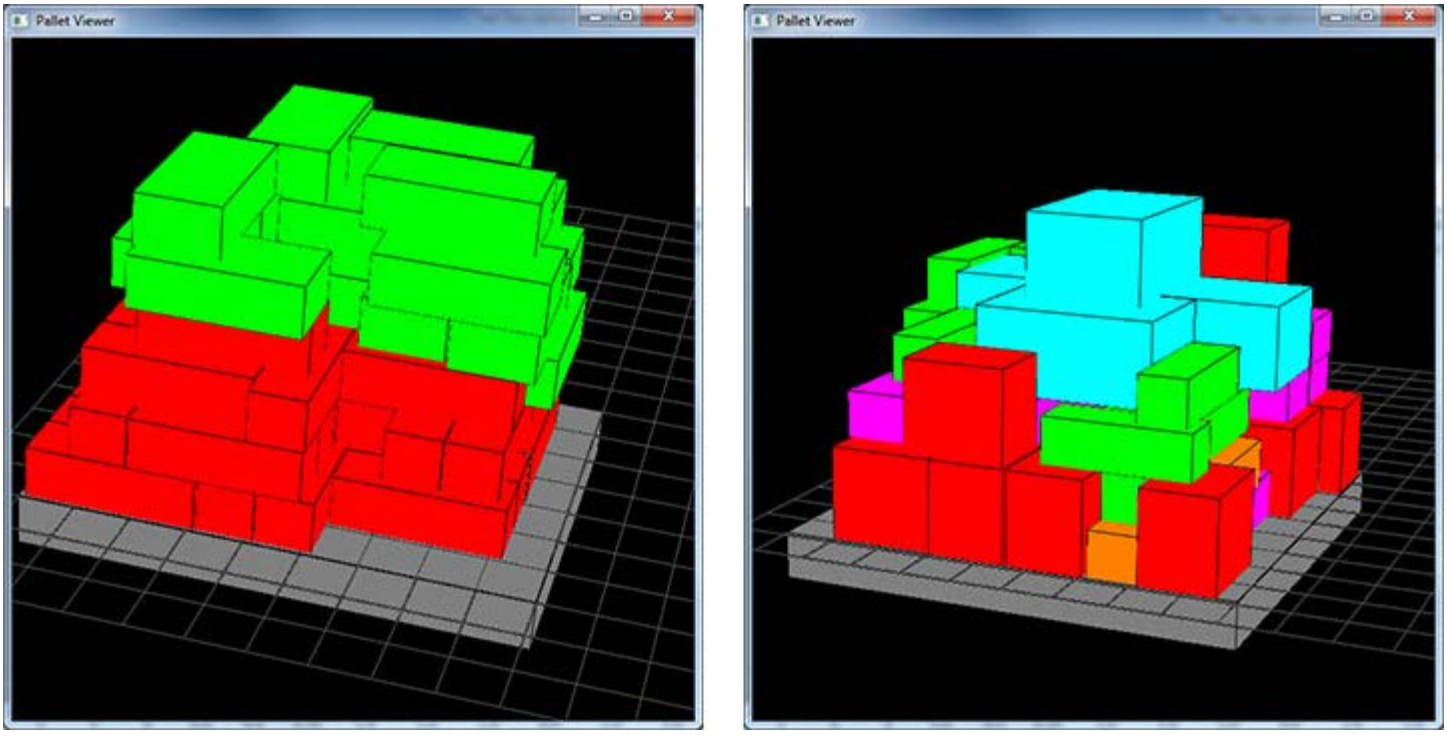

Figure 1: Sample pallet plans created by the RAMP algorithm

The Reactive Automated Mixed Palletizing (RAMP) algorithm scores each potential drop position for incoming packages by evaluating multiple criteria related to pallet stability and packing efficiency. The best score is selected as the target place position for that package. An example score-map of potential placement positions is shown in Figure 2. In cases where more upstream packages are visible, the RAMP algorithm will also consider how the current placement affects placement of future packages. The algorithm has been expanded to include buffering and non-rectangular cases, and the criteria thresholds can be adjusted to adapt the pallet structure for different applications. One of the primary goals of this approach is to allow for flexible scaling of a single palletizing algorithm from "fully reactive" to "fully known" applications.

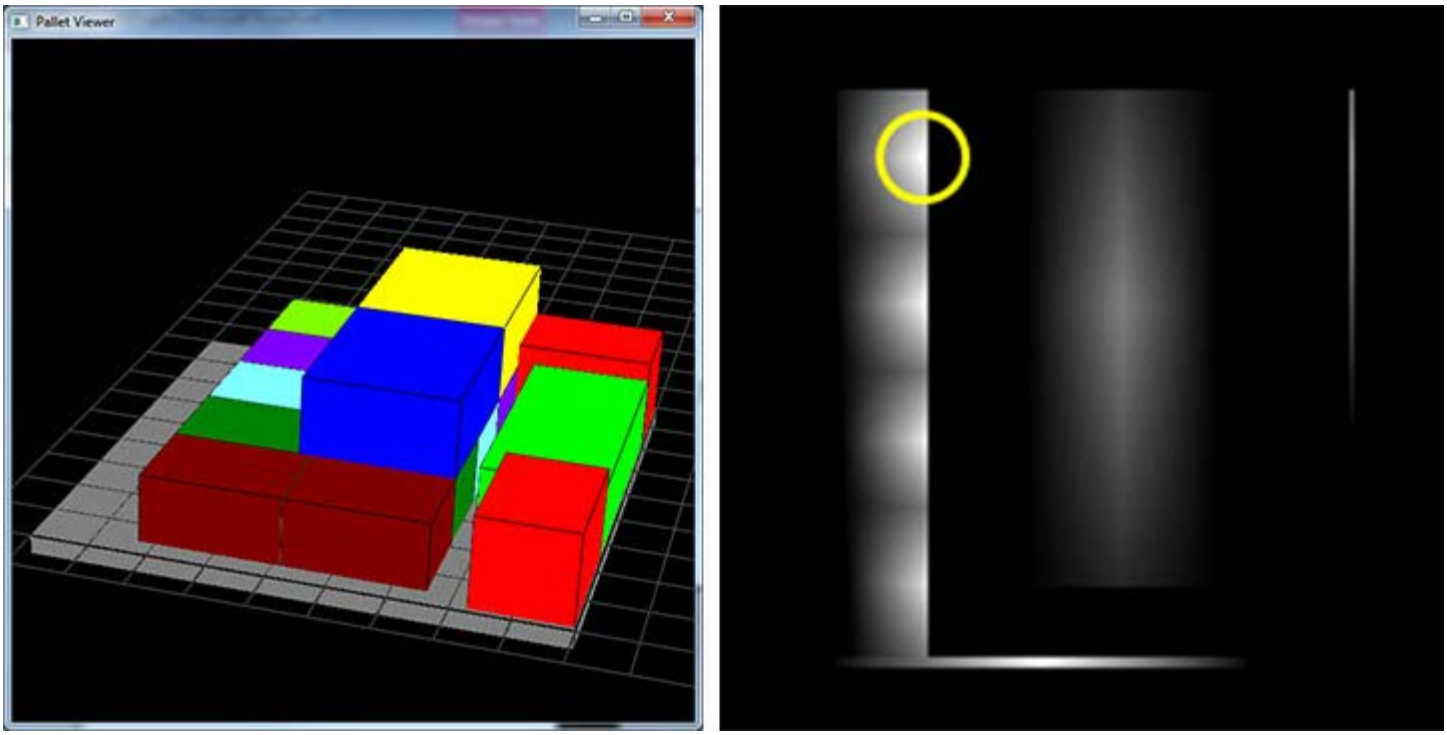

Figure 2: Score-map of potential placement positions on the given pallet

Accomplishments — The basic RAMP algorithm has been implemented as a C++ library, for flexibility to deploy in a variety of different production environments. The algorithm was evaluated using a set of test data and performance metrics developed by the National Institute of Standards and Technology. The RAMP algorithm was able to build good quality pallets even in very reactive (limited knowledge) cases. Future work will include continued refinement of evaluation criteria to improve the quality score of planned pallets. The RAMP algorithm will also be subjected to wider testing under a variety of incoming package configurations. Further testing will also help better understand the effects of evaluation criteria parameters on the resulting pallet structure. Finally, optimization is required to reduce the planning time in applications with more knowledge and control over the incoming package stream. SwRI is actively seeking interest from industry organizations to integrate and test the RAMP algorithm in an automated palletizing work cell.

Feasibility Investigation of Determining the Condition of Distribution Equipment in Live Power Systems Using Radar Technology, 10-R8761

Principal Investigator
Jake Casey-Snyder

Inclusive Dates: 04/04/17 – 08/04/17

Background — An electrical power distribution system comprises thousands of pieces of equipment distributed across the system, from transformers to switch gear, reclosers, and line splices. These pieces of equipment, much like the power lines that connect these devices together, are expected to be in operation for decades. However, there is a menagerie of conditions that lead to unexpected equipment failure resulting in interruption of service for customers and loss of revenue to the company. Current devices used to determine equipment condition require specialized test equipment operated by personnel that may even need to de-energize the equipment for inspection. A solution that can monitor equipment condition on a live system that can operate is being sought by power utilities.

Approach — The objective of this research was to determine if the condition of equipment can be measured by injecting high-frequency signals into the device. The signals that are reflected and transmitted were collected and compared to a baseline signal to measure the response change as the conditions of a piece of equipment are altered. This project focused on a distribution transformer and a power line splice. The transformer was interrogated to characterize device loading. The splice was interrogated to determine installation status and temperature changes. Simulation of a distribution transformer was also carried out to determine the feasibility of modeling the high frequency response of distribution devices.

Accomplishments — This project successfully captured the characteristics of transformer loading and splice installation and temperature using high-frequency signal injection. Results from this research project were pivotal in positioning SwRI to competitively respond to a solicitation in August 2017 related to electrical power equipment health monitoring. Additionally, the successful completion of this project has strongly positioned SwRI to develop equipment health monitoring solutions for electrical power utilities and technology providers.

SOUTHWEST RESEARCH INSTITUTE®

2017 IR&D Annual Report

Investigation of the Use of Machine Learning to Traffic Profile Prediction Capabilities, 10-R8762

Principal Investigators
Adam K. Van Horn
David Vickers
Angela Bos

Inclusive Dates: 04/11/17 – 08/11/17

Background — This project focused on augmenting the current traffic profile prediction capability developed as a part of a previous research effort, Traffic Profile Prediction (10-R8548), with machine learning to facilitate real-time data processing and timely predictions while incorporating additional data sources such as local weather. For this effort, a subset of data from Florida Department of Transportation District 5 Interstate 4 (FDOT D5 I-4) corridor was selected consisting of average speed, volume, and occupancy, along with corresponding weather condition data for four consecutive detectors along the I-4 corridor, (1765, 562, 563, 564) for both eastbound and westbound lanes.

Approach — Two promising state-of-the-art deep-learning techniques, convolutional neural networks (CNN) and long short-term memory networks (LSTM), were selected for evaluation. Both techniques preserve either spatial locality or temporal locality of adjacent samples. Additionally, a combination of the two techniques, a convolutional LSTM, was evaluated as well.

Accomplishments — This research effort demonstrated the advantages of deep-learning approaches for traffic profile prediction, especially during transition periods between free flow traffic and congestion, where simpler techniques, such as auto-regressive integrated moving average (ARIMA), tend to lag behind.

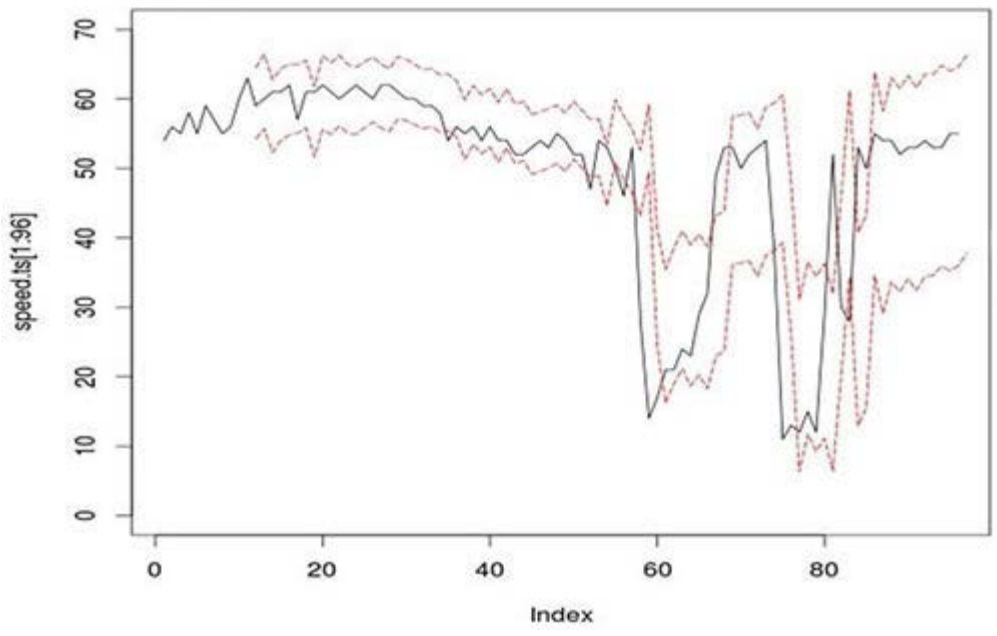

Figure 1: LSTM forecast

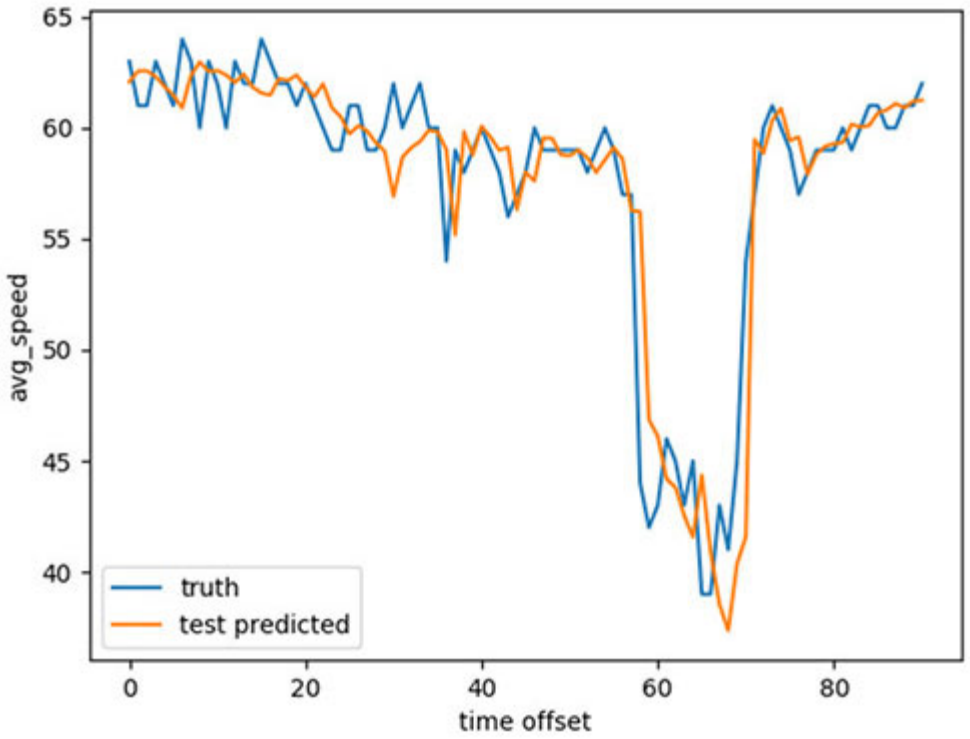

Figure 2: ARIMA forecast

2017 IR&D Annual Report

Investigation of the Application of Machine Learning to Distributed Temperature Sensing Data, 10-R8773

Principal Investigators
Maria Araujo
David Vickers
Heath Spidle
Samantha Blaisdell

Inclusive Dates: 06/05/17 – 10/05/17

Background — Between 2007 and 2012, leaks in the U.S. hazardous liquid pipelines network exceeded 100,000 barrels per year, a 3.5 percent increase from the previous five-year period. This expansion of leak events, combined with the increasing amount of pipeline infrastructure near urban centers and environmentally sensitive areas, has renewed the focus on the detection of leaks in hazardous liquid pipelines. One of the most prominent technologies currently being used for small leak detection is Distributed Temperature Sensing (DTS) systems, which comprise optoelectronic devices that measure temperatures by means of optical fibers functioning as linear sensors. In pipelines, a DTS cable containing fiber strands is placed next to and along the pipeline system. By utilizing Raman and Brillouin DTS, temperature changes can be detected along the pipeline against a pre-defined "baseline." These temperature changes, in turn, are used to detect and locate hydrocarbon leaks. However, these systems still have shortcomings in which leaks smaller than a certain size cannot be detected and, if the system's thresholds were lowered to detect those leaks, many false alarms would ensue. Rather than relying on thresholds and baselines, this research project investigated machine learning (ML) techniques for which classifiers could be trained to detect leak signatures to provide a more robust methodology for detecting leaks and also allow for the detection of smaller leaks than are currently detected by typical DTS systems, with low false alarm rates.

Approach — By leveraging approaches used in previous internal research projects 10-R8552 and 10-R8721, this research focused on:

- Investigation of the application of cluster-based classification ML techniques to the detection of pipeline leaks using DTS data.
- Investigation of state-of-the-art deep learning techniques for classification to support the detection of pipeline leaks using DTS data.
- Creation of an initial, proof-of-concept ML-based detection algorithm for leaks that exceeds the detection capabilities of current DTS systems.

Accomplishments — The project met its aforementioned objectives successfully. The proof-of-concept algorithm devised in this project resulted in a significant improvement over current state-of-art DTS algorithms by allowing the detection of several leaks that go undetected today by those algorithms. Additionally, the successful completion of this project has strongly positioned SwRI to develop capabilities for fiber-based pipeline leak detection technology providers.

SOUTHWEST RESEARCH INSTITUTE®

2017 IR&D Annual Report

Generation and Auto-Annotation of High-Precision Road Geometry Maps from Multi-Modal Sensor Data, 10-R8781

Principal Investigators
Kristopher C. Kozak
Marc Alban
Jerry Towler

Inclusive Dates: 07/01/17 – Current

Background — High-precision maps that define geometric features of a road network, such as lane centers, road boundaries, and traffic control devices like stop signs and crosswalks, are a key enabling technology for advancing the state of the art in ground vehicle automation. Existing mapping services, such as those from Google, HERE, and TomTom, rely on dedicated vehicles, expensive sensors, and teams of map editors to produce high-definition maps that are suitable for automated vehicles (AVs). Unfortunately, commercial map products have limited geographic availability and are typically not customizable, which significantly limits their usefulness outside of mainstream applications. Because of these constraints, a significant need currently exists for alternative mapping solutions that use sensors typically installed in AVs instead of specialized (and expensive) dedicated mapping systems.

There are several significant technical problems that must be addressed to create a fully functional and practical mapping system based on relatively low-cost, multi-modal sensors:

- Lower-cost sensors produce sparser, less-accurate measurements that are difficult to register together when measurements overlap (which can result in discontinuities and inconsistencies in the map).
- There are significant discrepancies between raw position measurements and local sensor registration, which must be resolved to create a consistent map.
- Auto-annotation of maps has been found to be very difficult and error-prone, so map annotation requires tooling for manual refinement.
- Extremely precise localization with respect to the map is required to take advantage of the precision and accuracy of the map.

Approach — To solve the identified problems, this project is focused on developing a novel combination of four techniques:

- Cross-modality feature matching to improve the accuracy of frame registrations.
- Nonlinear least squares optimization to optimize the map structure and improve overall precision and accuracy.
- Fully convolutional neural networks to automatically extract relevant road features and pre-populate map metadata.
- Centimeter-level precision localization, provided by SwRI's Ranger technology, to enable high-precision localization of map features with respect to a vehicle.

Accomplishments — This project is currently underway, so not all of the goals have been achieved. One major accomplishment to date is the development of a calibration tool for calibrating and aligning camera and Lidar sensors. This function is necessary for performing multi-modal sensor registration. Proper calibration and alignment is a prerequisite for collecting data for this project. Standard camera calibration methods and manual extrinsic parameter adjustment that have been used in the past could be performed

with several hours of effort; but, even in the best cases, yielded only a coarse "fit," which is not adequate for precision mapping.

The new automated process developed on this project enables calibration to be performed in real time, achieving calibrations that are much more accurate than previous methods in minutes rather than hours with measureable re-projection error statistics. As a result, this tool will not only facilitate the execution of this project, but also for calibrating almost any camera and Lidar pair, for which there are many applications outside of the mapping domain.

SOUTHWEST RESEARCH INSTITUTE®

2017 IR&D Annual Report

Multivariate Statistical Process Control for Cooling Towers, 14-R8656

Principal Investigators
Tom Arnold
David Ogden
John White

Inclusive Dates: 04/11/16 – 10/11/17

Background — SwRI operates 12 comfort cooling towers that support HVAC systems in office buildings on campus. Comfort cooling towers use approximately 20 percent of the cooling tower water consumed campus wide. SwRI operates 29 process cooling towers supporting labs in technical divisions. Process cooling towers use approximately 80 percent of the cooling tower water.

Cooling towers are managed, in part, by maintaining a target pH and conductivity level of the water in the tower. Fresh water, referred to as makeup water, can be added, or bleed water removed from the tower to maintain optimal levels. Prior to this project, pH, conductivity, makeup water usage, and bleed water readings were gathered by an outside contractor and reported on a weekly basis. This existing measurement and reporting process has missed system anomalies and resulted in significant water usage and financial costs to SwRI.

Approach — The objective of this project was to determine if multivariate statistical process techniques can be used to detect anomalies in cooling tower operation. Data on pH level, conductivity level, makeup water usage, and bleed water usage were collected in an automated fashion to enable the analysis and to perform more robust general monitoring. New communication cards were purchased and installed, meters were repaired, and sensors were connected to enable data collection.

Accomplishments — Analysis was performed to identify if the collected parameters could be used in multivariate anomaly detection. Because of incomplete water temperature readings at the time the project was completed, bleed water and makeup water were selected as the parameters to monitor with multivariate analysis. A calculation for the expected value of those parameters, each adjusted to average daily temperature, was identified. The difference between those calculated expected values and the actual measured value, delta x, for each parameter was then tracked. nSPCT multivariate analysis was used to monitor the difference between expected and measured bleed water usage (delta bleed), expected and measured makeup water usage (delta makeup), and the relationship of delta bleed to delta makeup each day. When performance of a tower exceeds the statistically established upper control limit for the monitored parameters, nSPCT signals an anomaly has occurred. Anomalies detected during the analysis phase to date have typically pointed to failing meters or installation issues (Figure 1). This tool will enable maintainers to detect malfunctioning equipment in the cooling tower system more quickly and easily, and with less manpower.

Completing the collection and integration of cooling tower supply and return temperature values is being carried on as additional research. The addition of these values will allow better calculations of the expected bleed water and makeup water volumes and provide monitoring that is more sensitive to change. This will provide greater coverage of the overall system and more sensitive anomaly detection.

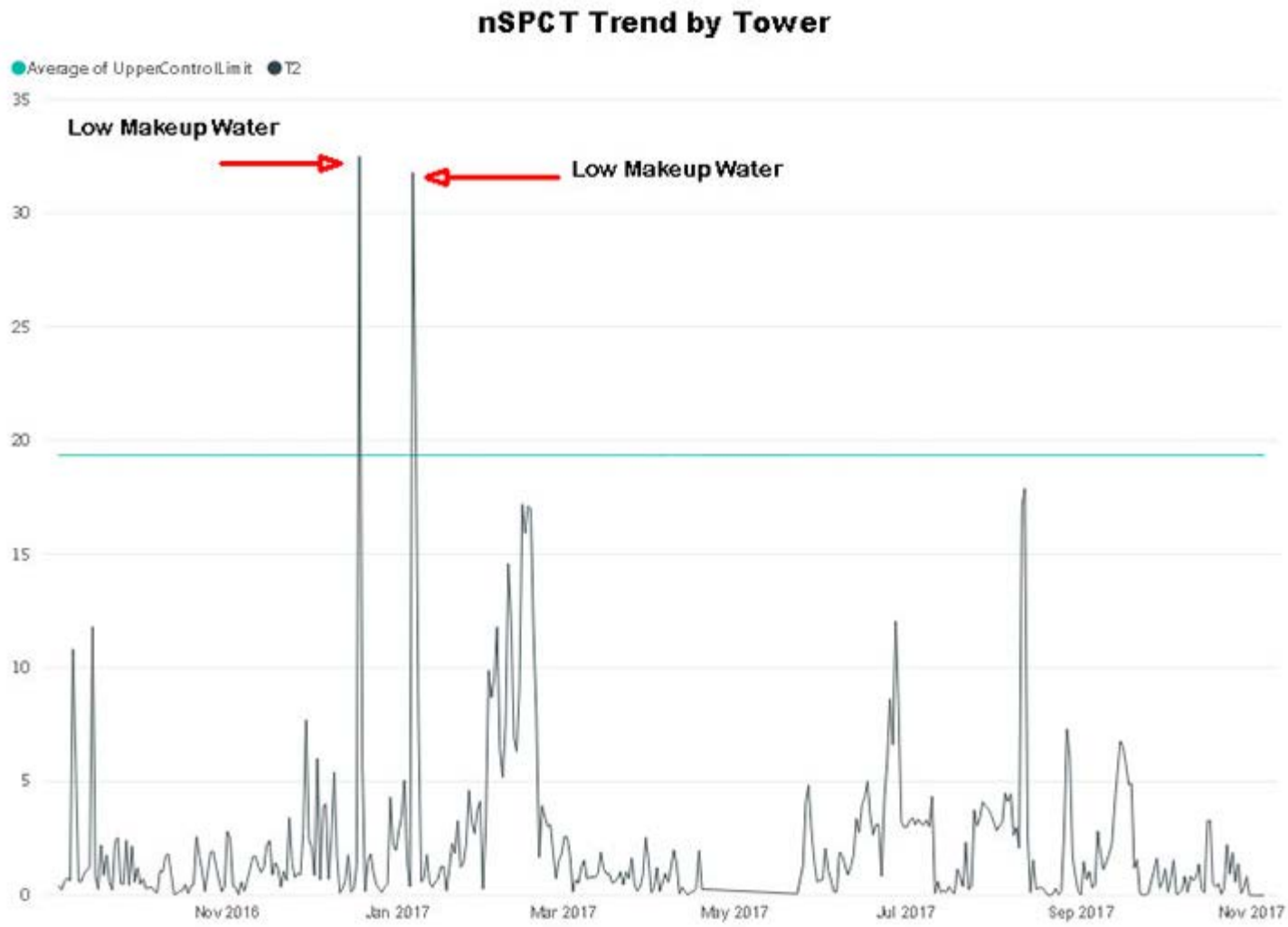

Figure 1: Detected anomalies during analysis phase.

2017 IR&D | IR&D Home

SOUTHWEST RESEARCH INSTITUTE®

2017 IR&D Annual Report

Fusion of Intelligence Data from Observables, 16-R8670

Principal Investigators
Jody Little
Spencer Vogel

Inclusive Dates: 06/22/16 – 10/22/16

Background — The focus of this project was to investigate methods to automate a manual work flow that is commonly performed by intelligence analysts. The work flow consists of a federated search among distributed information sources in different cloud-based data stores, semantically and contextually fusing the results, then generating human readable text-based synopses describing the results. Federated search is an information retrieval method that allows many disparate and heterogeneous information sources to be searched in parallel using a single query with the results being aggregated into a single cache. Semantic fusion is an information aggregation method that associates, correlates, and fuses data based on the meaning or intent of related data elements. Contextual fusion is an approach that associates and correlates data and information based on the context of how individual results relate to other results. Federated searches with subsequent semantic and contextual fusion are traditionally done by human intelligence analysts. However, with the growth of "big data" collection and storage, processing and exploiting large volumes of data that are scattered across many sources is an overwhelming and time-consuming task that, in many cases, is nearly intractable for humans to perform without missing key relationships. A goal of this project was to investigate and create automated capabilities to perform this cerebral task, and then provide intelligence analysts with linked synopsis of the results.

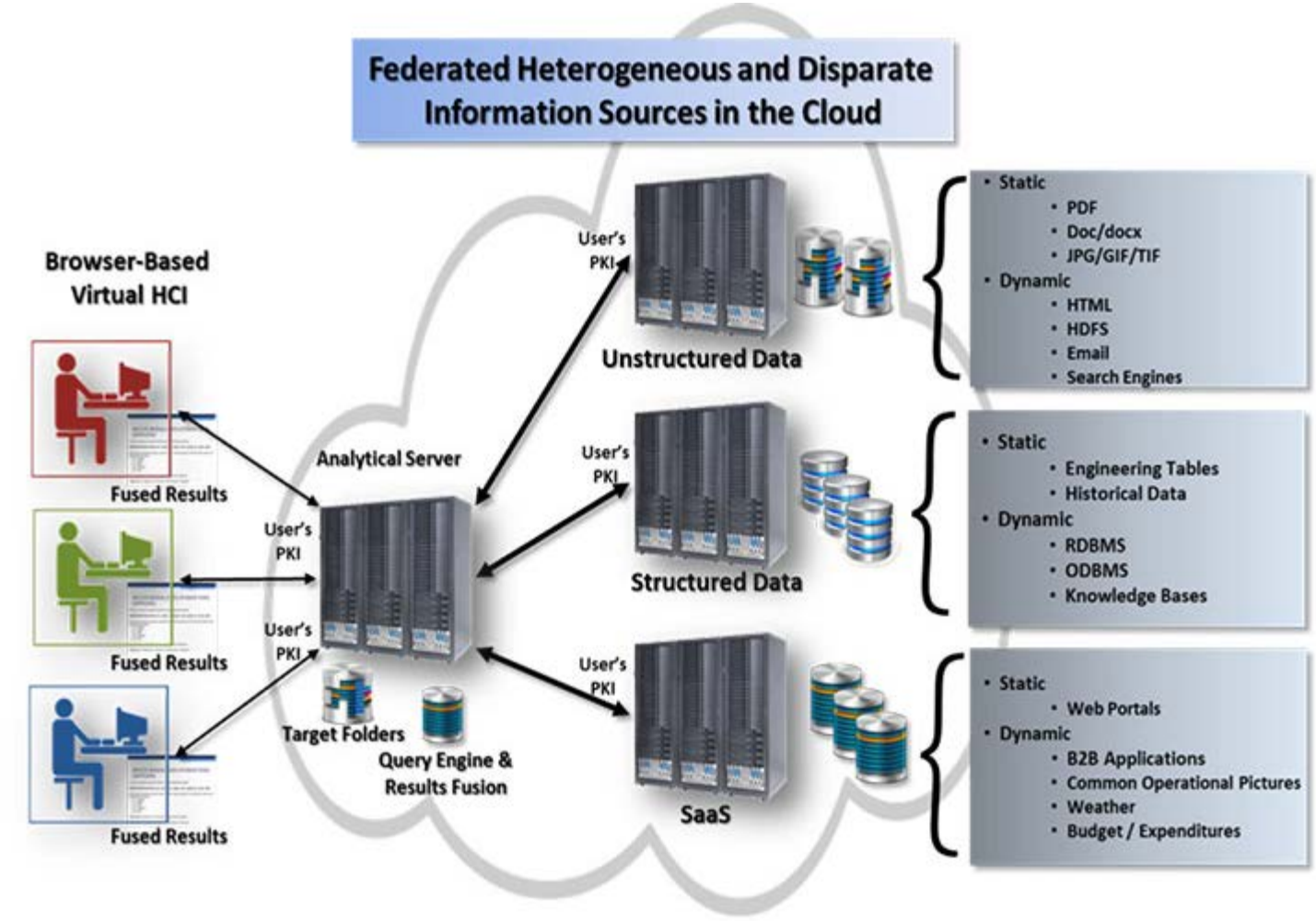

Figure 1: Intelligence exploitation is accomplished by individually searching federated information sources distributed across the entire intelligence community cloud, semantically and contextually fusing the results, and then autonomously generating text synopsis of the fused results in sentence and paragraph form.

Approach — This three-phase project began with an investigation of contemporary federated search capabilities and approaches currently in use on the World Wide Web. These search systems typically provide indexing and fast querying of disparate information sources. Because intelligence community clients desire open-source solutions, the team focused on open-source aggregation software during the first phase of the project. In the second phase, the research team studied and experimented with open-source semantic fusion systems that employ semantic networks to associate and correlate data. The team also worked with contextual fusion approaches developed in prior SwRI projects to fuse result elements based on their contextual relationships. An ontology was created and used to experiment with the contextual fusion approach. During the third phase, the research team studied and experimented with automated text summarization approaches that generate a topical synopsis from the fused search results. The automated text summarization approach was further explored to determine if a "summary of summaries" adequately provided a usable overview of all results.

Accomplishments — The project achieved the primary objectives of evaluating federated search approaches and tools, and evaluating semantic search approaches and tools to form a semantically enabled federated search and data fusion capability. The research team implemented federated search through a combination of web crawlers and direct-query agents that returned their results to Apache SOLR caches. Apache SOLR is an open-source search platform that indexes search results from multiple sites and returns recommendations for related content based on the search query's taxonomy. The SOLR application was extended to support indexing based on semantics among the data elements in the cached results. The research team also experimented with extending the cached SOLR results into ontology

representation and linking result elements contextually. This approach showed positive results, but it is highly language dependent because it requires the ontology to represent meanings of words in various contexts. Different languages often use varying contexts for meanings of words and phrases. The research team implemented automated text summarization and synopsis algorithms to provide synopses of fused search results in human readable form that is easily digested and understood by intelligence analysts. Since investigative intelligence analysis is often conducted using many different searches, fusion of multiple searches is also required. The research team also investigated and experimented with an automated summary of summaries to provide a high-level yet accurate overview of a particular search topic. The capabilities investigated and experimented within the research project are of contemporary interest to the intelligence community.

SOUTHWEST RESEARCH INSTITUTE®

2017 IR&D Annual Report

Development of an Omnidirectional MsT Probe for Guided Wave Testing of Plates, 18-R8707

Principal Investigator
Sergey Vinogradov

Inclusive Dates: 11/29/16 – 11/29/17

Background — The majority of vessels in processing plants such as refineries, chemical plants, electric power generation plants, and ships are manufactured from large plates welded together. Due to large surface area and access limitations, conducting nondestructive testing of these components is costly and time consuming using conventional inspection techniques such as eddy current testing, magnetic flux leakage, and bulk wave ultrasonic testing. Guided wave testing is an emerging method used to inspect these types of structures because of its ability to inspect comparatively larger areas from a single sensor location. The purpose of this project was to develop an omnidirectional guided wave probe with high circumferential resolution and automatic data collection, and to process the signals using synthetic aperture focusing technique (SAFT) imaging.

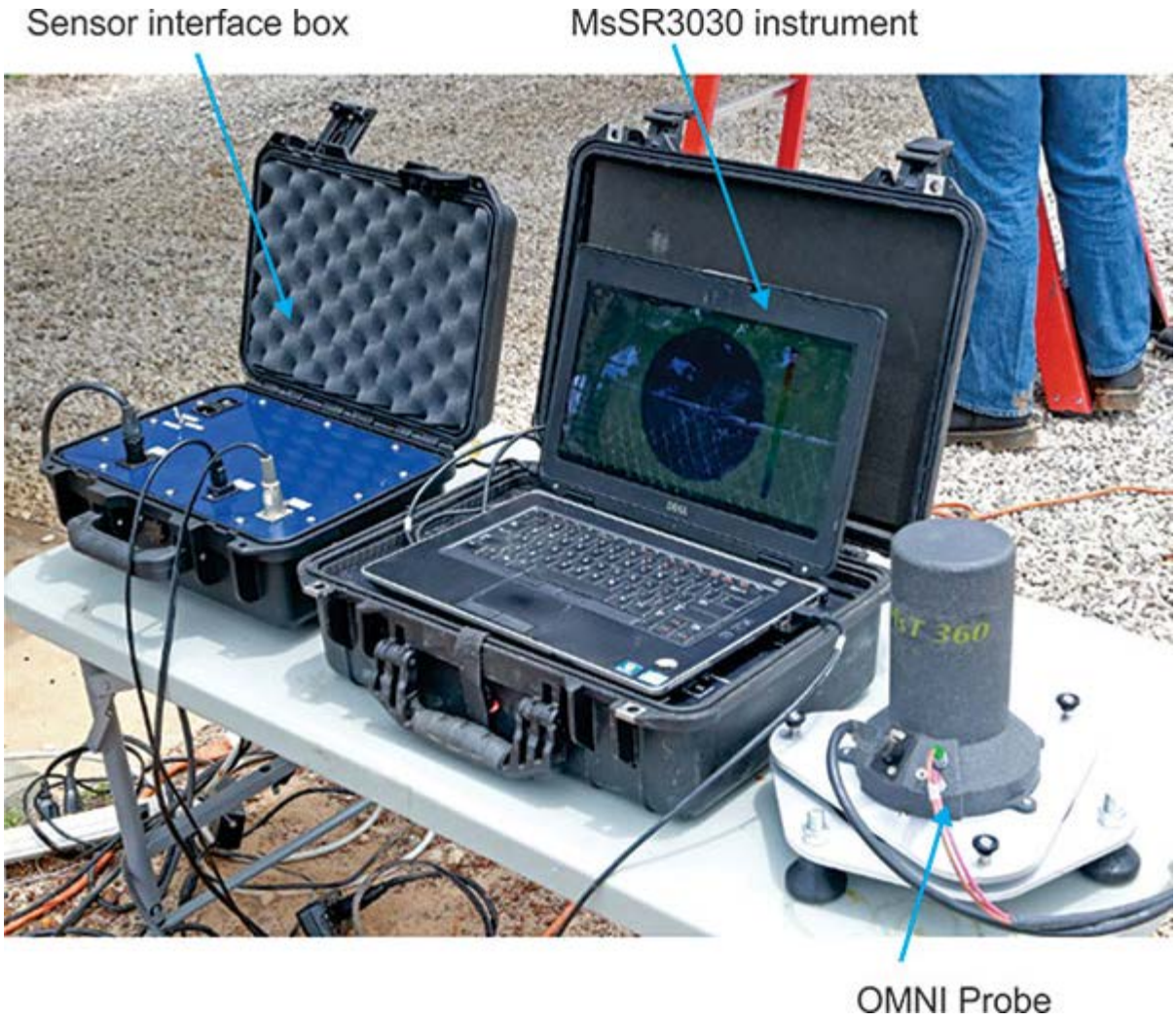

Figure 1: Omnidirectional probe package including a sensor interface box, MsSR3030R instrument and the production MsT360 probe.

Approach — A rotating plate MsT probe was used. The advantage of using plate MsT probes is that they have well-known beam characteristics in a wide frequency range. The probe uses a protective thin-wall metal cap between the probe and the tested structure and two layers of shear wave couplant – one layer between the probe and the metal cap and another layer between the metal cap and the tested structure. The data acquisition software and hardware were developed. For a field ruggedized version of the probe, a battery-operated sensor interface (motion control) box was fabricated. Data analysis software was developed in C++. The software allows for generating a report based on indications specified by the operator. SAFT imaging processing is embedded in the software for enhanced resolution. Figure 1 shows a sensor interface box, MsSR3030R instrument, and MsT 360 omnidirectional probe.

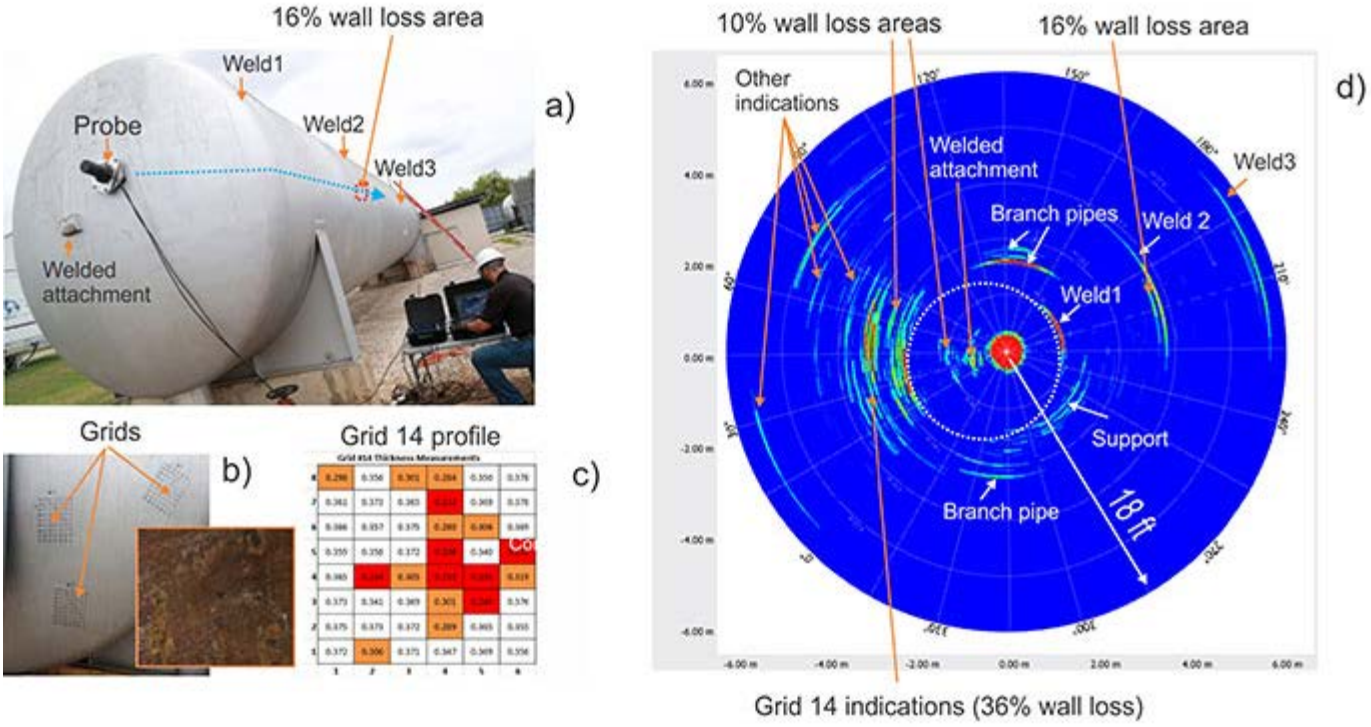

Figure 2: Testing on the storage tank: (a) omnidirectional probe mounted on the side cap of the tank, (b) grids used for taking UT readings in the areas with corrosion damage and a picture of corrosion, (c) corrosion profile of grid 14, (d) B-scan image of acquired data taken at 60 kHz center frequency.

Accomplishments — Testing on a retired storage tank showed the probe's ability to inspect over 1,000 square feet of structure surface within a 15-minute time frame. This coverage is more than three times the initial goal of this project (300 square feet). Figure 2 shows (a) an omnidirectional probe mounted on the side cap of the tank, (b) grids used for taking UT readings in the areas with corrosion damage and a picture of corrosion, (c) a corrosion profile of grid 14, and (d) a B-scan image of acquired data taken at 60 kHz center frequency. Testing of the probe on a mockup with known anomalies indicated that the smallest anomaly that was detected on 0.5 inch wall mockup at a 60 kHz test frequency was a 15-percent deep, 0.4 inch-diameter flat bottom hole located 6 feet from the probe.

On 24 inch OD pipe mockup with 0.25 inch wall thickness, the probe demonstrated high sensitivity to pitting type of corrosion with the depth starting from 0.5 mm (7 percent wall loss) when a short (3 feet) test range was used. Helical propagation pass of guided waves utilized by the probe makes it a very effective tool in finding corrosion and cracking in areas with complex geometry such as pipe supports (including welded supports) clamps or seam welds.

2017 IR&D Annual Report

Experimental Investigation of Co-direct Injection of Natural Gas and Diesel in a Heavy-duty Engine, 03-R8522

Principal Investigator
Gary Neely

Inclusive Dates: 01/01/15 – 12/31/16

Background — For the U.S. market, an abundant supply of natural gas (NG) coupled with recent greenhouse gas (GHG) regulations have spurred renewed interest in dual-fuel combustion regimes that utilize NG for the heavy-duty truck market. The GHG regulations stipulate that by 2017, truck engines shall emit 6 percent lower CO_2 emissions than the reference 2010 engines with an additional 6 percent reduction required by 2027. Combustion of methane (CH_4), the main constituent of NG, produces up to 20 percent lower CO_2 emissions due to its higher hydrogen content compared to diesel. However, because the NG is injected into the intake manifold, a homogeneous NG and air charge are subject to the compression process, packing some of the charge into piston crevice regions that are difficult to oxidize during the combustion process. These crevice losses lead to reduced engine efficiency and unburned CH_4 emissions that essentially offset the benefit of reduced CO_2 emissions of NG combustion, as methane is thought to have a strong global warming potential.

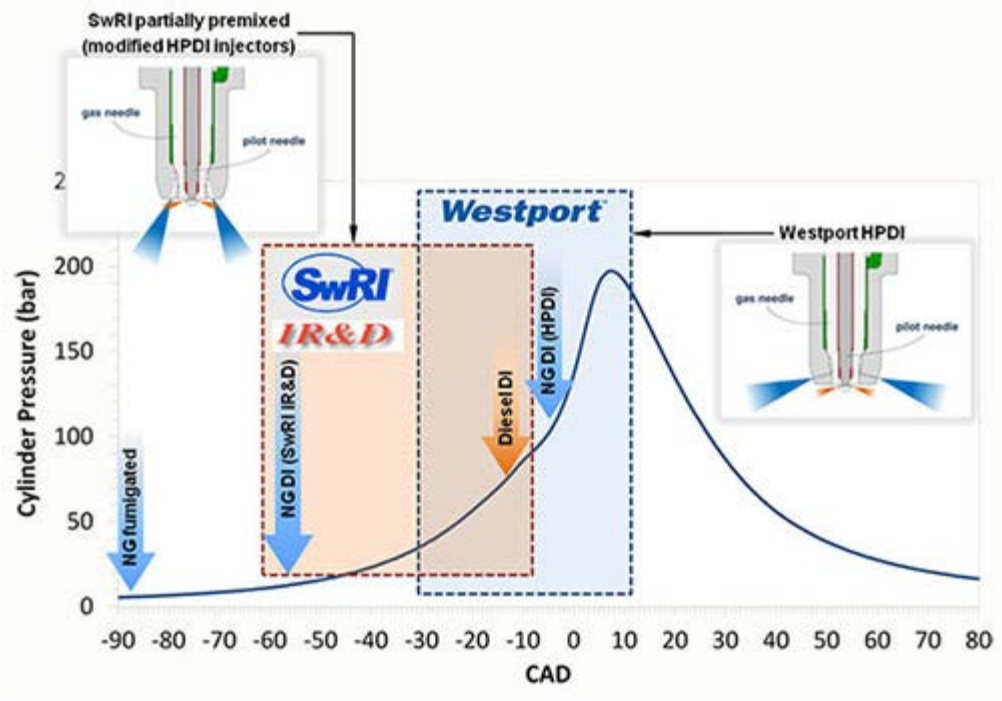

Figure 1: Dual-fuel Injection strategies. HPDI is production strategy while DI^2 is the strategy studied in this project.

Approach — This project was aimed at leveraging the unique co-direct-injection capability of the Westport™ High Pressure Direct Injection (HPDI) system to reduce the fuel penalty and methane

emissions associated with traditional introduction of natural gas (NG) in dual-fuel engines. The HPDI system was used to control the amount of NG pre-mixing by injecting NG during the compression stroke, which reduced the crevice packing issue of fumigated NG. The injection strategy investigated in this project, called DI^2, differed from the production HPDI strategy, as illustrated in Figure 1.

Accomplishments — By operating in the DI^2 combustion mode with the baseline injection nozzles, the engine efficiency was improved by more than 2.5 brake thermal efficiency points compared to the most efficient operation using the HPDI combustion strategy. At the same time, the measured combustion efficiency was improved to 98.6 percent, up from 97.1 percent measured for an equivalent fumigated combustion strategy. The improved combustion efficiency led to a 50 percent reduction in unburned CH_4 emissions compared to fumigated engine operation. In addition, modified injection nozzles with a narrower NG spray angle than the baseline injector (see Figure 2) were procured and evaluated on the engine to determine if further combustion loss reductions were available. As shown in Figure 3, the modified nozzles provided an additional 50 percent reduction in combustion losses at the engine condition tested.

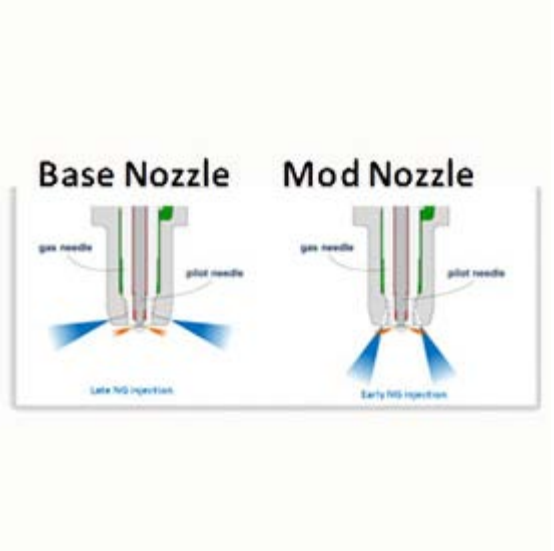

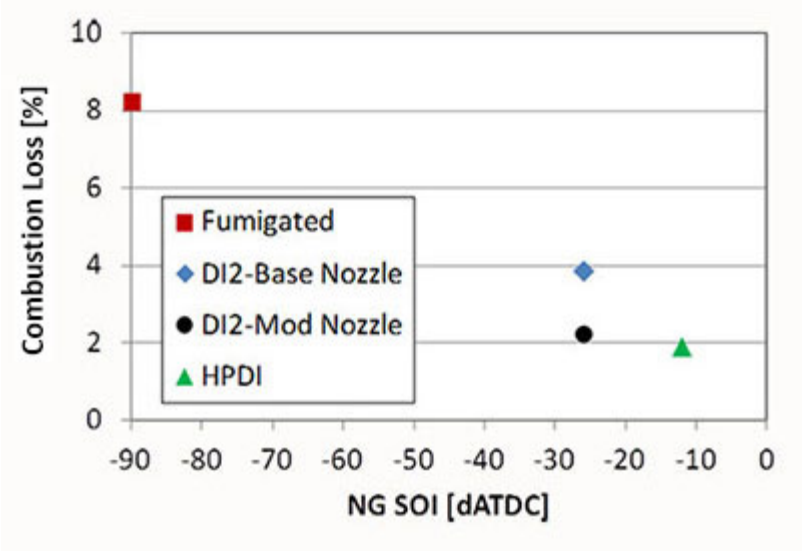

Figure 2: Baseline and modified injection nozzles.

Figure 3: Combustion losses for various dual-fuel combustion strategies at 1,500 rpm/9 bar BMEP: Fumigated, HPDI, and DI^2 with baseline and modified nozzles.

The results confirm that significant reductions in unburned CH_4 emissions can be achieved for dual-fuel combustion with advanced injection technologies, positioning the dual-fuel engine well for meeting future GHG regulations.

SOUTHWEST RESEARCH INSTITUTE®

2017 IR&D Annual Report

Investigation of the Durability of High-Efficiency Gasoline Engines, 03-R8596

Principal Investigators
Barry Westmoreland
Eric Randolph
Craig Wileman

Inclusive Dates: 10/01/15 – 04/03/17

Background — Two potential risks to adopting high-efficiency gasoline engine technologies that have been developed at SwRI are: The impact of rich operation on the durability of power cylinder components in Dedicated Exhaust Gas Recirculation (D-EGR) engines, and the potential for corrosion and condensation damage in the low-pressure EGR loop in High-Efficiency Dilute Gasoline (HEDGE) engines. These concerns are not limited to a specific engine type; rich operation concerns can arise in HEDGE engines, and the corrosion and condensation damage can arise in D-EGR engines at a lower level of risk. As SwRI works with clients to commercialize these technologies, their impact on durability needed to be understood and quantified.

Approach — The durability evaluation of a D-EGR engine was done using Radioactive Tracer Technology (RATT) in a 2.0L engine previously used as a development platform for D-EGR technology. The RATT process consists of creating labeling isotopes for unique engine parts of interest. As these parts wear, wear particles carrying the isotope markers build up in the lubricating oil and are circulated past a gamma ray detector that measures the occurrence of decay emissions of the radioactive isotope (Figure 1). By using different isotopes in the fuel-rich dedicated cylinder compared to the remaining stoichiometric cylinders, differences in wear rate were discernible in response to test control variables.

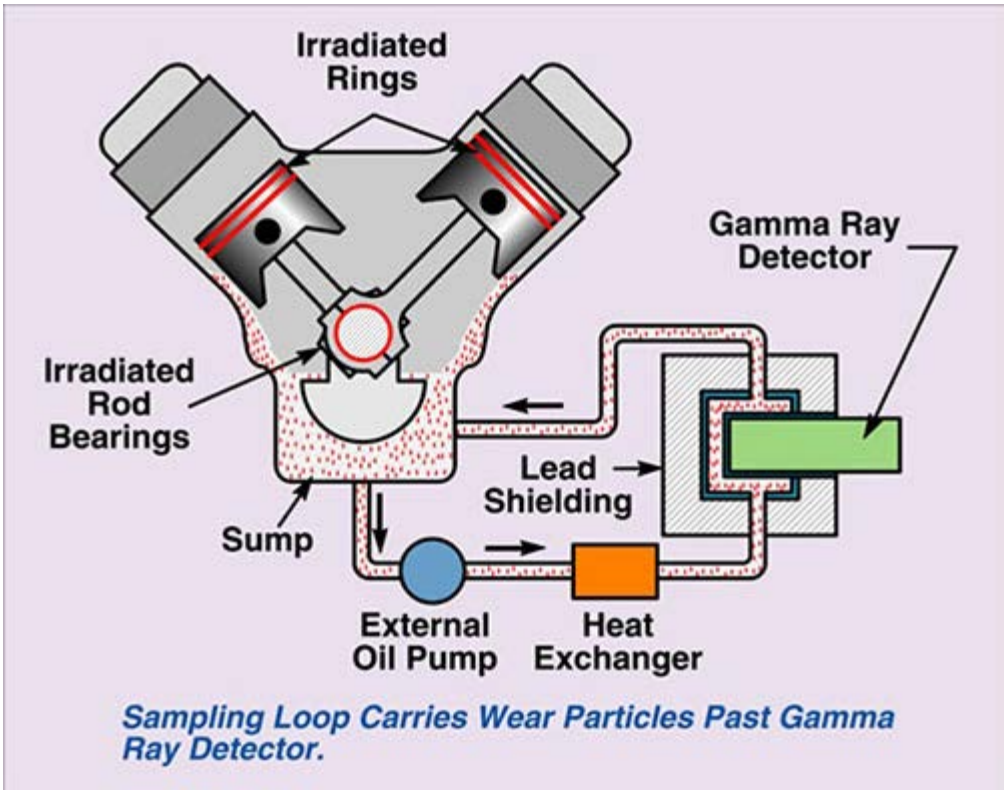

Figure 1: RATT indirect measurement orientation

The condensation and corrosion investigation was done using a different 2.0L engine previously used as a development platform for HEDGE technologies. The investigation involved analytical modeling to predict acid formation and the use of SwRI-developed corrosion probes, such as those shown in Figure 2, to measure *in-situ* corrosion rates under environmental and fuel chemistry parameter sweeps.

Accomplishments — The D-EGR durability study revealed a few areas of increased wear for the dedicated cylinder beyond the wear measured for the stoichiometric cylinders, but also found some conditions where the dedicated cylinder wear rate was below those of the stoichiometric cylinders. The findings could be used to further refine control strategies and power cylinder materials, yet no data gathered in this study suggested that D-EGR technology negatively affects overall engine durability.

Figure 2: Examples of multi-electrode corrosion probes

In the HEDGE engine evaluation, no corrosion was found based on the electrical current measured by the corrosion probes downstream of either the charge air cooler or the EGR cooler, even while condensate was present. Visual inspection of the corrosion probes also showed no physical evidence of corrosion and their current density was below what is generally expected for stable corrosion to occur. The overall results indicated that corrosion is not expected for condensate from EGR in a stoichiometric spark-ignited engine, even with gasoline fuels containing high levels of sulfur.

SOUTHWEST RESEARCH INSTITUTE®

2017 IR&D Annual Report

Advanced Model-Based SCR Controller for Advanced Multiple Component Catalyst Systems, 03-R8599

Principal Investigator
Christopher Sharp

Inclusive Dates: 10/01/15 – 10/31/16

Background — Over the course of the next 5 to 10 years, a new phase of more stringent emissions standards for NO_x is being implemented by the California Air Resources Board (CARB) and Environmental Protection Agency (EPA). These standards will require NO_x reduction efficiency more than 99 percent over certification test cycles, and greater than 99.5 percent when the system has achieved operating temperature. This will require the catalyst system to operate at high efficiency at temperatures well below the current mark of 200°C, a requirement that is triggering significant new Selective Catalytic Reduction (SCR) technology development. These new technologies and operating temperatures will place new requirements on the system controller. In addition, a high-performing system will need to have precise controls to maintain near complete conversion of NO_x, while at the same time avoiding undesirable secondary emissions of NH_3 and nitrous oxide (N_2O). To meet these challenges, NO_x emission controls systems will evolve with advanced technologies, multiple NO_x reduction devices and multiple NH_3 input locations are being proposed and evaluated. With the extensive system variations possible, there is a need for a flexible SCR controller that can be readily adapted to variety of different system configurations. This presented an opportunity for SwRI to develop such a control tool for multiple future emission control research and development projects.

The goal of the project was to develop a novel, modular SCR controller that would be adaptable to multi-bed catalyst systems. The core of the controller is a physics and chemistry-based kinetic model, but it is important to note that this is a "controls oriented" model, and therefore it must balance model fidelity with the ability to execute in real time using the computing resources available on an engine control unit (ECU). This implies a compromise between model complexity and execution time, and results in the need to use experimental data to empirically calibrate the model's kinetic constants. In addition, to provide precision control under real operating conditions, a robust real-time feedback mechanism would be needed.

Approach — The initial approach was to leverage previous model-based control efforts at SwRI to provide initial models. Data to support the development and calibration of the final model was provided by the unique facilities available at SwRI, including the Universal Synthetic Gas Reactor® (USGR®) and the Exhaust Composition Transient Operation Laboratory™ (ECTO-Lab™). State-of-the-art catalysts were available for this program for the Low NO_x development efforts that were being conducted on behalf of CARB. Based on the initial experimental data from the USGR, it became apparent that the previous models would not be sufficient, and therefore a new model was developed.

The basic objective of the urea dosing controller is to maintain a desired level of ammonia coverage on the SCR catalyst to achieve maximum reduction of NO_x. A schematic of the controller is given in Figure 1. The SCR model incorporates both a thermal component and a kinetic component. These are calibrated to each SCR catalyst using data from the USGR and the ECTO-Lab. For this program, the final calibrations were fine-tuned on an engine, but in the future these additional tuning experiments can be incorporated into the USGR and ECTO-Lab facilities. The model was used as a "coverage observer" within the controller, essentially providing a virtual feedback sensor for NH_3 storage, which cannot be measured. The model is a

0-D model, but several model elements are used in series to create a 1-D model of NH_3 coverage in the axial direction for each catalyst. This allows for precise prediction of spatial coverage on each catalyst bed that is modeled. The controller is calibrated to a given engine by supplying the catalyst dimensions, and then setting control loop gains and coverage targets based on laboratory testing of the system on engine.

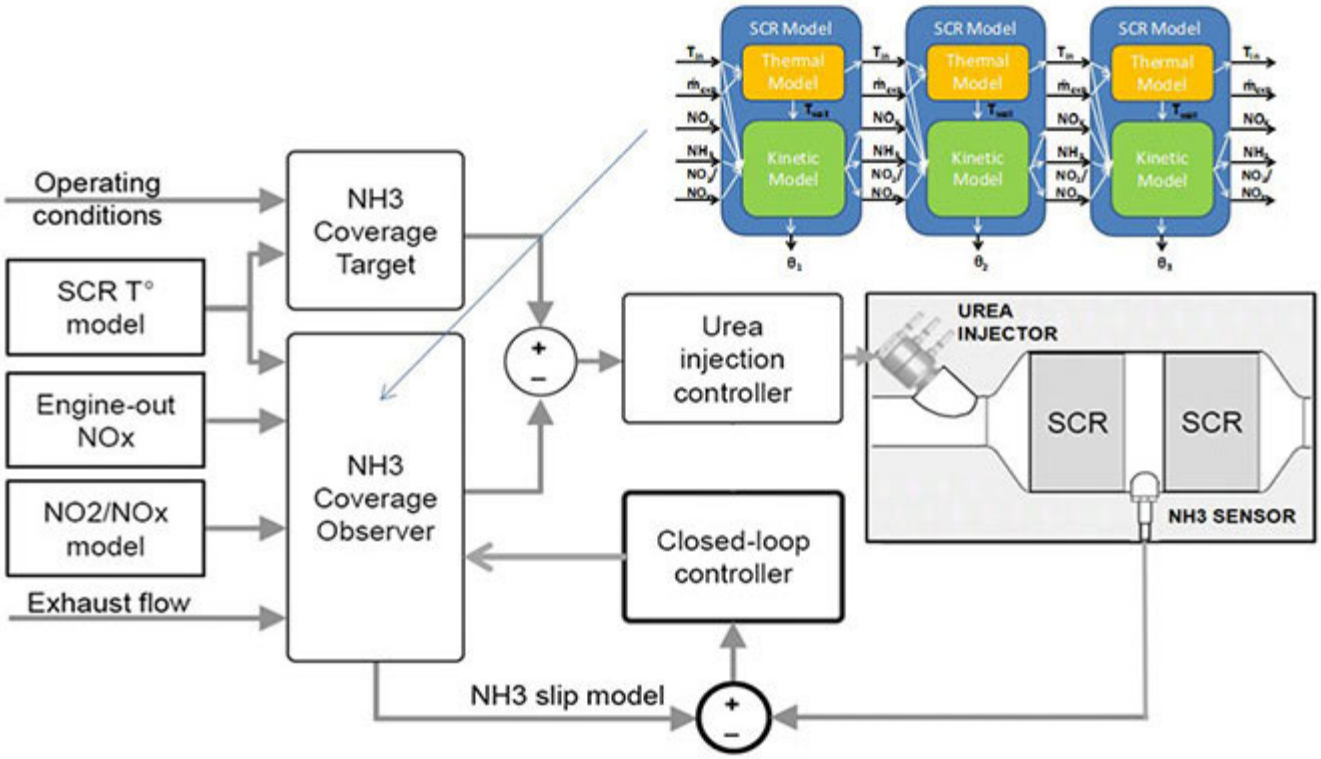

Figure 1: Advanced SCR model-based controller schematic

To enable maximum precision for very high NO_x reduction targets, more than 99.5 percent, a production ammonia sensor was used as a robust feedback mechanism. The sensor value is used to correct the model coverage estimates by comparing the model predicted NH_3 value at the appropriate location to the sensor value. This can be done in real-time to account for any model or measurement errors. As catalyst conditions change, the controller is continuously adjusting the NH_3 coverage on the catalysts to maintain optimum levels for maximum NO_x reduction and minimum NH_3 slip.

Accomplishments — The controller was successfully developed and calibrated to a set of advanced catalysts utilized in the CARB Low NO_x Demonstration program. They achieved high levels of NO_x reduction over a wide variety of duty cycles, using a single calibration. The capability of the controller allowed the demonstration test engine to achieve the goal of reaching a tailpipe NO_x target of less than 0.02 g/hp-hr, which is 90 percent below the current limit for heavy-duty engines. The controller reliably maintained tailpipe levels to below 0.01 g/hp-hr during operation under a variety of different duty cycles. A calibration process was developed to allow the control model to be adapted to other engines, catalysts, and applications.

SOUTHWEST RESEARCH INSTITUTE®

2017 IR&D Annual Report

Fast Catalyst Light-Off on a Heavy-Duty Natural Gas Engine, 03-R8620

Principal Investigator
Tom Briggs

Inclusive Dates: 01/01/16 – 12/31/16

Background — The purpose of this project is to develop methods for achieving faster light-off of the emissions catalyst on a heavy-duty natural gas engine, with less fuel consumption penalty than is possible with conventional engine controls. For emissions certification in the U.S., a heavy-duty engine is tested on the heavy duty federal test procedures (HD-FTP) test cycle, as shown in Figure 1. In this test procedure, it is critical to get the catalyst temperature up to 400°C as quickly as possible to control the emissions or the engine will not pass the test. In a demonstration project that SwRI has been executing for the California Air Resources Board (CARB), the tailpipe emissions from a 12-liter displacement natural gas engine have been reduced from the current requirement of 0.2 g/bhp-hr to 0.02 g/bhp-hr. In the process of achieving this reduction, the fuel consumption over the HD-FTP test cycle had to be increased by 2 percent to heat the catalyst quickly enough. This increased fuel consumption is not acceptable in a production system as the U.S. EPA is now targeting a 5 percent reduction in engine fuel consumption as part of new CO_2 standards. As most of the additional fuel consumption is in the first 20 seconds of the test cycle in order to heat the catalyst, this research was undertaken to develop other approaches to heating the catalyst that would have less or no fuel consumption penalty.

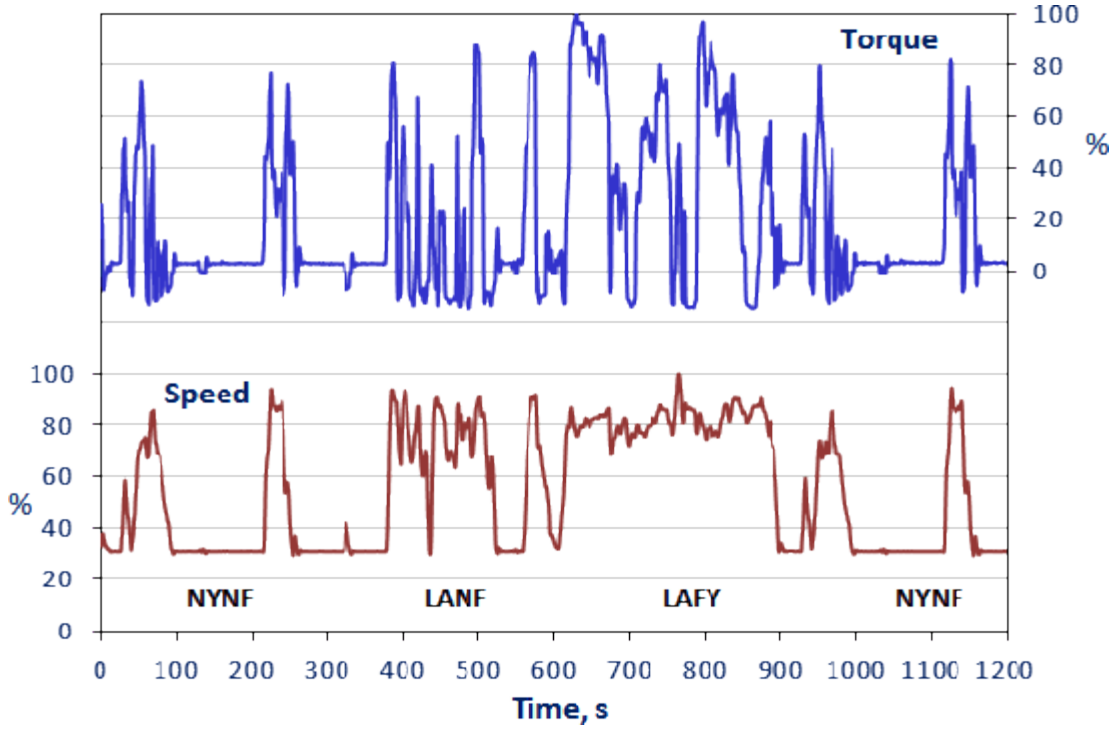

Figure 1: Heavy-duty engine Federal Test Procedure test cycle.

Approach — It is already known that most three-way catalyst formulations will allow the oxidation of H_2

and O_2 at very low temperatures (<100°C). Under normal circumstances an engine produces very little H_2 in the exhaust, but the Dedicated EGR development at SwRI has shown that significant H_2 production is possible under rich combustion. The first stage of the research is to characterize the catalyst response to these rich combustion products. This will provide guidance as to how the engine needs to be run to achieve fast catalyst heating. The next phase of the project is demonstrating methods for providing the rich products of combustion to the catalyst with less fuel consumption penalty. One strategy is to run the engine rich, but to use an air pump to supply additional air to the catalyst where it can react with the rich combustion products. This solution has been used in the light-duty gasoline engine industry before, but is relatively untested for heavy-duty engines. The other approach is to run the engine with three cylinders lean and three rich. This is expected to provide both H_2 and O_2 to the catalyst with minimal fuel consumption penalty and is expected to provide a path to extremely low engine emissions with good fuel consumption.

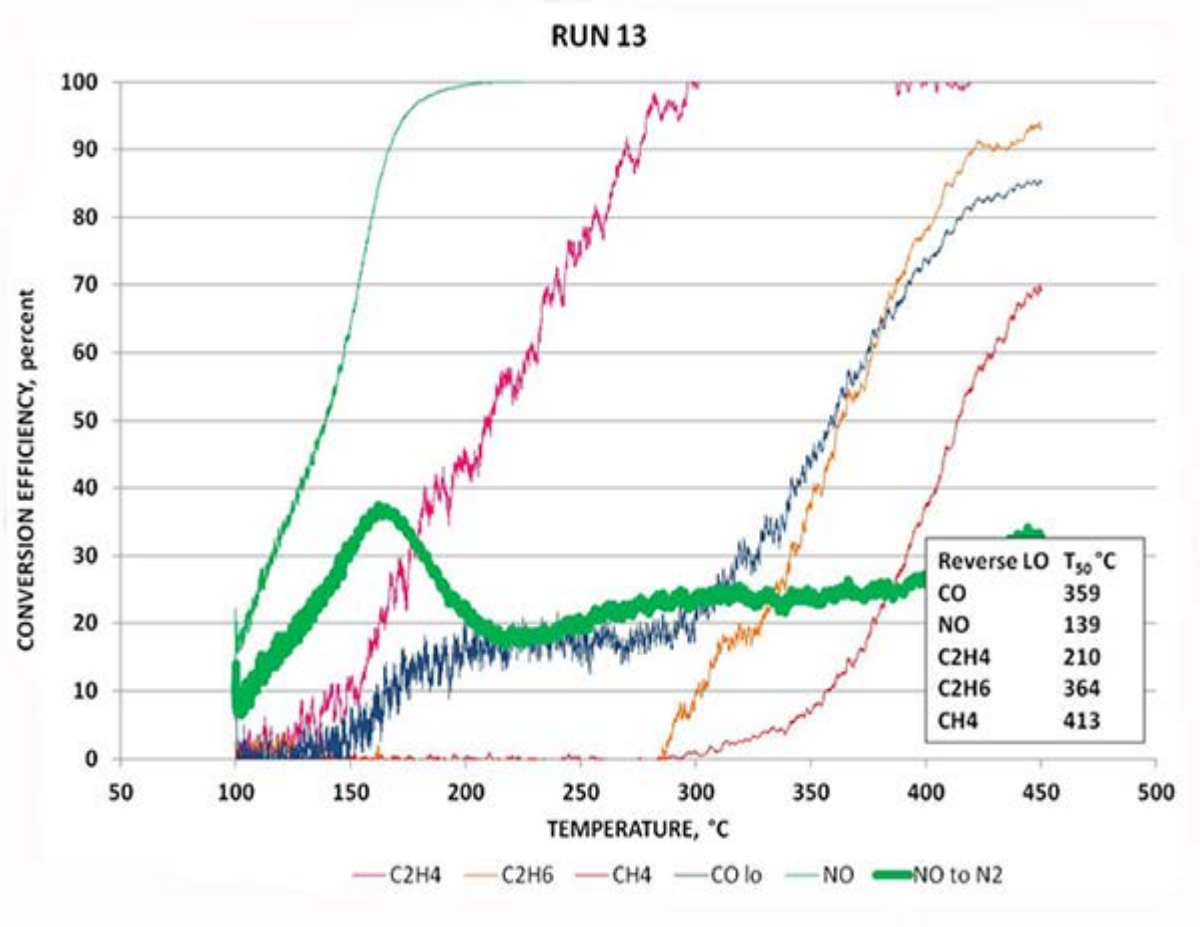

Figure 2: Catalyst bench testing.

Accomplishments — The catalyst bench testing has been completed, with suitable engine-out gas compositions identified. An example result is shown in Figure 2, which simulates operation at the rich combustion end of the intended study. It can be seen that the NO reduction begins at 139°C, which is significantly lower than for non-rich conditions. This result will guide our work to demonstrate on-engine solutions that can help achieve future emissions and fuel economy goals.

SOUTHWEST RESEARCH INSTITUTE®

2017 IR&D Annual Report

Dynamic Fast Charging of a Battery Pack without Significant Degradation in Capacity and Power Capability, 03-R8647

Principal Investigator
Bapi Surampudi

Inclusive Dates: 04/01/16 – 04/01/17

Background — Electrification of vehicles is becoming a more common way of meeting CAFE (Corporate Average Fuel Economy) standards and reduction of overall CO_2 emissions requirements. One of the challenges of designing an energy storage system for electric vehicles is to guarantee its life for the warranty period, while minimizing wait time during charging. Today, the state-of-the-art DC superchargers for the Tesla Model S can only charge up to 50 percent capacity in 20 minutes. The project utilized the Panasonic 18650 Tesla battery and focused on minimizing charge time. This battery uses the Nickel-Cobalt-Aluminum (NCA) chemistry.

Approach — SwRI identified six new charge profiles based on a deeper understanding of specially conducted calorimeter experiments that indicated different reaction characteristics during the charge process. Until a threshold state of charge (SOC), the reaction was predominantly endothermic. After reaching a threshold SOC, it turned exothermic as a function of SOC and at various levels of intensity. The endothermic SOC window is a good opportunity for high-current charge without increasing cell internal temperature. Through this research, charging algorithms were obtained as a function of SOC, end-of-charge voltage, and temperature. Moreover, the experiments indicated temperature regions suitable for most efficient charging, and resulted in directions for innovative thermal management.

The six new charge profiles along with two state-of-the-art profiles were used to conduct extensive life cycling tests (Figure 1). One aged sample from each charge profile was subjected to lithium plating (Figure 2) and the other to an overcharge tolerance test. The magnitude of rate of change of voltage with respect to charge (dV/dC) after aging is a proportional indication of magnitude of lithium plating damage. Four of these profiles (Table 1)

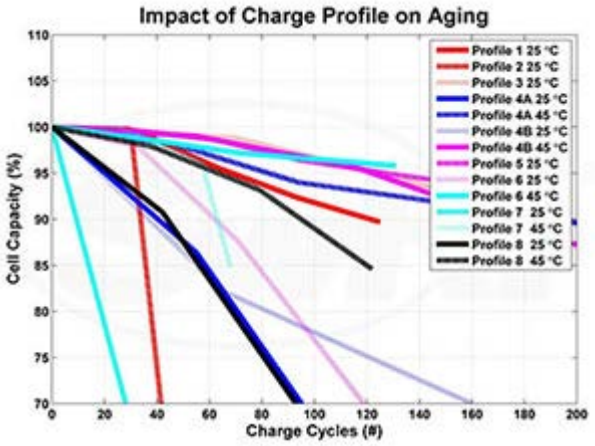

Figure 1: Impact of charge profile on aging.

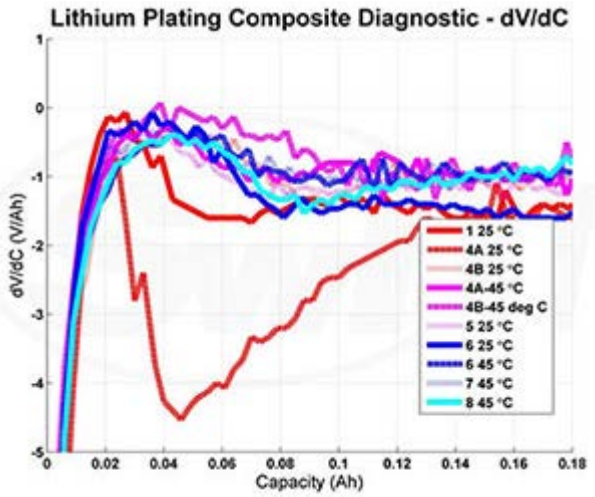

Figure 2: Lithium plating in cells aged with different charge profiles.

look promising in terms of a tradeoff between charge accepted, charge time, risk and aging. A normalized version of one of these best-candidate normalized charge profiles is shown in Figure 3. The profiles that are not acceptable mostly use aggressive current at room temperature.

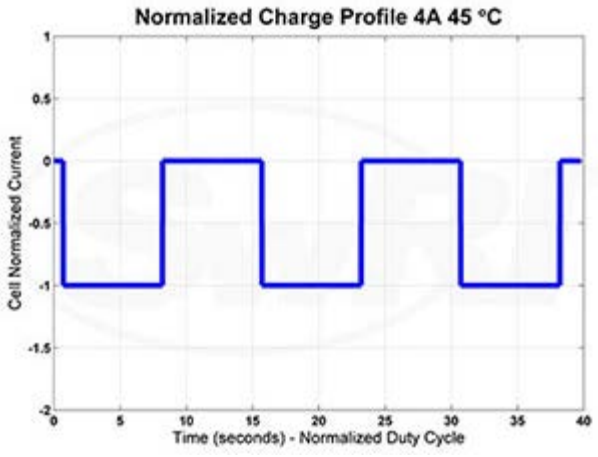

Figure 3: A best-candidate normalized charge profile.

Accomplishments —

- A pure constant voltage mode charge strategy to reduce charge time significantly for applications with no life requirements
- A test and analysis method to identify maximum current based on naturally occurring strong charge acceptance regions of SOC
- A thermal strategy to increase charge acceptance decrease degradation during cycling, reduce lithium plating and maximize overcharge tolerance
- A method to identify useable SOC that can minimize charge time and capacity degradation

Fast Charge Profile	1 Ah Charge Time/ Target Charge Time at BOL A	Charge Accepted = Actual/Rated Capacity at BOL B	OC Risk Factor C	LP Risk Factor D	Aging Factor E	Charge Metric CM=A*C*D*E/B
1 - 25 °C	1.50	0.91	0.71	0.50	0.25	0.15
2 - 25 °C	1.00	0.97	0.88	1.00	1.00	0.90
3 - 25 °C	2.50	0.81	0.72	1.00	0.25	0.56
4A - 25 °C	0.95	0.63	0.85	0.75	1.00	0.96
4B - 25 °C	0.95	0.53	0.82	0.25	0.25	0.09
4A - 45 °C	1.00	0.65	0.72	0.25	1.00	0.28
4B - 45 °C	0.95	0.50	0.84	0.25	0.25	0.10
5 - 25 °C	2.40	0.89	0.74	0.25	0.25	0.13
6 - 25 °C	1.00	0.85	0.78	0.50	0.75	0.35
6 - 45 °C	0.93	0.92	0.98	0.25	0.25	0.06
7 - 25 °C	0.65	0.94	0.77	1.00	1.00	0.53
7 - 45 °C	0.65	0.97	0.69	0.25	0.25	0.03
8 - 25 °C	0.75	0.80	0.77	1.00	1.00	0.72
8 - 45 °C	0.75	0.88	0.76	0.25	0.75	0.12

Age	Acceptable - 0.25, High = 0.75, Severe - 1
Lithium Plating	Low - 0.25, Moderate - 0.5, Severe - 0.75, Cell Failure - 1
	Profiles with best trade off
	Profiles with sub-optimal trade off
	Profiles not acceptable

Table 1: Summary of profiles with best charge metrics.

SOUTHWEST RESEARCH INSTITUTE®

2017 IR&D Annual Report

Fuel Economy Effect of Advanced Vehicle Hardware, 03-R8649

Principal Investigators
Matt Blanks
Jianliang Lin
Brent Shoffner
Kevin Whitney

Inclusive Dates: 04/01/16 – 11/06/17

Background — Aggressive greenhouse gas and fuel economy regulations require automakers to continually improve fuel economy of new vehicles. Consequently, automakers are requiring their suppliers to develop advanced vehicle hardware that contributes to these fuel economy goals. The objective of this research was to investigate the possible fuel economy gains that can be achieved using low-friction coatings on engine piston rings, as shown in Figure 1. A high precision measurement technique was used to determine a vehicle's fuel economy before and after a low-friction coating was applied to piston rings. This measurement technique yielded results that relate directly to global fuel economy regulations without the need to extrapolate from bench-style friction testing.

Figure 1: Engine piston rings after removal from engine

Approach — The low-friction coating was evaluated with SwRI's Direct Electronic Vehicle Control (DEVCon) system and a high-precision chassis dynamometer. DEVCon applies an electronic accelerator pedal position (APP) signal directly to the vehicle's engine control unit (ECU) and eliminates the variation normally introduced by a human driver. Figure 2 shows an example of continuous fuel flow measured from three repeat tests using both a human driver and DEVCon for vehicle control.

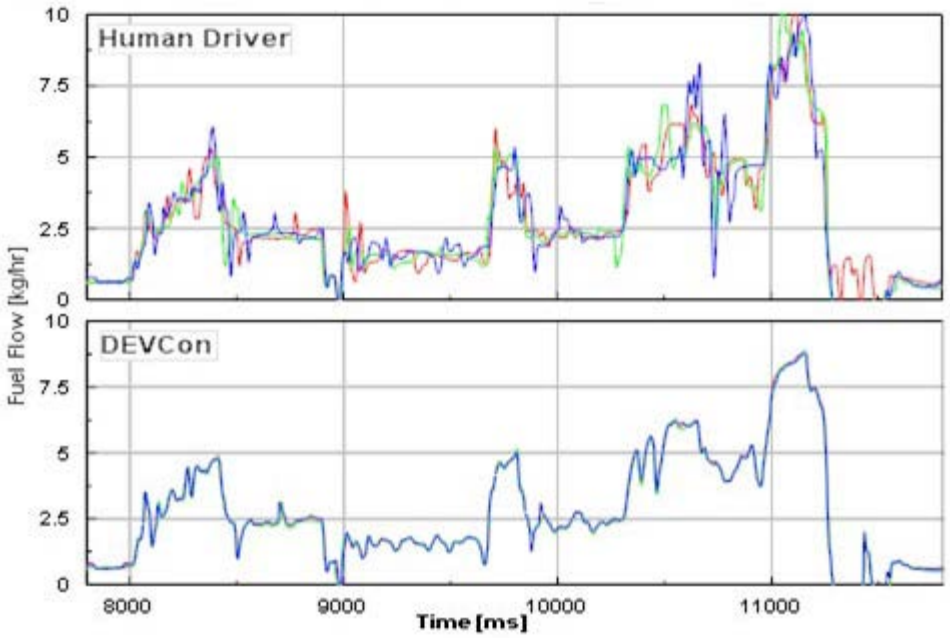

Figure 2: Continuous fuel flow measurement with a human driver and DEVCon

Accomplishments — The test vehicle's fuel economy has been measured over the Federal Test Procedure (FTP-75) and Highway Fuel Economy Test (HwFET) certification cycles using both the original manufacturer (OEM) piston rings and piston rings coated with a low-friction TiSiCN coating. Figure 3 gives the FTP-HwFET Combined Cycle test results for each configuration.

The first goal of this program was to determine the "engine rebuild" effect on fuel economy. The baseline or "OEM" results indicate that SwRI can completely disassemble and reassemble a vehicle's powertrain without causing a major shift in fuel economy. The second goal was to determine the fuel economy effect of SwRI's low-friction coating on piston rings. The SwRI-coated piston rings yielded an 0.82 percent improvement in fuel economy compared to the baseline rings.

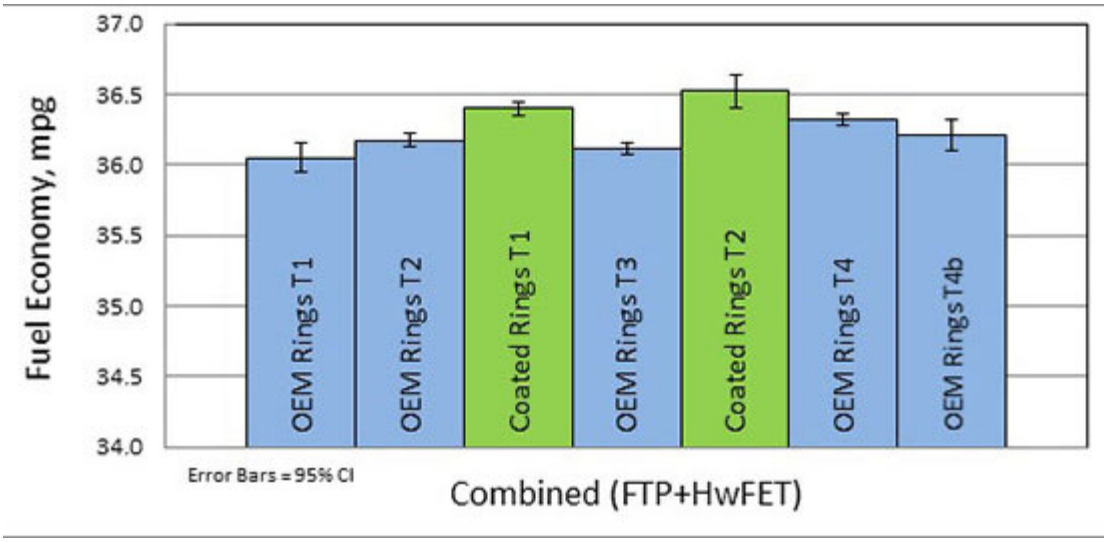

Figure 3: Vehicle fuel economy results with OEM and coated piston rings

SOUTHWEST RESEARCH INSTITUTE®

2017 IR&D Annual Report

Evaluation of Ionization Current as a Combustion Monitoring Tool in a Dual Fuel Engine, 03-R8668

Principal Investigator
Garrett Anderson

Inclusive Dates: 06/27/16 – 10/27/16

Background — Industry interest in large dual fuel engines has been growing because of favorable natural gas prices and environmental benefits. In addition, abnormal combustion (including knock) in large engines has been an active research and development topic in recent years. The Institute conducts research in this area for the CHEDE consortium and single-client projects.

Dual fuel engines are typically diesel engines that have been converted to burn natural gas while utilizing diesel fuel as an ignition source. These engines can exhibit knock much like spark ignited engines, which can lead to severe damage. Thus, an important part of the control system for an engine is to detect and control knock. Knocking combustion induces vibrations that are determined by engine geometry. This vibration is normally detected by accelerometers mounted on the engine block. Once detected, steps can be taken to reduce the knock before it damages the engine. However, this vibration can be difficult to detect in a large dual fuel engine because the frequency spectrum of interest can overlap with other mechanical vibrations.

Ion current has been used as a combustion monitoring tool in gasoline, diesel, lean-burn natural gas, and HCCI engines. The benefit of this tool is that it is cheaper than a cylinder pressure measurement system and provides some of the same information. Because of its reduced cost, it has been used as combustion feedback in production control systems to monitor for pre-ignition, misfire, and knock.

Approach — A probe was designed to extend through an existing passage in the engine head. It was constructed of stainless steel, Inconel, glass sealant and ceramic potting so that it could withstand the high temperatures of combustion.

An accompanying measurement circuit was also constructed that utilized an isolated operator amplifier and shunt resistor. This allowed for the measurement of current across the ionization gap when a large voltage was applied. This gap can be seen between the blue tube and gray wire in the cad model shown in Figure 1.

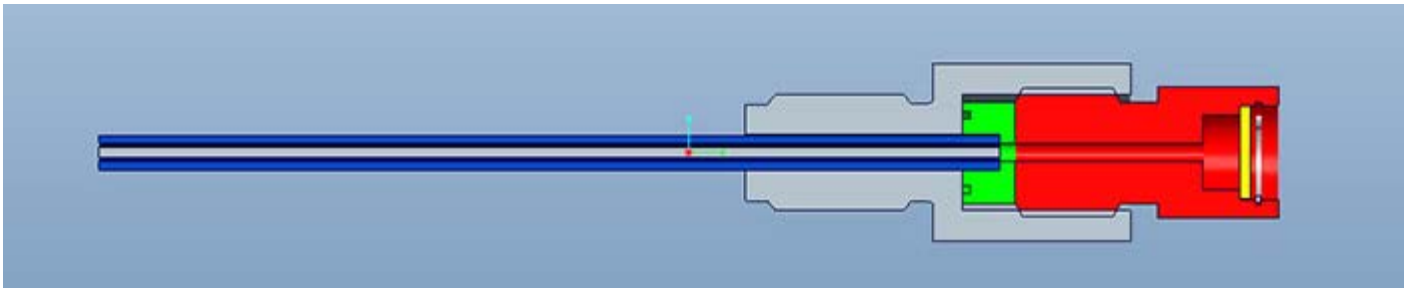

Figure 1: CAD model of ionization current probe.

Accomplishments — The main goal of monitoring combustion through ionization current measurement

was not a success, but the project was a not complete failure. A probe was designed that could withstand the harsh operating conditions of the engine. The specific instrument designed for this project did not function, but knowledge of how to construct a probe of this nature has been gained. It still may be worth pursuing this technology upon another engine platform that provides direct access to the combustion chamber. Dual fuel knock continues to be a topic of great interest. A probe placed in the cylinder may provide the feedback that is needed.

Figure 2: Dual-fuel, ionization current probe.

SOUTHWEST RESEARCH INSTITUTE®

2017 IR&D Annual Report

SULEV Potential for D-EGR Light Duty Passenger Vehicles, 03-R8689

Principal Investigator
Tom Briggs

Inclusive Dates: 08/30/16 – 01/03/17

Background — The purpose of this project is to evaluate the potential of leveraging unique features of the D-EGR combustion system to improve cold-start catalyst light off for light-duty passenger vehicles as part of a SULEV20 compliance strategy. SULEV20 is the most stringent emissions level in the world for passenger vehicles equipped with an internal combustion engine. To meet this emissions level, the vehicle must emit no more than 20 mg/mile of nitrous oxides plus non-methane hydrocarbons. In practice, the emissions from the vehicle once the catalyst system is warm are essentially undetectable so all of the measured emissions are from the cold-start portion of the emissions test when the catalyst is not yet hot enough to function. Modern engines with turbochargers are particularly difficult to make meet this emissions level as the turbocharger acts as a large heat sink, delaying the heating of the catalyst from the engine exhaust.

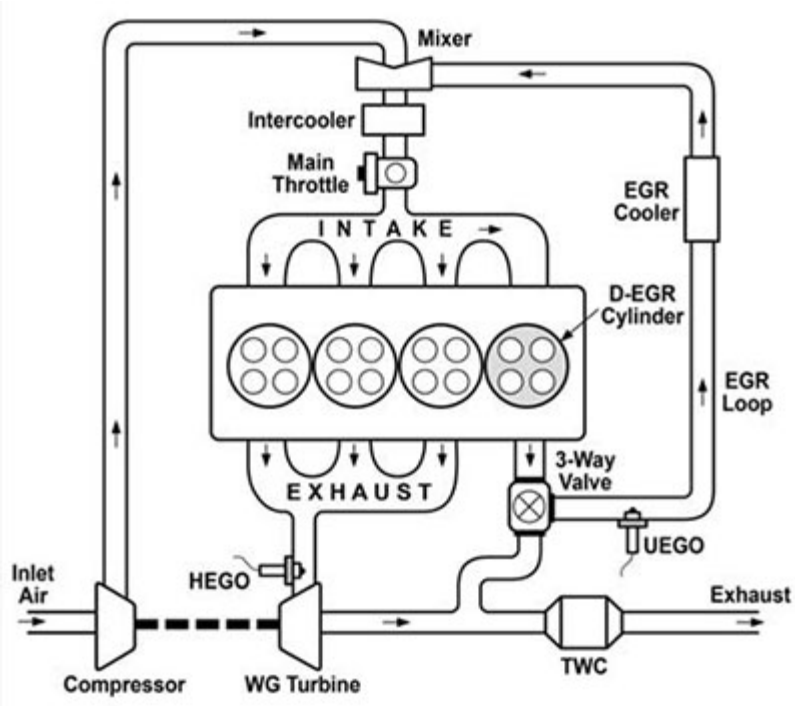

Figure 1: Typical configuration of an engine with D-EGR.

Dedicated EGR offers the potential to overcome this heat loss to the turbocharger, however, Figure 1 shows a typical configuration of an engine with D-EGR. Note the three-way valve immediately after the dedicated cylinder. Under cold-start conditions, this valve can be set to direct the exhaust from that cylinder directly to the catalyst, bypassing the turbocharger. This increases the thermal flux to the catalyst and heats the material faster. At the same time, the dedicated cylinder is operated slightly rich and the other cylinders slightly lean. The catalyst still receives a stoichiometric mixture of gases which allow it to operate, but these gases include hydrogen and oxygen. Catalysts will oxidize hydrogen at room temperature, creating more heat from the exothermic reaction. This also increases the temperature of the catalyst further. The combination of these were expected to significantly reduce the time for the catalyst to reach operating temperature, hence reducing the cold-start emissions and making SULEV20 a more attainable emissions level for turbocharged engines.

Approach — The study used the GT-Power modeling tool to predict the exhaust gas temperatures and catalyst temperatures for both conventional and D-EGR engine operation. Existing catalyst activity data was used to determine the impact of the modeled results on exhaust emissions and catalyst light off.

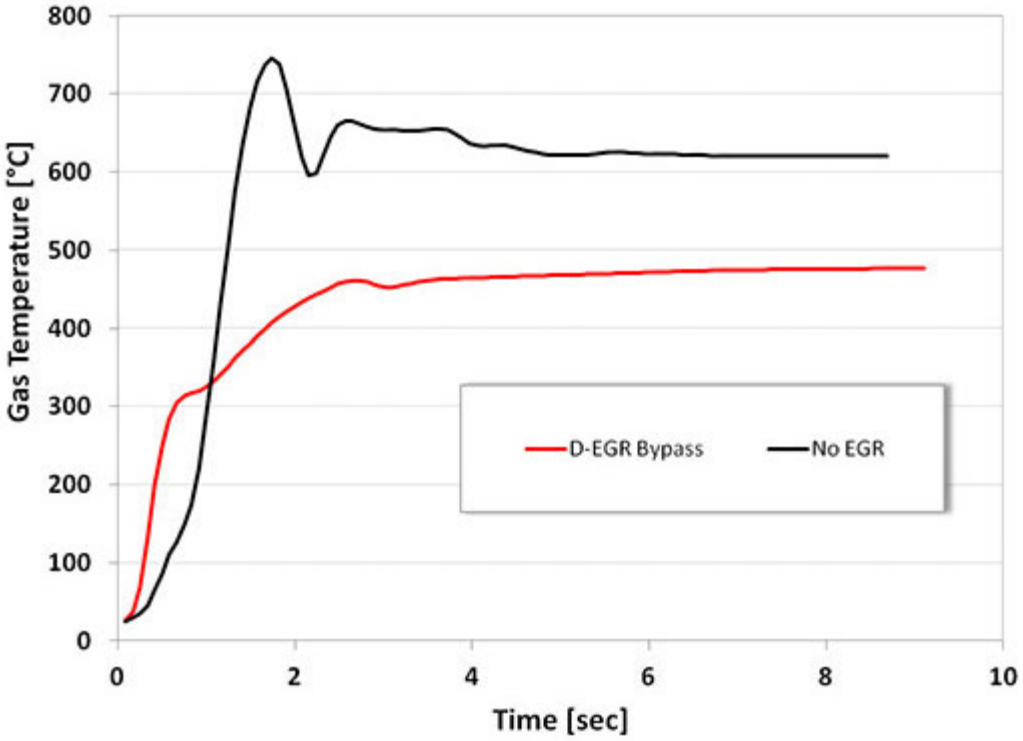

Figure 2: Gas temperature at catalyst inlet when running in D-EGR mode.

Accomplishments — The study showed that the gas temperature at the catalyst inlet reached 300°C when running in D-EGR mode in about half the time predicted for conventional operation, as seen in Figure 2. The model also showed that significant quantities of hydrogen and oxygen could be supplied to the catalyst with no penalty in hydrocarbon emissions, see Figure 3. Finally, existing catalyst bench test results showed that the presence of hydrogen and oxygen at the catalyst inlet reduced light-off temperatures for the catalyst by more than 50°C as seen when comparing Figure 4 and Figure 5. These coupled results indicate great potential for the D-EGR combustion system to enable SULEV20 emissions compliance for turbocharged engines in light duty passenger vehicles.

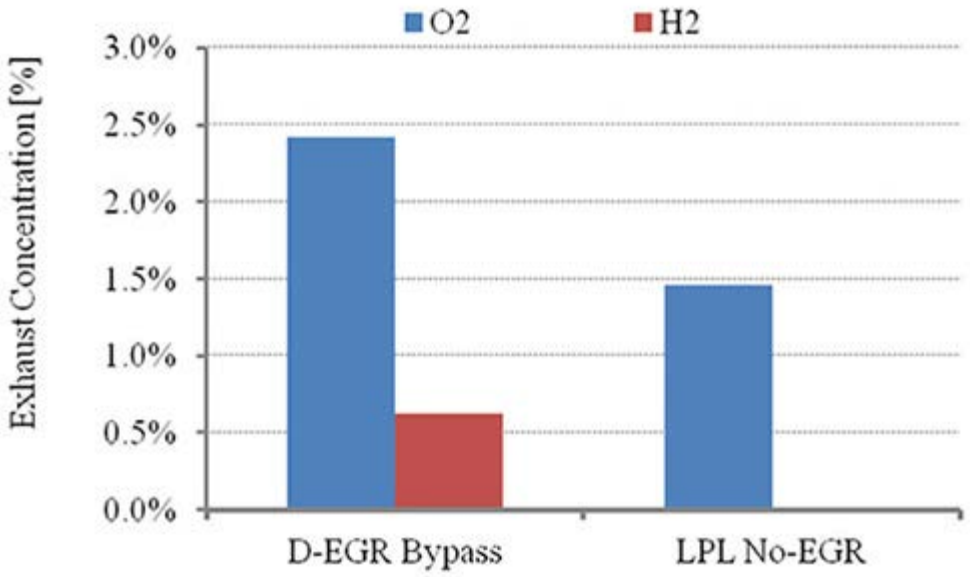

Figure 3: Hydrogen and oxygen supplied to catalyst with no emissions penalty.

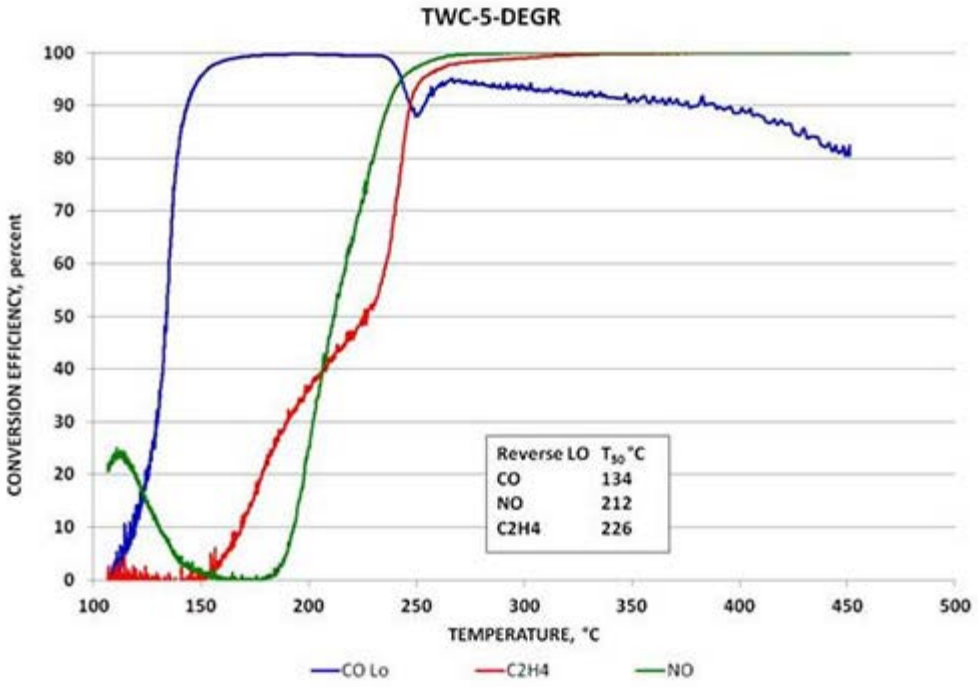

Figure 4: Temperature versus conversion, TWC-5 D-EGR.

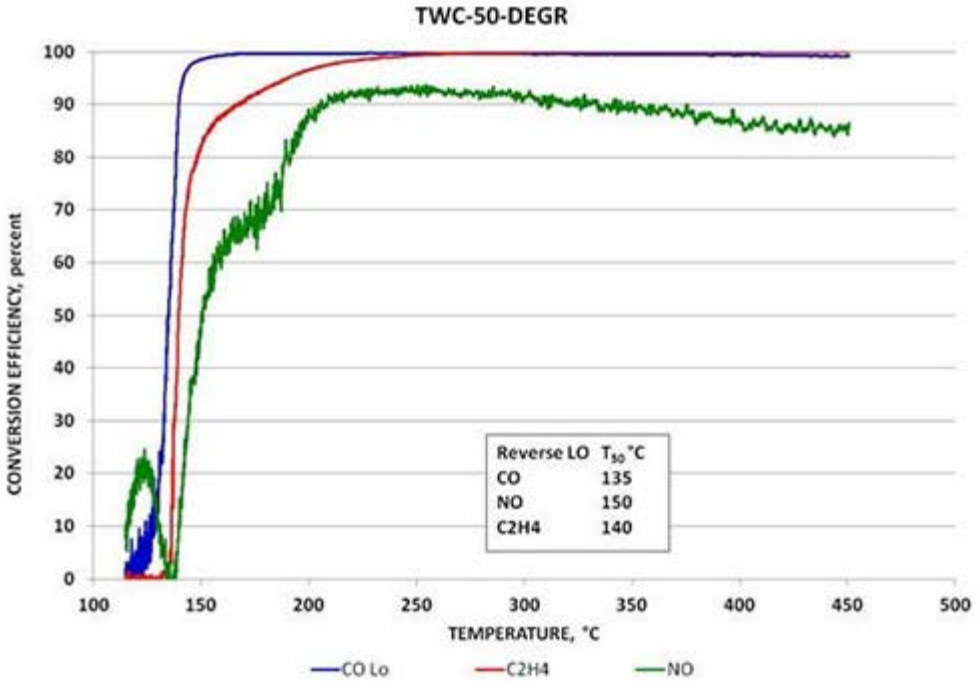

Figure 5: Temperature versus conversion, TWC-50 D-EGR.

SOUTHWEST RESEARCH INSTITUTE®

2017 IR&D Annual Report

Investigation of Dual-Fuel Engine to Achieve Tier 4 Final Emission Levels with no NOx Exhaust Aftertreatment, 03-R8694

Principal Investigators
Timothy J. Callahan
David P. Branyon
David P. Meyers
Ryan D. Johnson

Inclusive Dates: 09/12/16 – 01/12/17

Background — The latest U.S. Environmental Protection Agency (EPA) emission standards for large off-road engines (power >560 kW), known as Tier 4 Final (4f), are forcing manufacturers to use aftertreatment requiring "active control," meaning selective catalytic reduction (SCR) with urea injection to reduce oxides of nitrogen (NOx) and/or diesel particulate filter (DPF) with periodic regeneration to reduce particulate matter (PM). Implementation of SCR and/or DPF adds complexity in controls, packaging difficulties for mobile applications, and maintenance concerns. As the market faced these emissions regulations, a parallel demand for dual-fuel engines that run on natural gas and diesel emerged. The engines use pre-mixed natural gas admitted into the inlet air stream, with a diesel pilot used for ignition. This demand was originally driven by the price differential between natural gas and diesel fuel. In SwRI's development of large (>560 kW) dual-fuel engines for mine-haul trucks, it has been demonstrated that dual-fuel engines can easily meet Tier 2, and the hypothesis for this project was that dual-fuel engines may potentially meet Tier 4f without SCR or DPF aftertreatment, eliminating the aftertreatment packaging issue, and reducing operating cost by eliminating SCR.

Approach — A Tier 2 non-road diesel engine of 2.5-6 L/cyl displacement (>560 kW) was converted to dual-fuel operation by the addition of two precise, fast acting, state-of-the-art gas metering valves, close coupled natural gas-air mixers, intake throttles, and a high-pressure common rail injection system. The common rail injection system provided improved injection-to-injection accuracy at low injection quantities when compared to the stock injection system. An integrated control system was added to coordinate the diesel fuel injection event, natural gas metering, and intake air throttling. Natural gas substitution rate, diesel injection timing, diesel injection pressure, and overall equivalence ratio were optimized to meet the emissions standards and provide stable and knock free operation.

Accomplishments — The project clearly demonstrated the capability to reach Tier 4f without EGR or actively controlled aftertreatment (SCR or DPF) and with very high natural gas substitution above 90 percent even at moderate to low speeds and loads. The approach is envisioned as a relatively low cost, moderate modification route to achieving very high real-world substitution ratios. This approach should maximize the economic incentive by providing the quickest possible payback. Real-world substitution ratios above 90 percent are achievable on most duty cycles with no internal engine changes and at relatively low costs, both from a per-engine and an engineering investment perspective.

SOUTHWEST RESEARCH INSTITUTE®

2017 IR&D Annual Report

Methanol Fuel Testing on Port Fuel Injected Internal EGR, HPL-EGR and D-EGR® Engine Configurations, 03-R8713

Principal Investigator
Eric Randolph

Inclusive Dates: 12/05/16 – 03/20/17

Background — China is pursuing energy independence via multiple pathways, one of which is coal-derived methanol. Chinese engine manufacturers also are pursuing methods to reform methanol to fast-burning H_2 and high-octane CO to improve engine cold start, dilution tolerance, and efficiency. To further enhance efficiency, engine manufacturers can use cooled EGR, which improves knock tolerance. However, the dilution tolerance of the engine limits the degree of improvement. To expand the dilution limits, reformate can be introduced into the cooled EGR loop. SwRI's Dedicated EGR (D-EGR®) concept delivers both cooled EGR and reforms fuel to H_2 and CO through partial oxidation in the combustion chamber of a cylinder, or cylinders, dedicated to providing EGR. Because methanol differs from conventional gasoline in many respects, it was important determine the reformation behavior of methanol, as well as show the synergy of coupling methanol with D-EGR for leveraging the technology.

Approach — A 2.0L L4 engine was configured to operate on dedicated EGR, 25 percent cooled EGR and internal EGR. The compression ratio was increased to 12:1 to leverage the knock mitigation benefit of EGR and methanol. A comparison of the three EGR methods was executed to show the benefit of D-EGR over other EGR technologies (Table 1). The engine was operated on both methanol and HEEE Tier II certification gasoline to compare the fuel reformation behavior of methanol to conventional gasoline. Because D-EGR reforms fuel in the cylinder through partial oxidation under fuel-rich conditions, an enrichment sweep of the dedicated cylinder was executed on both fuels to compare the reformation behavior of each fuel.

Engine Configuration	Fuel
Internal EGR	Methanol
25% Cold EGR	Methanol
D-EGR	Methanol
D-EGR	HEEE

Table 1: Test setups

Accomplishments — Comparison of the three EGR technologies using methanol showed the benefit in brake thermal efficiency (BTE) of D-EGR over 25 percent cooled and internal EGR (Figure 1). This benefit in thermal efficiency with D-EGR was largely due to more complete combustion afforded by the fast-burning H_2. The reformation rate of H_2 for methanol was determined to be similar to conventional gasoline as well, as the rate of reformation was approximately 1.1 to 1.2 H_2 percent per 10 percent fuel enrichment in the dedicated cylinder. It was determined that the enrichment capability of methanol was much higher than gasoline. When running on gasoline, the engine could operate with up to 60 percent (D-phi of 1.60) fuel enrichment in the dedicated cylinder, which yielded 7 percent H_2 (Figure 2). Methanol's enrichment

limit was much higher at over 170 percent fuel enrichment, which led to H_2 concentrations of 19 percent. The results of this work were published with the Society of Automotive Engineers (SAE 2017-01-2285) and presented at the Society of Automotive Engineers International Powertrain Fuel and Lubricants Conference in Beijing, China, in October 2017.

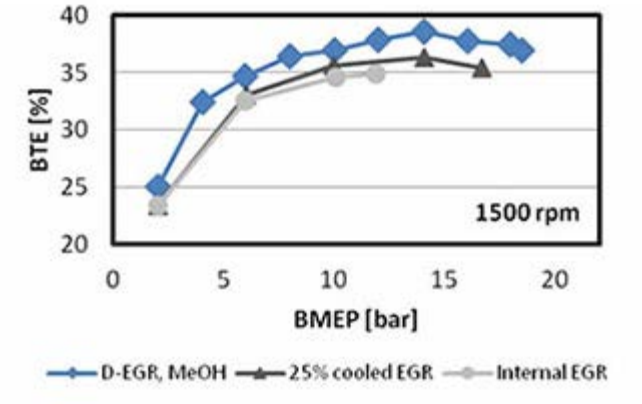

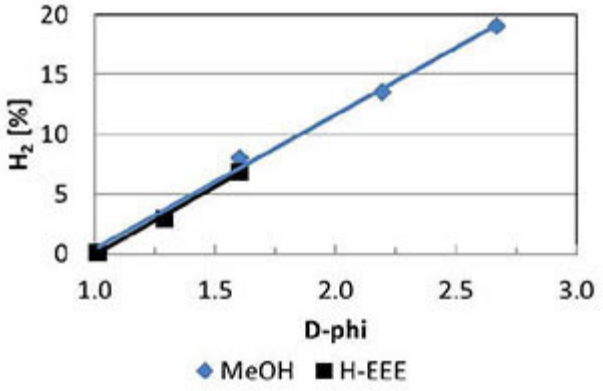

Figure 1: BTE comparison of the three EGR types on MeOH Figure 2: Methanol H_2 production at high enrichment. at 1,500 rpm.

2017 IR&D | IR&D Home

SOUTHWEST RESEARCH INSTITUTE®

2017 IR&D Annual Report

Development of Low Flow Capability and Lean / Rich Switching for SwRI's ECTO-Lab (formerly HGTR®) Technology, 03-R8714

Principal Investigators
Scott Eakle
Bradley Denton
Bryan Zavala

Inclusive Dates: 11/28/16 – 04/28/17

Background — The Exhaust Composition Transient Operation Laboratory (ECTO-Lab™) bench is a computer-controlled, multi-fueled, burner-based, continuous-flow reactor system designed to duplicate the lean exhaust conditions produced by medium-duty to line-haul size truck engines. The ECTO-Lab is a fully transient, full-size reactor type system. Unlike typical small-core gas reactor benches, which use bottled gas to simulate exhaust conditions, the ECTO-Lab produces a continuous exhaust flow through combustion of fuels and compounds, producing an exhaust gas composition that more accurately and precisely duplicates the array of gaseous species created from the combustion of diesel fuel in an engine. The exhaust gas conditions are generated through independent, model-based control and allow any combination of mass flow, temperature, NO_x, H_2O, and O_2 concentration within its window of operation. The flow and temperature window of operation is shown in Figure 1.

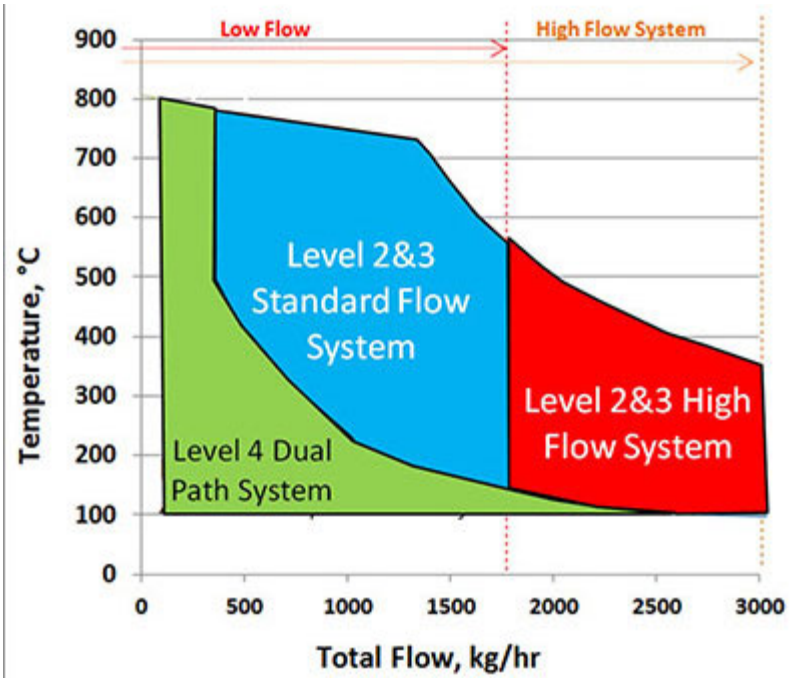

Figure 1: Flow and temperature window of operation for various FOCAS-HGTR configurations.

The original ECTO-Lab system was capable of generating up to 1,750 kg/h exhaust mass flow. In 2015, the system capability was expanded to 3,000 kg/h to simulate engine displacements up to 20L. A broad

range of operating conditions simulating engine displacements from 7 to 20L has been verified; however, lower flow rates cannot be achieved with the current architecture of the system. Therefore, flow rates less than 100 kg/hr cannot be achieved, which makes it difficult to simulate idle flow rates of medium sized engines and flow rates for engines with displacements of less than 7L.

Additionally, the current configuration operates lean due to the use of dilution air to control exhaust flow rate and temperature. Therefore, certain types of diesel aftertreatment components are unable to be evaluated with the current configuration due to its limitation of continuous lean operation. The Lean NO_x Trap (LNT) has been utilized in the light-duty diesel market as an alternative to conventional SCR for NO_x reduction. LNT requires periodic rich combustion events to release stored NO_x so that it can be reduced. At the start of this project, lean/rich switching could not be controlled on the ECTO-Lab, which limited the applicability of this system for evaluation of LNT performance. In addition to adding the low flow capability to evaluate light duty diesel aftertreatment systems, SwRI desired to add the capability to conduct rich/lean switching so that all diesel aftertreatment configurations can be evaluated on a single evaluation test bench.

There were two main objectives in this project:

- Design and develop methodology that enables accurate, low exhaust flow control so that all production intent diesel aftertreatment configurations can be evaluated.
- Perform research to develop methods that enable lean/rich switching of exhaust gas chemistry. With a single ECTO-Lab system, an operator would be able to simulate various exhaust profiles of diesel engine combustion strategies for aftertreatment control from 1 to 20L in displacement (approximately 30 to 3,000 kg/hr exhaust flow rate).

Approach — We began by utilizing bypass legs and small flow valves to create a system capable of lower flow rate control. The original ECTO-Lab system had a test leg and a dump leg that were dynamically controlled, allowing a portion of the exhaust to bypass the component under test, which enabled more transient operation and lower flow rates compared to controlling the blower flow rates alone. However, these valves were too large to achieve the exhaust flow rates required for light-duty applications. This project encompassed developing a system capable of switching between a lower flow regime and the standard flow regime without changing hardware. This mode of operation greatly expanded the dynamic flow range of the ECTO-Lab system. This wide range of dynamic operation was accomplished using new control models and software. To accomplish rich/lean switching, a more transient fuel control algorithm was necessary for improved burner lambda control on ECTO-Lab. A supplemental fuel injection supply in the combustor was implemented.

Once the modified approach to controls was developed, and exhaust design and supplemental fuel injection system were implemented, the new controls and control models were calibrated, tested, and refined. This work included both steady-state and transient control development. When satisfactory control of low flow was achieved, validation of low-flow capability was performed. This included replicating light-duty non-road drive cycles provided by the Advanced Combustion Catalyst and Aftertreatment (AC^2AT) consortium for a 1. L Doosan diesel engine.

Lean/rich switching on ECTO-Lab had some technical difficulties that resulted in unstable control of flow and temperature through the test components. Therefore, the lean rich switching development work was executed on SwRI's other version of the ECTO-Lab, which included a water-to-exhaust heat exchanger to provide independent control of flow, temperature, and stoichiometry. This allowed the combustor to operate near stoichiometric conditions without the use of dilution air for control of temperature. Therefore, the exhaust gas components consistent with a stoichiometric combustion system could be simulated. To control overall air-to-fuel ratio (AFR) entering the test component without impacting flow or temperature control, SwRI implemented a secondary dilution air supply, downstream of the combustor.

Accomplishments — Low flow was achieved through a redesign of the combustor exhaust system and modification of the model based controls for both flow rate and NO_x concentration. A new low-range exhaust flow meter (EFM) also was implemented to improve the accuracy of low flow rate measurements. Low flow was demonstrated on transient operating conditions that simulated a 1.8L Doosan diesel engine.

However, lean/rich switching proved unsuccessful on the ECTO-Lab system without the water-to-exhaust heat exchanger. If the AFR was commanded to a rich condition, dilution air would need to be diverted, making both temperature and flow rate controls uncontrollable. Again, the dilution air on the original ECTO-Lab design provides both temperature and flow management through the test components. To deploy an evaluation test stand capable of lean/rich switching for LNT evaluations, SwRI developed a new ECTO-Lab system based on the predominantly operated stoichiometric R-FOCAS burner. Unlike the previous generation ECTO-Lab, where the temperature and flow rate are controlled with dilution air, the new version of ECTO-Lab uses a water-to-air heat exchanger for temperature control. This allows for operation of the combustor near stoichiometric operating conditions without using dilution air for control of temperature. This allows for the simulation of exhaust gas components consistent with a stoichiometric combustion system.

In the new ECTO-Lab system, this novel configuration provides an additional leg for air dilution downstream of the combustor and located downstream of the water-gas heat exchanger. This dilution leg allows for continuous simulation of lean-burn exhaust systems and is used for secondary control of exhaust gas temperature. Since this dilution leg is not used as the only means of controlling exhaust gas temperature (as in prior versions of ECTO-Lab), flow through the leg can be turned off so the combustor can operate at stoichiometric and/or rich conditions to generate exhaust gas as observed for lean-burn combustions systems using catalyst technology such as Lean NO_x Traps (LNT).

SOUTHWEST RESEARCH INSTITUTE®

2017 IR&D Annual Report

Investigation of Regeneration Frequency, Ash Rate, and Soot/Ash Ratio Impact on Ash Loaded Diesel Particulate Filters, 03-R8716

Principal Investigator
Michael Chadwell

Inclusive Dates: 11/28/16 – 05/09/17

Background — Wall-flow diesel particulate filters (DPFs) have been required for every new on-road diesel-powered vehicle in the U.S. since 2007. Many non-road diesel-powered engines also now require a DPF to meet emissions regulations as well. The DPF traps particulate matter (PM) that is emitted from the engine. Much of this PM is in the form of carbonaceous soot, which can be periodically cleaned out through oxidation, known as regeneration. A small fraction of the captured PM is in the form of ash, which is derived from lubricating oil components as it is consumed in the engine. Because ash is comprised primarily of inorganic material, it cannot be oxidized; the DPF must eventually be removed and cleaned or replaced. Due to the service interval implications, ash storage requirements play a major role in determining the size of the DPF for a given application. By downsizing the DPF, vehicle manufacturers can reduce cost, reduce package size/complexity, and possibly reduce fuel consumption. DPF manufacturers must prove-out their designs to vehicle and engine manufacturers to win supplier contracts. Loading a DPF with ash in a lab environment can be very costly and time consuming: recent test durations have ranged from 1,000-5,000 hours. Reducing this test duration while maintaining ash that is representative of real-world ash would be very beneficial to clients. Therefore, the objectives of this research were: (1) modify the current ash-loading procedure to deposit ash in a more densely packed layer that more closely resembles field-returned DPFs and (2) reduce the time and cost required to load ash onto DPFs, thereby reducing overall cost of testing.

Approach — The current SwRI-developed ash-loading procedure was executed first to serve as a baseline. The baseline procedure (A) used a modified piston ring pack in the engine as well as a precisely controlled oil-doped fuel supply. Once the baseline was established, the cycle was modified to meet the research objectives. The first modification (B) sought to increase the ash density in the DPF by increasing the soot/ash ratio and by running more frequent active regenerations. The ash rate over the given operating cycle was expected to remain the same, thus the soot rate was increased to increase the soot/ash ratio. This was accomplished by increasing the amount of exhaust gas recirculation (EGR). In conjunction, the number of active regenerations was doubled to facilitate moving the ash toward the back of the inlet channels as the soot it is bonded to oxidizes. The modified cycle test was conducted and compared to the baseline. The final cycle modification (C) sought to increase the oil-consumption rate of the ash-loading engine to reduce the time required to reach the ash-loading target. This was accomplished by doubling the fuel oil doping rate (it was expected that increasing the oil consumption by 50 percent would increase the ash loading rate by 50 percent. In this case, the test duration was not fixed, but testing was stopped at the same load as the baseline and first result for comparison.

Accomplishments — Both research objectives were achieved with the methods developed in this investigation. Using SwRI CT scan capabilities, it was concluded that ash deposition was more densely packed (vs. baseline), which is shown in Figure 1.

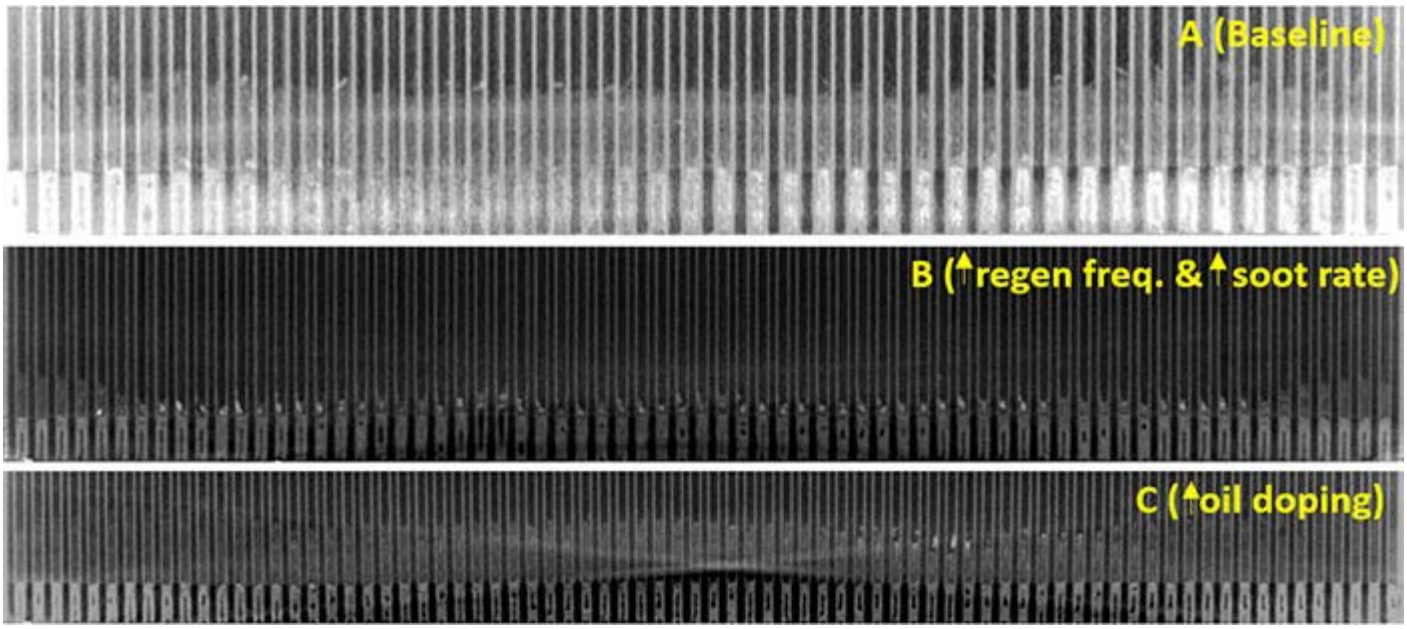

Figure 1: CT scan results comparing ash density at 5 g/L. Compared to the baseline (A), the increased density of method B (increased active regeneration frequency and increased soot rate) is profound. Method C (increased oil doping) showed ash density similar to A, which was expected, but achieved the load faster due to increased ash rate from increased oil doping.

The initial cycle modifications of increasing soot rate and increasing active regeneration frequency succeeded in replicating ash layers observed in field-return DPFs. The second objective was also met, which was done by increasing oil doping rate into the engine fuel supply. Ash density was unaffected from the baseline, but the ash loading rate was increased. In future projects, including the two large studies that have been awarded since the end of this project, the desired ash loading method will likely be a combination of the two improvements, i.e., increase soot/ash ratio and active regeneration frequency for enhanced ash density as well as increasing oil doping to increase ash rate.

SOUTHWEST RESEARCH INSTITUTE®

2017 IR&D Annual Report

Combustion Performance of CO_2 Only EGR and its Separation from an Exhaust Gas Stream Through Membrane Technology, 03-R8727

Principal Investigators
Eric Randolph
Jason Herrera
Graham Conway

Inclusive Dates: 01/27/17 – Current

Background — Exhaust Gas Recirculation (EGR) is a proven technology for efficiency improvement on gasoline and natural gas engines. The composition of EGR is determined by the engine's combustion and has a molar composition of about 13 percent H_2O, 14 percent CO_2 and the balance N_2 when the engine is operated at stoichiometric conditions. The physical and chemical properties of the EGR effect the thermodynamic behavior during the Otto cycle. Because triatomic molecules have lower ratio of specific heats than diatomic molecules, they negatively impact the efficiency of the engine compared to that of dilution with air. If CO_2 can be removed from the EGR gas stream (CO_2-reduced EGR), then the thermodynamic behavior of the EGR could be improved for increased engine efficiency. Further, because the concentration of H_2O is high in the exhaust stream, the dew point of the EGR stream could also be influenced with membrane separation technology by using CO_2-only EGR.

Figure 1: SwRI single cylinder engine

Approach — To determine their relative merits, EGR, CO_2-only EGR and CO_2-reduced EGR were tested on the SwRI single-cylinder engine (SCE) (Figure 1). This evaluation was performed at seven drive cycle representative speed-loads to determine the effects on combustion, knock, emissions, and boosting requirements. An evaluation at knock limited conditions and full load also was executed to assess the former, as well as the potential for enrichment mitigation.

In parallel with SCE testing, a CO_2 membrane was designed (Figure 2). The membrane in this design is based on an SwRI-patented technology. After fabrication, the membrane will be bench tested to determine

the membrane sequestration selectivity, flux rate, and stripper air requirements. The bench testing will also be used to assess the back-pressure penalty of the selective membrane.

Figure 2: Scematic of CO_2 selective membrane technology

Accomplishments — Comparison of the three EGR compositions has been tested to date. CO_2-only EGR had lower efficiency than conventional EGR due to its lower ratio of specific-heats. The engine also had a lower dilution tolerance with CO_2-only EGR, as the laminar burning velocity with CO_2-only EGR is lower due to the thermodynamic and chemical effects of CO_2. Alternatively, CO_2-reduced EGR had higher efficiency than conventional EGR due to its higher ratio of specific heats. The engine also had a higher dilution tolerance with CO_2-reduced EGR, as the laminar burning velocity with CO_2-reduced EGR is higher. The effort to scale the CO_2 membrane for automotive application is ongoing.

2017 IR&D | IR&D Home

SOUTHWEST RESEARCH INSTITUTE®

2017 IR&D Annual Report

Comparison of Accelerated Ash Loading Methods for Gasoline Particulate Filters, 03-R8729

Principal Investigators
Scott Eakle
Stephen Avery

Inclusive Dates: 01/01/17 – Current

Background — Particulate matter (PM) emissions from internal combustion engines have been of great interest. When evaluating the relative contributions of diesel- and gasoline-powered vehicles to ambient PM in the United States in 2000, the U.S. Environmental Protection Agency concluded that diesel-powered vehicles contributed 62 percent of the mobile source inventory, while gasoline-powered vehicles contributed 38 percent. However, the California Air Resource Board (CARB) predicted that 32 percent of PM emissions were from diesel-powered vehicles and 68 percent from gasoline-powered vehicles. Even though the results were not consistent, these studies demonstrated PM emissions from gasoline-powered vehicles can be significant.

With diesel particulate filters (DPF) implemented on diesel engines for US2007 heavy-duty diesel emissions compliance in the United States, tailpipe PM emissions from diesel engines were substantially reduced, often by 99 percent or more. It is understood that a conventional gasoline engine emits a higher number of particulates than those from a DPF-equipped diesel engine for comparable engine power ratings given the relatively small diameter of gasoline particulates. Due to these reasons, and the implications for public health, PM emissions from gasoline vehicles are coming under increasing scrutiny in the U.S. The European Union (EU) has already implemented a Particle Number (PN) standard for both on-highway heavy-duty and light-duty applications. Because the light-duty regulation (Euro 6c) does not exclude gasoline direct injected (GDI) applications (previous PM regulations were only specific to compression ignition engines), there has been an emergence of production-intent gasoline particulate filters (GPF) for light-duty GDI equipped applications.

Starting with MY2015 light-duty vehicles, CARB LEV III standards phased in a new 150,000-mile durability requirement, compared to the LEV II 50,000 and 120,000 mile standards. The combination of requiring a significant reduction in PM and an increase in the durability requirement may pose a concern for GDI applications equipped with a GPF. Since a conventional wall flow GPF captures a majority of solid material from the combustion process, the accumulation of inorganic components (i.e. wear metals from the engine or constituents found in the lube oil), termed as ash, will accumulate in the GPF over the lifetime of the application. Unlike organic components of PM, such as elemental carbon, that can be removed through a regenerative oxidation process, these inorganic components that accumulate are unable to be removed through traditional engine and aftertreatment management systems. Ash can only be removed through offline cleaning techniques. However, legislation requires that light-duty emissions control systems must be warranted for the full useful life (FUL) of the vehicle. Therefore, devices such as the GPF typically are not replaced and do not have recommended cleaning intervals due to the accumulation of ash.

Accelerating ash accumulation in particulate filters has been studied extensively since the emergence of the DPF for diesel applications. Various acceleration methods have been evaluated. Several have their drawbacks, however, as they may not accurately replicate the deposition mechanisms that are observed in real-world applications. Acceleration methods for ash accumulation all use lube oil as the primary driver since multiple studies have confirmed the dominant source of ash is related to engine lube oil

consumption.

While various methodologies have proven themselves accurate and effective for accelerated ash loading of the DPF, the physical and chemical mechanisms for ash loading of the GPF are vastly different and likely will require an alternative strategy.

To address the significant differences between the conditions for a DPF and GPF, we proposed to evaluate three methods for accelerated ash accumulation in the GPF:

- Add lube oil to fuel using a liquid flow controller
- Load ash using SwRI's ECTO-Lab technology (combust oil in a burner)
- Invert the lower compression ring on all pistons to increase oil consumption via realistic mechanisms

Approach — This project will be conducted in two phases, with the first phase consisting of evaluating various accelerated ash loading techniques. Each technique will be compared to a non-accelerated, field generated GPF for their ash deposition profile, ash composition, and GPF pressure drop performance. The second phase will determine the collective performance effect of soot and ash on the GPF.

Accomplishments — To date, two of the three accelerated ash accumulation methods have been evaluated, including doping the engine fuel supply with a known rate of lube oil and inversion of the lower compression ring on all pistons. At specified test break points, the GPF was removed from the accelerated ash loading engine and CT scans were performed to quantify the change in ash deposition profile. In addition to mapping the ash profiles, each GPF was characterized for pressure drop performance as a function of both ash and soot loading.

SOUTHWEST RESEARCH INSTITUTE®

2017 IR&D Annual Report

Heat Transfer Prediction in Internal Combustion Engines using Simulation, 03-R8755

Principal Investigators
Zainal Abidin
Anthony Megel
Bansal Shah

Inclusive Dates: 05/01/17 – Current

Background — Simulating and modeling internal combustion engines has become the standard in engine development by shortening development time and eliminating some hardware iterations that were required 20 years ago. SwRI has developed a combustion model (HEDGE mechanism) for gasoline engines as part of the HEDGE-III consortium and has been applied in a 3-D computational fluid dynamics (CFD) simulation. Diesel combustion studies have been conducted under the CHEDE-VI and CHEDE-VII consortia. SwRI has developed extensive procedures for simulating and analyzing cylinder head operation using the finite element approach (FEA). Generally, the combustion CFD and thermal FEA simulations are conducted separately with an interface boundary condition assumption. Because these phenomena are interdependent, separating the numerical simulations brings several inaccuracies. The primary objective of this research is to develop and validate a method to improve heat transfer prediction in the internal combustion engine by coupling the combustion CFD, thermal FEA, and cooling CFD. Better heat-transfer prediction improves combustion and wall heat loss prediction.

Approach — Three simulations will be conducted concurrently: combustion CFD, thermal FEA, and cooling CFD. Because the cyclic variation of the parameters for thermal FEA and cooling CFD is minor, both simulations will be conducted under a steady mode. The combustion CFD is conducted under transient conditions due to the highly transient process inside the combustion chamber. For the interaction, there will be an exchange between surface temperature and heat transfer at the interface. Between combustion CFD and thermal FEA, the frequency of data exchange will be studied to obtain the best coupling results.

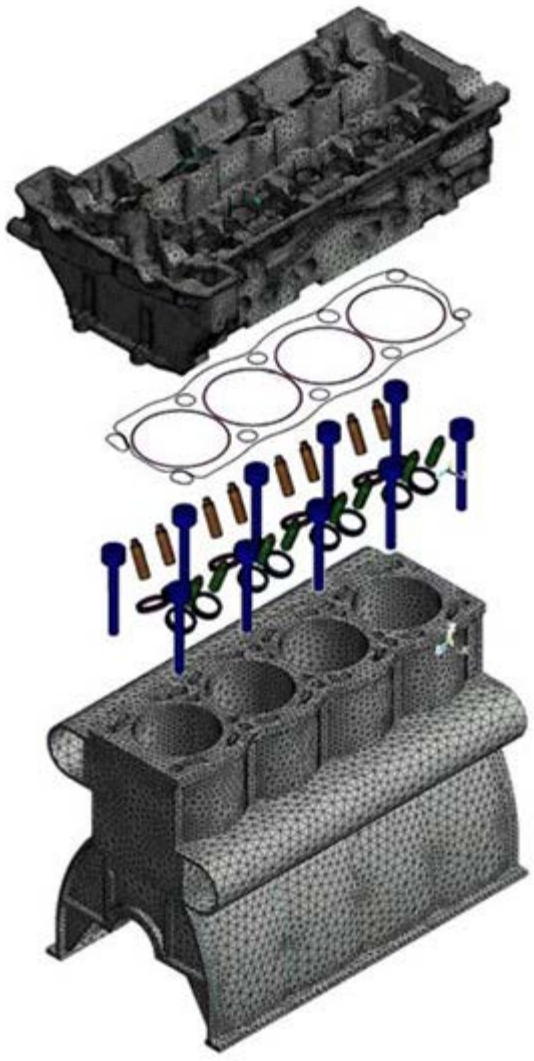

Figure 1: Meshing for engine block and head.

Accomplishments — The geometry preparation for the diesel engine simulation is almost completed. The geometry includes the cylinder block, head, cooling system and chamber. The boundary and model setup are underway and we will continue to simulate the model.

SOUTHWEST RESEARCH INSTITUTE®

2017 IR&D Annual Report

Characterization of High Pulse Energy Turbochargers, 03-R8757

Principal Investigators
Andrew Morris
Jason Miwa
Zainal Abidin

Inclusive Dates: 04/01/17 – Current

Background — The objective of the proposed research is to identify the critical parameters that determine the performance of high pulse energy turbocharger systems. The term 'high pulse energy turbocharger' refers to a turbocharger that provides exceptionally high isentropic efficiency when operated under highly pulsed flows. High pulse energy turbochargers are typically twin scroll turbochargers where the housing is separated into two volutes. However, not all twin entry turbochargers provide high pulse energy because other parts of the engine such as the exhaust manifold and turbine geometry appear to play an important role in efficiency as well. The SwRI-led Clean High Efficiency Diesel Engine (CHEDE-VI) program demonstrated that high pulse energy turbochargers have significant potential to improve fuel efficiency. However, turbocharger performance was much better than the cycle simulations had predicted due to the high pulse energy utilization. It was determined that engine simulation tools such as GT-Power do not accurately predict the performance of high pulse energy turbochargers. An issue with cycle simulation tools is that they use performance data from turbocharger gas stands that operate at steady state, while the engine may operate under a highly pulsating flow due to the different cylinder exhaust events. The CHEDE-VI program quantified and documented the impact of a high pulse energy turbocharger on engine BTE, but the physics are not fully understood.

Approach — Engine tests were conducted using multiple turbochargers, exhaust manifold designs, and test engines. The results of these tests provided a detailed characterization of gas flow, turbine speed and turbine performance. Data from the detailed characterization was used to set boundary conditions for the CFD simulation, and the model was evaluated to determine how well it matches the measured performance. The CFD model was used to quantify how different features in the exhaust ports, exhaust manifold, and turbine housing can impact the performance of the turbocharger. The results of the CFD simulation also were compared with the cycle simulation results to potentially highlight differences and areas for improvement. Finally, the results of the detailed experimental characterization and CFD simulation were used to generate a design concept for an improved turbocharger test stand. It is expected that a turbocharger test stand with

Figure 1: Three-dimensional computational fluids model of turbocharger system.

pulsating flows may provide the necessary test data to allow cycle simulation tools to accurately predict turbocharger performance. Improved modeling capability would allow researchers to better match high pulse energy turbos to engines and provide better fuel efficiency.

Accomplishments — The test engine was instrumented with high-speed pressure transducers in multiple locations around the turbine and compressor, and with a speed sensor to measure the instantaneous turbo speed in the crank angle domain. To test multiple turbochargers on the same engine, special adapters were needed. These adapters were designed with special care taken to ensure that the pre-turbine volume remained constant for both turbochargers, as this volume is thought to have a strong effect on the turbine performance. With the adapters procured, engine tests were conducted to examine the effects of speed and load on the turbine performance. From the high-speed data collected in these tests, the instantaneous scroll pressure ratio could be calculated. The scroll pressure ratio is simply the ratio of the pressure in one volute of the turbine to the pressure in the other volute. A scroll pressure ratio of one indicates even flow between the two sides, while values further away from one indicate uneven flow. By plotting the scroll pressure ratio vs. turbine pressure ratio for one complete engine cycle, it was demonstrated that the turbine is operating under highly pulsed and highly uneven flow. Figure 2 shows the differences between steady, even flow in gas stand tests and the actual operating conditions experienced by the turbine on the engine. Current activities include calibrating the CFD model to the experimental data collected, and continuing turbocharger evaluations.

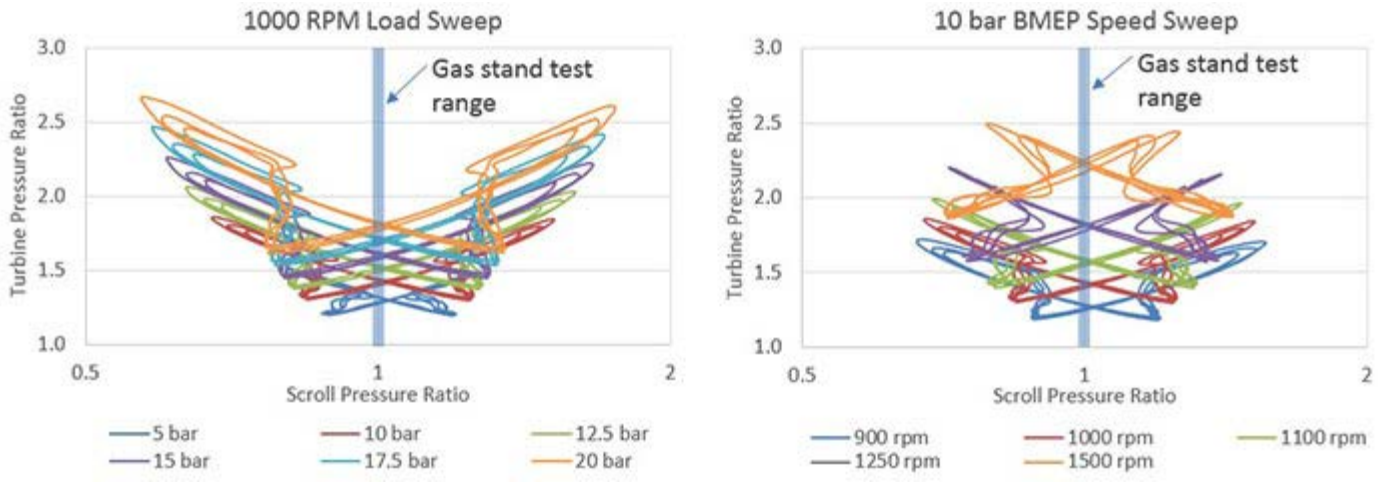

Figure 2: Comparison of turbine operating range on engine vs. gas stand tests for speed and load sweeps.

SOUTHWEST RESEARCH INSTITUTE®

2017 IR&D Annual Report

Evaluating System-Level Transient Performance of a Plug-In Hybrid-Electric Vehicle, 03-R8778

Principal Investigator
Peter Lobato

Inclusive Dates: 07/01/17 – Current

Background — Modern hybrid electric vehicles are designed to have their powertrains work as a complete system, rather than the sum of individual components. Testing them as a system allows us to identify what efficiency improvements can be made. Current vehicle testing procedures to determine fuel efficiency from hybrid and plug-in hybrid vehicles are not designed with the fidelity and precision needed for vehicle-level efficiency optimization. Because the engine, electric machines, gearing ratios, and power transfer devices are closely integrated and cannot operate without each other, future powertrain development requires much different methods, data acquisition strategies, and techniques compared to methods used with conventional vehicles. Figure 1 shows how tightly the electric motor and transmission are integrated in a previous Prius powertrain.

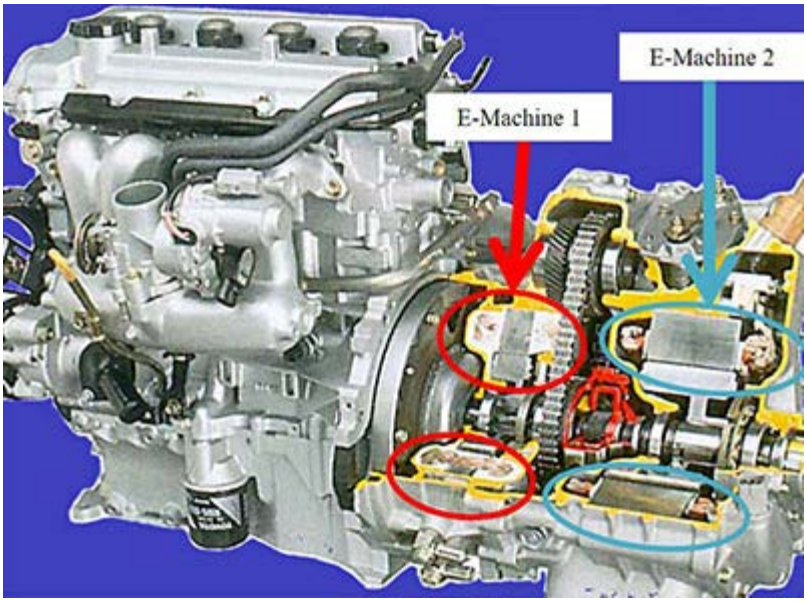

Figure 1: PHEV powertrain is highly integrated.

Approach — The objective of this project is to operate a test vehicle on a chassis dynamometer and analyze the flow of energy across individual subsystems of a plug-in hybrid vehicle. The hypothesis is that such an analysis will have the fidelity to identify and quantify available efficiency improvements. To conduct such an analysis, power will be measured throughout the vehicle's powertrain (Figure 2) in order to answer three main questions:

- Is there room for improvement in system-level performance using look-ahead technology with connected autonomous vehicles?
- Is there a difference between steady-state performance and transient performance, and can this knowledge be leveraged to improve vehicle transient efficiency?
- What potential exists for efficiency gains from lubricants tailored specifically to PHEVs?

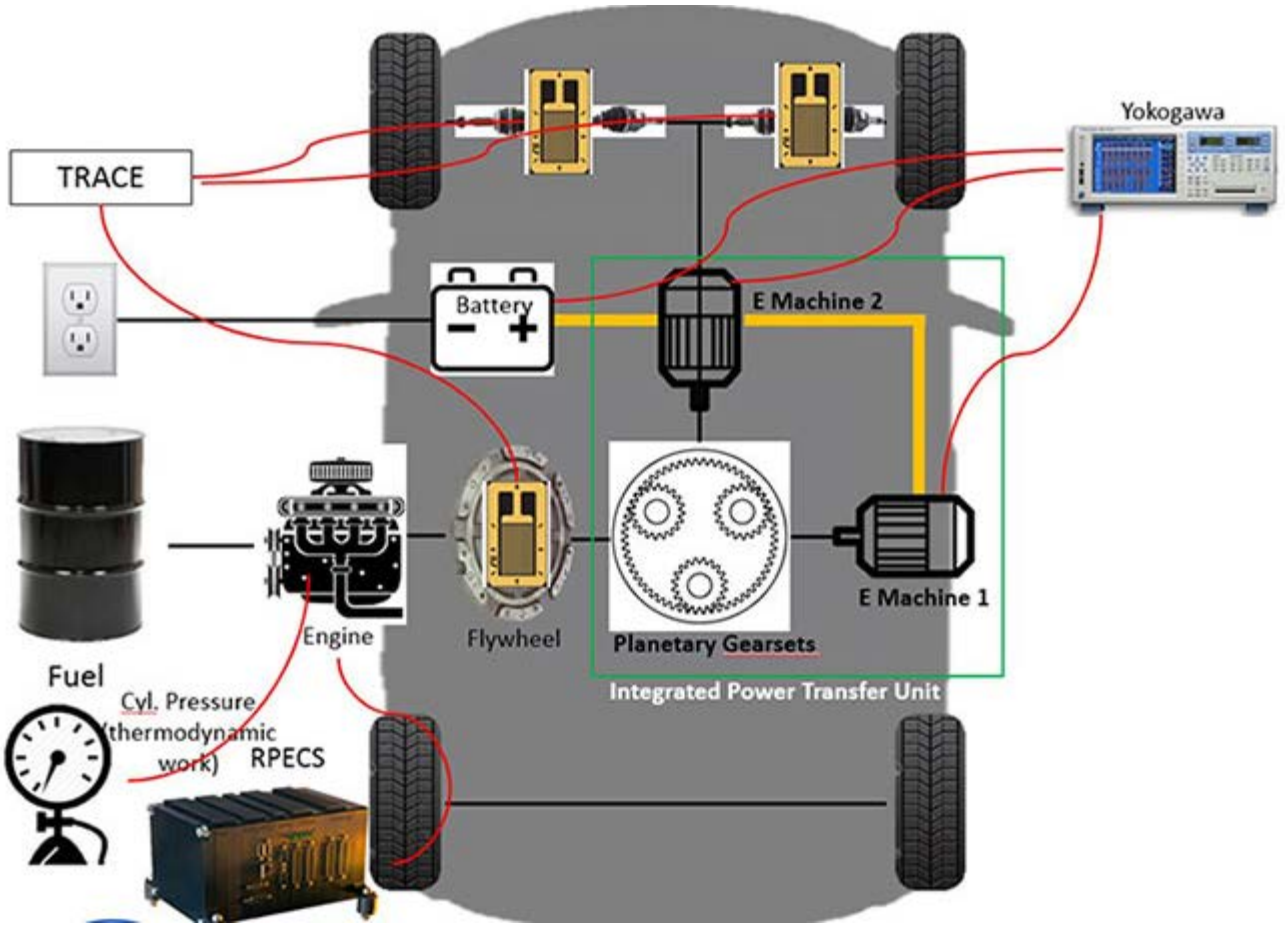

Figure 2: Vehicle instrumentation

Accomplishments — To date we have purchased a 2017 Toyota Prius Prime plug-in hybrid (Figure 3). After the vehicle was received, it was driven on one of SwRI's mileage accumulation dynamometers to break in the powertrain.

Figure 3: Test vehicle: 2017 Toyota Prius Prime

A key piece of instrumentation for this project is measuring engine-out torque. To do this, the coupling between the engine and power transfer unit (flywheel) was removed and re-designed to be a torque transducer. The vehicle's powertrain was removed and partially disassembled to gain access to the flywheel. The space around the flywheel (the inside of the transmission bell housing and rear face of the engine block) was measured precisely to determine how much space is available for modifications to the flywheel and associated electronics. In collaboration with other SwRI researchers, a Faro arm laser scanner is being used to generate a solid model of the interior space around the flywheel. Instrumentation is ongoing. Once all instrumentation for power measurements has been installed the vehicle will be re-assembled and chassis dyno testing will begin.

SOUTHWEST RESEARCH INSTITUTE®

2017 IR&D Annual Report

Development of a New Automotive Fuel Filter Test Method Incorporating Vibration and Cyclic Flow Test Parameters, 08-R8723

Principal Investigators
Larry Hollingsworth
Gary Bessee
Peter Wostarek
Christian Exposito
Paul Till

Inclusive Dates: 01/16/17 – Current

Background — Traditional filter efficiency test standards published by ISO and SAE require steady fluid flow and stationary fixtures that often are not representative of the filter environment in its actual application. Further, filter technology has evolved for some filter classes such that standardized tests do not adequately differentiate filter models. This research project was aimed at creating a diesel fuel filter test procedure that incorporated cyclic fluid flow rates and controlled structural vibration to provide an evaluation that better simulated the environment of the filter in application that can differentiate filters based on their performance relative to the dynamic conditions.

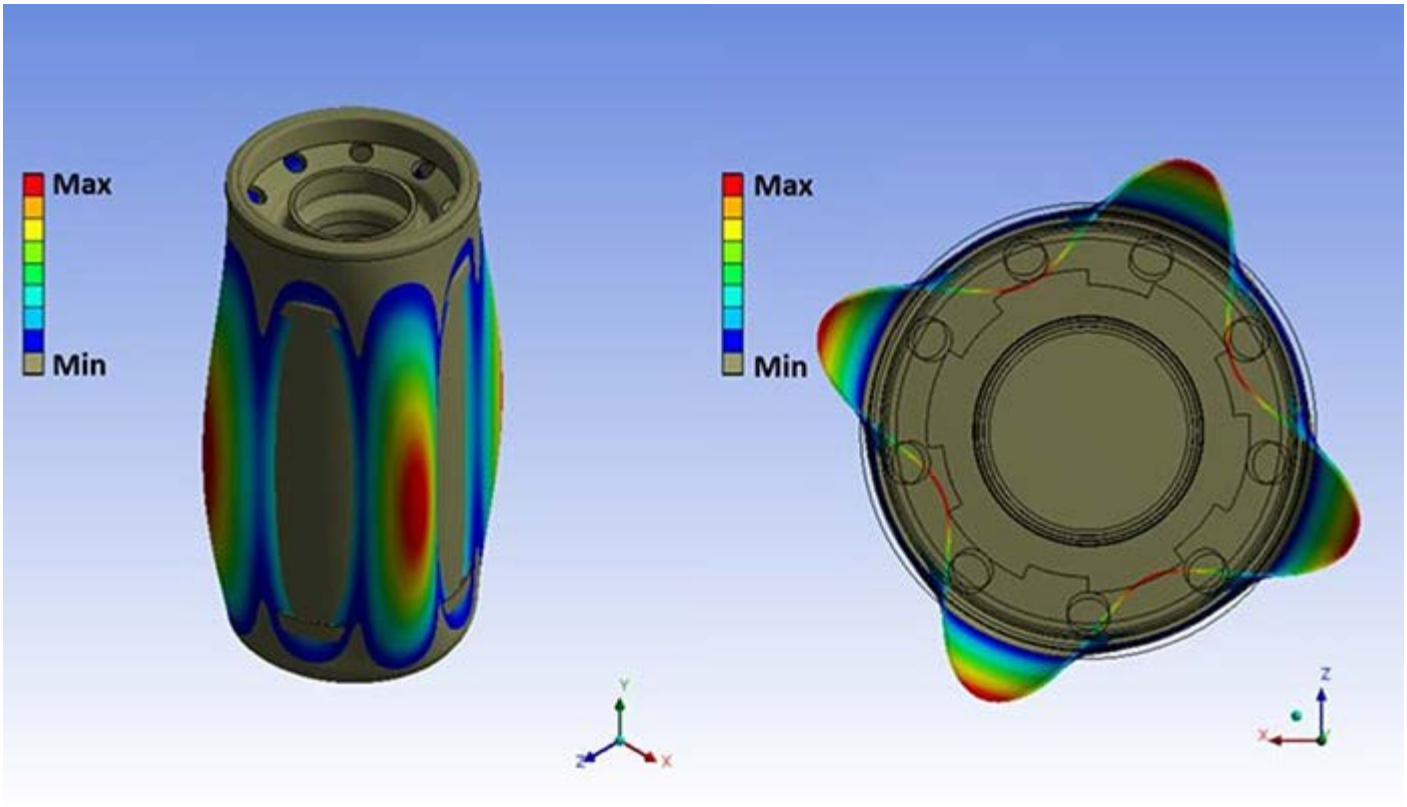

Figure 1: Low-order vibration mode shape of filter shell.

Approach — From heavy-duty diesel vehicle and filter manufacturer recommendations, a spin-on type

diesel fuel filter with several competitive models was chosen as a research candidate. The filter was analyzed from a structural dynamics perspective to determine the effects of filter mounting design, natural vibration modes and frequencies of the filter/mount system, and filter motion due to vibration input. Figure 1 displays a filter shell mode predicted from a dynamic finite element model. This structural perspective of the filter motion was coupled with directions from vehicle manufacturers regarding the expected vibration and flow cycling seen in vehicles. The candidate filters were then evaluated on a filter efficiency test stand that was adapted to provide cyclic flow patterns and drive the filters with vibration. The cyclic flow patterns were varied to study the particles detected downstream of the filter due to varied flow amplitude changes and rates of flow change. Figure 2 illustrates particle counts detected downstream of a filter after flow rate changes. Particle detection downstream of the filters was also used to evaluate various vibration spectra having different amplitudes, frequency ranges, and inclusion or omission of filter system structural resonances. Determining cyclic flow and vibration conditions critical to filter performance were then used to define a final test protocol. Finally, models from competitive filter manufacturers were evaluated using the final test protocol.

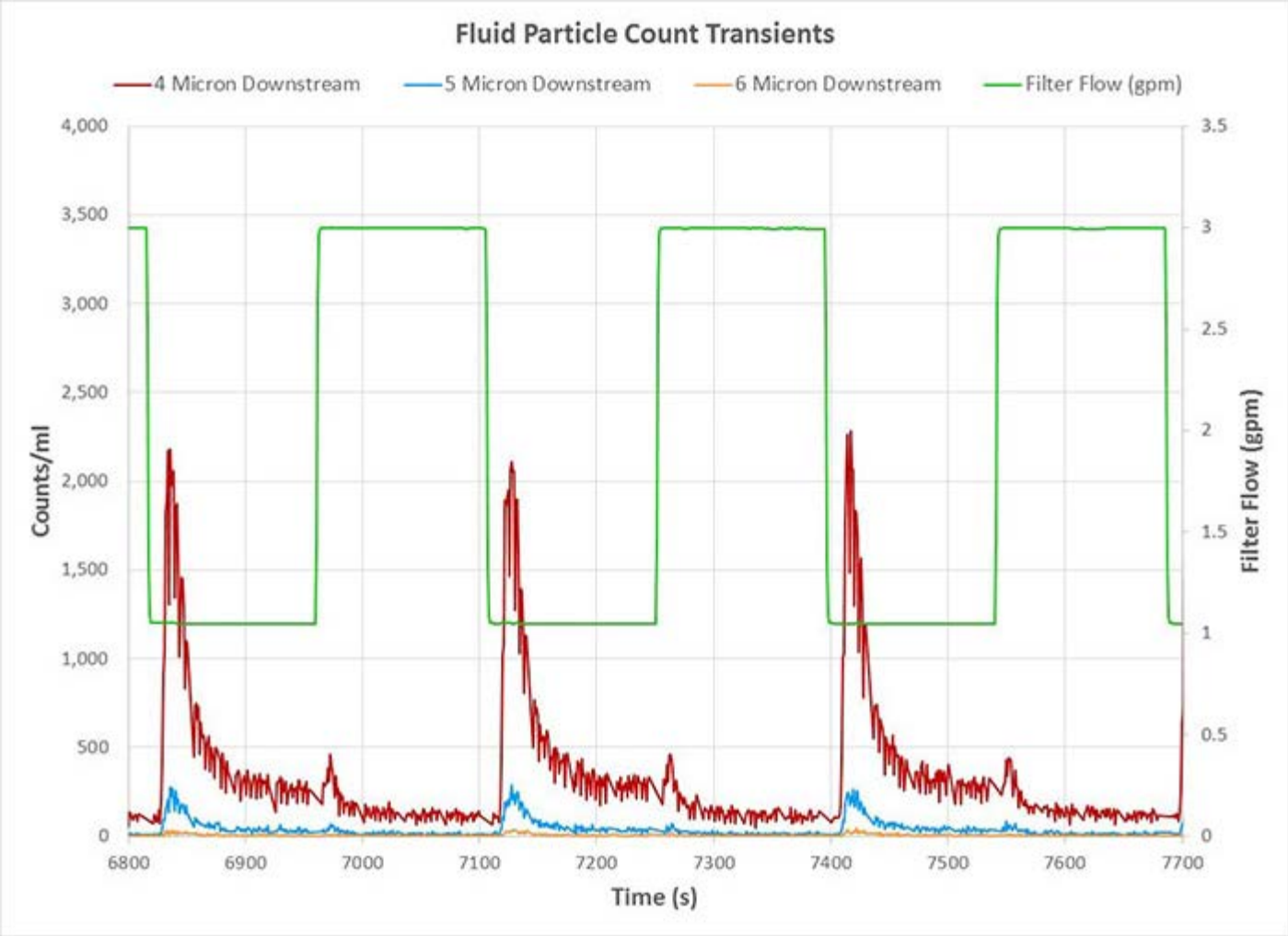

Figure 2: Filter downstream particle transients due to flow change.

Accomplishments — Filter efficiency has been found to depend strongly on both cyclic flow and vibration, both of which can be controlled to create a repeatable test protocol. In particular, rapid flow rate changes produce a particle release downstream that can be several hundred or thousands of particles higher than the steady flow condition. Vibration input coupled to key structural resonances can itself significantly decrease filter efficiency as well as amplify the downstream particle release after flow change events. Final competitive filter evaluation using the developed test protocol is scheduled but not complete at this time.

SOUTHWEST RESEARCH INSTITUTE®

2017 IR&D Annual Report

Investigation of Drought Intensity and Periodicity in South Texas Using Chemical Records in Bat Guano Cores, 15-R8519

Principal Investigators
Leanne Stepchinski
Rebecca Nuno
Nathaniel Toll

Inclusive Dates: 12/04/15 – Current

Background — Understanding the periodicity and severity of droughts can be a critical component when predicting future recharge in groundwater availability modeling. Paleoclimate proxies can be used to discern information about past climates such as temperature and amount of rainfall. This information can assist in identifying patterns of historical drought, which in turn can be used to predict future drought conditions. In semi-arid areas, such as south-central Texas, limited climate proxies are available for estimating regional historical precipitation variability. Bat guano deposits, however, offer a potential alternative record of the paleoclimate to complement traditional climate proxies such as tree rings and speleothems. When identified, paleoclimatic trends such as drought periods can be used to inform conceptual models of recharge rates and durations for use in groundwater resource assessment and modeling. The goal of this study was to explore the potential for using bat guano deposits in caves as an alternative paleoclimate record in south-central Texas.

Approach — The goal of this project was to determine whether the frequency, severity, and longevity of droughts could be identified using anion, cation, and isotopic chemical markers sampled from guano cores. This study used guano extracted from the Bracken Bat Cave, located in Comal County, Texas, USA. Chemical marker data ascertained from guano samples were assessed for their utility to provide a basis for determining historical climatic cycles in central Texas. Radiocarbon (^{14}C) and stable isotopic data ($^{2}H/^{1}H$, $^{15}N/^{14}N$, and $^{13}C/^{12}C$), along with other supporting chemical data, were used to establish age and chemical signatures associated with core sample depths. Mineralogical data were used to analyze whether diagenetic processes affected guano composition over time.

Accomplishments — Guano core collected from Bracken Cave was sub-sampled and analyzed for chemical and isotopic data. Past guano mining, cave breakdown, and guano saturation prevented the collection of deeper guano deposits present in the cave and limited the time frame of this analysis to approximately 35 years. While a medium-to-long-term climate record was not available in this study, successful sampling and sub-sampling methods were developed, and analytical results helped to indicate responsiveness of guano to short-term climatic events. Staff extended their expertise of isotopic analysis to include paleoclimate proxies, which can be applied to studies in hydrogeologic and recharge analyses to enhance opportunities for water resource evaluation funding.

SOUTHWEST RESEARCH INSTITUTE®

2017 IR&D Annual Report

Understanding the Fluid Behavior of Planetary Regolith Materials, 15-R8651

Principal Investigators
Danielle Y. Wyrick
Hakan Başağaoğlu
Justin Blount

Inclusive Dates: 04/01/16 – 04/01/18

Background — Common to all solid planetary bodies is surface regolith, unconsolidated material typically comprised of dust and broken rock fragments. On Earth, the regolith contains high amounts of organic material and biological weathering, and is subjected to effective aeolian and fluvial processes that serve to round individual grains and sort sediments by size. Less well understood is the behavior of regolith materials on airless bodies, where minimal erosional processes keep individual grains at a high degree of non-sphericity. Gully formations and fluvial-like features on the small asteroids Vesta and Helene have been attributed to several hypotheses, but none has explored the role of grain size and shape distribution on the dynamic and static behavior of the regolith on airless planetary bodies. Understanding the effects of grain shape and size has significance beyond geology, including targeted drug delivery. Recent Institute advances in multi-phase Lattice-Boltzmann numerical modeling, including simulating non-Newtonian fluids, suggest that 2-D simulations of densely packed multiple angular-shaped particles are not only feasible, but may have wide ranging modeling applications in both geological and biomedical fields.

Approach — The objectives of this project are twofold: to understand how grain size and shape affect material properties such as cohesion, friction angle, and porosity, as well as dynamic behavior such as angle of repose; and improve existing Institute modeling capabilities of complex geologic and biologic problems by including arbitrary shape particles and Bingham fluid flow behavior. Existing models have already been translated to allow for computational optimization of the code, including increasing the number of modeled particles, size, shape, and fluid type. Current upgrades to the Lattice-Boltzmann modeling approach, including non-Newtonian viscosities such as dilatant, pseudoplastic, and viscoeleastic fluid flows, have been augmented with Bingham fluid capabilities, allowing for modeling of a wide range of conditions, from creeping (low Reynolds numbers) to moderately turbulent flow regimes.

Accomplishments — The project is currently in progress, with completion of early experimental and modeling tasks. We developed different particle shapes, and coded for ease of incorporating additional subroutines for more complicated particle geometries. We validated our new Lattice-Boltzmann model against previously published simulation results with a circular and an ellipsoid particle in a Newtonian fluid, and then modeled the settling trajectories and velocities of particles of different shapes. This new modeling approach may help resolve outstanding questions regarding the fundamental behavior of regolith materials on airless bodies, but more importantly, the increased modeling capabilities will allow for immediate applications toward the space science and biomedical fields.

2017 IR&D Annual Report

Development of an Integrated Surface Water-Groundwater Model for Semi-Arid Environments, 15-R8759

Principal Investigators
Beth Fratesi
Nate Toll
Rebecca Nunu

Inclusive Dates: 04/01/17 – Current

Background — During this project we are exploring methods to fully integrate surface-water flow models with groundwater flow models in semi-arid karst watersheds. This will allow for accurate assessment of the effect of groundwater management practices (i.e., large-scale pumping) on river flow and the reciprocal effect of changes in surface-water flow on groundwater. Precipitation and recharge in arid and semi-arid climates, and a conduit-dominated flow groundwater regime indicative of a karst carbonate system, need to be accommodated to evaluate the water resources of western Texas, in particular, and all other arid and semi-arid environments. Although integrated surface-water/groundwater models developed for less-challenging environments have met with some success, application of a fully coupled surface-water/groundwater model to a karst aquifer with a very high ratio of evapotranspiration to precipitation has not been achieved.

The primary research element of this project is to investigate and simulate the dynamic hydraulic interactions between a surface-water flow regime and groundwater flow regime in response to varying precipitation (i.e., droughts) and water-management actions, such as developing and implementing large-scale groundwater well fields. This investigation will culminate in the development of a fully coupled surface-water/groundwater model suitable for arid and semi-arid environments, and karst carbonate aquifers.

Approach — The project team is conducting an in-depth review of software packages that profess to accommodate coupled surface-water/groundwater flow and interaction. After an initial phase of research into the documented capabilities of these packages, likely packages are being evaluated by constructing a groundwater model and a surface-water model of the Devils River watershed. Once the separate models have undergone initial calibration, they will be coupled. The project plan includes contingencies for additional scripting that may be needed to complete the coupling, incorporate recharge into both the surface-water and groundwater regimes, and insure that conduit/matrix hydraulics are accurately accommodated in the coupled model.

Accomplishments — To date, an in-depth review of software documentation has been completed using a structured evaluation process, resulting in the selection of three packages for further testing. Construction of a surface-water and groundwater model of the Devils River watershed using these packages is currently underway. A detailed schematic for coupling the two models is being constructed for each of the three software packages.

SOUTHWEST RESEARCH INSTITUTE®

2017 IR&D Annual Report

Predicting Induced Permeability from Geomechanical Modeling of Hydraulic Fracturing, 15-R8760

Principal Investigators
Kevin J. Smart
Alan P. Morris
David A. Ferrill
Ronald N. McGinnis
Biswajit Dasgupta

Inclusive Dates: 04/01/17 – Current

Background — Fluid flow through rock is the fundamental process in most energy extraction endeavors, including hydrocarbon exploration and production, and enhanced geothermal energy production. In most unconventional oil and gas resource plays, extraction of hydrocarbons from self-sourced reservoirs (e.g., Eagle Ford, Wolfcamp, Marcellus, Bakken, Barnett, Monterey, and Niobrara Formations) is technically challenging because the natural system matrix permeability is very low. A combination of long, horizontal wells (laterals) and aggressive stimulation (hydraulic fracturing to create new fractures and connect to existing fractures) is necessary for economic fluid recovery. For a typical onshore U.S. unconventional well, 60 percent or more of the total well cost goes toward the post-drilling (stimulation) activities. Improvements in the planning and pre-stimulation prediction of hydraulic fracturing are of ever-increasing importance to the economic viability of most unconventional plays.

Approach — The objectives of this project are to improve predictive modeling of reservoir stimulation activities by investigating alternative approaches for converting simulated continuum-based inelastic strains into fracture volumes (fracture porosity) and quantitative predictions of induced fracture permeability; and fully integrating natural discontinuity information (e.g., derived from wellbore data or discrete fracture networks) so that contributions of both induced and natural fractures are captured in the analyses. Pre-completion estimates of increased porosity and permeability resulting from reservoir stimulation are highly sought after by our clients in the energy extraction industry.

This project builds on our established geomechanical approach to hydraulic fracture modeling, which has employed primarily continuum-mechanics-based, finite-element methods using inelastic (permanent) strains as proxies for the induced fractures. This approach does not explicitly simulate discontinuity formation and therefore does not provide a direct measure of permeability enhancement of the system. While these analyses have been successful in simulating complex fracture patterns that our clients consider to be more realistic than standard industry approaches – and therefore useful in well planning and design – the lack of induced fracture volume (porosity) and permeability information is hindering the next major advance in modeling induced hydraulic fracturing. A viable option for advancing this work is to incorporate a new user-defined constitutive model into our fundamental continuum-mechanics approach that will explicitly calculate an induced fracture aperture variable. When integrated over the simulation domain, this approach can provide a quantitative measure of the porosity and permeability enhancement. An alternative technique that we are exploring and comparing is an integrated finite element-discrete element modeling approach that explicitly allows new fracture formation and therefore computation of new fracture volume.

Accomplishments — A user material model implemented in FLAC was tested by replicating experimental rock tests that used a dog-bone geometry under triaxial extension loading conditions. Axial strain versus

differential stress derived from the numerical simulations showed a close similarity to the experimental test results. Further, the numerical simulations provided insights into the location, type (tensile versus shear), and magnitude of induced fractures in the samples as a function of applied confining pressure.

SOUTHWEST RESEARCH INSTITUTE®

2017 IR&D Annual Report

Injection Wells and Induced Seismicity, South Central Texas, 15-R8772

Principal Investigators
Alan P. Morris
Ronald R. McGinnis
David A. Ferrill
Kevin J. Smart
Nathaniel Toll

Inclusive Dates: 06/01/16 – 10/03/17

Background — Induced seismic activity has become a focus of substantial media attention and public interest. In this project we performed a baseline study of a new long-term, large-volume injection program associated with the San Antonio Water System's Twin Oaks desalination plant. In 2016, San Antonio Water System (SAWS) started desalination operations at its Twin Oaks facility south of San Antonio. The project extracts brackish water from the Carrizo Formation, passes the water through a reverse-osmosis treatment to remove the dissolved solids, and uses the processed water to supplement the water supply of the City of San Antonio. The waste saline brine is then injected into disposal wells somewhat down-dip (toward the coast) from the extraction wells. We constructed a 3-D geologic framework model of the locale, and using the injection data to date, simulation scenarios were run to parameterize the risk of induced seismicity related to the injection program.

Approach — The location of the disposal wells is close to known or suspected faults (Figure 1), and experienced a magnitude 3 earthquake in 1984. Fashing, Texas, the location of a magnitude 4.8 earthquake in 2011, is approximately 25 miles to the south-southeast.

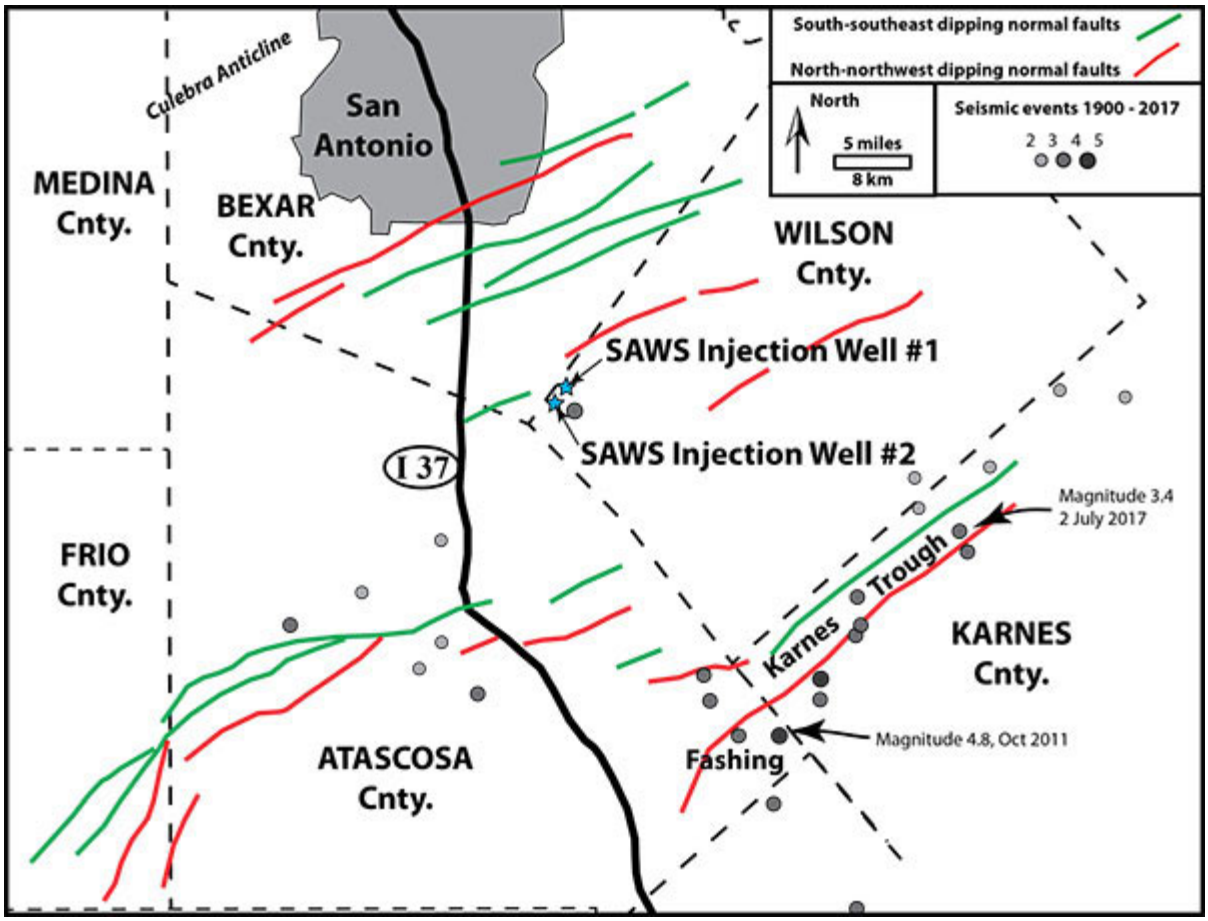

Figure 1: Locations of the two currently operating disposal wells south of San Antonio. Also shown are the principal mapped faults and earthquake epicenters from the period 1900 to present.

Two Freedom of Information Act Requests were submitted by SwRI legal counsel and these resulted in SAWS providing us with all the well completion records, and the minute-by-minute injection records for the first seven months of operation (October 2016 to April 2017), followed by the minute-by-minute injection records for the period April 2017 to August 16, 2017.

A geologic framework model was constructed using PETREL software, and key elements of the model were transferred into 3DStress® software, which was used to develop a stress and permeability model to run simulations of the proposed injection programs for the disposal wells and evaluate likelihood of fault reactivation. This is an approach that we used to perform a “look back” at the Youngstown, Ohio, earthquake sequence.

Using the 3DStress® model, we simulated a range of scenarios to evaluate the risk of induced seismicity (if any) resulting from injection activity. We have recently developed analytical tools for use in 3DStress to simulate injection well effects on fault and fracture stability, and these were used to develop a range of scenarios designed to evaluate the critical risk factors for induced seismicity (stress state, permeability architecture, and the presence, orientations, and locations of faults in the vicinity of the injection site).

Accomplishments — The technical accomplishments of this project include:

- Successful building of a 3-D geologic model of the area of interest south and east of San Antonio.
- Creation of a viable stress model for the volume under study.
- Testing of permeability scenarios and the parameterization of viable candidates for permeability architecture to be used in simulations.
- Simulations using discretized versions of SAWS two injection wells' pressure and flow rate histories indicate that:
    - Pressure perturbations generated by the injection wells can propagate 10s of km away from the

injection site
- Fault sensitivity to reactivation by pore pressure perturbation is not simply a function of proximity to the injection site, but also depends on location with respect to the injection well(s) and the permeability architecture, and on the orientation and geometry of the fault experiencing pore fluid pressure change.

SOUTHWEST RESEARCH INSTITUTE®

2017 IR&D Annual Report

Development of Computational Fluid Dynamics Framework for Characterization of High Energy Arcing Faults (HEAF) in Nuclear Power Plants, 20-R8680

Principal Investigators
Debashis Basu
Marc Janssens
Karen Carpenter

Inclusive Dates: 11/01/16 – 11/30/16

Background — A high energy arcing fault (HEAF) can occur in an electrical system or component through an arc path to ground or lower voltage, if sufficiently high voltage is present at a conductor with the capacity to release a large amount of energy in an extremely short time. A HEAF is characterized by a sudden release of electrical energy through the air, and the energy transfer from the arc to the air leads to a sudden air pressure rise in electrical installations followed by release of hot gases from the installations. This creates a hazard for the surrounding equipment as well as nearby personnel. Because HEAF experiments are expensive, using computational fluid dynamics (CFD) to numerically simulate HEAFs is a viable and cost-effective analysis tool for determining the zone of influence (ZOI) of a HEAF for different types of high energy electrical cabinets. HEAF events initiate with an arc that heats and ionizes the surrounding environment to several thousand degrees Celsius, making it electrically conductive; the temperature increases as a result of self heating induced by the current. Simulation of the HEAF phenomenon involves modeling the plasma-state gas as well as thermo-fluid analysis. The plasma-state gas is affected by the electromagnetic force, induced by the current, the plasma state gas pressure gradient, and the rate of heat generation. The electromagnetic field significantly influences the overall flow and thermal field in the computational domain.

We used existing commercially available CFD tools to develop a computational framework for numerically simulating the high-velocity mass and energy transport that occurs during HEAFs that pose a fire risk to nuclear power plants. The project also evaluated the feasibility of modifying existing CFD tools to accurately simulate the effects of selected HEAF events in nuclear power plants. Project staff members were able to successfully couple the fluid dynamic solver with the electromagnetics solver to obtain accurate estimates of the effects of the Lorentz force and the electromagnetic forces on plasma characteristics. The project demonstrated a proof-of-concept model for this coupled analysis. Preliminary results using this coupled model appear promising and can be used to do detailed HEAF modeling in nuclear power plants. Computed results showed good qualitative agreement with observed results.

Approach — We used CFD and other numerical techniques to achieve the objectives. In particular, the modeling efforts focused on the following:

- Setting up a computational model framework to numerically simulate the pressure rise and energy flow of the hot gases due to a HEAF event in a high energy electrical enclosure.
- Determining how far the computational domain must be extended beyond the electrical cabinet to capture all targets that could potentially be damaged or ignited, and optimized the mesh to minimize impact on run time.
- Computing the thermal field within an enclosure with arc formation and also analyzing the effect of the arc on the temperature after the arc is extinguished.

Comparing two approaches for representing an electrical arc when simulating HEAF events. In the first approach, a simplified model based on experimental data specified the open arc energy as a source term in the CFD calculations used to calculate the pressure, velocity, and temperature responses. The Navier-Stokes equations were solved in this approach with a specified heat source term to model the arc energy. The more-detailed second approach involved a coupled simulation of multi physical fields related to the arc, using electromagnetic equations to calculate the Lorentz force, which in turn provided a source term in the Navier Stokes fluid momentum equations. This second approach involved coupling the Navier Stokes equations with Maxwell's equations for the electromagnetic field. We compared the two approaches based on the predicted temperature and pressure within the compartment and the degree of agreement with the experimental results.

Accomplishments — The major accomplishments of the project are as follows:

- We used existing commercially available CFD tools to develop a computational framework for numerically simulating the high velocity mass and energy transport that occurs during HEAFs that pose a fire risk to NPPs.
- We also evaluated the feasibility of modifying existing CFD tools to accurately simulate the effects of selected HEAF events in NPPs.
- We were able to successfully couple the fluid dynamic solver with the electromagnetics solver to get an accurate estimation of the Lorentz force and electric field for realistic prediction of plasma characteristics.
- We demonstrated a proof-of-concept model for this coupling analysis. Preliminary results using this coupled model have been very promising and can be used for detailed HEAF modeling in NPPs.
- Our preliminary analysis and comparison between the two approaches found that the coupled Maxwell-Fluent approach provides a more realistic solution to HEAF problems consistent with experimental observations.

SOUTHWEST RESEARCH INSTITUTE®

2017 IR&D Annual Report

Assessment of Limitations in Current Approaches to Analyses of Seismic Liquefaction Potential, 20-R8698

Principal Investigators
Kevin J. Smart
Biswajit Dasgupta

Inclusive Dates: 10/10/16 – 02/10/17

Background — Liquefaction is a complex process whereby saturated or partially saturated cohesionless granular media lose shear strength because of increase in pore pressure under cyclic shear stress induced by seismic ground motion. The loss of shear strength results in a "liquid-like" behavior of the otherwise solid material. Liquefaction has been a major cause of damage to buildings and other structures during large earthquakes, and assessing the potential for soil liquefaction to disrupt infrastructure is important for local, state, and federal regulatory agencies as well as commercial organizations. A semi-empirical relationship for assessment of liquefaction potential was developed based upon a case history database of earthquakes prior to 1985. In addition to the semi-empirical approach, a number of soil liquefaction constitutive models have been developed that are used for coupled fluid-mechanical analysis under dynamic loading to model the basic mechanisms that can lead to liquefaction and subsequent ground instability.

Approach — The objectives of this project were to evaluate the currently available soil liquefaction models in terms of their critical input soil parameters related to liquefaction resistance, and study the influence of one or two key demand parameters (e.g., duration of ground motion, intensity of ground motion) on the prediction of liquefaction potential provided by each approach. Four currently available soil liquefaction models (Roth, Finn-Byrne, UBCSAND, PM4SAND) were evaluated in terms of their critical input soil parameters related to liquefaction resistance. We also studied the influence of a key demand parameter (i.e., intensity of ground motion) on the prediction of liquefaction potential provided by each approach. Study sites near Christchurch, New Zealand, were selected where liquefaction was observed following two large earthquakes – the September 4, 2010, Mw 7.1 (Darfield) earthquake and the February 22, 2011, Mw 6.3 (Christchurch) earthquake.

Accomplishments — The Roth and PM4SAND models performed similarly in that they generally predicted liquefaction at similar subsurface locations in response to loading from both the 2010 and 2011 earthquakes. The UBCSAND model results were similar to the Roth and PM4SAND results at shallow depths. In some cases, however, the UBCSAND model predicted liquefaction at greater depths where liquefaction would not be expected. The Finn Byrne model did not provide reliable results, suggesting that it requires calibration of input parameters before application.

SOUTHWEST RESEARCH INSTITUTE®

2017 IR&D Annual Report

Proof-of-Concept Biosphere Model to Calculate Human Radon Doses Applicable to Buried Radioactive Waste Exposure Scenarios, 20-R8775

Principal Investigators
Patrick LaPlante
Daniel Speaker
Osvaldo Pensado

Inclusive Dates: 06/26/17 – 10/26/17

Background — The purpose of this project was to develop a proof-of-concept environmental transport and dose model that implements a radon inhalation radiation dose calculation capability applicable to buried radioactive waste facility exposure scenarios. Radon is a naturally occurring chemically inert radioactive gas that forms from the radioactive decay of radium-226 and uranium. Radon typically is associated with natural uranium deposits, soils overlying uranium-bearing rock formations, and various types of radioactive waste. Radon readily diffuses through unsaturated fractures and pores in rocks and soils, as well as through building materials. Inhalation of radon decay products (e.g., polonium-210 and lead-210) can be a major contributor to radiation dose when radium-226 is present. U.S. regulatory agencies consider calculated potential radon doses when evaluating radioactive waste disposal licensing actions involving radium-226 bearing wastes. These evaluations typically apply complex long-term performance assessment models that simulate release and environmental transport of waste materials and estimate radiation doses to hypothetical members of the public.

Approach — The technical approach involved an initial development of the radon transport and dose model using simulation software and followed a typical model development process. The model design objectives included addressing applicable features and processes, such as waste facility engineered barriers; release of radon to the geosphere and biosphere; variable sources and transport geometries; an inadvertent future human intrusion scenario involving construction of a hypothetical future residence at the waste facility site; potential human receptors located at the site boundary and within the onsite residence; attenuation of radon and decay product transport by multiple subsurface geologic layers and by the concrete foundation of the hypothetical residence; radon flux from the soil surface to air followed by air transport and dispersion beyond the site boundary; radioactive decay and ingrowth; and potential accumulation or loss of radon decay products that could affect dose calculations.

To address radon transport within the soil or the atmosphere, several networks were constructed (called cell-nets) of individual mixing cell calculations that were implemented in a manner that was appropriate for gas transport through solid media and air. These mixing cell calculations uniformly and instantaneously distribute mass within the available pore space within each cell. By linking multiple cells together using software features that implement advective and diffusive mass transfers between mixing cells, the project team developed radon transport models that simulate advective and diffusive transport using calculations that are mathematically equivalent to the solution of a coupled system of differential equations by finite differences (a cell represents a finite-difference element). The simulation software numerically solves the coupled system of finite-difference equations to compute the contaminant mass present in each cell and mass transfers as a function of time. The cell-nets were implemented in the model to simulate movement of radon gas through the soil by diffusion and through the air by advective transport with lateral and vertical dispersion. Following transport, the model calculates airborne concentrations at receptor locations and

radiation doses based on the time individuals spend in each environment. The model was tested to evaluate whether it performed within expectations. A screenshot of the air transport submodel in Figure 1 shows the construction and information flow. Figures 2 and 3 show calculated radon concentrations with time and transport distance in the soil and air, respectively.

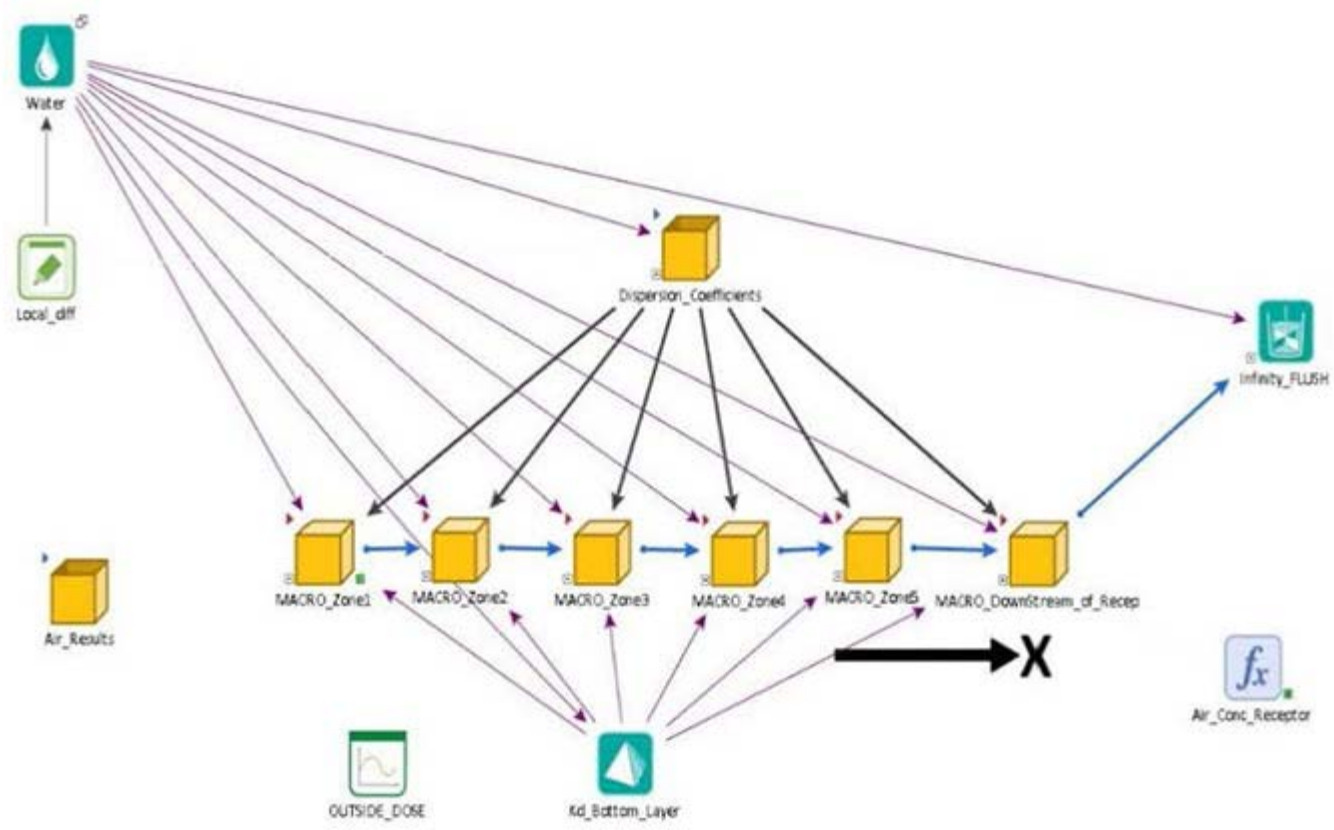

Figure 1: Airborne radon advective transport submodel.

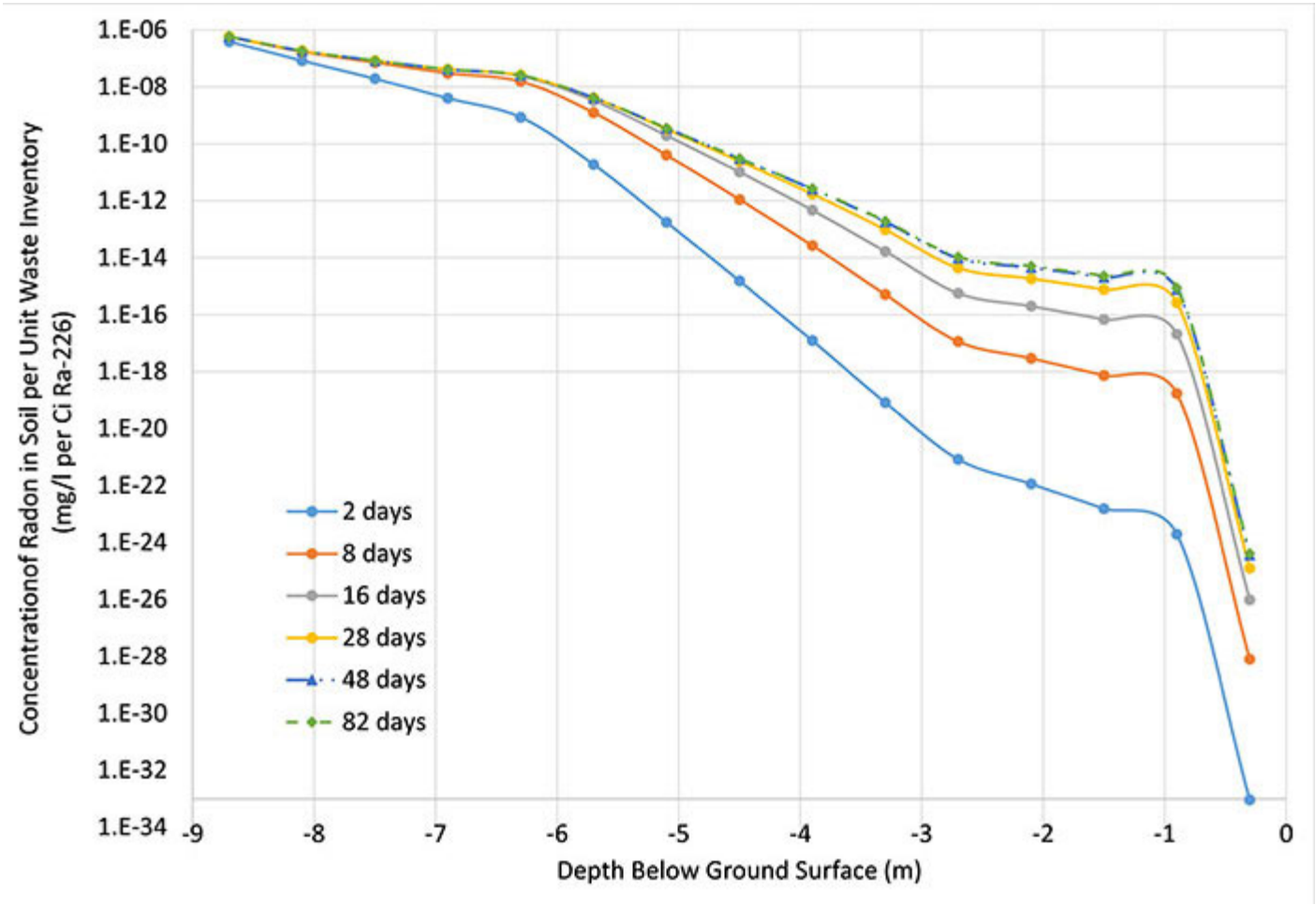

Figure 2: Calculated radon concentrations in soil by transport distance and time.

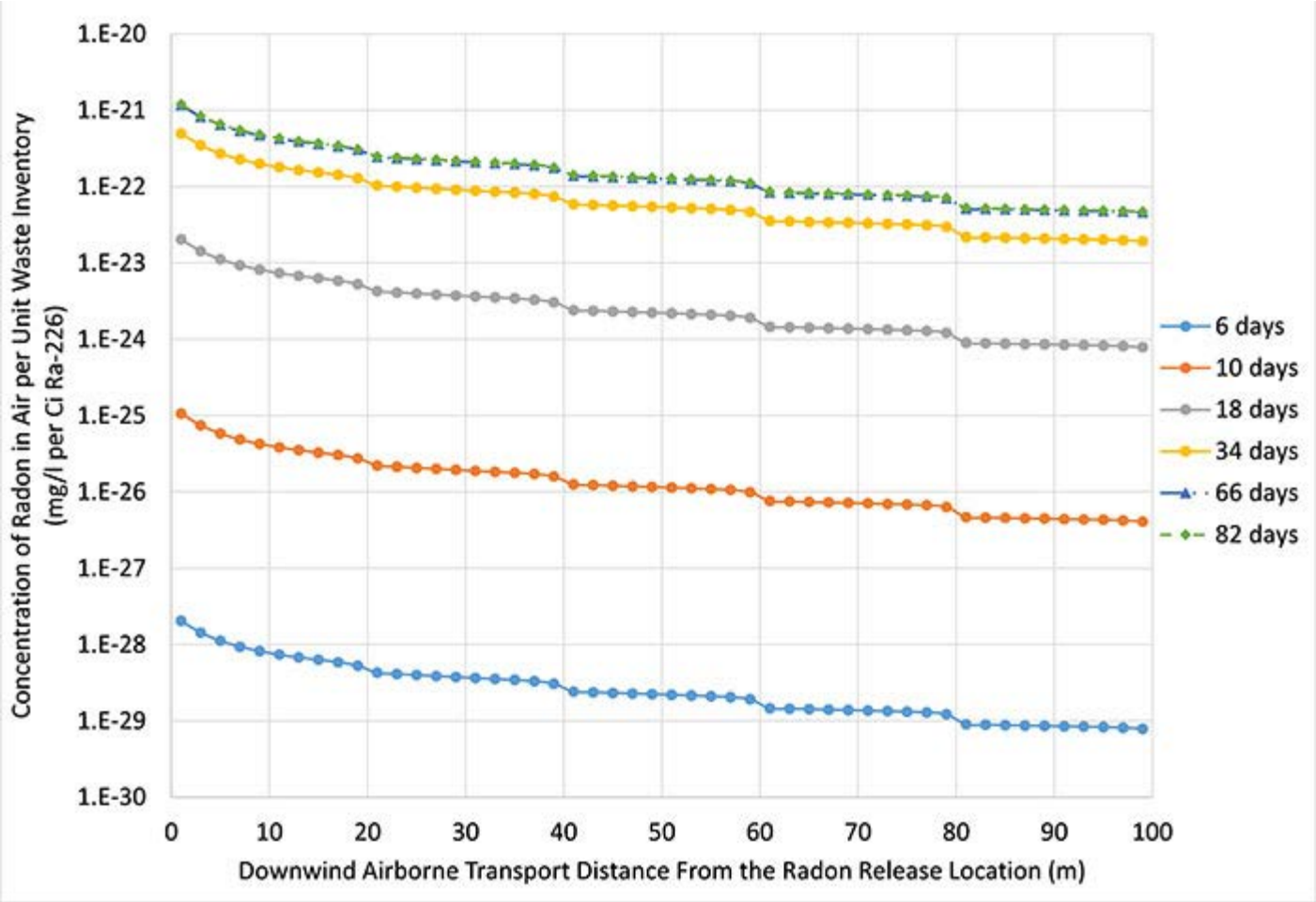

Figure 3: Calculated radon concentrations in air by transport distance and time.

Accomplishments — An environmental radon transport and dose model was developed that implements calculations applicable to evaluation of buried radioactive waste facilities. The project demonstrated SwRI staff could quickly and efficiently conceptualize a complex modeling problem and develop an applicable mathematical model using available simulation software. The radon model incorporates the planned features and includes submodels for the radium source, geologic (soil) transport, residential basement, air transport, and receptor dose calculations. Initial verification tests and analysis of model results provided a measure of confidence that the model is functioning as designed. External client funding has been received to continue developing and testing a variant of the model in accordance with applicable quality assurance procedures.

2017 IR&D | IR&D Home

SOUTHWEST RESEARCH INSTITUTE®

2017 IR&D Annual Report

Model Based Gas Turbine Health Monitoring, Diagnostics, and Optimization Using Typically Sparse Performance Data, 18-R8601

Principal Investigators
Jacob Delimont
David Ransom
Craig Nolen

Inclusive Dates: 10/01/16 – 03/30/17

Background — In the current economic and political environment, there is a push for operators using gas turbines for power generation and other industrial uses to achieve higher operating efficiencies. One way that owners and operators of gas turbines believe they can increase operating efficiencies is by using high-fidelity physics-based models. This allows the end user to analyze machine performance, plan for performance upgrades, and evaluate use cases and operating conditions not originally envisioned by the original equipment manufacturers (OEMs). Physics-based performance modeling is used extensively in the design of gas turbines for both aerospace and industrial applications. However, the models developed by the OEMs are considered proprietary. Owners and operators of gas turbines do not have access to these models for use in reliability-centered maintenance, plant scheduling, process optimization, or for predicting the performance impact of proposed machine modifications. Without access to the original models of the OEMs, the end users are left with the options of paying an OEM to perform the analysis for them, creating their own physics-based model based on engineering assumptions, or using trend-based tools that lack flexibility.

Figure 1: GE 7FA rotor during maintenance.

Approach — Modeling a gas turbine requires knowledge of the gas turbine, which can be gained from manufacturers' specifications and data collected from an operating gas turbine. During a maintenance outage at a local power plant, shown in Figure 1, instrumentation was installed and used to collect operating data. This data was used to develop a functioning model of the gas turbine including maps of turbomachinery component performance, shown in Figure 2, to allow for off-design performance predictions.

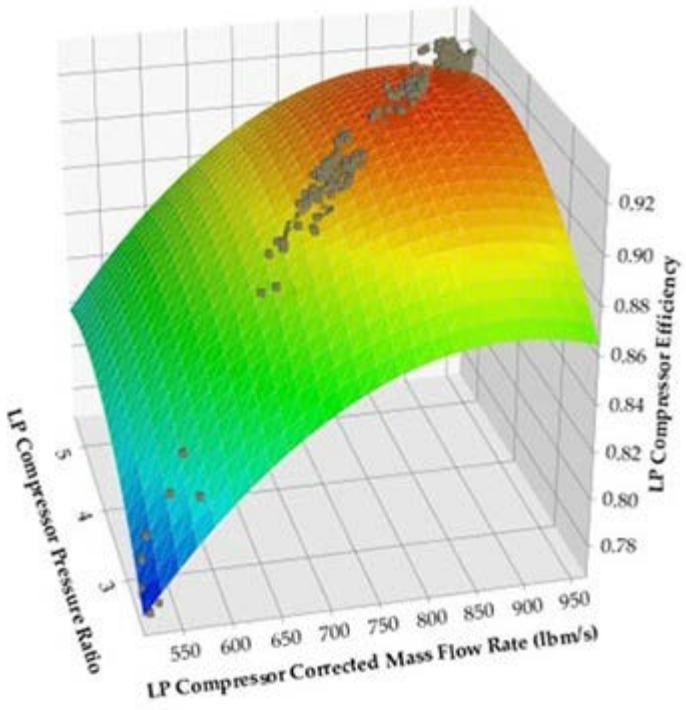

Figure 2: Gas turbine compressor performance map.

Accomplishments — Beginning with almost zero knowledge about the GE 7FA gas turbine, the project team was able to build an off-design performance model using only collected plant data and publicly available information on the turbine. The key objective of developing a model of the GE 7FA engine that can be used to solve "what-if" scenarios was accomplished. This demonstrated the use of plant-gathered experimental data to build turbomachinery performance maps capable of off-design operation predictions.

2017 IR&D | IR&D Home

SOUTHWEST RESEARCH INSTITUTE®

2017 IR&D Annual Report

Field Testing of Rotating Equipment Vibration Modes Using Operational Modal Analysis, 18-R8608

Principal Investigators
Jason Wilkes
J. Jeffrey Moore
Tim Allison
Natalie Smith
Jonathan Wade
Klaus Brun

Inclusive Dates: 11/16/15 – 05/16/17

Background — The energy industry, particularly the natural gas and hydrocarbon segments, depend on the centrifugal compressor to produce, process, liquefy, and transport many different gases. Centrifugal compressors use one or more impellers to impart angular momentum to the flowing gas to produce an increase in pressure, often referred to as head. As the head developed in the compressor increases, the pressures and fluid densities surrounding the impellers and the rotor assembly become higher and affect the dynamic behavior of the rotor, including shaft and impeller seals, axial thrust balance pistons, and impellers. Although state-of-the-art methods are often used to predict the stability of such rotating equipment prior to commissioning in the field, these units are commonly shop tested using externally mounted shakers to assess rotordynamic stability at various operating conditions. This process is costly and requires modifications to the compressor to allow for the installation of an exciter at one end of the shaft.

In recent years, a new technique has been successfully used to measure the dynamic stability of compressors using only the excitation caused by the pressurized gas as it interacts with the shaft and impellers. This process is termed operational modal analysis (OMA). This technique has been applied in other industries for some time; however, its application in rotating equipment is relatively new and is not well understood. The objective of this project was to advance the state of the art for applying OMA to rotating equipment, providing expertise in a market that is sure to grow in the next decade.

Figure 1: C33 compressor during commissioning.

Approach — An industrial high-pressure compressor was procured, installed, commissioned, and operated at SwRI's Turbomachinery Research Facility (TRF) to validate the capability of OMA in rotating equipment. The setup of this compressor is similar to hundreds of industrial compressors operating in the oil and gas industry across the globe. High-speed dynamic shaft vibration data were recorded during operation of this unit, and post processed using an OMA algorithm to refine analysis methodology and evaluate accuracy of the results.

Accomplishments — In agreement with the expected project outcomes, developed OMA modal results compare favorably to predicted modal results, and publication of the research findings will follow soon. Additionally, the research program was critical in the setup of a new high-pressure industrial compressor and test loop at SwRI that has already enabled new and exciting experimental work.

SOUTHWEST RESEARCH INSTITUTE®

2017 IR&D Annual Report

Development and Validation of Liquid-Liquid Separation Modeling Techniques, 18-R8622

Principal Investigators
Amy B. McCleney
Steven T. Green
Rebecca A. Owston

Inclusive Dates: 01/01/16 – 07/01/17

Background — Separating liquids and gases is a critical part of chemical production plants, oil and gas production operations, and many other industrial processes. Separators are composed of large vessels with complex internals to promote coalescence of liquid droplets and/or eliminate mist from gas. The design of multiphase separators is a nontrivial task, requiring complex separation physics and knowledge of fluid properties, flow rates, and inlet mixing conditions. It has long been known that separator performance is strongly dependent on the operating conditions of the flow, pressure, and fluid properties. However, most of the available data, design guidelines, and prediction models are based on air/water analyses at atmospheric conditions because of the high cost of testing at field-like conditions. Separator modeling using computational fluid dynamics (CFD) represents an economical option for design, but caution must be used in the setup and interpretation of the data. Many examples are available in the literature of poor agreement between simulation results using particular models and experimental/field data. Therefore, there is a need for reliable methods to simulate separator efficiency and performance for oil and gas industry applications. The objective of this work was to demonstrate the ability to perform accurate CFD modeling of liquid-liquid separation by validating CFD simulation results against test data being collected under a separate Joint Industry Project (JIP) with industry participants.

Approach — A three-dimensional solid model of the test separator and internals was created as the basis for the simulations carried out in two software packages, ANSYS® Fluent® and STAR-CCM+®. Benchmark CFD simulations comparing the accuracy and complexity of different separator modeling techniques/simplifying assumptions were conducted using two different software packages. After developing a suitable emulsion rheology submodel and determining the optimum submodels within each software package for obtaining high-accuracy, liquid-liquid separation results, a total of 11 parametric simulations were then carried out that varied the viscosity, flow rate, and water cut in the separator. These parameters corresponded to the test parameters used during experimental testing, where liquid-liquid separation efficiencies and concentration values were collected and compared to the numerical results for both the benchmark and parametric simulations. Overall, there was excellent agreement between the CFD results and the laboratory test results.

Accomplishments — The project team developed a set of best practices for the setup, execution, and post-processing of CFD simulations for modeling liquid-liquid separators in each software package.

- A technical paper regarding the multiphase modeling approach for gravity separators was presented at the Offshore Technology Conference (OTC) in May 2017.
- A second paper and a corresponding presentation highlighting the differences in the performance of the two CFD software packages have been fully prepared, and an abstract has been submitted to the OTC technical committee to present this work at the 2018 conference, to be held in Houston.
- A third paper and a corresponding presentation highlighting the emulsion rheology submodel that was created during this project have been prepared. It is anticipated that these will be submitted and

presented to the Society of Petroleum Engineers International (SPE) Technical Conference and Exhibition (ATCE) in 2018.

SOUTHWEST RESEARCH INSTITUTE®

2017 IR&D Annual Report

Acoustic-Induced Vibration Testing, Modeling, and Mitigation, 18-R8730

Principal Investigators
Brandon Ridens
Jeffrey Bennett
Tim Allison
Sarah Simons
Klaus Brun

Inclusive Dates: 01/01/17 – Current

Background — The purpose of this project is to develop a better understanding of acoustic-induced vibrations (AIV) on pressurized gas pipelines that will then enable SwRI to develop and demonstrate mitigation strategies that will reduce the dynamic pressures on the piping that cause AIV failures. AIV is a phenomenon that has been known to cause high-frequency metal fatigue failures at piping discontinuities that present a stress concentration, such as branch connections or pipe supports. Acoustic noise generated from upstream flow restrictions providing high pressure ratio, such as control valves or relief valves, can excite high-frequency acoustic modes and piping shell modes, generally in the range of 100 to 3,000+ Hz, within the main pipeline. These alternating stresses can result in high-cycle metal fatigue failures within minutes of operation.

Figure 1: Installed test section (orange) in the parallel configuration.

The current industry best practice is to follow an empirically based guideline to screen for high-risk conditions. The guideline offers few options (often impractical) for reducing the risk of failure from AIV. SwRI currently offers screening of AIV conditions in pipelines by following the aforementioned industry guidelines, selecting stiffening rings through representative finite element modeling, and applying several mitigation techniques for the piping. However, if an AIV problem is predicted, SwRI can only help select a stiffening ring or recommend a limited set of structural mitigations, which may not be adequate for reducing stresses below allowable levels. Two avenues of mitigation strategies will be considered in this project: reducing the excitation source and strengthening the structure.

Approach — Understanding AIV excitation is accomplished through a combination of data analysis of reduced-power testing, computational modeling, and full-scale testing. The first step in the process is detailed design and construction of a full-scale test article, shown in Figure 1, which is used for both stages

of testing. Finite element modeling is used to confirm preliminary predictions that AVI excitation mode coincidences are possible within the test piping. Next, reduced-power testing is conducted, operating the test article in two configurations through a range of backpressures and flow rates to compare against predicted mode coincidences. The third step involves detailed analysis of the test data to better understand AIV, performing computational modeling, and developing a mitigation design using the computational model predictions. The final step is to prove the mitigation strategy in a full-power test by applying it to the previously used test article.

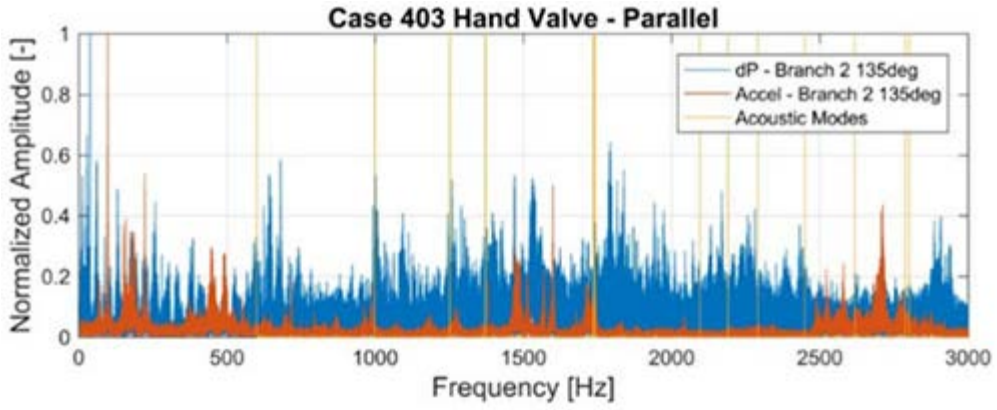

Figure 2: Frequency spectrum comparison of dynamic pressure, vibration, and predicted acoustic modes at Branch 2 during case 403.

Accomplishments — The reduced-power testing has been completed and recorded data have been fully processed. Coincidences were found between mechanical and acoustic responses and confirmed with experimental data from the reduced-power testing, as shown in Figure 2. A custom-designed computational fluid dynamic (CFD) model was made to analyze the fluid system and was validated using recorded test data, as shown in Figure 3. Next, a pulsation dampener design was chosen as the AIV mitigation technique to be used in the full-scale testing. A conceptual design has been defined based on common dampener characteristics and the results of the small-scale AIV testing. The full-scale testing remains to be completed. The full-scale test, which will produce a “broadband” acoustic noise disturbance that simulates the sound power experienced downstream in a piping system, will produce data that will be used to confirm predictions from a three-dimensional CFD model of the AIV event.

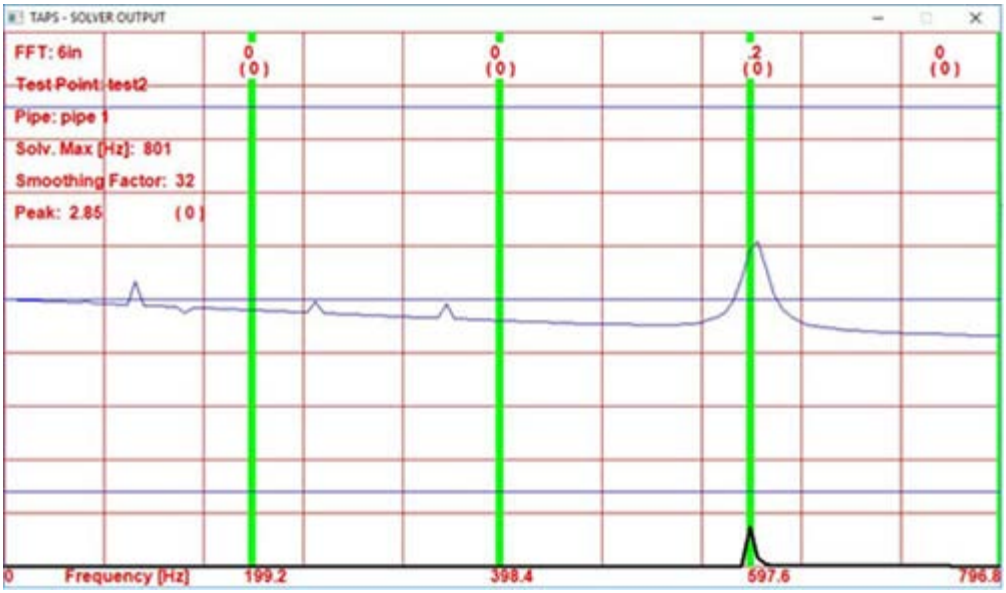

Figure 3: Modal results of the test corresponding to recorded laboratory data.

SOUTHWEST RESEARCH INSTITUTE®

2017 IR&D Annual Report

Tie Bolt Rotor Modeling and Design: Joint Bending Stiffness and Tie Bolt Preload Requirements, 18-R8766

Principal Investigator
Aaron Rimpel

Inclusive Dates: 05/15/17 – 09/15/17

Background — Constructing turbomachinery rotors from built-up sections – comprising impeller stages, spacers, and stub shafts – held together with a central tie bolt is an accepted practice. One design issue pertaining to these "tie bolt rotors" relates to accurate prediction of shaft bending stiffness, which is essential to establishing adequate margin between shaft running speeds and rotor bending critical speeds. For tie bolt rotors, the interface between adjacent shaft sections (e.g., butt joint, Hirth coupling, or Curvic coupling) has a contact stiffness that would act to reduce the effective bending stiffness compared to a solid shaft with otherwise identical dimensions. This stiffness is affected by the interface contact pressure, which is controlled by tie bolt preload force, and by surface finish, joint geometry, etc. Inaccurate prediction in the design stage results in the need to "tune" the rotordynamic models *a posteriori* based on free-free natural frequencies measured in modal bump tests. This situation also runs the risk of needing to implement design changes or modifications if critical speed margins are found to be compromised after the rotor has been manufactured. The primary objective of the current research has been to develop a modeling approach to accurately simulate the bending stiffness of joints common in built-up rotors assembled with central tie bolts. The current scope has been limited to variations of butt joints (with and without pilot fits), though extension to applications with Curvic and Hirth joints could be subjects of future work. A second objective sought to establish a methodology for specifying the range of tie bolt preload force required for a tie bolt rotor with multiple joints.

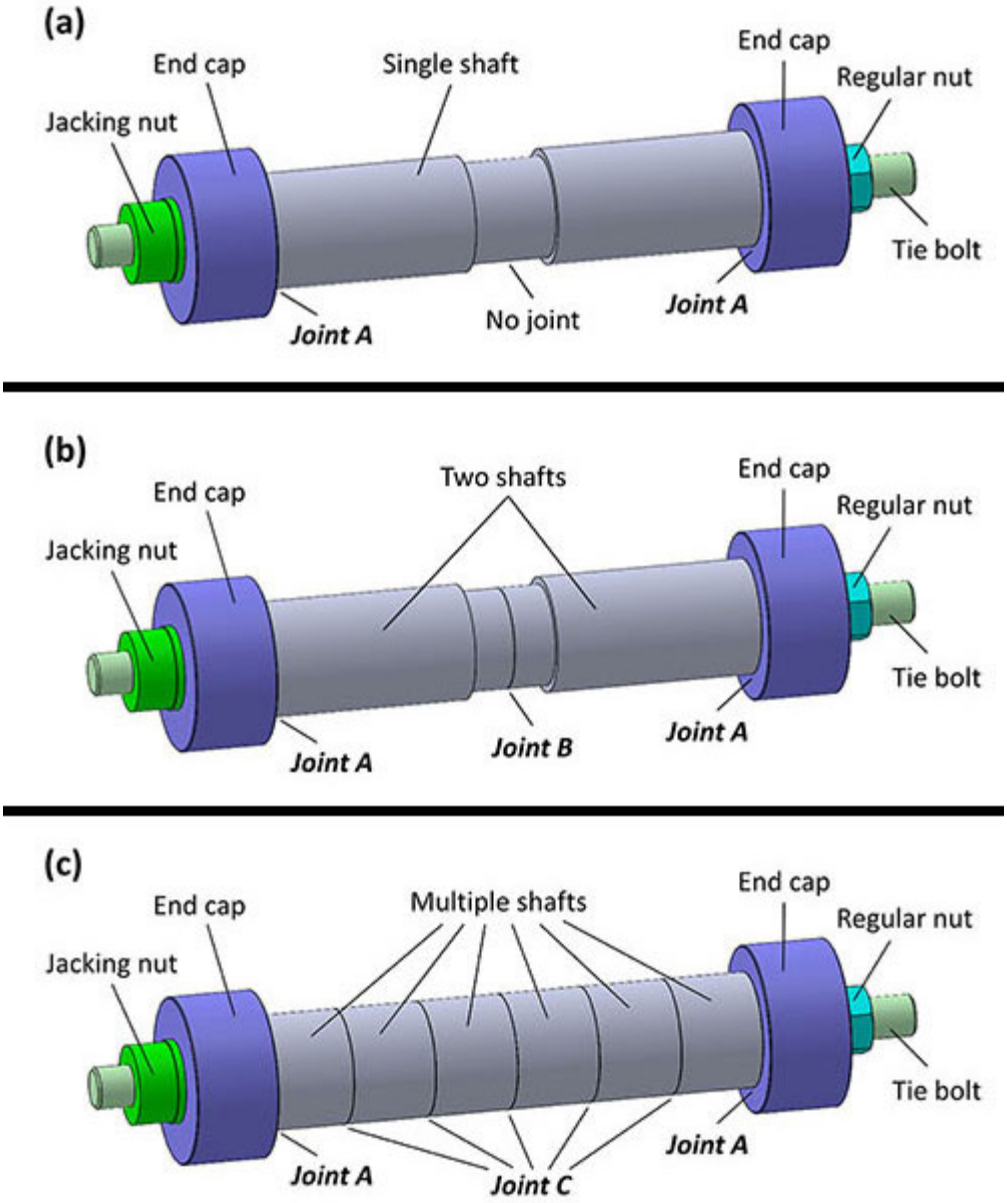

Figure 1: Model of tie bolt rotor test articles: (a) solid shaft, (b) two-piece shaft, (c) multi-piece shaft

Approach — An empirical contact stiffness model was created by analyzing measured natural frequencies from tie bolt rotor test articles (see Figure 1) for a range of tie bolt preload forces and comparing with finite element analysis (FEA) predictions. The contact stiffness effect was simulated using a thin layer of material with a smaller modulus of elasticity than the shaft. The empirical model was created from one of the test cases, then it was implemented in simulations for all other test cases to validate its general applicability.

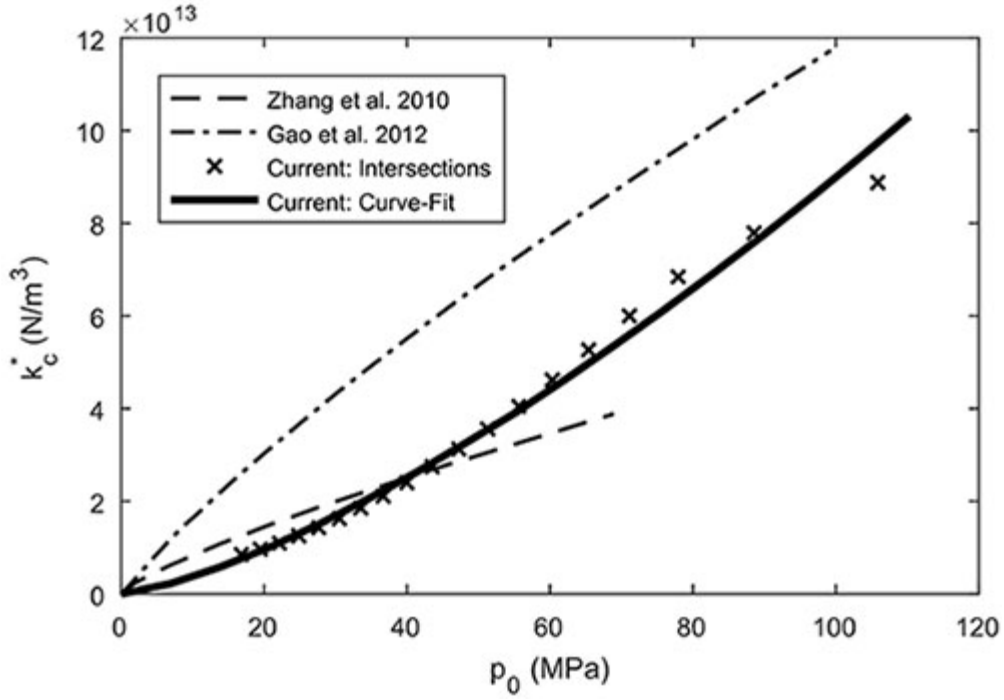

Figure 2: Contact stiffness model comparison

Accomplishments — The empirically obtained contact stiffness model (Figure 2) improved the ability to predict shaft natural frequencies for all tie bolt rotor configurations tested. To illustrate, Figure 3 presents a comparison of the measured natural frequencies to simulations with and without using the contact stiffness model for one of the test cases. The test data show how shafts with more joints are affected by the contact stiffness effect ("Butt (N)" configuration has one more joint than the "Solid (N)" configuration), and the respective contact model predictions ("FEA Contact") demonstrate the improvement over the baseline case ("FEA Baseline").

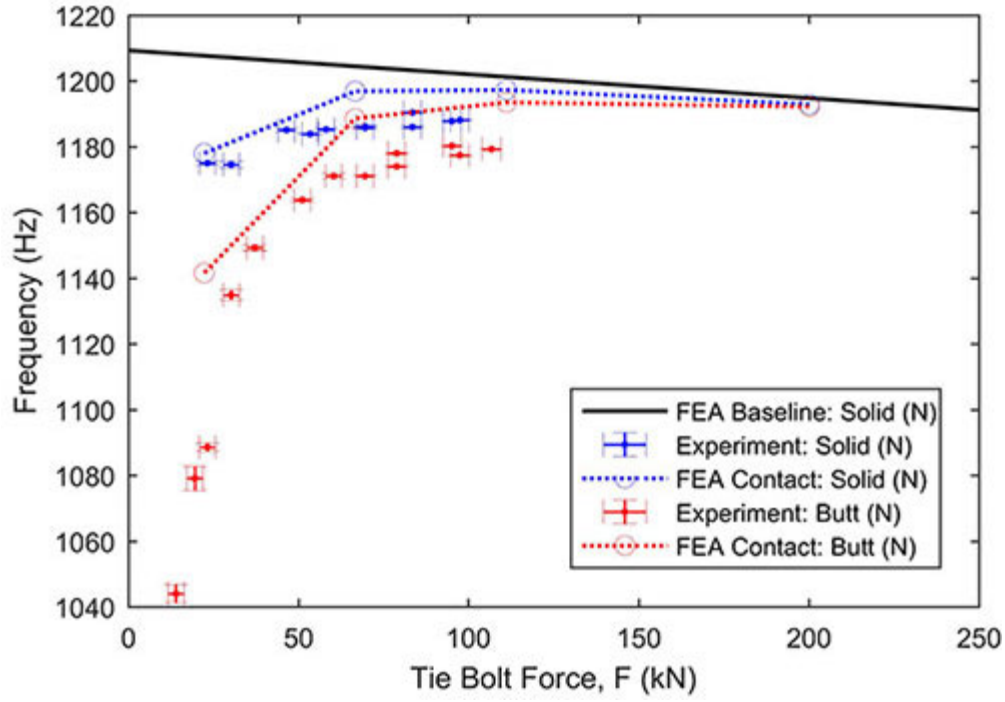

Figure 3: Natural frequency measurements and predictions: narrow solid and butt joint shafts

SOUTHWEST RESEARCH INSTITUTE®

2017 IR&D Annual Report

Optical Level Sensor for Cryogenic Applications, 18-R8771

Principal Investigators
Shane Coogan
Carolyn Day
Thomas Moore

Inclusive Dates: 05/25/17 – 07/28/17

Background — The purpose of this project was to develop an accurate liquid level sensor for cryogenic fluids such as liquid hydrogen. Highly accurate level sensors are needed in liquid test facilities to control processes and to validate other level sensing technologies. Accuracy requirements can be severe for validation applications. For instance, precise propellant utilization in space launch vehicles requires that the vehicle control system know the tank levels with low uncertainty. The facility used to validate and calibrate the vehicle system must be an order of magnitude more accurate than the accuracy requirement of the end application.

While many level sensing options are commercially available for common industrial fluids, these conventional sensors cannot provide highly accurate measurements in liquid hydrogen. The stratified temperature environment, low density, and low dielectric constant limit the applicability of ultrasonic- and radar-based sensors, while weight-based methods are limited by the accuracy of load cells. Liquid hydrogen is an important commodity for space vehicles and is also relevant to energy systems that consume large quantities of hydrogen gas. Developing a practical high-accuracy sensor for this application provides a needed technology and improves SwRI's ability to pursue cryogenic projects. The objective of this project was to build a liquid hydrogen level sensor prototype and to perform initial risk reduction testing with water/air and with liquid nitrogen.

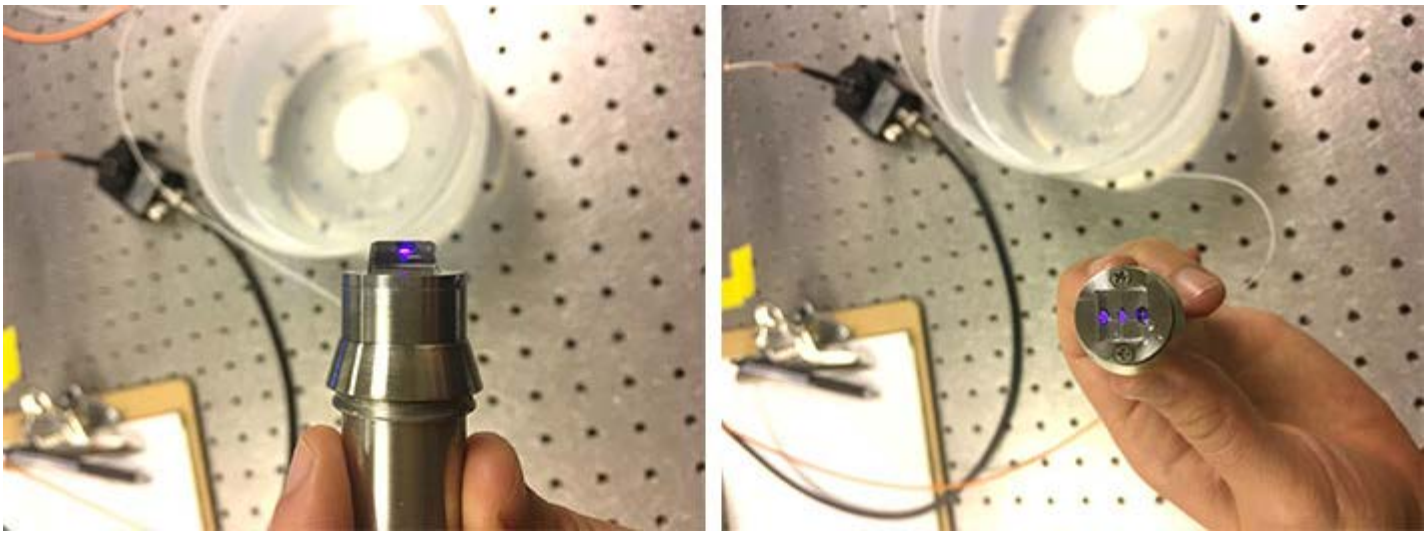

Figure 1: Fused silica prism in machined housing with laser turned on.

Approach — The sensor design is based on reflex gauges used in high-pressure steam systems. The liquid surface of saturated hydrogen, high-pressure water/steam, and other fluids operating near the critical

point is difficult to observe because of the similar refractive indices between the liquid and vapor phases. Reflex gauges allow for the direct visual inspection of the liquid level in these situations by sharpening the visual distinction between phases. A 45-degree angle cut into the surface of the viewing glass that contacts the fluid causes light to reflect completely when the glass is in contact with vapor, but to refract when it is in contact with liquid. The glass appears bright when vapor is present, but dark when liquid is present. A sensor was built using off-the-shelf optical components and a custom-machined mount that was designed to fit in a 3/4 in. Swagelok fitting. A laser was coupled to the sensor and the light output was read and sent to an oscilloscope, allowing a signal to be seen that varied based on whether liquid or vapor was present at the level of the prism, and accordingly if the laser light was reflected or not. The fused silica prism and mount can be seen in Figure 1. This was put into a test apparatus that allowed liquid nitrogen to flow past the sensor. The presence of liquid at the location of the laser on the fused silica prism can be determined with this sensor, making it a highly accurate point measurement.

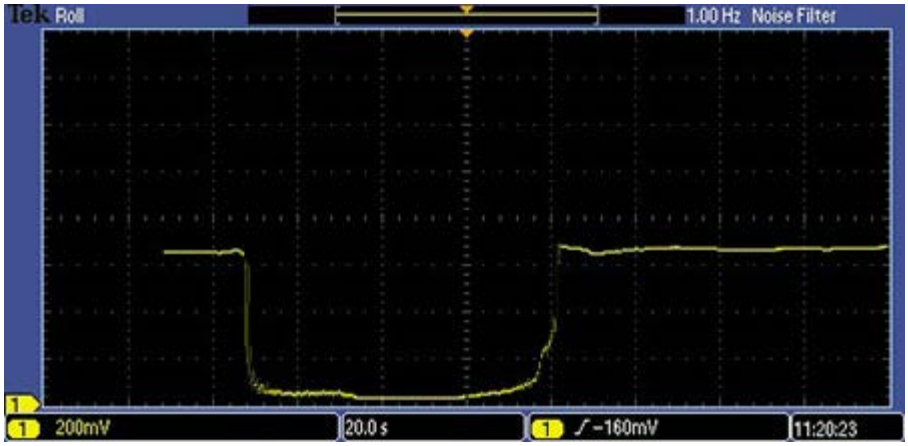

Figure 2: Oscilloscope output from liquid nitrogen test.

Accomplishments — This project facilitated the successful design, fabrication, and testing in a pressurized cryogenic system of an optical level sensor. The sensor distinguished between liquid and vapor in all tests performed, and the signal was observed to align with direct visual and audible inspection of the liquid nitrogen flow. Hydrostatic testing to 300 psia demonstrated that the sensor mechanical design is adequate for most cryogenic applications. Figure 2 shows the results from one of the liquid nitrogen test runs. The signal recording begins with no flow (vapor). The valve on the liquid nitrogen dewar was then opened, and the signal dropped immediately when liquid nitrogen was flowing past the sensor. The dewar was then closed, and the signal rapidly returned to the vapor signal level.

SOUTHWEST RESEARCH INSTITUTE®

2017 IR&D Annual Report

Investigation of the Effects of Inlet Flow Distortion on the Performance of Centrifugal Compressors, 18-R8780

Principal Investigators
Pablo C. Bueno
Kevin Hoopes

Inclusive Dates: 07/01/17 – Current

Background — The objective of this project is to understand the impact of swirl distortion on centrifugal compressor performance and develop a method to analyze it experimentally and numerically. The aerodynamic performance of a centrifugal compressor depends strongly on the velocity and total pressure profile of the flow when it arrives at the inlet. Thus, one of the primary goals of the design of the inlet piping is to ensure that the flow is as uniform as possible at the inlet plane. Many manufacturers and operators today still use design guidelines that were developed in the 1960s and 1970s and that have not been updated since then. It has been shown that designs that rely only on these guidelines can result in significant flow distribution problems that significantly affect the performance of the machine. Because the performance of each machine is unique, there are no general reduced-order methods that can be used to predict the performance losses caused by improper inlet piping design. This presents an opportunity to develop a process that can predict, on a case-by-case basis, the shape of the velocity profile as it arrives at the impeller and how it will affect the performance of the compressor.

Approach — Computational fluid dynamic (CFD) simulations will be used to quantify the uniformity of the velocity profile and amount of swirl at the compressor inlet plane for different piping layouts. The effect of those layouts on the performance of a generic impeller wheel will then be tested in the Single Stage Test Rig (SSTR). The data from the experimental study will be used to validate the CFD simulations and to develop an understanding of how compressor performance is influenced by the incoming flow. The amount of swirl will be varied by increasing the length of the section of straight pipe between the last elbow in the layout and the impeller.

Accomplishments — To date, the impeller has been designed and sent for fabrication. The impeller is shown in Figure 1.

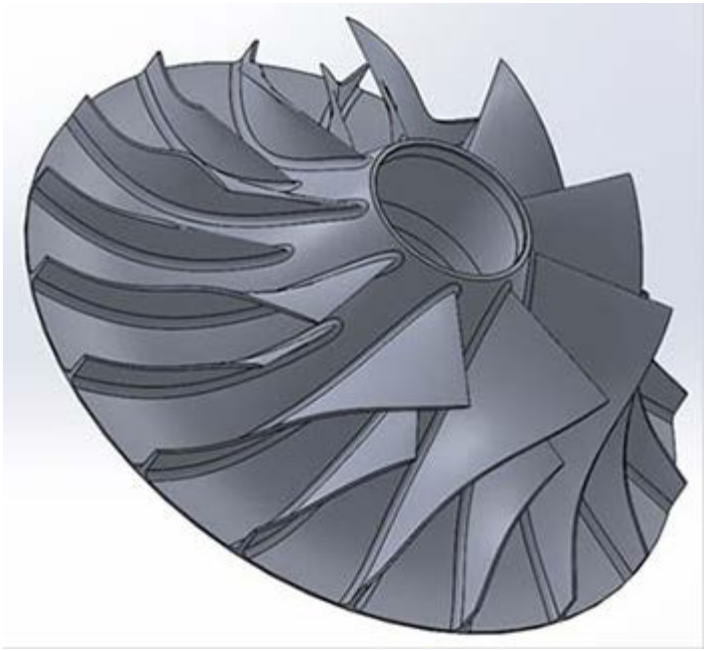

Figure 1: Custom-designed impeller for inlet distortion studies.

All instrumentation has been procured and is currently being integrated into the SSTR. In the meantime, preliminary tests have started using an impeller that was provided by a customer as shown in Figure 2.

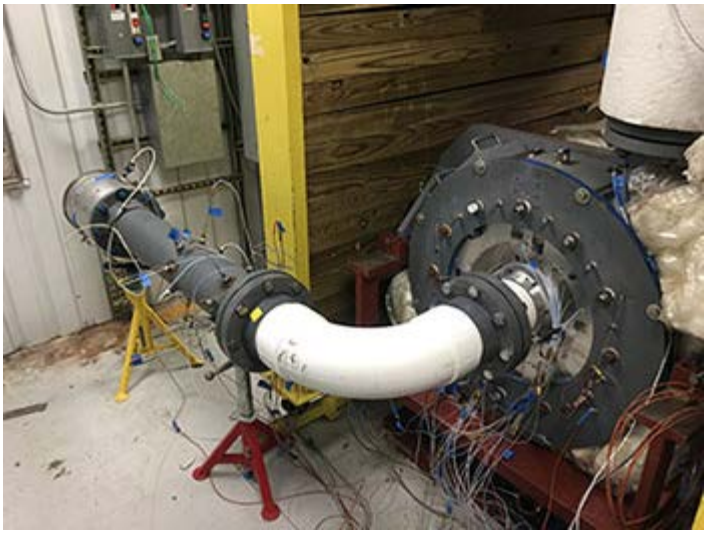

Figure 2: Experimental testing of inlet flow distortion in the SSTR with the elbow 2 diameters upstream of the impeller.

CFD simulations of the flow in the inlet piping have also started. The swirl pattern for the configuration shown in Figure 2 is shown in Figure 3.

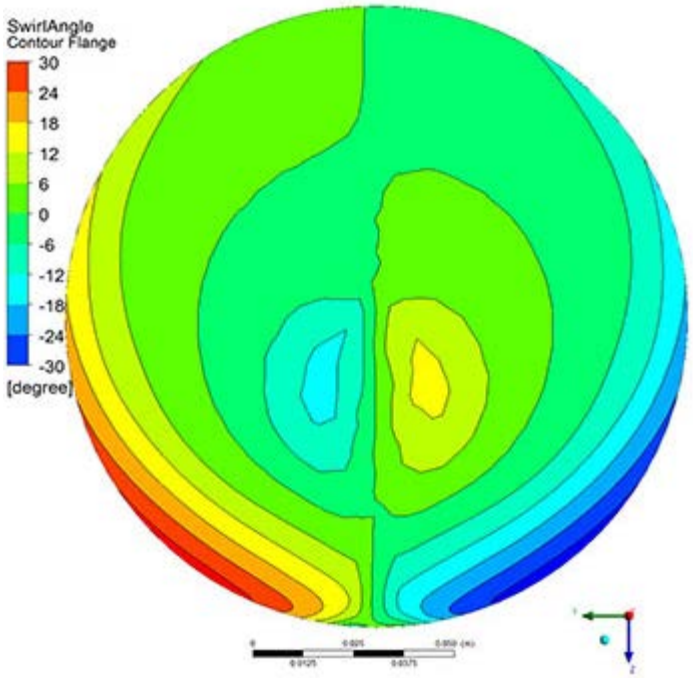

Figure 3: Swirl pattern of the inlet flow with the elbow 2 diameters upstream of the impeller.

SOUTHWEST RESEARCH INSTITUTE®

2017 IR&D Annual Report

Inexpensive and Rapid Production of Microfluidic Parts, 11-R8719

Principal Investigators
Chris Hackert
Domenick Leto
Cole Buss
Alan Craig

Inclusive Dates: 12/05/16 – 03/06/17

Background — Microfluidics is a growing technology area encompassing items such as inkjet printer heads, lab-on-a-chip technology, and sensors for hazardous chemicals and biological agents. Microfluidic channels are typically less than 1 mm in lateral dimension, and often in the range of 100 µm or smaller. The small distances involved enable very high gradients in temperature, concentration, or pressure. A special sub-field of microfluidics is the microreactor, in which sensitive or dangerous reactions can be managed with great precision or in small quantities. This is achievable because of highly controllable reactant flow rates, lack of turbulent flow creating variable concentrations, high surface-to-volume ratio for catalytic processes, and high heat transfer rates to the structure leading to good temperature control of the reaction.

Approach — Our proposed concept was that a combination of high-resolution additive manufacturing with electroplating may be used to produce inexpensive yet precise microfluidic structures made of chemically resistant materials such as nickel metal. Stereolithographic additive manufacturing devices (SLA) use a highly focused light beam to solidify a curable liquid resin. Recent SLA machines have been developed with ~30-µm spot size, allowing the direct printing of microscale devices. The curable resin, however, does not have the properties desirable for many microfluidic applications since the resin is a poor conductor of heat and not resistant to corrosive chemicals. Our concept was to print the channel spaces as a form (or mold) using a high-resolution SLA device, and then either electroplate nickel or cast the part into low-melting point metal to create the actual microfluidic device. Unwanted SLA resin then would be removed by an appropriate acid or solvent, leaving the nickel microchannels behind.

Accomplishments — We were successful in producing sample microfluidic structures in inexpensive 3-D additive manufacturing printers using two methods: direct electroless nickel plating and casting into metal. Along the way, we found that the nominal printer resolution is not necessarily the resolution of the produced part: longer and shorter exposure times can lead to addition and removal of cured resin from the part boundaries, respectively. Adjusting the exposure time and scaling the design of the part can compensate for this issue. High-resolution metrology may be necessary to ensure design fidelity. Other lessons learned are that high-resolution embossed features need structural support to remain intact and stable before final curing. Substrate layers and buttresses may be needed to maintain the shape of the part. The cured resin was surprisingly difficult to dissolve chemically. Casting worked well for all microfluidic elements at the 200-mm scale, but only for simple channels at the 100-mm scale. Surface tension of the liquid metal and fragility of narrow walls appears to be the limiting factor. Use of a vacuum oven (to eliminate air bubbles) and a mold-release agent was helpful.

SOUTHWEST RESEARCH INSTITUTE®

2017 IR&D Annual Report

Method Development for Production of Energetic Bimetallic Materials, 11-R8770

Principal Investigators
Nathan Weyandt
Charles Baker
Domenick Leto

Inclusive Dates: 05/31/17 – 10/02/17

Background — The objective of this project was to develop reliable methods by which energetic bimetallic materials could be produced at SwRI. Bimetallic reactions are alloying reactions between two metallic elements that can rapidly release a large amount of energy. The common production method used (atomic vapor deposition) is complicated and suffers significant issues with some of the desired metal pairs.

Approach — The two methods specifically identified for this internal research project were electrophoretic deposition (EPD) and block copolymer lithography (BCL). EPD is a process that uses an electric field to migrate and deposit suspended particles from a solution onto a desired conductive substrate. SwRI developed a simple 3-D printed device to support the substrates and opposing electrodes in electrolyte during the process. EPD experiments were performed with two flat plate electrodes vertically immersed in a 100 mL suspension of nanoparticles. Titanium, boron, nickel, aluminum, silicon, and zirconium particles were prepared under an argon atmosphere and sonicated into solution (two elements per test trial). Corrugated stainless steel ribbon, stainless steel sheets, and gold-coated microarray substrates were used as the electrodes. Potential was supplied by a power amplifier with provisions to control the pulse characteristics. After deposition, the cathode substrate was slowly removed from the suspension and air-dried in a fume hood. The solid loading, electrode spacing, electrode type, deposition time, applied potential, and pulse duration were varied in the EPD experiments.

In the BCL process, metal salts are co-dissolved with a block copolymer consisting of a hydroxyl-terminated polyethylene oxide block and a poly(2-vinylpyridine) block, PEO-b-P2VP. The expectation was that the di- and tri-valent metal ions would have interactions within the P2VP block segments, preventing mixing of metal ions. The metal-salt solutions were mixed in equimolar ratio and allowed to dry slowly at 75 percent relative humidity. The samples were then heated to 150°C in argon to drive off the remaining water and phase-separate the block copolymer segments. Finally, the material (droplet or film) was heated to 500°C under a hydrogen atmosphere to reduce the ions to metal. The primary variables for the BCL tests were the choice of bimetallic pairs (among Al, Ni, B, Ti, and Pd) and the choice of the metal salt anion.

Accomplishments — In each electrophoretic deposition test trial, the method resulted in codeposited metals on the substrate, but not as a solid film and with poor adhesion (Figure 1). Furthermore, when tested for ignition characteristics, the materials showed some sparking at the point of electrode contact with no evidence of propagation or sustained ignition.

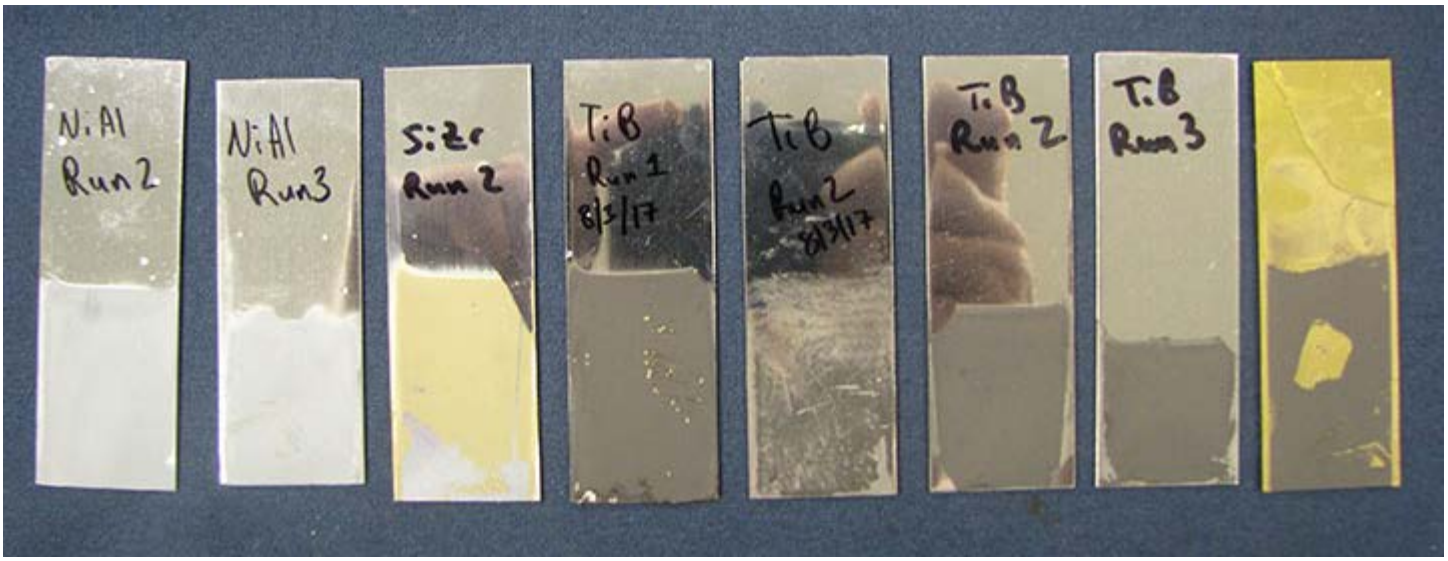

Figure 1: Representative results of EPD films deposition.

In the majority of the block copolymer lithography trials, the material formed a thin gel that hardened to bits of solid metallic film that fragmented during the final hydrogen baking stage of the process. In the final two test trials the material formed a transparent, gel-like spherical mass, which hardened to a metallic sphere following the hydrogen baking process (Figure 2). When tested for ignition, none of the materials showed evidence of sparking or igniting. Furthermore, the materials did not show evidence of being conductive.

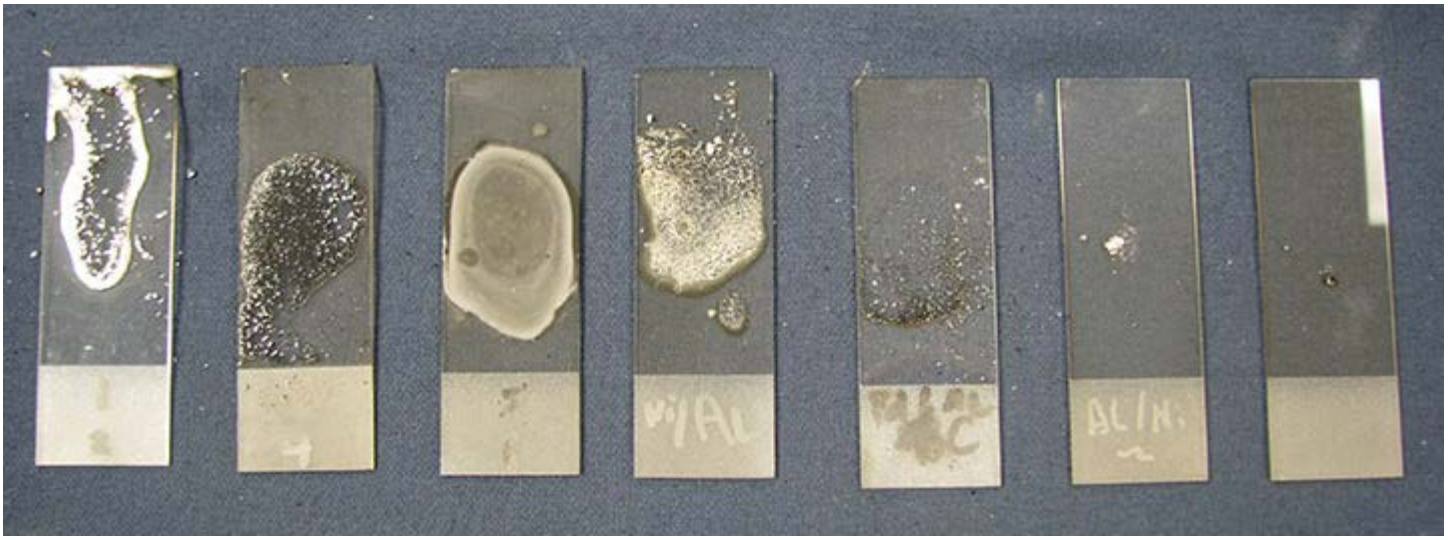

Figure 2: Materials resulting from seven BCL test trials.

SOUTHWEST RESEARCH INSTITUTE®

2017 IR&D Annual Report

A Bundt Pan Electrostatic Analyzer for an Open Ion Source for MASPEX, 15-R8709

Principal Investigators
Ryan Blase
Amy Lopes
Greg Miller

Inclusive Dates: 10/11/16 – 02/11/17

Background — The purpose of this project was to design, simulate, fabricate, and test an open ion source for the MAss Spectrometer for Planetary EXploration (MASPEX) instrument. An open ion source is important in planetary orbiter and flyby mass spectrometers to measure ions and reactive neutrals in planetary atmospheres. A typical closed ion source with a gas inlet system cannot measure the abundance of ions and reactive neutrals precisely as ions are neutralized and reactive neutrals react with surfaces or other molecules during wall interactions inside the gas inlet system and closed ion source. Open ion sources can measure these ions and reactive neutrals but have a reduced sensitivity in comparison to closed ion sources. We set out to develop a novel open ion source, termed the Bundt Pan Electrostatic Analyzer (ESA, Figure 1), to enhance the sensitivity of the device to ions and neutrals compared to the current state of the art. The proposed effort was in support of Enceladus Life Finder, a New Frontiers 4 proposal featuring MASPEX as a payload instrument.

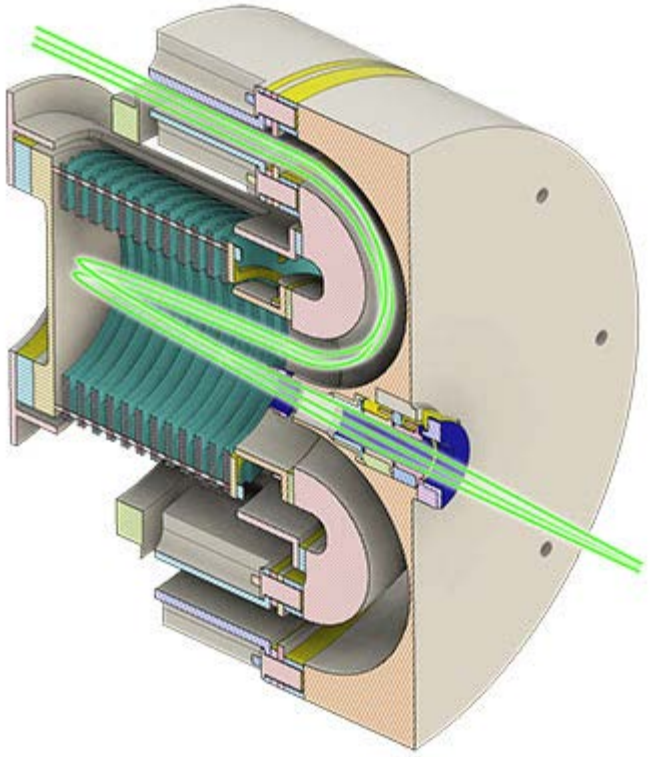

Figure 1: 3-D CAD cross section of the Bundt Pan ESA open ion source with ion trajectories.

Approach — The open ion source was termed a Bundt Pan Electrostatic Analyzer (ESA) due to its resemblance to a bundt cake pan. We simulated and ray traced the ion trajectories through the optical design with SIMION. When the design achieved acceptable energy acceptance and efficient ion transmission through the device we then moved to the mechanical engineering design of the open ion source. The open ion source was mechanically designed in an engineering drawing package with mounting, insulation, and electrical connections of all ion optical components considered. The majority of the pieces of the mechanical design were then fabricated in SwRI's Precision Machining Facility with the reflectron lens elements of the design fabricated by an outside contractor. After receipt of all machined parts, the open ion source was assembled and mounted on a single aluminum plate to be fitted inside the vacuum chamber (Figure 2). The open ion source was then tested with an ion gun at the entrance to the Bundt Pan ESA. Experimental difficulties and time limitations did not allow transmission and detection of the ion beam through the entire device, but ion beam current

was successfully measured on the back plate of the reflectron.

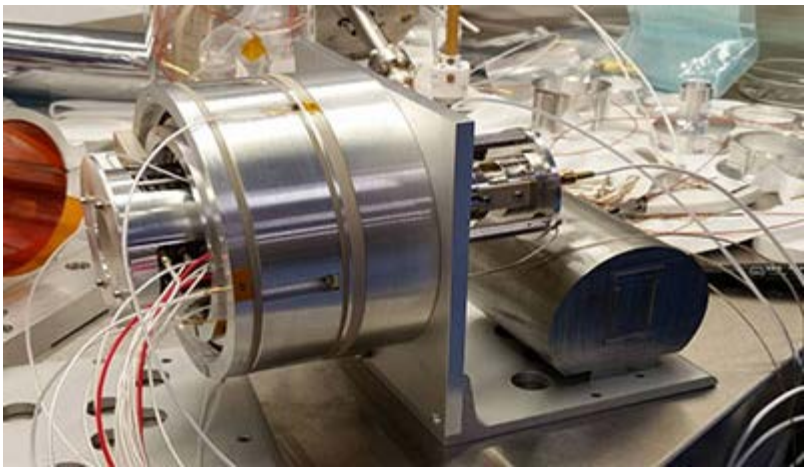

Figure 2: Photograph of the fully assembled Bundt Pan ESA open ion source.

Accomplishments — We successfully designed, simulated, and fabricated the Bundt pan ESA open ion source. The design requirements of an energy acceptance of 15 percent (0.15) and angular acceptance of ±5° were confirmed and the optical design showed efficient transmission through the entire device through SIMION simulation results. Efficient ion transmission through the device allows for co-axial injection of the exiting ions to MASPEX for mass spectral analysis. The mechanical design was inserted into a vacuum chamber and tested with an ion gun. Ion beams were successfully transmitted through the ESA and measured at the back of the reflectron.

SOUTHWEST RESEARCH INSTITUTE®

2017 IR&D Annual Report

Fabrication and Testing of High Voltage Optocouplers for Space Applications, 15-R8712

Principal Investigators
Armando De Los Santos
Dennis Guerrero

Inclusive Dates: 10/31/16 – 03/01/17

Background — High voltage power supplies (HVPS) have long played an integral role in many scientific instruments in the space sciences, powering analytical sensors used to investigate the solar system around us. SwRI has a long and successful history in building these highly specialized HVPS for our own instrument needs, as well as for outside clients. We have also specialized in a particular type of high voltage (HV) control circuit stepping or sweeping output. This type of circuit typically uses high voltage optocouplers as the main control element. These are very specialized devices that have proven to be a challenge to build properly. In recent years, these devices began to suffer failures deep into the supplies' environmental testing regime and in one instance after launch. Extensive investigations by SwRI and NASA personnel identified numerous weaknesses in the two commercially available parts.

To combat these problems, an internal research project (15-R8388, Development of High Voltage Optocouplers for Space Applications) was conducted to design, build, and test two different HV optocouplers while focusing on new topologies, materials, and improved construction techniques using more reliable components. Several iterations of each HV optocoupler were built and tested leading to an evolution of components, materials, and fabrication methods that resulted in very robust units. A modified version of the developed HV optocouplers was designed, built, and tested to fit into an existing power supply design. As a result of the screening and radiation testing, many things were learned. The cumulative effect of issues caused the yield on parts for this program to be approximately 50 percent. Solutions to resolve these issues were proven on subsequent builds.

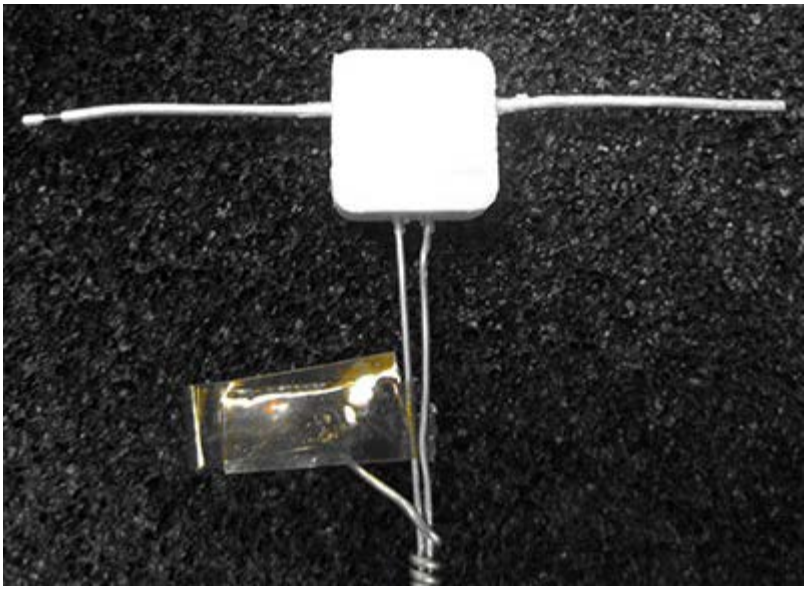

Figure 1: SwRI 100SW1502 standard high-voltage optocoupler.

For use on multiple near term space instrument programs for the NASA Europa Mission, we designed two standardized units that have simplified assembly, additional component pre-screening with a revised pre-cure to increase yield and reliability, and minimal partial discharge issues (improved clearances), all while being seamlessly integrated into the proposed power supplies. Prototypes of these devices were built and initial measurements were very good. A larger number of units of each type were needed to subject to thermal cycling, burn-in, and life testing to uncover any potential long term issues. This effort had to occur

before the referenced programs above made their final part selection.

Approach — The tasks planned for this project included:

- Acquiring materials and components required for building up to 20 parts
- Pre-screening (inspection and testing) of all components
- Modifying available molds to accommodate recent design changes
- Re-laying out and building the small internal PC board to accommodate recent design changes
- Fabricating new devices
- Preliminary electrical testing of new devices
- Thermal cycling, burn-in, partial discharge, and life testing of new devices.

Accomplishments — Most of the proposed work was successfully completed through this project with life testing continuing. With good test results and high yield, several instrument programs as mentioned above have selected these parts while the selection process for other instrument programs is still in progress.

A photograph of the SwRI 100SW1502 Standard High Voltage Optocoupler is shown in Figure 1.

SOUTHWEST RESEARCH INSTITUTE®

2017 IR&D Annual Report

Development of a Lunar Advanced Vacuum Apparatus (LAVA), 15-R8734

Principal Investigators
Edward Patrick
Marius Necsoiu
Preston Karnes

Inclusive Dates: 01/03/17 – Current

Background — Expertise in handling ultrahigh vacuum (UHV) systems is common, as is expertise in handling soil or other unconsolidated materials. Handling soil under UHV conditions is very uncommon. However, this expertise and capability is essential in the laboratory when grappling with the issues surrounding the surface environments of primitive solar system bodies such as Mercury, the Moon, the moons of Mars (Phobos and Deimos), and the asteroids, not only in terms of the science investigation of these planetary bodies, but also in terms of the engineering designs demanded by both remote and *in situ* instrumentation of these primitive surfaces. The purpose of this project is to produce science data relevant to the permeation and diffusion of volatiles and gases at the lunar surface. These data will then be used to support future missions to the Moon. Dubbed the "Lunar Advanced Vacuum Apparatus" (LAVA), this laboratory setup will permit measurements of the time taken for gases introduced at the base of a column of JSC-1A lunar soil simulant to reach an ion gauge and a mass spectrometer for recording. Varying permeability rates of various gases (He, Ne, Ar, N_2, CO_2, etc.) will be used to inform current models as to how these gases diffuse through, evolve, and trap at the lunar surface. The assumption is that those volatiles discovered at the lunar south pole by the LCROSS mission originated with ancient comet or asteroid impactors, or were released from the lunar interior during subsurface disturbances or moonquakes.

Approach — A column containing the pedigreed JSC-1A lunar soil simulant will be dispensed into a 2,000 ml graduated cylinder within which is placed tubing to introduce gas to the base of the column. Gas will be introduced at the base of this column of pulverized, granular, volcanic material at a specific point in time and its detection time will be recorded at the ion gauge and mass spectrometer. The diffusion behavior of each gas species will be measured according to its unique physical and chemical properties.

Accomplishments — The 2,000 ml graduated cylinder has been placed in the LAVA chamber and gate valve has been installed. Work continues on the vacuum "hopper" that will drop the simulant into the cylinder and chamber after first being degassed by a separate baking, sorting, and adsorbed gas evacuation. Lessons learned during this effort are being used in a current collaborative project with the Korean Institute of Civil Engineering and Technology (KICT) to advise them on the present construction and fabrication of their Dirty Thermal Vacuum Chamber (DTVC).

SOUTHWEST RESEARCH INSTITUTE®

2017 IR&D Annual Report

Enhancing the Efficacy of a Chlamydia Subunit Vaccine Through Encapsulation, 01-R8584

Principal Investigator
XingGuo Cheng

Inclusive Dates: 09/01/15 – 01/25/17

Background — Chlamydia trachomatis (CT) is the world's leading cause of sexually transmitted diseases (STD) and the most commonly reported STD in the U.S. and Texas. Chlamydia infection may result in pelvic inflammatory disease, complications such as ectopic pregnancy and infertility in women, in addition to epididymitis in men, pneumonia in infants, and even blindness. A peptide, or protein-based, vaccine candidate has been demonstrated to have a high degree of efficacy in two animal models of genital chlamydial infection. However, there is a need to further develop this promising vaccine in terms of longer-lasting protective immunity, easy and effective delivery, and improved efficacy in order to transition into humans. The objective of this project is to develop an effective, novel, encapsulated subunit Chlamydia vaccine that will be validated in an established animal (mouse) model of genital chlamydial infection. We hypothesize that the encapsulated vaccine formulation will perform better (e.g., higher and longer protective efficacy, longer stability, and fewer side effects) than the non-encapsulated vaccine formulation.

Approach — For the technical tasks, we will perform encapsulation and characterization of subunit chlamydial antigens along with selected adjuvants, and *in vivo* evaluation of the performance of free and encapsulated vaccines.

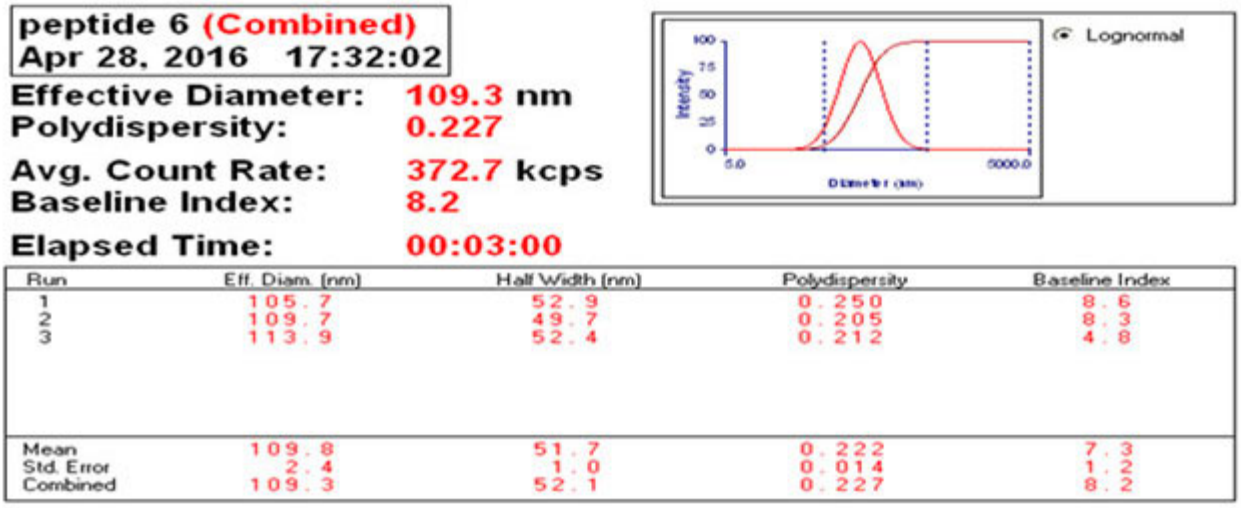

	Liposome-Peptide 6	Liposome-Peptide 8	Liposome-Peptide 10	Liposome-Peptide 12	Liposome-CPG
Particle size (nm)	109.8 ± 2.4	132.6 ± 1.8	136.7 ± 1.2	141.4 ± 0.8	128 ± 0.7
Z-potential (mV)	-64.54 ± 3	-68.42 ± 2.6	-64.07 ± 3.45	17.34 ± 2.04	-30 ± 0.96

Figure 1: Particle size and zeta potential of each liposomal-peptide nano vaccine formulation before mixing.

Accomplishments — We performed peptide solubility, successfully encapsulated five different subunit peptide antigens, and also fabricated and characterized liposomes encapsulating an adjuvant (CPG) (Figure 1). An animal vaccination study demonstrated that liposome-chlamydial protease/proteasome-like activity factor (CPAF), liposome-peptide, and peptide-only vaccination induced a robust Chlamydia muridarum specific Th1 cellular response. Compared to other vaccination groups, the liposome-peptide vaccination resulted in faster clearance of infection after a challenge with bacteria (Figure 2). Liposome-peptide vaccinated animals displayed minimal oviduct dilatation (Figure 3). These results indicate that apart from enhancing resolution of infection, vaccination with liposome-peptide induces protection against oviduct pathology.

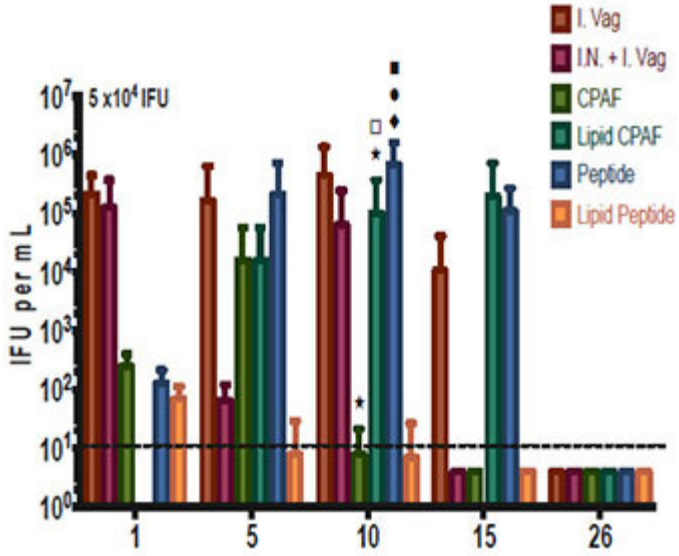

Figure 2: Percentage of mice shedding bacteria. Four-to-five-week-old female C57BL/6 mice (n = 8) were immunized intra-nasally with whole EB, CPAF, lipid CPAF, peptide, lipid peptide, or PBS (mock), and booster immunizations were given on days 12 and 29. Fifteen days after the final immunization, mice were challenged intravaginal with 5x10⁴ IFU of C. muridarum.

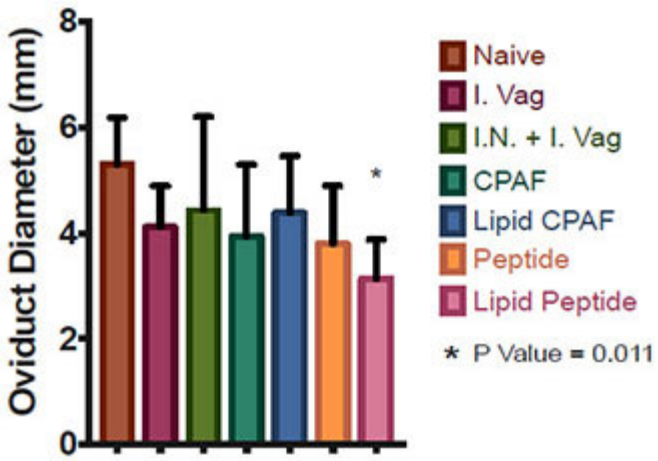

Figure 3: Upper genital tract pathology following genital challenge in immunized mice.